

**Design, Synthesis and Characterisation of
Fluorescent Purine Nucleosides Containing Rigid
'Phenyl-ethynyl-phenyl-' Moieties: Identification of New
 $\text{Pd}_2(\text{dba-Z})_3$ Catalysts for Sonogashira Cross-couplings**

QIONG XU

Ph.D.

University of York

Chemistry

November 2015

Abstract

This thesis describes the design, synthesis and characterisation of novel fluorescent purine nucleosides, which directly address the general lack of commercially available analogues for studying DNA and RNA polymerases in a biological context. C8 purine modification is an advantageous position for fluorescent-labelling that can potentially minimise interactions along the Watson-Crick base pairing edge. An organic rigid-rod system, namely a 'phenyl-ethynyl-phenyl-' group was linked to the purine, inducing adequate fluorescence properties. A series of C8-modified purine nucleosides, containing highly conjugated linear ethynyl linker motifs, were synthesised, employing Sonogashira cross-coupling chemistry and catalytic Pd/Cu. The development of new Pd catalysts capable of performing these reactions was deemed necessary for these Sonogashira cross-coupling reactions, exploiting the ligand properties of olefins (alkenes).

A series of dibenzylidene acetone (dba-Z) alkene ligands and their novel Pd complexes were synthesised and characterised. Detailed NMR spectroscopic and TEM analyses were required to determine the composition and structure of the dinuclear 'Pd-dba-Z' complexes. The Pd₂(dba-Z)₃ complexes were found to be useful catalysts for use in the cross-coupling reactions of suitably halogenated nucleosides. A library of adenosine and guanosine compounds has been prepared, using the newly developed Pd catalysts.

Molecular self-assembly is principal to many areas of study in biology and supramolecular chemistry. The biophysical behaviour of the synthesised fluorescent nucleoside compounds has been examined and a detailed study by UV-Vis and fluorescence spectroscopy. The solvatochromism properties of the compounds are reported. DMSO showed the largest quantum yields in comparison with other solvents for all the fluorescent nucleosides. While in water, the quantum yields were found to be relatively small, values are workable in a biological context. The modified-guanosine and adenosine analogues exhibit photophysical characteristics which may prove useful in future studies.

The development of a C-H bond functionalisation methodology for the catalytic direct arylation of inosine at the C8 position has been investigated. Such chemistry is advantageous for the introduction of aromatic groups, avoiding pre-functionalisation (halogenation) of the nucleoside substrates, as compared to traditional cross-coupling reactions, *e.g.* Suzuki-Miyaura. Some limitations with the methodology have been identified.

In a separate strand to the thesis, the design, synthesis and characterisation of platinum complexes containing phosphine-alkene ligands, based on a chalcone-ferrocene framework, is detailed (within Appendix A). Platinum complexes containing either the 'Lei' ligand and/or 'ferrocenyl-derived-Lei' ligand have been further characterised.

Contents

Abstract.....	2
Contents	3
List of Schemes.....	7
List of Figures	9
List of Tables	12
List of Accompanying Material.....	13
Acknowledgements.....	15
Author's Declaration.....	17
1 Introduction.....	19
1.1 The structure of DNA and RNA	19
1.1.1 Nucleosides, nucleotides and nucleic acids	20
1.1.2 Conformations of double stranded DNA	21
1.1.3 Higher ordered nucleic acid structures	22
1.2 Chemical synthesis of DNA – solid phase oligonucleotide synthesis	26
1.3 Modification to the structure of oligonucleotides.....	27
1.3.1 Fluorescent nucleotide analogues	27
1.3.2 Synthetic modifications to the phosphate	29
1.3.3 Synthetic modifications to the ribose.....	31
1.3.4 Synthetic modifications to the nucleobase.....	33
1.3.5 C8-modified nucleosides	36
1.4 Pd-catalysed functionalization of unprotected oligonucleotides	38
1.4.1 Ligand synthesis for cross-coupling reactions with Pd catalysis.....	38

1.4.2 Pd-catalysed cross-coupling in organic synthesis.....	42
1.4.3 Other Pd-catalysed cross-couplings of nucleosides and nucleotides.....	47
1.4.4 Pd-catalysed C-H functionalisation of nucleosides.....	49
1.5 Aims and Objectives.....	51
1.5.1 Aims.....	51
1.5.2 Objectives.....	51
2 Synthesis of new Pd catalysts containing dba-Z ligands, including hydroxylated derivatives.....	53
2.1 Introduction.....	53
2.2 Synthesis of hydroxylated-dba Pd complexes.....	56
2.2.1 Synthesis of the ligand for Pd ₂ (3-OH-dba) ₃ •(3-OH-dba).....	56
2.2.2 Synthesis of the ligand for Pd ₂ (4-OH-dba) ₃ •(4-OH-dba).....	57
2.2.3 Synthesis of the complex [Pd ₂ (dba-3-OH) ₃ •dba-3-OH].....	58
2.2.4 Synthesis of the complex Pd ₂ (4-OH-dba) ₃ •(4-OH-dba).....	61
2.3 Synthesis of hydroxylated– and alkyloxy–dba Pd complexes.....	63
2.3.1 Synthesis of the ligand for [Pd ₂ (4-OH,4'-alkyloxy-dba) ₃ •(4-OH,4'-alkyloxy-dba)].....	63
2.3.2 Synthesis of the ligand for Pd ₂ (4-OH, 3'-alkyloxy dba) ₃ •(4-OH, 3'-alkyloxy dba).....	70
2.3.3 Synthesis of the ligand for Pd ₂ (3-OH, 4'-alkyloxy dba) ₃ •(3-OH, 4'-alkyloxy dba).....	72
2.3.4 Preparation of the ligand and complex for Pd ₂ (3-OH, 3'-alkyloxy dba) ₃	73
2.3.4 Synthesis of the complex of Pd ₂ (4-OH, 4'-alkyloxy dba) ₃ •(4-OH, 4'-alkyloxy dba).....	73
2.3.6 Synthesis of the complex of Pd ₂ (4-OH, 3'-alkyloxy dba) ₃ •(4-OH, 3'-alkyloxy dba).....	75
2.4 Synthesis of alkyloxy dba Pd complexes.....	76
2.4.1 Synthesis of the ligand for Pd ₂ (4,4'-alkyloxy-dba) ₃ •(4,4'-alkyloxy-dba).....	76
2.4.2 Synthesis of the ligand for Pd ₂ (3, 3'-alkyloxy dba) ₃ •(3, 3'-alkyloxy dba).....	77
2.4.3 Synthesis of the complex of Pd ₂ (4-alkyloxy-dba) ₃ •(4-alkyloxy-dba).....	77

2.5	Transmission electron microscopy (TEM) analysis	79
2.6	Active Pd ratio from the $[\text{Pd}_2(\text{dba})_3]$ complexes.....	82
2.7	Conclusion	86
2.8	Experimental	87
3	Synthesis of highly conjugated linear ethynyl nucleosides	107
3.1	Introduction.....	107
3.2	Sonogashira alkylation of unprotected 8-modified fluorescent nucleosides	108
3.2.1	Sonogashira alkylation of unprotected 8-bromoguanosine and adenosine.....	108
3.2.2	Pd catalyst activity towards Heck and Sonogashira cross-coupling reactions	112
3.2.3	Modification of multiple alkyne motif on C8 nucleosides	115
3.4	Guanine-quartet study involving 8-alkynylated purines.....	125
3.4.1	Synthesis alkylation of 8-modified for G-quartet study	125
3.4.2	NMR study.....	126
3.5	Attempts to synthesise precursor compounds for solid-phase synthesis	126
3.6	Conclusion	129
3.7	Experimental.....	130
4	Photophysical Characterisation of Modified Nucleosides.....	153
4.1	Introduction.....	153
4.1.1	Principles of fluorescence.....	153
4.1.2	Fluorescent Nucleosides Analogues	155
4.1.3	Extinction coefficient and quantum yield.....	156
4.2	UV-vis spectroscopy.....	158
4.3	Fluorescence spectroscopy.....	160
4.4	Photophysical characterisation of C-8 modified nucleosides.....	164

4.5 Solvatochromism	165
4.6 Conclusion	175
4.7 Experimental	176
5 C-H direct arylation of nucleosides	180
5.1 Introduction.....	180
5.2 Direct arylation reactions of inosine.....	180
5.3 Substrate scope in the direct arylation reactions.....	181
5.4 Conclusion	183
5.5 Experimental	184
6 Conclusions and Future Work	192
6.1 General Discussion	192
6.2 Synthesis of Pd catalysts for 8-modified fluorescent nucleosides.....	192
6.3 Synthesis of highly conjugated linear ethynyl nucleosides	193
6.4 Photophysical characterization of modified nucleosides.....	193
6.5 C-H direct arylation of nucleosides	194
6.6 Future Work	194
Abbreviations.....	198
References.....	1

List of Schemes

Scheme 1.1 Chiral diene catalysed Suzuki cross-coupling.	40
Scheme 1.2 Reaction of 1,3-diiminoisoindoline with <i>cis</i> -[PdCl ₂ (CNR ₁) ₂].	40
Scheme 1.3 Synthesis route of the Pd complex.	40
Scheme 1.4 Suzuki-Miyaura cross-coupling with 4-bromoacetophenone and Ph ₄ BNa.	41
Scheme 1.5 The Sonogashira cross-coupling reaction.	43
Scheme 1.6 Proposed mechanism of Pd-catalysed Sonogashira cross-coupling reaction.	43
Scheme 1.7 Structure of TPPTS and TXPTS.	44
Scheme 1.8 Sonogashira reaction with 5-IdU and phenylacetylene in aqueous solvent form.	44
Scheme 1.9 The Sonogashira reaction of 5-IdU and alkynes in aqueous solvent.	44
Scheme 1.10 Sonogashira cross-coupling of 8-bromopurine nucleosides.	45
Scheme 1.11 Sonogashira coupling of phenylalanine analogues.	45
Scheme 1.12 Sonogashira cross-coupling of guanosine with phenylacetylene.	46
Scheme 1.13 General Heck reaction.	46
Scheme 1.14 Mechanism of the Heck reaction.	46
Scheme 1.15 Heck coupling of 5-IdU using Pd(OAc) ₂	47
Scheme 1.16 Synthesis of (adenin-8-yl) and (adenine-6-yl)phenylalanines.	47
Scheme 1.17 Structures of phosphine ligands L1–L3.	48
Scheme 1.18 Suzuki cross-coupling with 7-iodotubercidin and boronic acids.	48
Scheme 1.19 One-pot synthesis of 8-substituted NAD derivatives.	49
Scheme 1.20 First example of C-H arylation of purine nucleosides.	50
Scheme 1.21 Coupling of 5-IdU and thiophene.	51
Scheme 2.1 The dba ligand effects in a general cross-coupling catalytic cycle.	54
Scheme 2.2 Synthesis of ligand 3	56
Scheme 2.3 Acid-catalysed synthesis of ligand 5	57
Scheme 2.4 Synthesis of [Pd ₂ (dba-3-OH) ₃ ·dba-3-OH] 6	58
Scheme 2.5 Synthesis of [Pd ₂ (dba-4-OH) ₃ ·dba-4-OH] 7	61
Scheme 2.6 Synthesis of compound 9	63
Scheme 2.7 Attempted synthesis of compound 10	64
Scheme 2.8 Synthesis of compound 12	64
Scheme 2.9 Synthesis of compound 10	64
Scheme 2.10 Synthesis of decane compound 14	65

Scheme 2.11 Synthesis of compound 15.	65
Scheme 2.12 Synthesis of compound 16.	66
Scheme 2.13 Synthesis of compound 18.	66
Scheme 2.14 Synthesis of compound 19.	67
Scheme 2.15 Attempted synthesis of compound 21.	67
Scheme 2.16 Synthesis of compound 20.	68
Scheme 2.17 Synthesis of compound 24.	68
Scheme 2.18 Synthesis of compound 25.	69
Scheme 2.19 Synthesis of 4-OH, 4'-OHexyl dba compound 26.	69
Scheme 2.20 Synthesis of compound 27.	71
Scheme 2.21 Synthesis 4-OH, 3'-OHexyl dba compound 28.	71
Scheme 2.22 Synthesis of 3'-OH, 4-alkyloxy dba compound 29.	72
Scheme 2.23 Synthesis of 3-hydroxy compound 30.	73
Scheme 2.24 Synthesis of 3'-OH, 3'-alkyloxy dba compound 31.	73
Scheme 2.25 Synthesis of Pd complex 33.	74
Scheme 2.26 Synthesis of Pd complex 34.	76
Scheme 2.27 Synthesis of symmetrical hexane-dba 35.	77
Scheme 2.28 Synthesis of ligand 36.	77
Scheme 2.29 Synthesis of complex Pd complex 37.	78
Scheme 2.30 The kinetic equilibrium processes of $\{Pd^0(dba)_2 + nL\}$ in oxidative addition reactions.	82
Scheme 2.31 Addition of PPh_3 to 'Pd-dba-Z' complex 37.	82
Scheme 3.1 Synthesis of 8-bromo-(deoxy)adenosine 39(41) and 8-bromo-(deoxy)guanosine 43(45).	110
Scheme 3.3 Attempted synthesis of compound 49 for use in ReactIR™ studies.	112
Scheme 3.4 Comparison of two routes for synthesising target compound 59.	116
Scheme 3.5 Synthesis of 8-Bromoinosine 61.	116
Scheme 3.6 Synthesis of acetate-protected group on (deoxy)guanosine derivatives 70 and 71.	125
Scheme 3.7 Protection of 74 for solid-phase synthesis.	128
Scheme 3.8 Synthesis of uridine phosphoramidite 75.	129
Scheme 5.1 Synthesis of C-H bond direct arylation of inosine.	180
Scheme 5.2 Synthesis of 1-iodopyrene 87.	183

List of Figures

Figure 1.1 A schematic of the double helical structure of DNA and a detailed helical structure of DNA.....	19
Figure 1.2 Structure of nucleosides and nucleotides.....	20
Figure 1.3 The two most common conformations adopted by the ribose unit.....	21
Figure 1.4 Watson-Crick base-pair.....	22
Figure 1.5 <i>Anti/syn</i> nucleoside equilibrium and base flip.....	23
Figure 1.6 Structure of G-quartets.....	23
Figure 1.7 Two sets of 6 aromatic proton resonances in D ₂ O.....	24
Figure 1.8 NMR spectrum showing changes consistent with formation of a G-quartet.....	25
Figure 1.9 Solid-phase synthesis cycle.....	26
Figure 1.10 Possible nucleoside/nucleotide modifications on guanosine (as an example).....	28
Figure 1.11 Typical modifications sites in natural and unnatural analogues, R = ribose/deoxyribose.	28
Figure 1.12 Examples of commercially-available modified fluorescent adenosine analogues. ⁴⁹	29
Figure 1.13 5-fluoro-2'-deoxyuridine-5'- <i>O</i> -tetraphosphate (Um-PPPP-FdU).....	29
Figure 1.14 Fluorescent AppAMC and ApppBODIPY analogues.....	30
Figure 1.15 Fluorescent polymerase compound, ANS-dATP.....	30
Figure 1.16 TNP-ATP happens as an equilibrium fusion depending on the pH environment.....	31
Figure 1.17 3'- <i>O</i> -(2-aminoethylcarbamoyl) modification of ribose.....	32
Figure 1.18 Structures of coumarin-labeled ATP analogues.....	32
Figure 1.19 Naturally-occurring fluorescent nucleosides. R = ribonucleosides.....	33
Figure 1.20 Push-pull-type purine nucleoside-based fluorescent sensor.....	34
Figure 1.21 Tor's redox active f metal-containing luminescent linkers.....	34
Figure 1.22 Pyrene-labelled uridine and cytidine nucleosides (R = uridine).....	34
Figure 1.23 Pyrene-labelled fluorescent guanosine derivatives (λ_{\max} and λ_{em} values given in nm). 35	
Figure 1.24 Examples of nucleobase ring-modified systems.....	35
Figure 1.25 Examples of extended-ring nucleobase systems.....	36
Figure 1.26 The interaction edges in Guanine. ⁹²	37
Figure 1.27 A C8 fluorescent-labelled adenosine derivative.....	37
Figure 1.28 C8-substituted cinnamyl adenosine analogues.....	38
Figure 1.29 Examples of C8 modified purine analogues.....	38
Figure 1.30 Common ligands used in cross-coupling chemistry.....	39
Figure 1.31 Structure of Pd ^{II} complexes.....	41
Figure 1.32 Comparison of direct C-H functionalization and traditional cross-coupling methods. 50	

Figure 2.1 Substituted dba-Z ligands and their Pd ⁰ complexes.	53
Figure 2.2 Target synthesis of ligands and Pd catalysts for 8-modified fluorescent nucleosides....	55
Figure 2.3 ¹ H NMR spectrum and ¹ H- ¹ H COSY spectrum of [Pd ₂ (dba-3-OH) ₃ ·dba-3-OH] 6 (in CD ₃ OD, 400 MHz at 300 K).....	59
Figure 2.4 Three conformations in dba.....	60
Figure 2.5 ¹ H NMR spectrum and ¹ H- ¹ H COSY of [Pd ₂ (dba-4-OH) ₃ ·dba-4-OH] 7 (in CD ₃ OD, 400 MHz, 300 K).	62
Figure 2.6 ¹ H NMR spectrum of 26 and by-product of 26 (35) (in CDCl ₃ , ref. δ 7.26, 400 MHz). 70	
Figure 2.7 ¹ H NMR and ¹ H- ¹ H COSY spectrum of Pd complex 33 (in THF-d ₈ , ref. δ 3.58, 1.72, 400 MHz).....	74
Figure 2.8 ¹ H NMR and ¹ H- ¹ H COSY spectrum of Pd complex 37 (in CDCl ₃ , ref. δ 7.26, 400 MHz).	78
Figure 2.9 Example electron micrograph of large Pd particles derived complex 6 , approx. 200nm.	80
Figure 2.10 Example electron micrograph of Pd particles derived from complex 7	80
Figure 2.11 Example electron micrograph of a Pd particle of complex 33 . Inset shows histogram of particle diameter (nm), approx. 5-10 nm, across a sample of nanoparticles (<i>n</i> = 104).....	81
Figure 2.12 Example electron micrograph of a Pd particle of complex 37 . Inset shows histogram of particle diameter (nm) across a sample of nanoparticles (<i>n</i> = 24).	81
Figure 2.13 ³¹ P NMR spectrum of ‘Pd-dba-Z’ complex 37 in R.T. (CD ₂ Cl ₂).	83
Figure 2.14 ³¹ P NMR spectrum of the [Pd ⁰ ₂ (dba) ₃ ·dba] at R.T. (CD ₂ Cl ₂).	84
Figure 2.15 ³¹ P NMR of Pd complex 33 under different temperatures (CD ₂ Cl ₂).	85
Figure 3.1 Previous work on the synthesis of 8-alkynylated guanosine and adenosine derivatives.	107
Figure 3.2 Possible coordination of 8-BrG to Pd under basic conditions compared with 8-BrA. 108	
Figure 3.3 Homocoupled product from reaction of Sonogashira alkylation of unprotected 8-bromoguanosines/adenosines.....	112
Figure 3.4 Screening the activity of novel Pd catalysts 1 mol% against the Sonogashira cross-coupling reaction of 8-bromoguanosine 43 to give 46	113
Figure 3.5 Screening the activity of novel Pd catalysts against the Sonogashira cross-coupling reaction of 8-bromoadenosine 39 to give 47	114
Figure 3.6 ¹ H NMR spectrum of compound 65	118
Figure 3.7 Equilibrium of the <i>anti-syn</i> relationship 120	
Figure 3.8 Conformation flip from <i>anti</i> to <i>syn</i> 120	
Figure 3.9 Equilibrium of the <i>anti-syn</i> relationship..... 121	

Figure 3.10 ^1H - ^1H coupling constants between the proton signals on the furanose ring.....	123
Figure 3.11 Stack ^1H NMR spectra for synthesise precursor PhCCPhCC-dG for solid-phase synthesis.....	128
Figure 4.1 Jablonski (electronic transitions) diagram.....	154
Figure 4.2 Quantum yield equation.....	154
Figure 4.3 Jablonski (energy) diagram.....	155
Figure 4.4 Beer-Lambert Law.....	156
Figure 4.5 UV-vis spectrum for varying concentrations of PhCCPhCC-(deoxy)adenosine 62(63) , in DMSO at 20 °C.....	159
Figure 4.6 UV-vis spectrum for varying concentrations of PhCCPhCC-(deoxy)guanosine, 64(65) , in DMSO at 20 °C. The arrows show the absorption peaks.....	159
Figure 4.7 PhCCPhCC-guanosine 64 absorption concentration dependence (standard deviation of the mean is plotted).....	160
Figure 4.8 Absorption and emission spectrum for PhCCPhCC-(deoxy)adenosine, 62(63) , in DMSO at 20 °C.....	161
Figure 4.9 Absorption and emission spectrum for PhCCPhCC-(deoxy)guanosine, 64(65) , in DMSO at 20 °C.....	161
Figure 4.10 Concentration study of fluorescence excitation for PhCCPhCC-guanosine 64 in DMSO (emission = 476 nm).....	162
Figure 4.11 Absorption spectra of C8 modified nucleosides (approx. $C = 2.5 \times 10^{-6}$ M).....	163
Figure 4.12 Emission spectra of C8 modified nucleosides (approx. $C = 2.5 \times 10^{-6}$ M).....	164
Figure 4.13 Solvatochromic effect on fluorescence of PhCCPhCC-(deoxy)adenosine 62(63) (1.5×10^{-6} M) at 20 °C.....	166
Figure 4.14 Solvatochromic effect on fluorescence of PhCCPhCC-(deoxy)guanosine (1.45×10^{-6} M) at 20 °C.....	167
Figure 4.15 Anthracene and quinine sulphate – reference compounds.....	167
Figure 4.16 Lippert-Mataga plot for PhCCPhCC-(deoxy)adenosine.....	173
Figure 4.17 Lippert-Mataga plot for PhCCPhCC-(deoxy)guanosine.....	173
Figure 4.18 Attempted correlation between orientation polarizability (Δf) and quantum yield for PhCCPhCC-(deoxy)adenosine.....	173
Figure 4.19 Attempted correlation between solvent dielectric and quantum yield for PhCCPhCC-(deoxy)adenosine.....	174
Figure 6.1 Angled DNA mismatching duplex.....	195
Figure 6.2 Micellar catalysis study.....	195

List of Tables

Table 2.1 ¹ H NMR data for [Pd ₂ (dba-3-OH) ₃ ·dba-3-OH] (CD ₃ OD, 400 MHz).	60
Table 2.2 ¹ H NMR spectroscopic data for [Pd ₂ (dba-4-OH) ₃ ·dba-4-OH] (CD ₃ OD, 400 MHz).	63
Table 2.3 ¹ H NMR spectroscopic data for complex 33	75
Table 2.4 ¹ H NMR data for complex 34	76
Table 2.5 ¹ H NMR data for complex 37	79
Table 2.6 Active Pd ratio of ‘Pd-dba-Z’ complexes determined by NMR and elemental analysis.	84
Table 3.1 Various attempts to affect the cross-coupling of 8-bromoguanosine 43	111
Table 3.2 Pd catalyst activity toward a Heck cross-coupling reaction of a pyrimidine nucleoside 50 and alkene 51	115
Table 3.3 Modification at C8 of adenosines/guanosines/uredines/inosines.	117
Table 3.4 Yield comparison for the cross-coupling reaction in PC and DMF.	119
Table 3.5 ¹ H and ¹³ C NMR chemical shift data of natural ^a and modified nucleosides. ^b	122
Table 3.6 NMR ¹ H- ¹ H spin-spin coupling constants and ratio of C2’-endo to C3’-endo of nucleosides from data given in Table 3.5 ^b	124
Table 3.7 G-Quartets study with various conditions.	126
Table 4.1 Photophysical properties for 8-modified nucleosides.	164
Table 4.2 Solvent dependence of fluorescence emission for C8 modified nucleosides.	168
Table 4.3 Stokes shifts for C8 modified nucleosides.	168
Table 4.4 Quantum yield of C8 modified nucleosides in different solvents.	169
Table 4.5 Effect on solvent on the fluorescence properties of PhCCPhCC-Adenosine.	170
Table 4.6 Effect on solvent on the fluorescence properties of PhCCPhCC-deoxyAdenosine.	170
Table 4.7 Effect on solvent on the fluorescence properties of PhCCPhCC-Guanosine	171
Table 4.8 Effect on solvent on the fluorescence properties of PhCCPhCC-deoxyGuanosine.	171
Table 4.9 Effect on solvent on the fluorescence properties of PhCCPhCC-Inosine.	172
Table 5.1 Yields obtained for the direct arylation reaction of inosine using different Pd catalysts.	181
Table 5.2 Substrate scope in the direct arylation of inosine using various aryl iodides.	182

List of Accompanying Material

Appendix (on CD)

Appendix A Pt complexes of alkene-phosphine ligands (*contains discussion of results*)

Appendix B Spectroscopic data for compounds (NMR spectra, X-Ray data, photophysical characterization)

Appendix C Spectroscopic data for photophysical characterisation

***Be fearless in your choices
and don't be afraid to be yourself.***

– Britney Spears

Acknowledgements

Undertaking this PhD has been a truly life-changing experience for me as an international student who first came out from her home. The journey of the PhD life has been incredible. I am glad to be at this stage of my life and grateful to every one of them.

At the outset, I would like to thank the most my supervisor, Professor Ian Fairlamb for giving me this wonderful opportunity to join the IJSF group and to work on such an interdisciplinary project. Thank you for your support, great ideas and endless advice. Also thank you for having so much enthusiasm for research, discussing work with you was always inspiring and uplifting. I have been extremely lucky to have a supervisor who cared so much about my work, and who responded to my questions and queries so promptly. I would also like to thank all the members in IJSF group at University of York. I am indebted to them for their help. I would like to thank Dr. Christoph Baumann for the biology part of my project, which was an invaluable part of my PhD work. Furthermore, I gratefully acknowledge the funding support received towards my PhD from the Chemistry Department, Dr. Tony Wild, for three years of Wild Scholarship.

I greatly appreciate the support from all the Chemistry and Biology technical staff, Dr. Meg Stark (TEM), Dr. Adrian Whitwood (X-ray crystallography), Dr. Karl Heaton (MS), Heather Fish and Pedro Aguilar (NMR spectroscopy), Graeme McAllister (CHN) and Dr. Charlotte Elkington (various support, not only for technical support). Special thanks should also be given to Steve Hau for his generous help.

I must express my gratitude to the music practice rooms of University of York, which provided a much needed form of escape from my studies. I am also greatly indebted to the huge double room that Wentworth College provided me for three and half years and the porter from Wentworth College, David Dale.

Thank you to all my family. Without their unconditional love and support I could not have accomplished anything. My parents have always been beside me and made me the person I am today.

Life would not have been enjoyable and cheerful without my friend, Molan Liu. She made sure that I never felt alone. There are no words to convey how much I love her and I truly thank her for sticking by my side during this most fantastic moment.

Author's Declaration

I declare that the work in this thesis, submitted for the degree of Ph.D., is my own original work, except where due reference is made to other authors, and has not been previously submitted by me at this, or any other university.

CHAPTER 1

INTRODUCTION

1 Introduction

1.1 The structure of DNA and RNA

Since the 1940s it has been known that DNA (2'-deoxyribonucleic acid) was the carrier of genetic information.¹ A clear X-ray diffraction image of DNA (B-form), named Photograph 51, was taken by Rosalind Franklin in 1952, and provided key information that was essential for developing a model of DNA.² Watson and Crick used what they saw in Photograph 51 as the basis for their study, and in 1953 built the model of B-form duplex DNA, then the famous model of DNA began to be understood.^{3,4} This field has revealed the genetic information of every living organism. DNA is a biological informational macromolecule polymer composed of a linear backbone of 2-deoxyribose units interlinked via 3'-5' phosphodiester linkages (Figure 1.1).

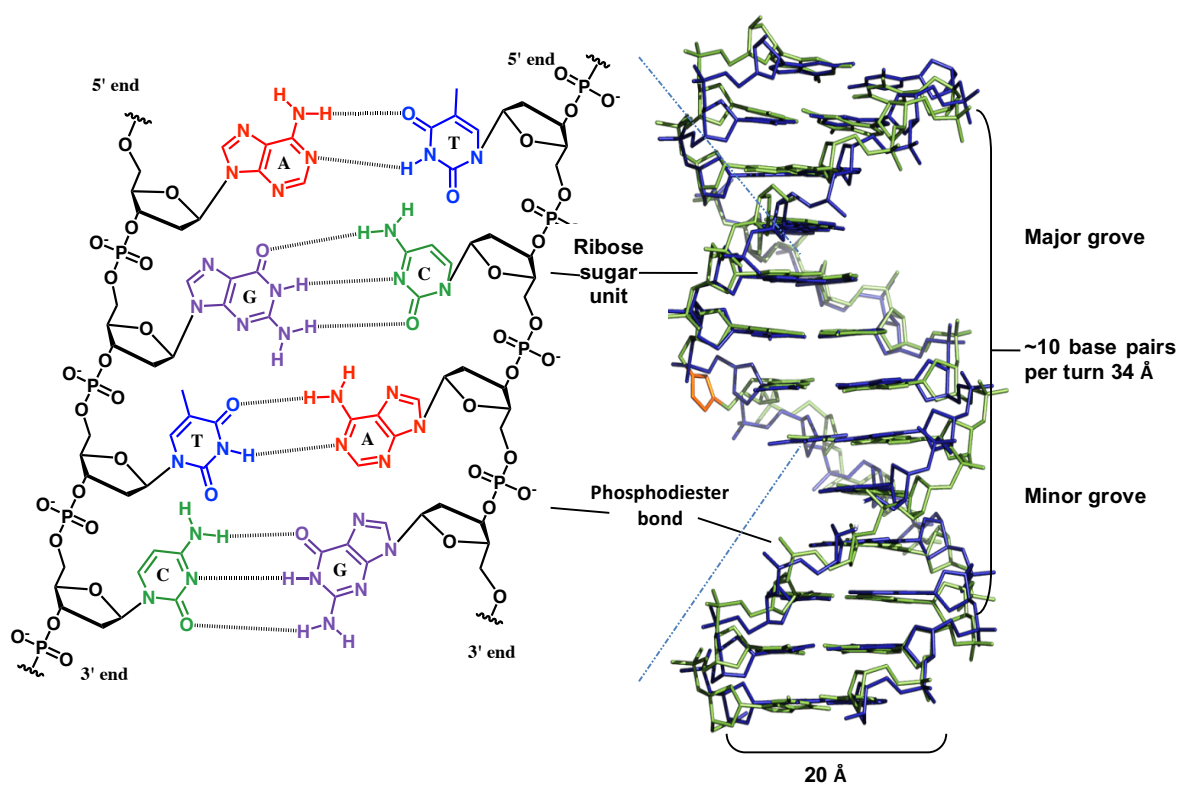


Figure 1.1 A schematic of the double helical structure of DNA and a detailed helical structure of DNA. Adapted image taken from website:

http://static.newworldencyclopedia.org/8/87/DNA_orbit_animated_small.gif, accessed 26/11/2015.

The deoxyribose bound to a nucleobase is known as a nucleoside, while the phosphate ester containing a nucleoside is known as a nucleotide. Nucleotides consist of a nitrogen heterocycle (the nucleobase), a pentose and a phosphate. The phosphate group plays a role as a “bridge” linking nucleotides in a phosphate-diester backbone. Each DNA macromolecule is paired by hydrogen bonding (through the nucleobases) with a complementary strand, holding this complex ‘super-molecule’ in its lowest energy conformation, and the two anti-parallel DNA strands twist about each other to form a right-handed double helix defined by minor and major grooves.

1.1.1 Nucleosides, nucleotides and nucleic acids

There are two nucleic acids that carry genetic information: 2'-deoxyribonucleic acid (DNA) and ribonucleic acid (RNA). They each consist of four nucleotides that differ in their nucleobases, three of which are found in both nucleic acids, and one which is different. DNA differs from RNA in that the ribose sugar contains one less hydroxyl substituent, that is, ribose and 2'-deoxyribose are present in RNA and DNA respectively. DNA is double-stranded, whereas RNA usually consists of a single strand. The nucleosides can be arranged into two categories according to the type of nucleobase, the purines (5,6-bicyclic heterocycle), and the pyrimidines (6-membered heterocycle). Also one of the bases differs with the exchange of the pyrimidine present in DNA, thymine, for uracil within RNA (a methyl group is placed at the C5 position in thymidine) (Figure 1.2).

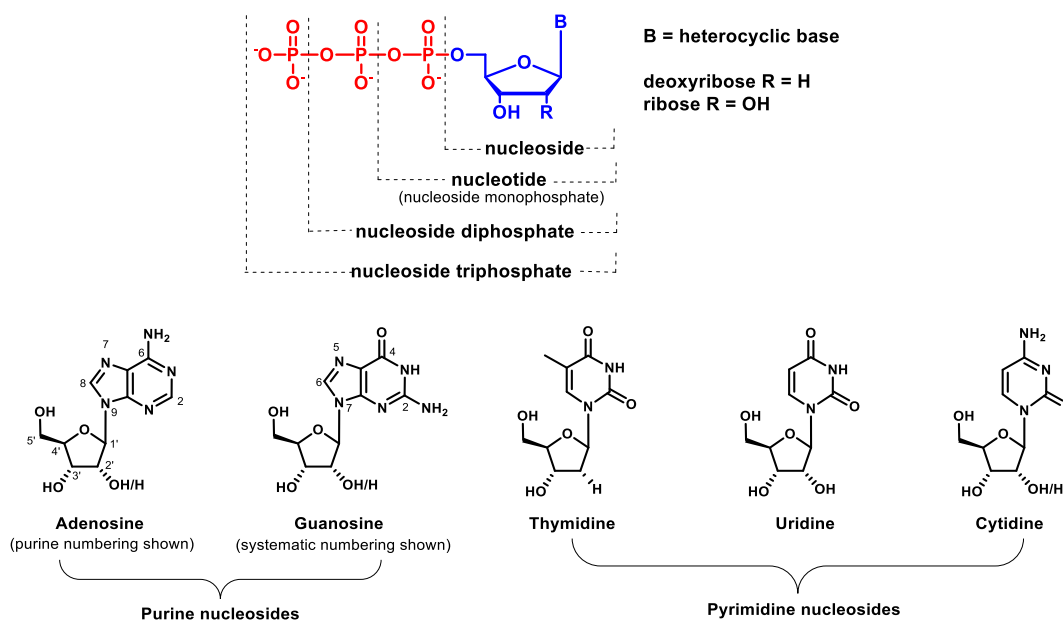


Figure 1.2 Structure of nucleosides and nucleotides.

The natural nucleosides contain 2'-deoxyribose and ribose ring systems. The sequence of bases carries genetic information, and this precise base pairing is crucial to DNA replication, DNA transcription and RNA translation into protein. In most organisms DNA is the storage form of the genetic code, while the transcription of RNA is required for genetic code translation into proteins.^{5,6}

1.1.2 Conformations of double stranded DNA

In the most common double-stranded DNA structure, B-form double helix, the antiparallel strands form a right-handed helix where the stacked base pairs stick perpendicular to the axis of the helix. The backbone of DNA and RNA consists of the alternating phosphate-ribose (or 2'-deoxyribose) chain. Conformational variation occurs from restricted bond rotations within the ribose unit to give a different ribose ring pucker (five-membered rings can form a range of different conformations). This puckering of the ribose can be determined by spin coupling by ¹H NMR spectroscopic analysis, as it is caused by the torsional relationship of adjacent C-H bonds within the sugar ring. DNA and RNA undertake two different stereoelectronic conformations due to this puckering of the sugar (Figure 1.3).

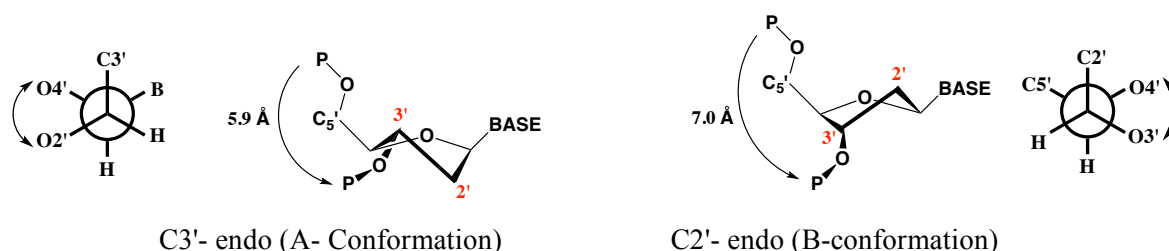


Figure 1.3 The two most common conformations adopted by the ribose unit.

In fact, there are twenty distinct sugar ring puckered conformers that could be summarised by the pseudorotational cycle.⁷ The two conformations shown in Figure 1.3 are almost exclusively found, as they have the lowest energy states and directly affect the forming structure of DNA and RNA. In the B form, the conformation is stabilised by a gauche effect between the 3'-OP group and the endocyclic O4'. The O4' and the O3' are in a gauche conformation. However, for the A-conformation, only to the 2'-OP group is in the gauche conformation between O4' and O2'. In the absence of a 2'-OP group, the C2'-endo conformation is favoured, as is the case of DNA. However, in the presence of a 2'-OP group, as is the case of RNA, the conformation is stabilized by a gauche effect between the 2'-OP group. Note that there is an exception for cytidine nucleosides, which favour the C3'-endo conformation due to an intermolecular H-bond, which is longer than expected. The hydrogen bond of cytidine of the C2'-endo conformation is exceptionally weak for a pyrimidic nucleoside.⁸ These two conformations, in solution, are in equilibrium with an energy separation of < 2–5 kJ mol⁻¹.⁹

There are various factors that affect the conformation of DNA; these are the local chemical environment, substituent electronegativity, nucleobase stereochemistry, temperature, pH, and solvent polarity. High salt environments stabilize B-conformation,¹⁰ however, the presence of less polar solvents such as ethanol or trifluoroethanol can promote a transition to A-conformation structures.^{11,12}

1.1.3 Higher ordered nucleic acid structures

Not long after the DNA double helix structure was determined, other structural variants of oligonucleotides were discovered. DNA can adopt an *anti*-parallel double helix with the complementary Watson-Crick base pairs stabilised through specific hydrogen bond interactions and non-canonical base interactions (Figure 1.4).

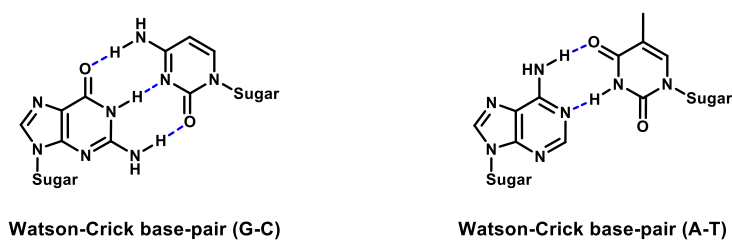


Figure 1.4 Watson-Crick base-pair.

Hoogsteen base pairs are formed alongside the major groove edge of nucleic acid duplexes, applying the N7 position of the purine base (as a hydrogen bond acceptor) and C6 amino group (as a donor), which keeps it away from the normal Watson-Crick (N3-N4) base pairs. Furthermore, non-Watson-Crick base pairs are generally observed in RNA structures. That is, a RNA triplex can exist when both Watson-Crick and Hoogsteen base pairs are present. In some cases, such as the example shown in the adenosine structure in Figure 1.5, Watson-Crick and Hoogsteen base pair can be transferred under different circumstances. Al-hashimi¹³ *et al.* surprisingly noted the transition pattern between Watson-Crick and Hoogsteen base pairing in a double helix, as shown in Figure 1.5. They found that adenine (A) pairs with thymine (T) using Watson-Crick hydrogen bonds 99% of the time. However, adenine can flip to form Hoogsteen hydrogen bonds, *ca.* 1% of the time. Guanine and cytosine base pairs undertake a similar transition in structure.

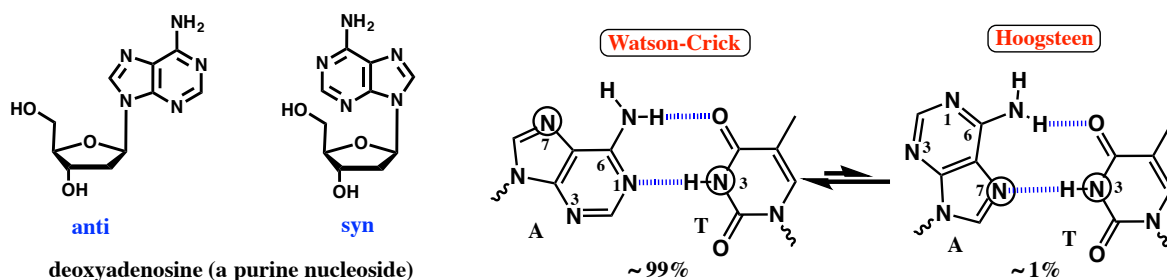


Figure 1.5 *Anti/syn* nucleoside equilibrium and base flip.

Molecular self-assembly is ubiquitous in nature and has now developed as a new approach in biology and supramolecular chemistry.¹⁴ Under certain circumstances, involving two rather special nucleic acids, G-quadruplexes can be formed. G-quadruplexes are four-stranded DNA structures that form when guanine residues participate in Hoogsteen hydrogen-bonding in a square-planar symmetrical array, which are commonly referred to as G-quartets (Figure 1.6).¹⁵

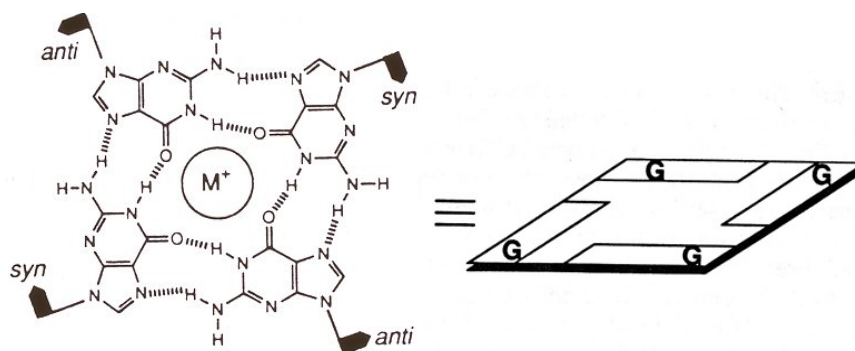


Figure 1.6 Structure of G-quartets (Figure taken from ref. **15** with permissions, G-quadruplexes in promoters throughout the human genome, Huppert, J.L.; Balasubramanian, S. *Nucleic Acids Res.* 2007, 35, 406-9, Permission rights obtained 26th November 2015. Copyright Nucleic Acids Research 2007).

Each base is both the donor and acceptor in a Hoogsteen base pair. The structure involves two different glycosidic conformations (*syn*-like and *anti*-like, Figure 1.5), which because of the rotation around the β -glycosyl bond alternates between the *syn*- and *anti*-conformations. Considering these stereochemical aspects, which are determined by C2'-*endo*/C3'-*endo* sugar pucker equilibrium, the *syn/anti* glycosidic conformation determines the orientation of the G-quartets. G-quartets stacking to form a quadruplex was first acknowledged as being the starting point for aggregation of 5'-guanosine monophosphate.¹⁵ The bases undertake self-recognition and self-assembly routes, resulting in a complex supramolecular structure built on the formation of cyclic tetrameric entities, stabilized by the presence of a metal-ion, *e.g.* typically by Na^+ or K^+ ions, which bind the best.^{15,16}

The G-quadruplex structure has been implicated in regulating gene transcription,¹⁷⁻¹⁹ recombination,²⁰ chromosome stability^{21,22} and programmed cell death.²³ Ligands that can stabilize G-quadruplexes form at the telomeric end of chromosomes, which are also the site of action of specific anti-cancer compounds.²⁴ The G-quadruplex can also be used as fluorescent base probes.²⁵ To confirm the presence of a G-quartet, spectroscopic and spectrometric methods can be used, *e.g.* NMR and MS.^{26,27} Wetmore and co-workers found that the 8-aryl-guanine moiety exhibits a *syn*-conformational preference, as determined by ¹H and ¹³C NMR spectroscopic analysis. A conformational shift from *anti* (natural conformation) to *syn* correlates with a downfield shift of H2', C1', C3' and C4' signals and an upfield shift of the C2' signal.^{28,29}

Lilley *et al.* identified that hexadeoxynucleotide d(TG₄T) exhibits two sets of 6 aromatic proton resonances in D₂O as the temperature is changed (Figure 1.7).³⁰ There was one resonance ($\delta = 7.42$), which formed at higher temperature, and another at lower temperature ($\delta = 8.11$). This revealed a slow exchange occurring between the two conformations on the NMR timescale.

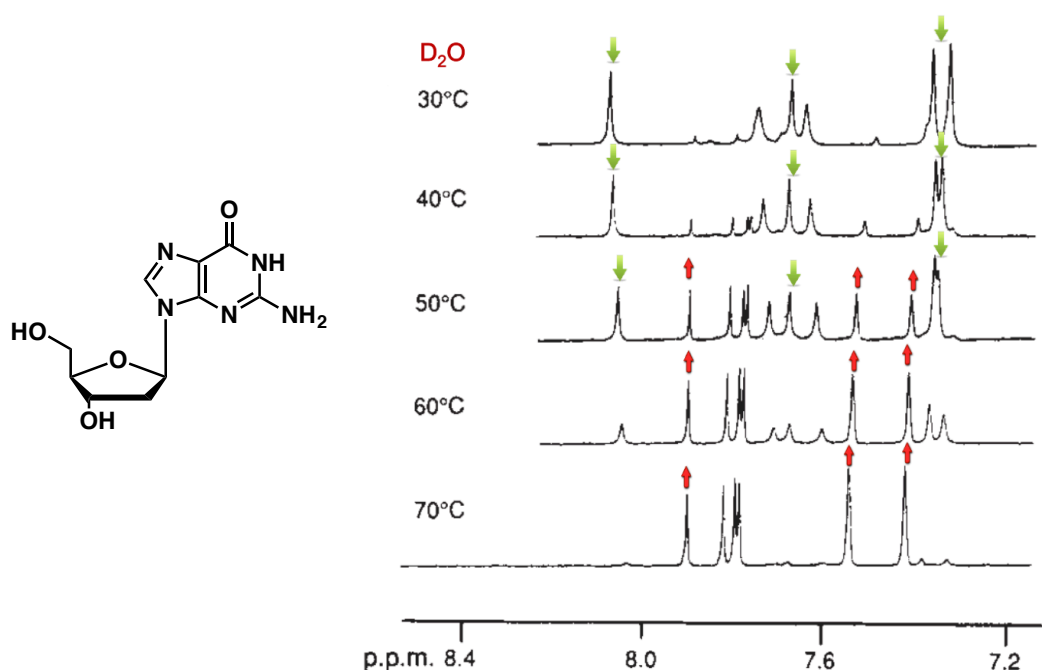


Figure 1.7 Two sets of 6 aromatic proton resonances in D₂O (Figure taken from ref. **30**: NMR study of parallel-stranded tetraplex formation by the hexadeoxynucleotide d(TG₄T), Aboul-ela, F.; Murchie, A. I. H.; Lilley, D. M. *J. Nature* 1992, 360, 280-282, Permission rights obtained 25th November 2015. Copyright Nature 1992).

Abboud *et al.* studied a (*N,N*-dimethylaniline)guanosine derivative that showed evidence for self-assembly (Figure 1.8).³¹ They employed *d*₆-DMSO because the intermolecular H-bonding interactions were suggested to be minimized. There was no evidence for self-assembly at room temperature (a). However, in CD₂Cl₂ at room temperature self-assembly occurred. As shown in Figure 1.8, between $\delta = 7.0$ and 7.8 (spectrum b), there is the appearance of a broad proton signal, which suggests formation of the proposed G-quartet was incomplete. When the temperature was lowered to -30 °C, a well-defined spectral pattern has been shown and it was considered to be the formation of a G-quartet (c).

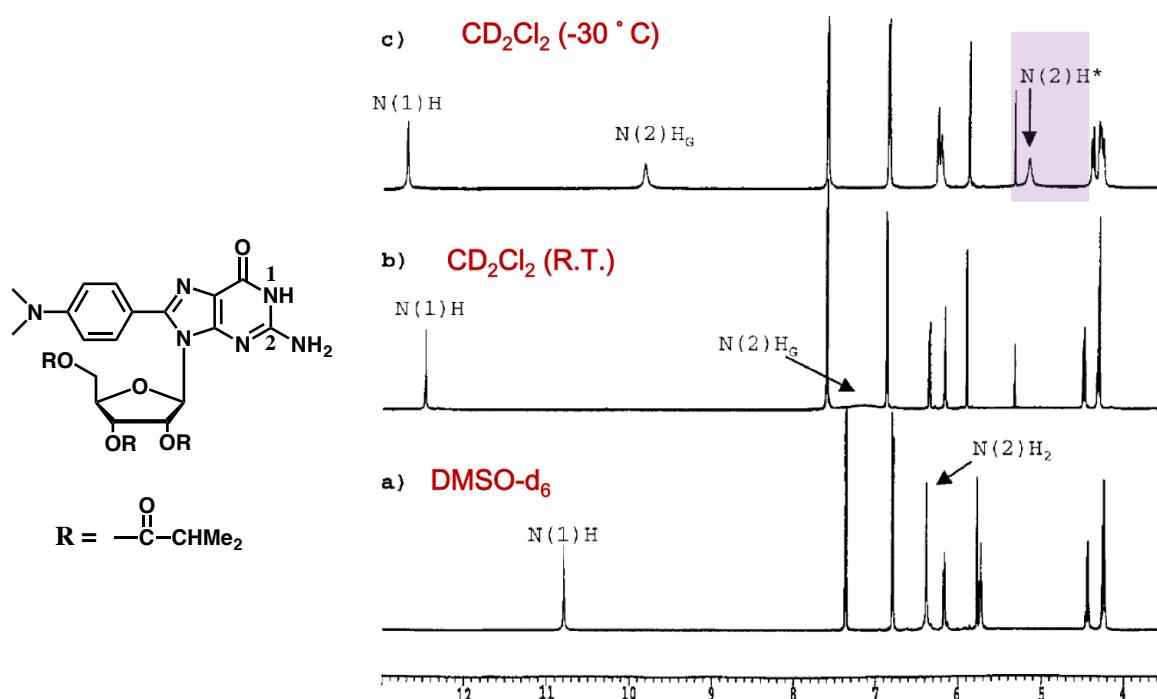


Figure 1.8 NMR spectrum showing changes consistent with formation of a G-quartet (Figure taken from ref. 31: A G-Quartet Formed in the Absence of a Templating Metal Cation: A New 8-(*N,N*-dimethylaniline)guanosine Derivative, Sessler, J. L.; Sathiosatham, M.; Doerr, K.; Lynch, V.; Abboud, K. A. *Angew. Chemie Int. Ed.* 2000, 39, 1300-3, Permission rights obtained 26th November 2015. Copyright Angewandte Chemie 2000).

To characterise the structural information on G-quartets, the following methodology can be used: (1) differential pulse voltammetry; (2) atomic force microscopy; (3) dynamic light scattering; (4) solution X-ray scattering; (5) temperature gradient gel-electrophoresis; (6) NMR G4 characterization; (7) Scanning Tunnel Microscopy, *etc.*³²⁻³⁵ The G-quartet surfaces in areas ranging from structural biology and medicinal chemistry to supramolecular chemistry and nanotechnology. It has been

studied *in vitro* and *in vivo*, and they have been found in the transcripts of diverse organisms, ranging from viruses to humans.^{36,37}

1.2 Chemical synthesis of DNA – solid phase oligonucleotide synthesis

The chemical synthesis of a small fragment of DNA (referred to as oligonucleotides) is important for the research of nucleic acids and their function in biological systems. Nucleic acids are synthesised from the 3'-end to the 5'-end. Therefore, the solid-phase oligonucleotide synthesis proceeds from the protection of the 3'-hydroxyl of the nucleoside bound to the support-bound, which has a 5'-DMT protecting group (Figure 1.9).^{38,39} The DMT protecting group at the 5'-position is then removed under acidic conditions. The free hydroxyl can then couple to another nucleoside phosphoramidite. Unreacted 5'-hydroxyl groups can be capped using acetic acid and 1-methylimidazole, to prevent further reaction in the next cycle of the synthesis, while also allowing the removal of shorter oligonucleotides at the end of the synthetic route. The successive addition of nucleotide phosphoramidites is used for the next cycle of the synthesis.

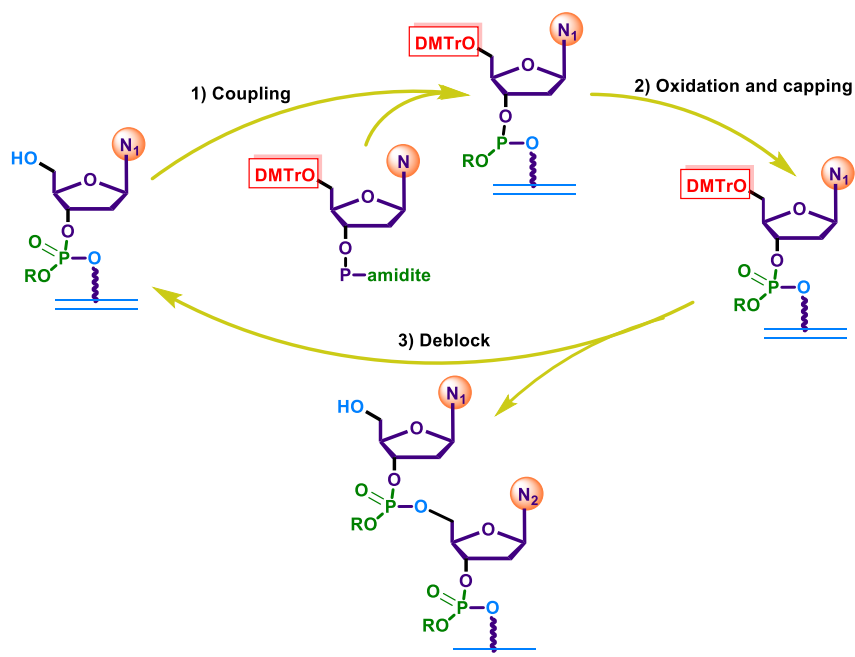


Figure 1.9 Solid-phase synthesis cycle.

1.3 Modification to the structure of oligonucleotides

Modification strategies for fluorescent-labelling of DNA and RNA are the most common detection approaches used in DNA and RNA diagnostics, sequencing and genomic analysis.⁴⁰ The methods for fluorescent modification strategies have been investigated for biomolecular analysis and can be summarised into two main methodologies: a) modification of the fluorophore *via* solid-phase oligonucleotide synthesis; b) post-synthetic labelling. The first methodology requires certain phosphoramidite monomers, which are attached to typical modifications sites (Figure 1.11). This method is usually required for more complicated monomers, which are not commercially available and is not desirable if the monomers are unstable during the biological process being studied. The second methodology is achieved from the reaction of an amino-modified monomer in the oligonucleotide and active phosphonate ester of the fluorophore.⁴¹

1.3.1 Fluorescent nucleotide analogues

Modified fluorescent oligonucleotides can be used as probes of DNA and RNA helix-to-coil transitions, DNA or RNA chain elongation, mechano-chemical coupling in motor proteins and cellular-signal transduction progresses. Fluorescent oligonucleotides that emit fluorescence only in the presence of targets have been used as fluorescent probes. Fluorescent nucleoside analogue probes incorporated into nucleic acids offer valuable options for the research on the dynamics, structure, and recognition properties of biomolecules.⁴² Fluorescence is particularly useful where a strong signal away from any background signals of the chemical structure can be detected.

Nucleosides and nucleotides can be chemically-modified so that they can be used as probes in biological systems.⁴³ A variety of spectroscopic labels are commonly used to study biological systems, depending on the specific requirements of the system being investigated and the information required. The synthesis of fluorescent nucleosides analogues, which are sterically less bulky, but retain the desired fluorescent properties, is important, as these are valuable as fluorescent probes. Modifications can be made at almost every position, but can be divided into three possible approaches to nucleotide modification (Figure 1.10).⁴⁴⁻⁴⁶ The expanded nucleotides can be characterised by their extended conjugation of natural nucleotides through the fusing of additional aromatic rings system. It results in enhanced photophysical properties.

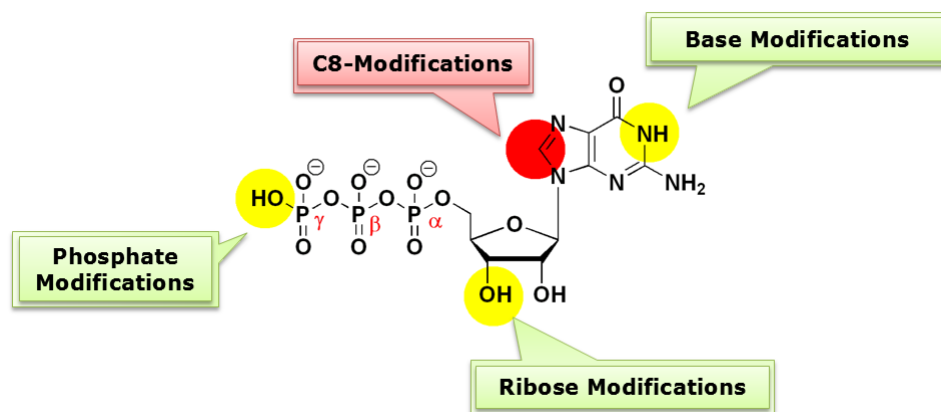


Figure 1.10 Possible nucleoside/nucleotide modifications on guanosine (as an example).

The modified fluorescent groups can be adjacent to the triphosphate by substitution of the terminal phosphate, ribose moiety, or coupling to the nucleobase. For the base modifications, it also has typical modification sites in naturally-occurring nucleosides, which generally requiring unnatural analogues (Figure 1.11).⁴⁴⁻⁴⁶ The chemical tag should extend the fluorescence, while exhibiting similar biochemical physical properties to the non-modified molecule.⁴⁷

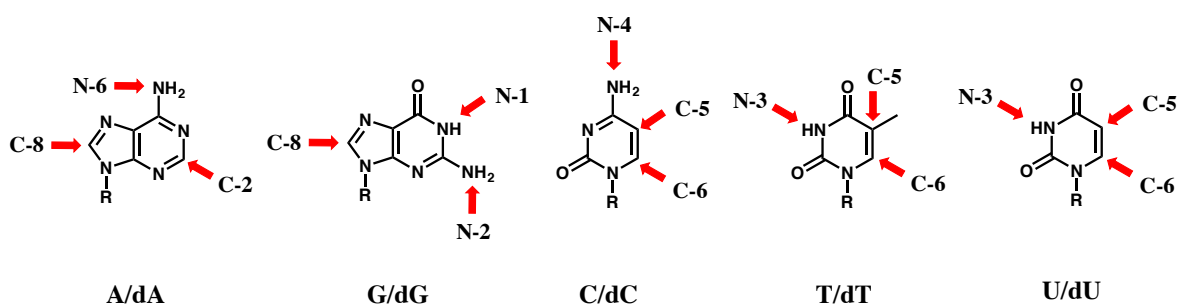


Figure 1.11 Typical modifications sites in natural and unnatural analogues, R = ribose/deoxyribose.

Currently there is a demand for the modified fluorescent oligonucleotides,⁴⁸ and several precursors are commercially-available, but expensive (Figure 1.12). However, molecules like λ -thio-bodipy-ATP,⁴⁹ containing γ -phosphate labels, which are cleaved upon nucleotide incorporation into oligonucleotides, lose their fluorescent character. The alexa532-EDA-ATP,⁴⁹ a modified ribose label, also has been found out a limited application as λ -thio-bodipy-ATP so far. Therefore, although they are commercially-available, they are not entirely suitable for fluorescent studies with nucleic acids. With these many options available, it is important that the fluorophore is cautiously selected to achieve optimal experimental results.

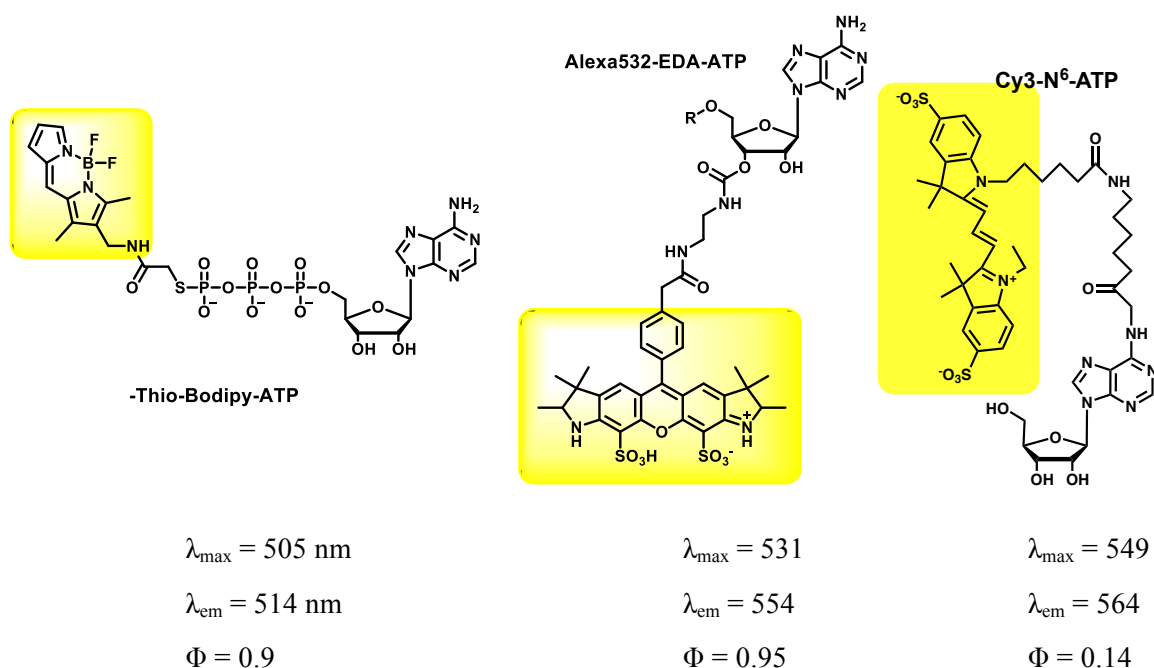
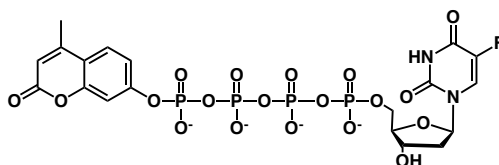


Figure 1.12 Examples of commercially-available modified fluorescent adenosine analogues.⁴⁹

1.3.2 Synthetic modifications to the phosphate

Modified nucleotides containing a terminal phosphate might be advantageous in the design of antiviral therapeutics, or act as a tool for defining the structural role of the active site of proteins.⁵⁰ Srinivasan and co-workers⁵¹ designed and synthesised a potential probe 5-fluoro-2'-deoxyuridine-5'-*O*-tetraphosphate (Figure 1.13), modifying the terminal phosphate group (Um-PPPP-FdU). This probe allows quantification of cellular internalization; DNA incorporation of nucleotide-based chemotherapeutic agents may offer useful mechanistic insights. Um-PPPP-FdU employed a 4-methylumbelliferyl fluorophore, which involved a ZnCl_2 -mediated coupling of imidazolide of 4-methylumbelliferone phosphate with 5-fluoro-2'-deoxyuridine-5'-*O*-triphosphate (FdUTP).



$$\lambda_{\max} = 355 \text{ nm}$$

$$\lambda_{\text{em}} = 460 \text{ nm}$$

Figure 1.13 5-fluoro-2'-deoxyuridine-5'-*O*-tetraphosphate (Um-PPPP-FdU).

Brenner and co-workers⁵² modified diadenosine polyphosphate analogues, containing fluorophores, by replacement of one of the nucleosides. Examples include Appp-S-(7-diethylamino-4-methyl-3-(4-succinimidylphenyl)) coumarin (ApppAMC) and Appp-S-(4-(4-difluoro-5,7-dimethyl-4-bora-3a,4a-diaza-sindacine-3-yl) methylaminoacetyl) (ApppBODIPY) (Figure 1.14), which form a class of AMP fluorophore diphosphate compounds. These compounds showed better biological characteristics than purine mononucleotides (lifetime *in vivo* and stabilization for long-lived enzyme).

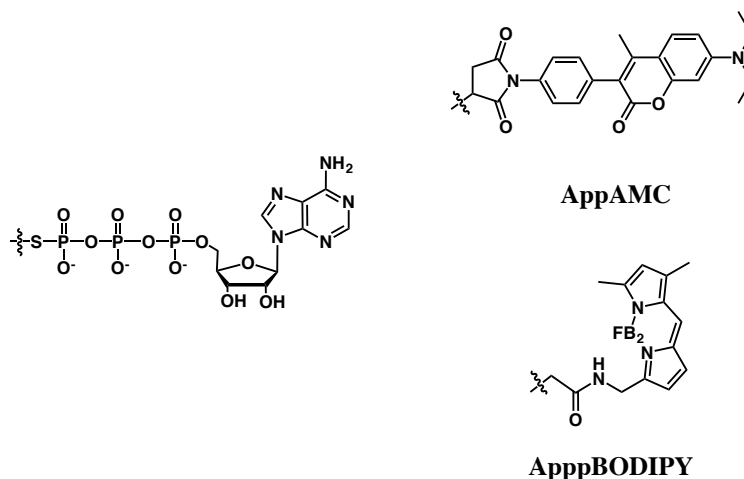


Figure 1.14 Fluorescent ApppAMC and ApppBODIPY analogues.

Synthetically-modified nucleotides ANS-dATP (Figure 1.15), containing 1-aminonaphthalene-5-sulfonate (ANS) attached to the terminate phosphate, were synthesized and used as a fluorescent probe by Hardin and co-workers.⁵⁰ Multiple studies demonstrated that the polymerase was able to use the gamma-modified nucleotides. Molecular modelling studies showed that an ANS attachment to the terminate phosphate may sterically hinder the γ -phosphate which can lead to base-mispairing; therefore, a mismatching base pair will not adopt an appropriate orientation for incorporation of the nucleotide.

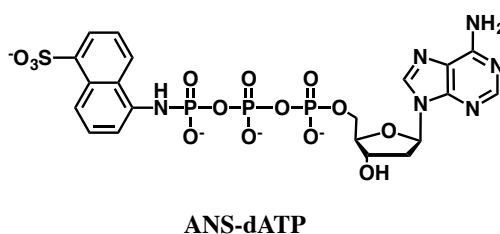


Figure 1.15 Fluorescent polymerase compound, ANS-dATP.

Similar modified adenosines exhibit absorbance at 315 nm and emission at 460 nm ($\Phi = 0.8$).⁵³ The uracil triphosphate analogues were synthesized by the same method, exhibiting similar fluorescence properties – absorbing at 360 nm, and emitting at 464 nm.⁵⁴

Generally, the modification of the terminal phosphate group as a fluorescent motif can be used, although during the process of the incorporation of the nucleotide the γ -phosphate label is cleaved. This is a limitation as the fluorophore is no longer linked to the nucleotide, resulting in a modified-RNA with no-fluorescent properties. As a result, phosphate-modified nucleotides are less suitable for use as fluorescent probes.

1.3.3 Synthetic modifications to the ribose

Over the past decades, synthetically modified oligonucleotides have improved their utility as fluorescent probes. For the purpose of using 5'-triphosphatases, modifying the ribose moiety at the 2'- or 3'- hydroxyl is a practical approach which avoids the use of bulky modifying chemical groups. One of the first reported ribose-modified derivatives was by Hiratsuka and co-workers.^{55,56} They reported 2',3'-*O*-(2,4,6-trinitrocyclohexadienylidene)adenosine triphosphate (TNP-ATP) (Figure 1.16), which could exchange within an equilibrium with altering pH.

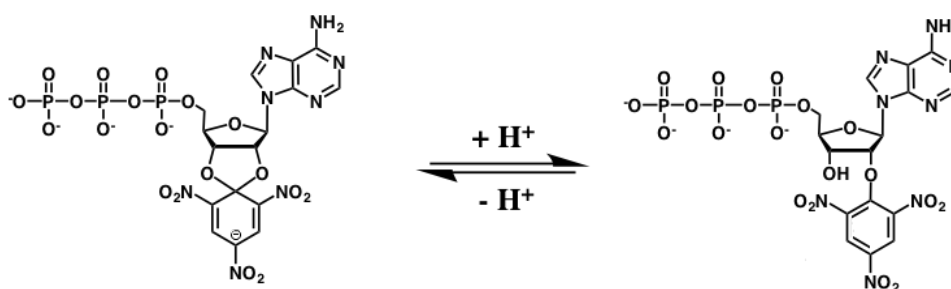


Figure 1.16 TNP-ATP happens as an equilibrium fusion depending on the pH environment.

Various fluorescent analogues with ribose modification have been synthesised. Among these, the chemical modification was made to 2'-*O*-(2-aminoethylcarbamoyl) or 3'-*O*-(2-aminoethylcarbamoyl) of the ribose (Figure 1.17).⁴⁷

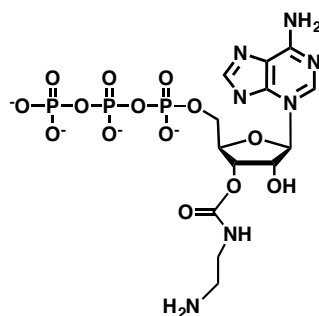


Figure 1.17 3'-O-(2-aminoethylcarbamoyl) modification of ribose.

A free amino functional group attached to the ribose-ring allows a variety of different groups to be attached to the nucleotide to give fluorescent ribosemodified analogues. A leading example is 3'-O-(2-aminoethylcarbamoyl)ATP (edaATP) (Figure 1.18).⁵⁷ The synthetic method used was based on that reported by Cremona *et al.*⁵⁸ The three fluorescent molecules, shown in Figure 1.18, have been synthesised using a similar methodology. The ribose-modified nucleotides, such as edaATP and mantATP, undergo base-catalysed exchange between 2'- and 3'-hydroxyl positions on the ribose ring. The two isomers are chemically distinct and may be incorporated differently by proteins, which can influence the fluorescence properties. This type of modified derivatives can be compared to historical modifications on the ribose ring including 3'-deac-edaADP, while the novel synthesized 3'-but-edaADP and 3'-mbcADP analogues exhibited higher quantum yields.

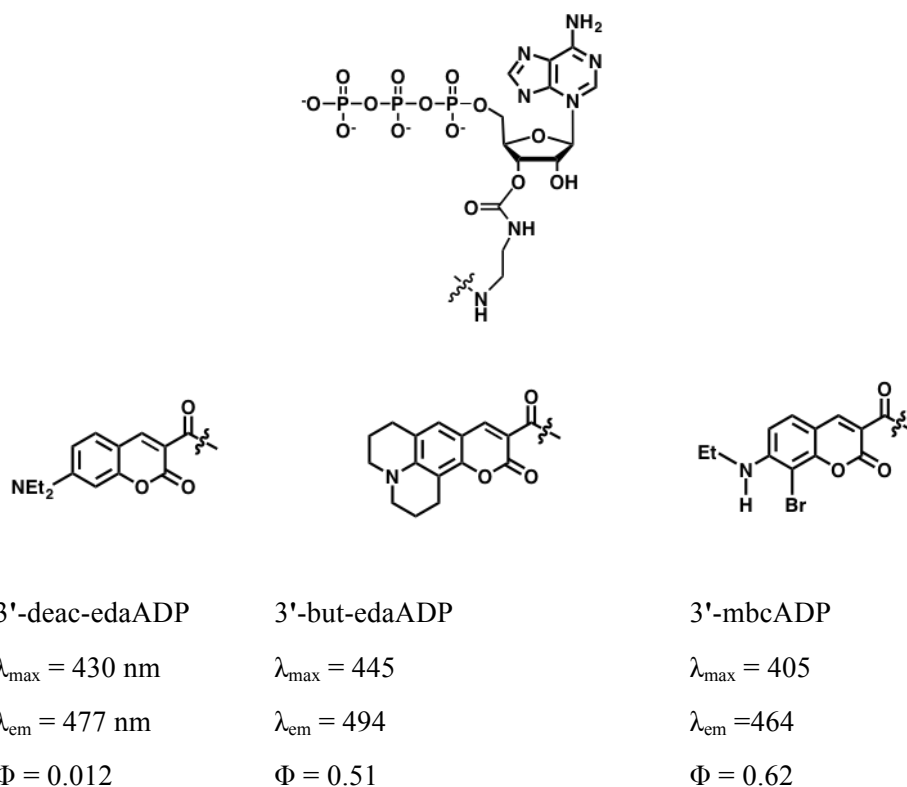


Figure 1.18 Structures of coumarin-labeled ATP analogues.

In general, short DNA or RNA molecules are vulnerable to nuclease digestion and inactivation. Therefore, to stabilize such oligonucleotides, ribose modifications are usually required.⁵⁹ Nevertheless, modification of the ribose, linking with a fluorescent group via the 2'-OH or 3'-OH groups can cause inhibition of the elongation of DNA (in replication) and RNA (in transcription). These modifications can exhibit variable effects on transcription elongation, especially at the 2'-position, where the effect of inhibited transcription elongation is most dramatic.⁶⁰

1.3.4 Synthetic modifications to the nucleobase

Naturally-occurring nucleosides found in DNA and messenger RNA are normally non-fluorescent. Some naturally-occurring modifications on nucleobases, *e.g.* *N*⁷-methylguanosine,⁶¹ 4-thiouridine,⁶² wyosine derivatives,^{63,64} or *N*⁶-acetylcytidine⁶⁵ are useful fluorescent probes for tRNA (Figure 1.19).

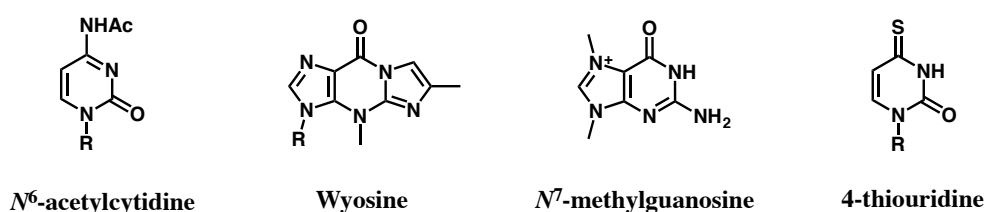


Figure 1.19 Naturally-occurring fluorescent nucleosides. R = ribonucleosides.

However, due to they have inherent low quantum yields and weak emission, when incorporated into oligonucleotides, they cannot be used for studying the structure and dynamics of tRNA.^{66, 67} The naturally-occurring fluorescent base analogues are relatively limited for further study, therefore, the design and synthesis of novel modified nucleosides that can act as probes in the oligonucleotides are needed.

Nucleobase modifications have been widely evaluated, including: a) ring substitution analogues in which a fluorophore substitution group links to the ring system of the nucleobase; b) extended ring analogues with conjugates which extend the conjugation of the π system through bonded aromatic rings; c) amino extensions in which a substituent directly attaches to the amino group of the nucleobase, *i.e.* adenosine derivatives. As the utility of these derivatives is limited, no further comment is made here.

1.3.4.1 Ring substitution analogues

Guo and co-workers⁶⁸ presented a method to improve the fluorescent properties by a push-pull system (Figure 1.20). In this fluorophore, the purine part performed as the chromophore; an electron-donating amino group functioned as a push effect incorporate into the C6 position of purine. Meanwhile, an electron-withdrawing aryl group was linked to the C8 position of the purine to increase the conjugated system and employ a pull effect.

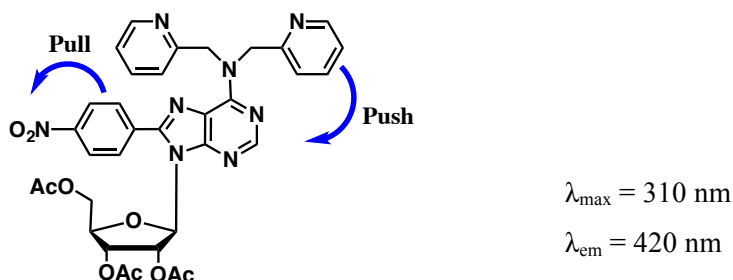


Figure 1.20 Push-pull-type purine nucleoside-based fluorescent sensor.

Interestingly, Tor and co-workers have reported the synthesis of Ru^{II}- and Os^{II}-containing nucleosides (Figure 1.21),⁶⁹ where the complexes are covalently attached to the 5-position in 2'-deoxyuridine. These Ru^{II} and Os^{II} derivatives transformed into their phosphoramidites and then into modified oligonucleotides. The Ru^{II} moiety exhibits a long lived excited state, $\tau = 2.78 \mu\text{s}$, correlated with a relatively high emission quantum efficiency, $\Phi = 0.137$. In contrast, the Os^{II} moiety is non-emissive, $\tau = 0.078 \mu\text{s}$ $\Phi = 0.0003$, which serves as a quencher of the Ru^{II} excited state.

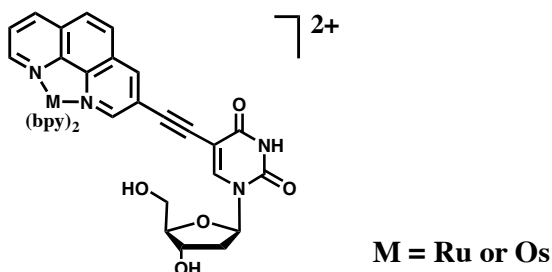


Figure 1.21 Tor's redox active metal-containing luminescent linkers.

Saito and co-workers have synthesised uridine and cytidine base-discriminating fluorescent nucleosides probes (Figure 1.22).⁷⁰ The fluorescence of the PyU/A base pair duplex was not quenched due to the stabilisation.



Figure 1.22 Pyrene-labelled uridine and cytidine nucleosides (R = uridine).

Interestingly, Saito and co-workers later synthesised novel push-pull-type fluorescent guanosine derivatives with conjugation of a pyrene, substituted with electron-withdrawing groups, to C8 position (Figure 1.23).⁷¹

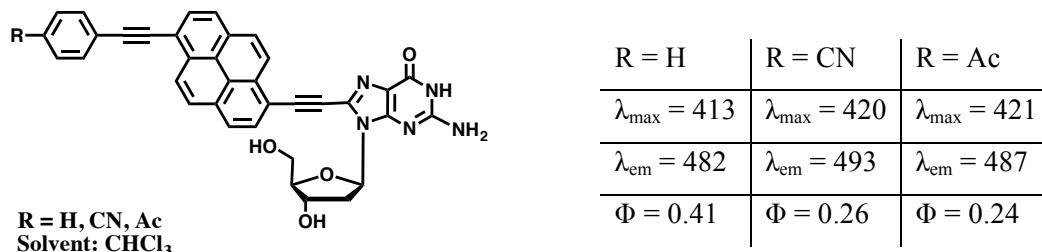


Figure 1.23 Pyrene-labelled fluorescent guanosine derivatives (λ_{max} and λ_{em} values given in nm).

The other modified bases shown in Figure 1.24 are fluorophore-linked nucleotides, in which aromatic moieties are attached.^{72–75}

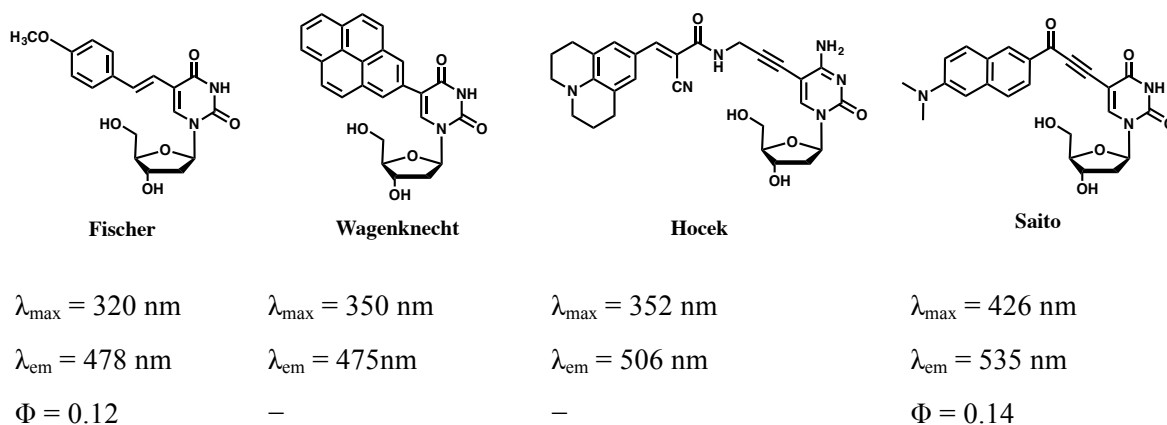


Figure 1.24 Examples of nucleobase ring-modified systems.

1.3.4.2. Extended ring analogues

A large class of fluorescent properties have been introduced by extending the π -conjugation through appending heterocycles and fluorophores to the natural base.⁴² These properties have been developed from the following categories: size-expanded,⁷⁶ pteridine,⁷⁷ polycyclic aromatic hydrocarbon⁷⁸ and isomorphous base analogues.⁷⁹ Many of these analogues maintain the Watson-Crick base-pair hydrogen bonding face; so that they can still form stable duplexes during incorporation into DNA, as they can maintain the ability to hybridize. However, the major disadvantage of these fluorescent

oligonucleoside analogues is that they exhibit significantly lower quantum yields, which limit their use in some specific fluorescence applications.⁸⁰

Various modified extended ring analogues are shown in Figure 1.25.⁸¹⁻⁸⁵ While the addition of rather bulky aromatic rings to the natural nucleobases also displays an enhanced photophysical properties. Some of them display relatively high quantum yields, although their fluorescence lifetimes have not been determined. These extended ring modified nucleobases retain their W-C hydrogen bonding face, with rather large aromatic rings, to interact in normal W-C base pairing. They are all red shifted absorption bands compared to their natural nucleobase derivatives, which results in an emission band near the visible range and rather high quantum yields.

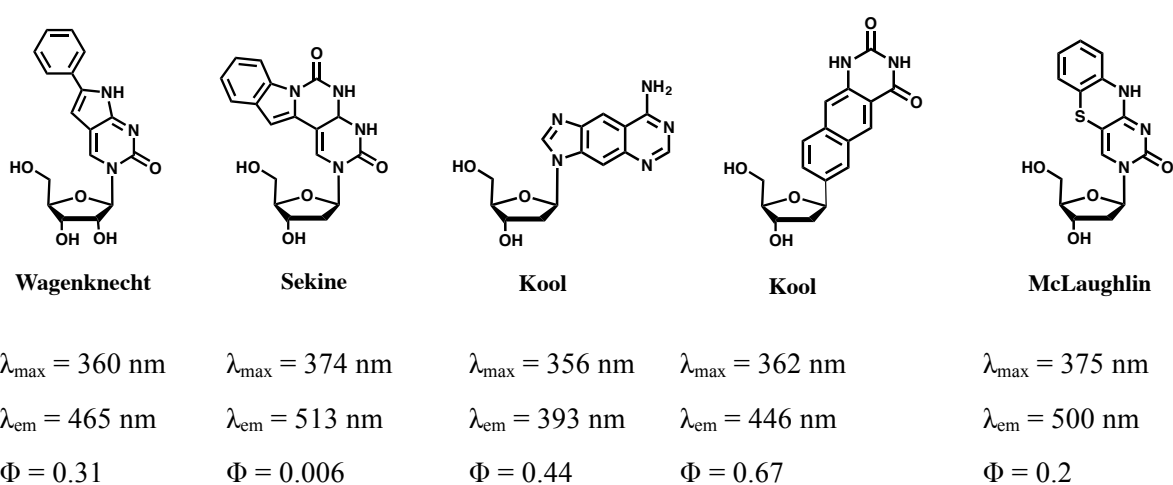


Figure 1.25 Examples of extended-ring nucleobase systems.

1.3.5 C8-modified nucleosides

C8-modified purines, their nucleosides, and phosphoramidites have been synthetic aims for more than 60 years. Their value as fluorescent probes has attracted researchers to study and they also have therapeutic uses.⁸⁶⁻⁸⁸ There are many synthetic methods for derivatisation of the C8-modified purines, mainly utilising the 8-bromo substituted purine nucleoside, as a selective bromination of the purine can readily make available many C8-functionalised materials.⁸⁹ Several strategies have been studied including a pyrimidine or selective C8-modification of an unsubstituted purine. These strategies have been shown less expansive in terms of scope and use.⁹⁰ C8-aryl purine nucleosides can be synthesised *via* the Suzuki cross-coupling reaction have given access to a diverse range of analogues and, in turn, the phosphoramidite derivatives, which have been used to afford modified oligonucleotides.⁹¹

Normally, the drawback of base-modification strategies is the potential inhibition of the Watson-Crick base-pairing. If one were to take adenine nucleotide modifications as an example, there are

three main modification positions for the linkage with a fluorophore (see back Figure 1.11). Labels can be added on the C2 position of the nucleobase. Unfortunately, this will inhibit the Watson-Crick edge (Figure 1.26).⁹² Although there are many probes which exhibit little interference they cannot be used for studying DNA duplexes or RNA with secondary structures based on Watson-Crick base-pairing. Therefore, a better position for labelling nucleotides is at the C8 position, which is removed from the Watson-Crick base-pairing edge.

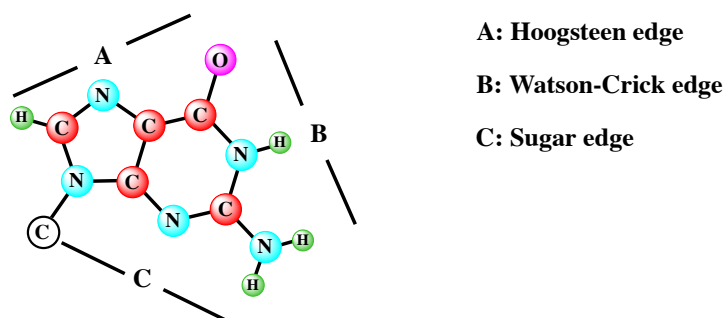


Figure 1.26 The interaction edges in Guanine.⁹²

Saito and co-workers also studied the C8 fluorescence-labelled adenosine derivative (Figure 1.27),⁹³ which was introduced for the detection of thymine bases on a target DNA. The molecule has the advantage of utilising known chromophores, whose photophysical properties are well studied, and connecting them to the native nucleobases whose hydrogen bonding ability is also known.

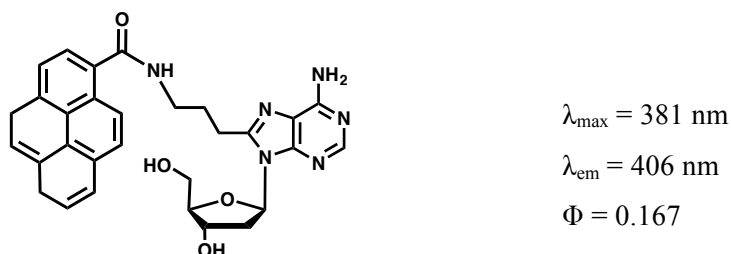


Figure 1.27 A C8 fluorescent-labelled adenosine derivative.

Fisher and co-workers have developed and synthesised a series of C8 substituted cinnamyl adenosine analogues (Figure 1.28).⁹⁴ They also computed their HOMO and LUMO energy levels, which could explain the correlation between emission wavelength and quantum yields of these compounds. Using the calculation of the HOMO-LUMO gap of these analogues enables prediction of the absorption wavelength for a specific analogue. Their research allowed confirmation of the chemical structure and fluorescence characteristics of these molecules, allowing researchers to design practical fluorescent nucleoside probes.

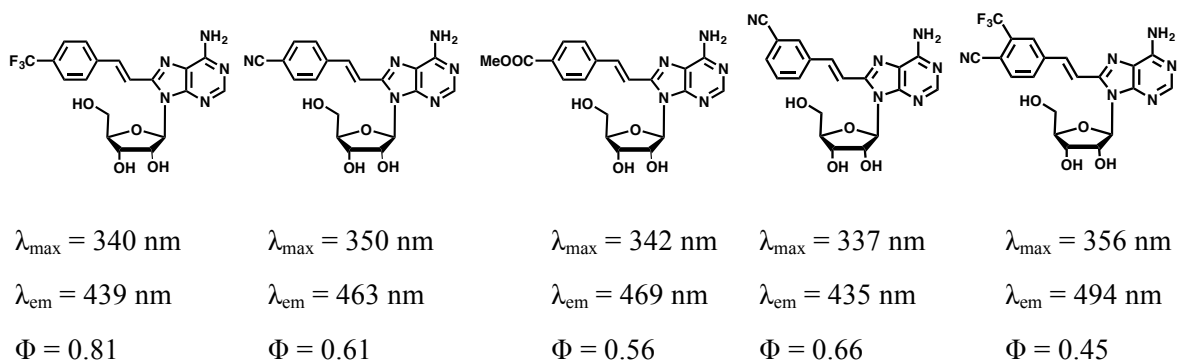


Figure 1.28 C8-substituted cinnamyl adenosine analogues.

Various C8 modification examples are given in Figure 1.29,^{95–98} including an example of an 8-alkynylated purine nucleoside previously synthesised and photophysically-assessed within our research group in York.

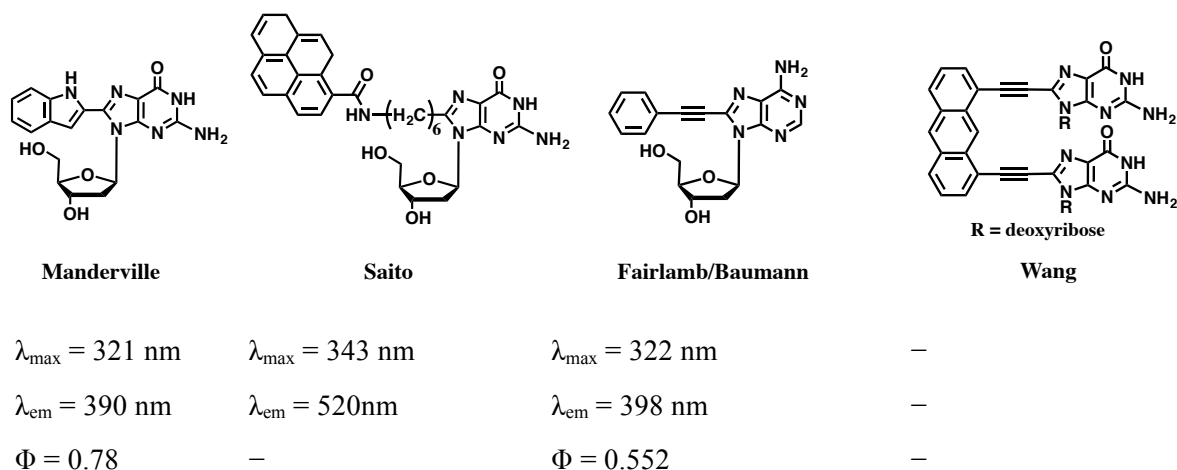


Figure 1.29 Examples of C8 modified purine analogues.

1.4 Pd-catalysed functionalization of unprotected oligonucleotides

1.4.1 Ligand synthesis for cross-coupling reactions with Pd catalysis

The use of carbon-carbon bond forming reactions, cross-coupling of organohalides with nucleophilic olefins or alkynes catalysed by Pd, with the absence or presence of an activated ligand, co-catalyst or base has become more and more important for synthetic chemistry. The synthetic progress of new forms of catalyst for organic reactions is a significant field of chemical synthesis, as the demand grows for rational organic synthesis under mild conditions, in high yields, and high selectivity.⁹⁹ A common strategy in homogeneous catalysis is the formation of novel ligand structures in combination

with a transition metal centre.¹⁰⁰ Furthermore, the appropriate activators, additives, and reaction media are also vital factors and variables affecting catalytic activity.

Many Pd catalysts are used for various types of C-C bond-forming reactions. Their reactivity, stability and selectivity can be tuned by ligands, such as phosphines, carbenes and amines.¹⁰¹ These ligands can be divided into the following types: a) monodentate ligands, which means the ligands have only one donor atom giving two electrons to a metal centre; b) bidentate ligands, which have two donor atoms; c) polydentate ligands, which have more than two donor atoms, often three or four.

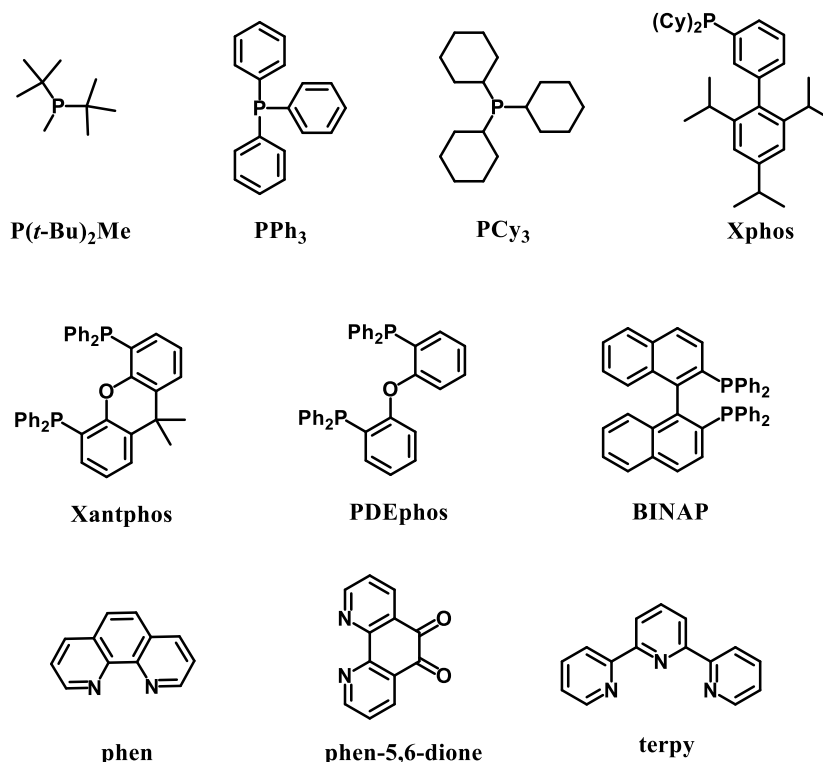
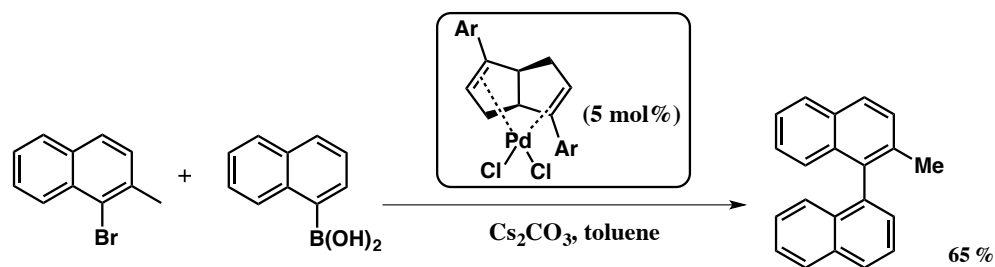


Figure 1.30 Common ligands used in cross-coupling chemistry.

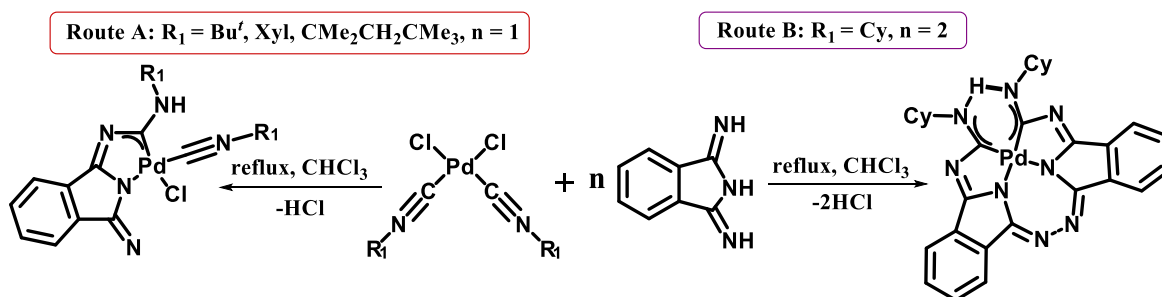
Furthermore, if a bidentate or a polydentate ligand is bonded with the same central metal ion or atom forming a ring system, that is called a chelating ligand. When a monodentate ligand binds with a metal ion through more than one site, it is called ambidentate ligand. For the past several decades, many researchers have developed and modified ligands for cross-coupling reactions (Figure 1.30).

Lin and co-workers introduced the first asymmetric Suzuki-Miyaura cross-coupling using Pd-diene complexes with an *ortho*-formyl group, to give axially chiral biaryls (Scheme 1.1).¹⁰² One chiral non-racemic Pd complex promoted the first atroposelective Suzuki-Miyaura cross-coupling reaction that delivered the coupling product in 65% yield and 60% ee. The additional free ligand promotes the asymmetric induction.



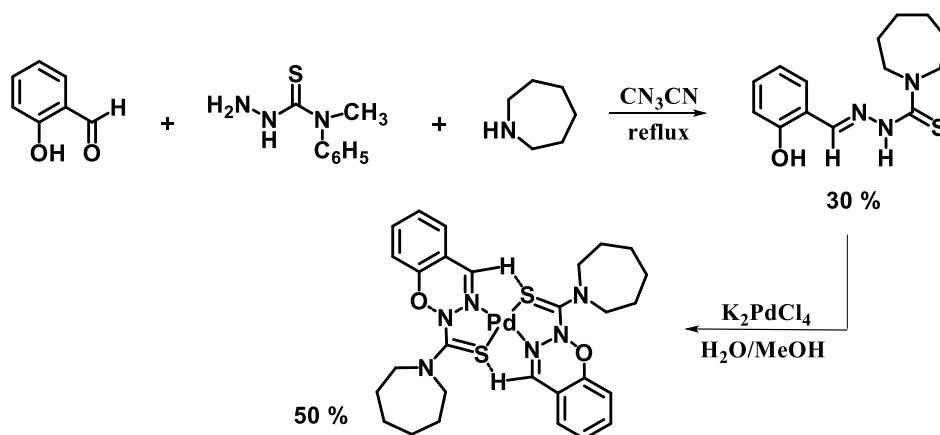
Scheme 1.1 Chiral diene catalysed Suzuki cross-coupling.

Chay and co-workers explored a novel type of aminocarbene ligands with palladium-mediated coupling between 1,3-diiminoisoindoline and isonitriles in combination with *cis*-[PdCl₂(CNR₁)₂] (Scheme 1.2).¹⁰³ In the reaction, 1,3-diiminoisoindoline behaves as both nucleophile (via the imine NH) and chelator (via the amide HN moiety), affording a bidentate carbene species. They also tested these complexes in Suzuki-Miyaura cross-coupling of aryl bromides and iodides with phenylboronic acids, exhibiting good catalytic activity.



Scheme 1.2 Reaction of 1,3-diiminoisoindoline with *cis*-[PdCl₂(CNR₁)₂].

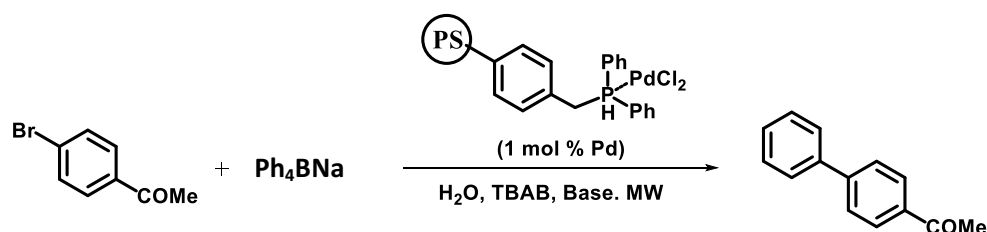
Kostas *et al.* developed the synthesis of a novel palladium complex derived from salicylaldehyde N(4)-hexamethyleneiminylthiosemicarbazone in two steps (Scheme 1.3).¹⁰⁴



Scheme 1.3 Synthesis route of the Pd complex.

Their preliminary catalytic studies were conducted using conventional heating at 100 °C for 24 h. This Pd complex contained two thiosemicarbazone moieties in a bidentate mode *via* the azomethine nitrogen and the sulphur atom, creating two five-membered chelate rings. Their results indicated that the microwave irradiation can promote the Suzuki-Miyaura cross-coupling of aryl bromides and chlorides with phenylboronic acid in DMF-H₂O (70%:30%, v/v).

Bai *et al.* introduced a Suzuki-Miyaura cross-coupling of bromoarenes with tetraphenylborate via polystyrene-supported Pd catalysis under microwave irradiation (Scheme 1.4).¹⁰⁵ The polystyrene-supported Pd catalysts (cross-linked with divinylbenzene) were stable to air and high temperatures, and were highly efficient over more than six recycles (yields of 90-93 %, using 1 mol% Pd). A presynthesised polymeric Pd^{II} precatalyst, with K₂CO₃ and TBAB at 120 °C under microwave irradiation, was found to be the optimal catalyst system



Scheme 1.4 Suzuki-Miyaura cross-coupling with 4-bromoacetophenone and Ph₄BNa.

Tanaka and co-workers have synthesised and characterised two Pd^{II} complexes [[PdCl(bnqp)](PF₆) and [PdCl(bbnp)](PF₆)] (Figure 1.31),¹⁰⁶ which have terpyridine-type tridentate ligands with benzo-1,5-naphthyridin-2-yl groups. From the X-ray diffraction study, they found that the Pd-Cl bond in each compound were significantly distorted because of the steric hindrance of the hydrogen atoms at the position of benzo-1,5-naphthyridin-2-yl groups.

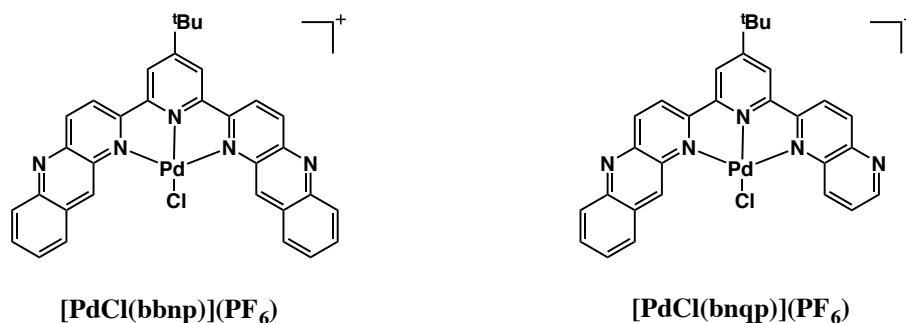


Figure 1.31 Structure of Pd^{II} complexes.

1.4.2 Pd-catalysed cross-coupling in organic synthesis

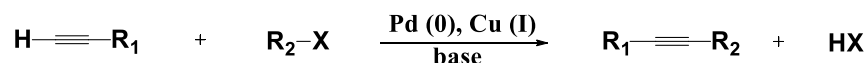
During the past forty years, Pd catalysts have played an important role in organic chemistry and developed a growing number of Pd-catalysed reactions allowing the introduction of functional groups and formation of novel organic molecules. The importance of Pd-catalysed cross-coupling reactions in organic synthesis is highlighted by the award of the Nobel Prize for Chemistry in 2010 to Heck, Negishi and Suzuki.¹⁰⁷

Pd-catalysed cross-coupling is a process whereby two different hydrocarbon fragments assemble on the Pd via the formation of Pd-C bonds. It is generally used for the synthesis of sp^2 - sp^2 or sp - sp^2 bonds, due to the problems associated with β -hydride elimination at sp^3 carbon centres. However, recent research shows that the latter problems can be solved.^{108,109} Two substrates are coupled to one another with the aid of a Pd catalyst, resulting in the formation of a new C-C single bond, as seen in the earlier section for Suzuki- Miyaura cross-coupling.

Generally, cross-coupling reactions require a halogenated (or pseudohalogen) species, which can be coupled to an organometallic reagent with Pd. The organohalide oxidatively adds to the Pd^0 catalyst to give a Pd^{II} species. Then the Pd^{II} species can undertake transmetalation with the organometallic reagent, followed by reductive elimination to generate the cross-coupled product, and Pd^0 catalyst. Pd-catalysed cross-coupling reactions have been used in the synthesis of base-modified nucleosides and nucleotides.^{110,111} Coupling with a variety of nucleophilic reagents to form C-C or C-X bonds can be achieved. Also with Pd catalysis, direct arylation by C-H bond functionalization allows the synthesis of base-modified nucleosides.

1.4.2.1 Sonogashira cross-coupling reaction

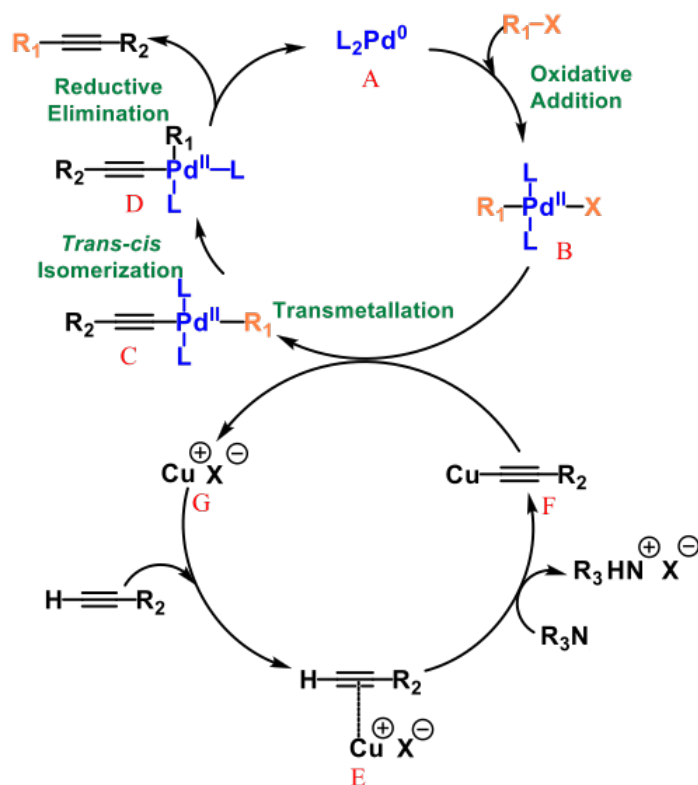
The Sonogashira cross-coupling reaction is a C-C bond formation process that leads to the coupling of sp -hybridized carbon atoms of terminal alkynes and sp^2 -hybridized carbons of halides (aryl and vinyl halides), catalysed by Pd^0 with a Cu^I co-catalyst in the presence of a base (Scheme 1.5). The reaction was discovered in 1975 by Sonogashira *et al.* by using $PdCl_2(PPh_3)_2$ as the precatalyst and CuI as the co-catalyst at room temperature.¹¹²



R_1 = alkyl, alkenyl, heteroaryl, aryl;

R_2 = vinyl, heteroaryl, aryl; X = halide, triflate, etc.

Scheme 1.5 The Sonogashira cross-coupling reaction.



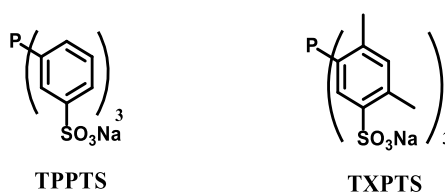
Scheme 1.6 Proposed mechanism of Pd-catalysed Sonogashira cross-coupling reaction.

A The mechanism of the Sonogashira reaction is still not well understood, but so far the mechanism is proposed to proceed *via* two catalytic cycles (Scheme 1.6).¹¹³ The first “Pd cycle” starts with the formation of the Pd^{II} complex (B) using an aryl halide and Pd^0L_2 (A) in an oxidative addition reaction.¹¹⁴ Then in the transmetalation step, the Pd^{II} complex participates in the copper cycle and transfers the halide to the acetylide *via* the copper acetylide species (F) in the copper cycle and forms the complex (C) and releases copper halide CuX (G). The two ligands change their orientation from *trans* (C) to *cis* (D) in the *trans/cis* isomerization process, which gives it the correct geometry for the next step. In the final reductive elimination step, Pd^{II} is reduced to Pd^0 , giving regenerated active catalyst.¹¹⁵

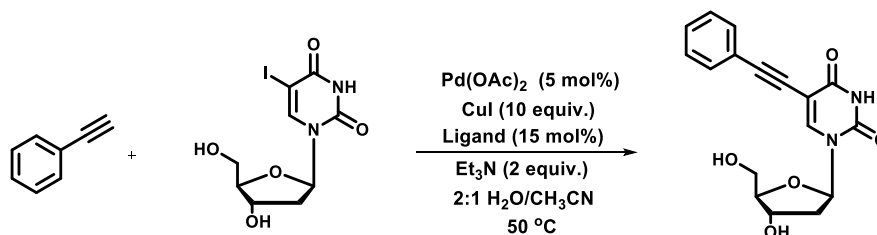
Alkynylation of nucleosides is one important modification strategy for the synthesis of chemically-modified biomolecules. The advantage of this modification is that this strategy can have less influence on DNA conformation.¹¹⁶

The first case of the Sonogashira cross-coupling for purine nucleosides was the coupling of 2-IA with alkynes in DMF, using $\text{PdCl}_2(\text{PPh}_3)_2$ as precatalyst and CuI as co-catalyst, developed by Miyasaka and co-workers.¹¹⁷

Cho *et al.* provided one of the first examples of Pd catalysts applied in aqueous Sonogashira couplings of unprotected 8-bromopurines and 5-iodouridine (5-IdU) under mild conditions.¹¹⁸ Cho and co-workers made the aqueous phosphine ligands for the Sonogashira cross-coupling for unprotected 5-IdU and phenylacetylene and the TXPTS and $\text{Pd}(\text{OAc})_2$ system achieved 90% conversion of 5-IdU to the product within 1.5 h (Scheme 1.3). It was shown to be an effective catalyst system for the coupling and the TXPTS ligand compared well with TPPTS (Scheme 1.8).

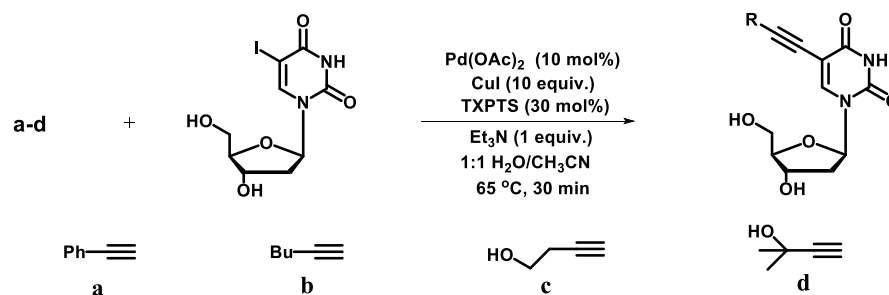


Scheme 1.7 Structure of TPPTS and TXPTS.



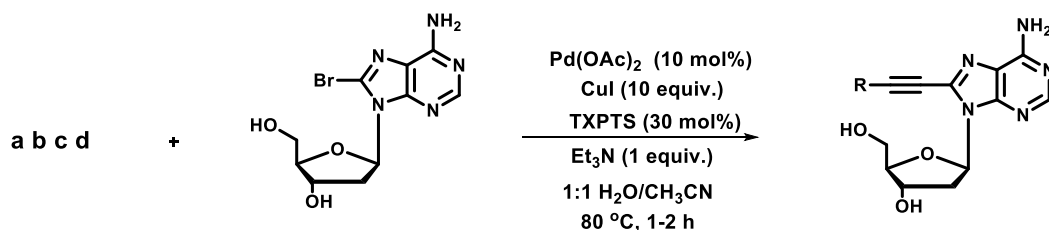
Scheme 1.8 Sonogashira reaction with 5-IdU and phenylacetylene in aqueous solvent form.

Alkyl-substituted alkynes gave lower yields of 42 % and 55 % respectively. Furthermore, the more sterically hindered alkyne gave an 84 % yield of product (Scheme 1.9).



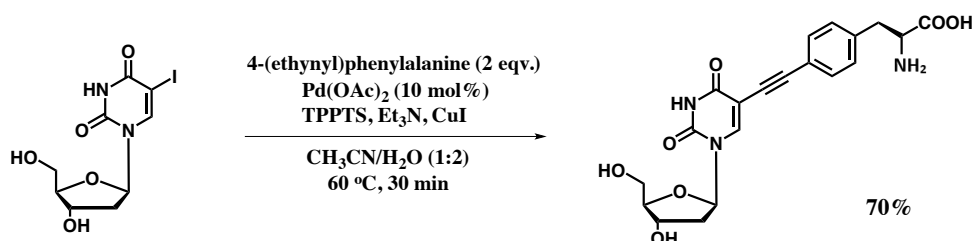
Scheme 1.9 The Sonogashira reaction of 5-IdU and alkynes in aqueous solvent.

The optimized alkynylation conditions were found to be 10 mol% Pd(OAc)₂, 10 mol% CuI, 30 mol% TXPTS as ligand, and 1 equiv. of triethylamine in 1:1 H₂O/CH₃CN, 80 °C, which was employed in the aqueous Sonogashira cross-coupling of unprotected halonucleoside with terminal alkynes. Under the optimized conditions, both phenylacetylene and alkyl-substituted alkynes gave relatively high yields of desired product with no side products. Both 8-BrdA and 8-BrdG reacted to give products with high yields (Scheme 1.10).



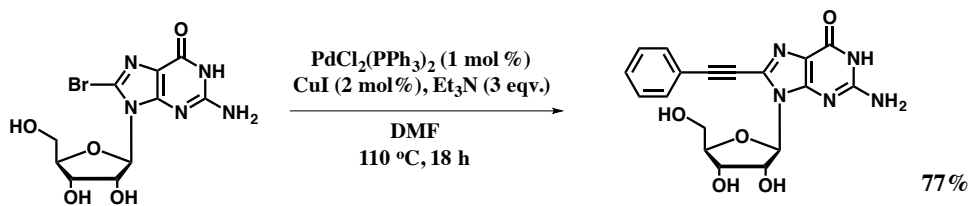
Scheme 1.10 Sonogashira cross-coupling of 8-bromopurine nucleosides.

Hocek and co-workers developed an aqueous Sonogashira cross-coupling reaction catalysed by Pd(OAc)₂/TPPTS in triethylamine as base and CuI as additive in a mixture of CH₃CN/H₂O solvent system to gain the product as an amino acid moiety (Scheme 1.11). A similar protocol for the synthesis of phenylalanine derivatives with deoxyadenosine at the C8 position was reported by Hocek *et al.*¹¹⁹



Scheme 1.11 Sonogashira coupling of phenylalanine analogues.

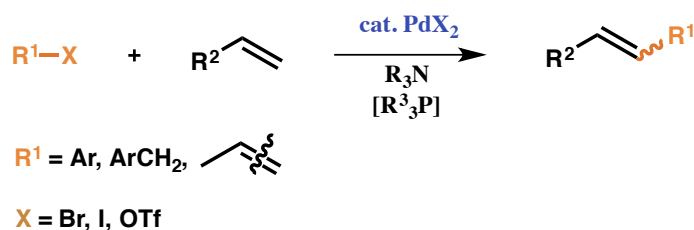
In previous research by Fairlamb and Baumann, Sonogashira cross-couplings of unprotected purine nucleosides have been investigated, including the first synthesis of an unprotected 8-bromoguanosine (Scheme 1.12). Various C8 modified adenosines and guanosines were synthesised by Sonogashira cross-couplings mediated by a PdCl₂(PPh₃)₂ precatalyst and CuI as co-catalyst. The optimal conditions for these reactions were 2 mol% Cu and 1 mol% Pd.¹²⁰



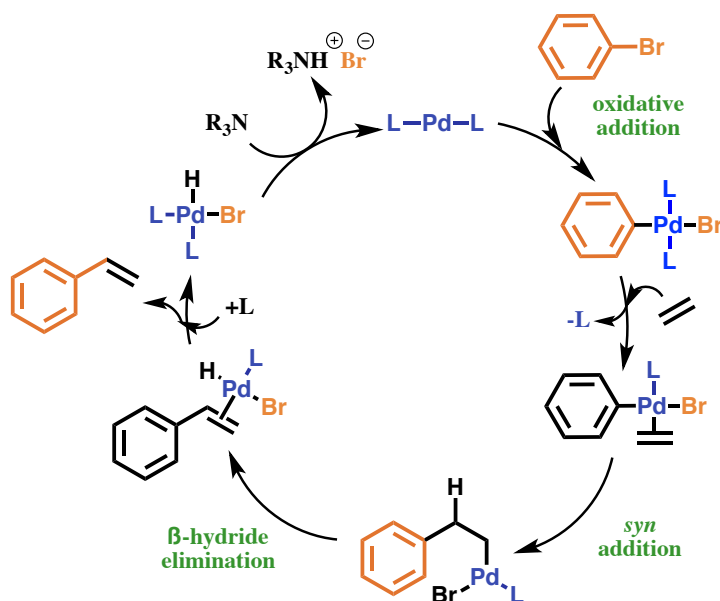
Scheme 1.12 Sonogashira cross-coupling of guanosine with phenylacetylene.

1.4.2.2 Heck reaction

The palladium-catalysed Mizoroki–Heck reaction is the most effective methodology for the vinylation of aryl/vinyl halides or triflates. This reaction, a C–C bond is formed in the presence of a base (Scheme 1.13). If a Pd^{II} source is used in a Heck reaction, it must be reduced to Pd^0 before entering catalytic cycle (the same is the case for the Sonogashira cross-coupling reaction).



Scheme 1.13 General Heck reaction.

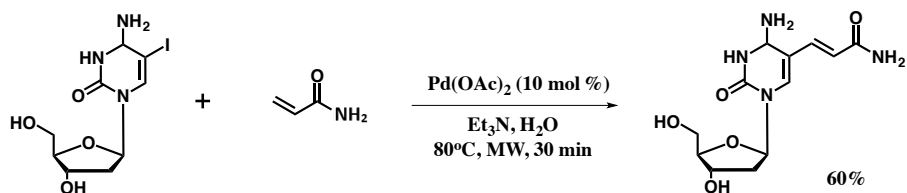


Scheme 1.14 Mechanism of the Heck reaction.

The first step of the catalytic cycle is an oxidative addition of the aryl halide to a Pd^0 complex (Scheme 1.14). The oxidative addition gives a σ -aryl– Pd^{II} halide, which first coordinates to the alkene and then undertakes a *syn* addition of the alkene. β -hydride elimination gives a hydrido– Pd^{II} halide

ligated to the arylated alkene. After dissociation from the arylated alkene, the hydrido-Pd^{II} halide undertakes a reversible reductive elimination to regenerate the active Pd⁰ complex. The base shifts this equilibrium to the Pd⁰ catalyst by quenching the hydrogen halide.

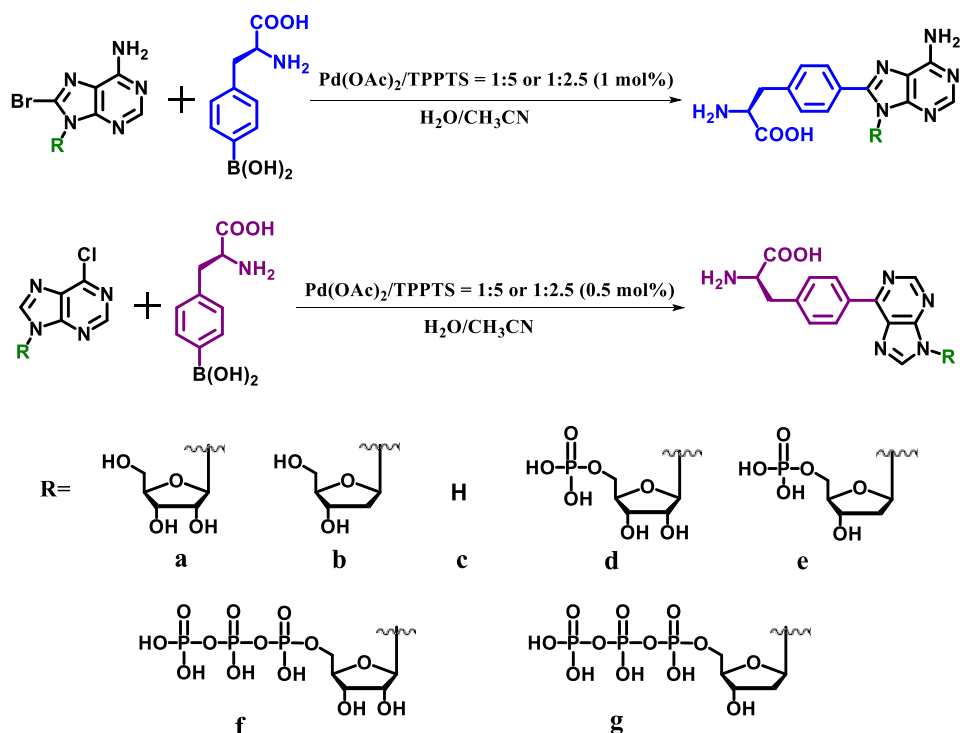
The most recent example of the cross-coupling of unprotected nucleosides involving Heck coupling of 5-IdU with acrylates, employs Pd(OAc)₂ (10 mol %) as the precatalyst at 80 °C, as reported by Len and co-workers (Scheme 1.15).¹²¹ Et₃N acted as a base and a ligand in these reactions and the addition of water also assisted catalysis.



Scheme 1.15 Heck coupling of 5-IdU using Pd(OAc)₂.

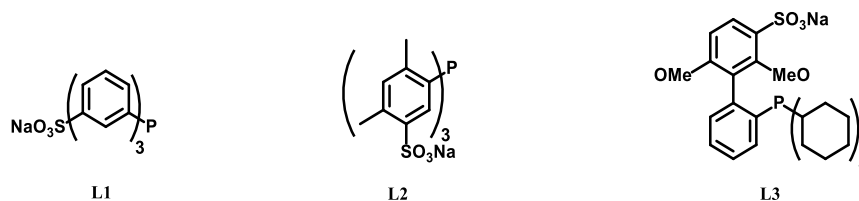
1.4.3 Other Pd-catalysed cross-couplings of nucleosides and nucleotides

In 2006, Capek *et al.* published an efficient single-step synthesis of (purin-8-yl) and (purin-6-yl) phenylalanines using the Shaughnessy method¹²² for Suzuki cross-coupling reactions between unprotected 8-bromo- and 6-chloroadenosine nucleosides **a** and **b** and simple arylboronic acids in aqueous media, as well as coupling of nucleotides (Scheme 1.16 and Scheme 1.17).¹²³



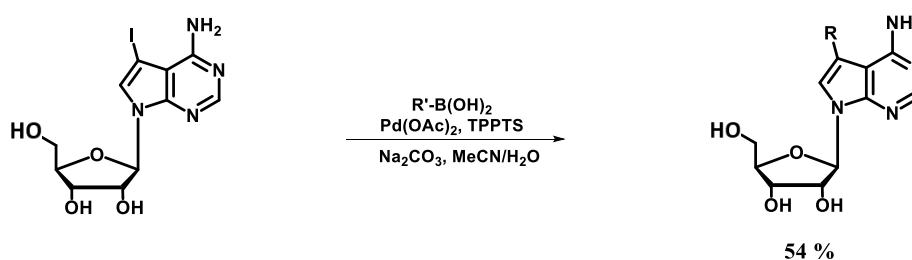
Scheme 1.16 Synthesis of (adenin-8-yl) and (adenine-6-yl)phenylalanines.

For the synthesis of 4-(adenin-8-yl) phenylalanines **a** and **b**, classical heating achieved high yields, while for the synthesis of (purin-6-yl) phenylalanines, microwave-mediated conditions gave the product in excellent yield. With a 9-unsubstituted 8-halopurine base **c** the reaction was conducted under optimised microwave conditions and gave **c** in a yield of 84 %.



Scheme 1.17 Structures of phosphine ligands L1–L3.

Bourderioux *et al.* reported the synthesis of 7-heteroaryl-7-deazaadenosines conducted with single step aqueous Suzuki cross-coupling between 7-iodotubercidin and boronic acids in the presence of Pd(OAc)₂, TPPTS ligand, and Na₂CO₃ as a base (Scheme 1.18).¹²⁴



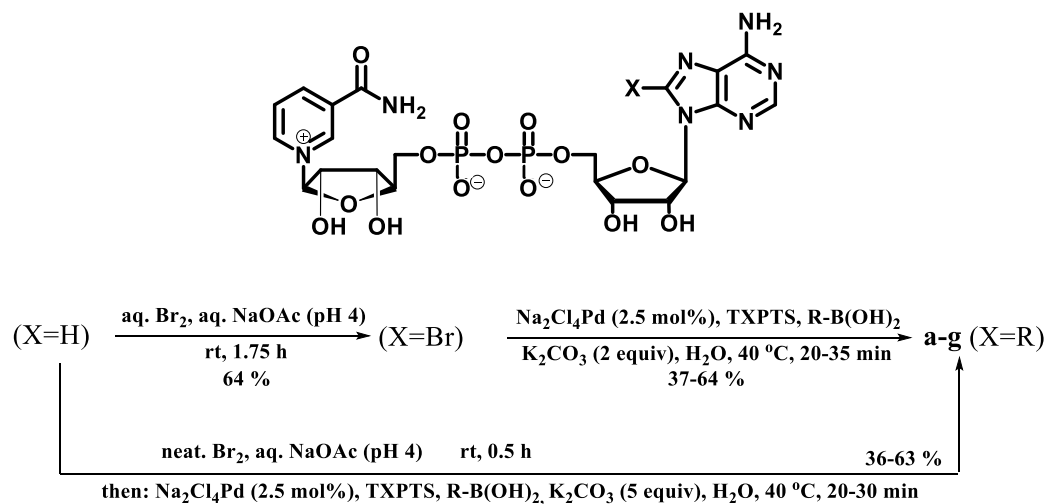
	-R (-R')	Products (yields)		-R (-R')	Products (yields)
a		1a (48%)	e		1e (77%)
b		1b (82%)	f		1f (63%)
c		1c (72%)	g		1g (9%)
d		1d (77%)	h		1h (82%)

Scheme 1.18 Suzuki cross-coupling with 7-iodotubercidin and boronic acids.

Nucleosides **a-b** exhibited potent cytostatic effects (nanomolar GIC₅₀) over a wide range of tested cell lines, comparable to Tubercidin or Doxorubicin and better than Clofarabin. The reactivity of 7-aryl-7-deazaadenine ribonucleosides was lower than the 7-heteroaryl-7-deazaadenine ribonucleosides. It has been found to possess cytostatic effects at low nanomolar concentrations with the potency

comparable to clofarabine. Furthermore, the compounds **b**, **c**, **d**, **f**, **g** were noncytotoxic against normal human fibroblasts, which indicated a promising therapeutic index under *in vitro* conditions.

In 2011, Pesnot *et al.* developed a study of a new and efficient synthetic approach facilitating the synthesis of 8-bromo-NAD (NAD: nicotinamide adenine dinucleotide, Scheme 1.19).¹²⁵



Scheme 1.19 One-pot synthesis of 8-substituted NAD derivatives.

The optimised cross-coupling conditions employed electron-rich phosphine ligand, TXPTS (tris(4,6-dimethyl-3-sulfonatophenyl) phosphine trisodium salt), which promoted the Suzuki cross-coupling of 8-bromo-adenosine at 40 °C within 1 h. Use of neat bromine instead of bromine-water limited the bromination time to 30 min.

1.4.4 Pd-catalysed C-H functionalisation of nucleosides

The field of C-H bond functionalisation emerged in the 1970s. C-H bond functionalisation has its own advantages compared to traditional cross-coupling methodologies. Unlike traditional cross-couplings, C-H functionalisation does not need pre-functionalisation of the substrates, therefore it does not need extra reaction steps to produce the target molecule (Figure 1.32). These advantages can reduce synthesis time and cost. The process is more efficient if the C-H bond is directly converted into the M-C bond in the catalytic cycle. C-H bond functionalisation can have some drawbacks, *e.g.* non-selective C-H bond activation and often stoichiometric side products are generated, *e.g.* Cu salts. C-H functionalisation can be defined as the coupling of a C-H and C-X (X = halide or similar activating group) mediated by a transition metal. In this case, Pd-catalysed C-H functionalisation has been chosen as the platform to demonstrate Pd-catalysed intramolecular C-H arylation reactions.

After primary oxidative addition of a Pd^0 species into a C-X bond, a C'-H bond in close proximity can be activated to form a "Pd(C)(C')L₂". Reductive elimination to form a new C-C bond in the usual way is then possible.

Traditional Cross-coupling Methodologies

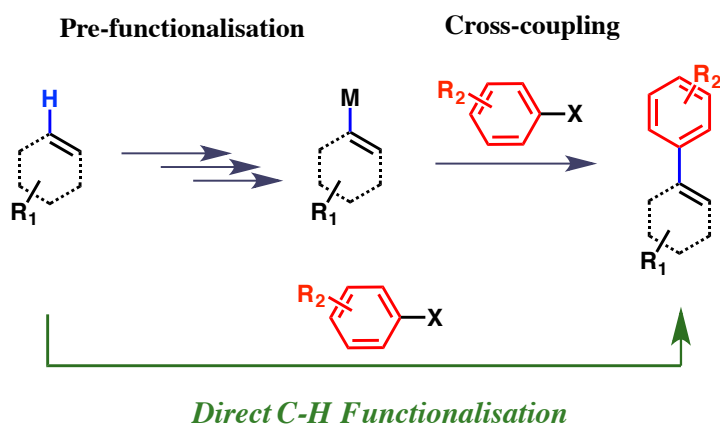
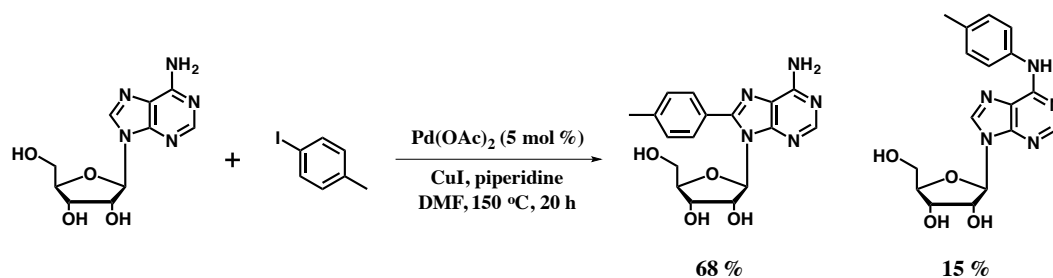


Figure 1.32 Comparison of direct C-H functionalization and traditional cross-coupling methods.

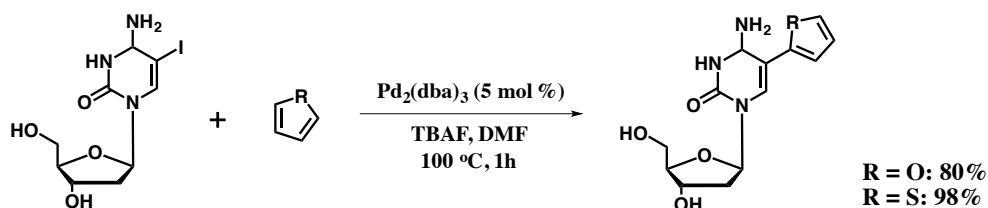
Purine nucleosides react with aryl iodide coupling partners. Hocek and co-workers first conducted a C-H arylation of purine nucleosides (Scheme 1.20).¹²⁶ They have developed 8-(4-methoxyphenyl)purine nucleosides which are directly coupled with aryl iodides by $\text{Pd}(\text{OAc})_2$ (5 mol%) using CuI in DMF at 150 °C. Unfortunately, when the C-H arylation was applied to adenosine, a mixture of C8 and N6 products (side-product) was observed in 5:1 ratio.



Scheme 1.20 First example of C-H arylation of purine nucleosides.

The Fairlamb research group improved the selectivity for C8 arylation of adenosine by using Cs_2CO_3 instead of piperidine alone.^{127,128} The piperidine aids the reduction of $\text{Pd}(\text{OAc})_2$ to give Pd^0 . This research also revealed that the guanine moiety disfavoured C8 direct arylation, when compared to the related adenines.

Electron-deficient pyrimidines are much more difficult to synthesise by direct arylations. Wnuk and co-workers¹²⁹ used electron-rich heterocycles to overcome this difficulty. They directly coupled 5-IdU with furan, and thiophene by using 5 mol% Pd₂(dba)₃•(dba) and TBAF in DMF (Scheme 1.21).



Scheme 1.21 Coupling of 5-IdU and thiophene.

1.5 Aims and Objectives

1.5.1 Aims

The principle aims of the project are to:

- i. Design and synthesise novel and tuneable dba ligands and Pd catalysts for aqueous cross-coupling reactions, with a focus on purine derivatives.
- ii. Design, synthesise and characterise highly conjugated linear ethynyl purines, as a new class of purine fluorescent probes.
- iii. The C-H bond activation of appropriate nucleosides.

1.5.2 Objectives

The objectives of the research detailed within this thesis are to:

- i. Devise synthetic methods for Sonogashira cross-coupling reactions, using bespoke designed Pd catalysts, containing aryl-substituted dibenzylidene acetone 'dba-Z' ligands.
- ii. Screen the activity of the aqueous Pd catalysts against the Sonogashira cross-coupling reaction of 8-bromoguanosine or adenosine with terminal alkynes.
- iii. Characterise Pd nanoparticles and 'active Pd' ratios from Pd catalysts using TEM techniques, NMR and MS analysis.
- iv. Characterise and understand the fluorescent behaviour of 8-alkynylated nucleosides, especially containing multiple alkyne 'Ph-CC-Ph-CC-' motifs by fluorescence spectroscopy and UV-Vis spectroscopy, including solvatochromic studies.
- v. Develop C-H bond functionalisation methodologies for accessing 8-arylated inosine derivatives.

CHAPTER 2

SYNTHESIS OF PD CATALYSTS FOR 8- MODIFIED FLUORESCENT NUCLEOSIDES

2 Synthesis of new Pd catalysts containing dba-Z ligands, including hydroxylated derivatives

2.1 Introduction

$[\text{Pd}^0(\text{dba})_3 \cdot \text{dba}]$ has been widely used as a catalyst in synthetic chemistry and as a precursor complex for coordination chemistry (dba = *E,E*-dibenzylideneacetone). The Fairlamb group developed a ligand design concept based on tuning the C=C bonds within dba-framework, making remote substituent modifications to the aryl groups (Figure 2.1).¹³⁰ Close attention was paid to the synthesis and application of $\text{Pd}^0_2(\text{dba-Z})_3$ complexes (Z = dba aryl substituents). Remarkable and differential catalytic performance in cross-couplings, such as Suzuki-Miyaura and Heck reactions, was observed. Changing the electronic properties of dba in $[\text{Pd}^0_2(\text{dba-Z})_3]$ affects the rate of oxidative addition, the first committed step in a cross-coupling catalytic cycle. The extent of back-donation between the Pd^0 and the alkene ligand could be influenced by changing the aryl substituents (Z) on dba. An electron-withdrawing substituent could increase π -backdonation (reducing the rate of oxidative addition), whereas an electron-donating substituent could destabilise π -backbonding (increasing the rate of oxidative addition). The use of $[\text{Pd}^0_2(\text{dba-Z})_3]$ complexes therefore affects the release of the active Pd^0 catalyst, which is accelerated by the donating properties of dba-Z ligand.¹³¹

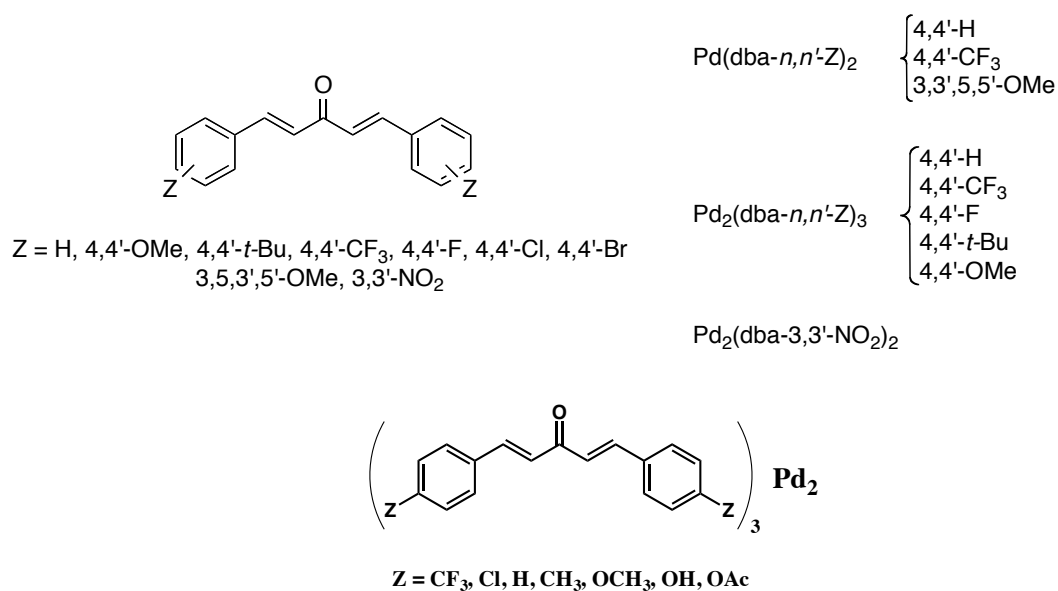
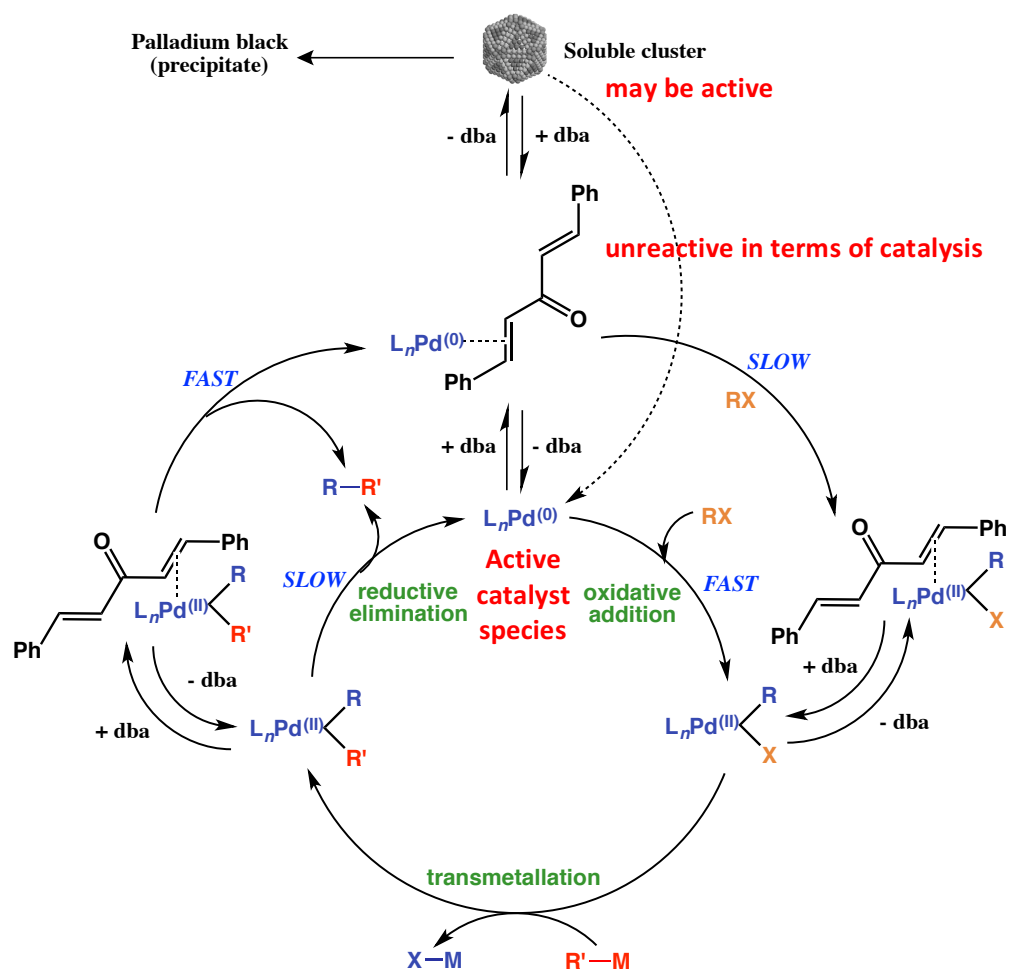


Figure 2.1 Substituted dba-Z ligands and their Pd^0 complexes.

Goodson and co-workers¹³² later synthesised a hydroxylated dba-Pd catalyst precursor complex shown in Figure 2.1, with the idea that the phenolic hydrogens would become deprotonated under basic reaction conditions, which could find application in Suzuki-Miyaura polycondensation reactions.

Amatore and Jutand *et al.*¹³³ presented strong evidence (using electrochemical methods) indicating the non-innocent behavior of dba ligands in the oxidative addition reactions of *in situ* generated Pd⁰L₂ species with aryl iodides. In the case of [Pd⁰(dba)L₂] (L = PPh₃) the dba ligand was not as labile as previously assumed, requiring as much as 50 equivalents of PPh₃ to replace it completely, *i.e.* dba has a higher affinity than PPh₃ for [Pd⁰(PPh₃)₂S] (where S = solvent) to give [Pd⁰(dba)(PPh₃)₂]. Therefore, the dba ligand controls the concentration of the highly reactive Pd⁰L_n species (L = monodentate ligand; *n* = 1 or 2).



Scheme 2.1 The dba ligand effects in a general cross-coupling catalytic cycle (note: oxidative addition is fast where X = I and slow where X = Cl), as proposed by Fairlamb *et al.*

It is important to note that the dba brings the rates of the individual steps of the catalytic cycle closer to each other (subsequent steps are usually rate-limiting, *e.g.* transmetallation), taking advantage of a faster oxidative addition where needed or through stabilization of Pd⁰. By increasing the equivalent of dba or monophosphine will lead to a slower reaction as the amount of [Pd⁰L_nS] is reduced; while by increasing the electron density of the phosphine, the equilibrium will move towards [L_nPd⁰(dba)]. The soluble Pd cluster (aggregated Pd) may also affect oxidative addition rates (Scheme 2.1). It was suggested that there is an antagonistic effect of the high reactivity of Pd⁰L_n species and the equilibrium relative to the unreactive [L_nPd⁰(dba)], and possibly Pd⁰ cluster species.

The dba ligand appears to play a non-innocent role in the majority of cross-coupling reactions, even influencing other steps such as β-hydrogen elimination. The purity of common Pd pre-catalysts, particularly in the case of [Pd⁰₂(dba)₃·dba] has also been of concern.^{134,135} Arguably this is important in mechanistic studies where the purity of the material is critical for the accurate measurement of reaction rates and catalytic turnover. [Pd⁰₂(dba)₃] can generate PdNPs, under reducing conditions with heating, indeed even in the solid-state (on standing on the shelf, for example). It has also been suggested that the PdNPs derived from Pd₂(dba)₃ could play an important role in catalytic oxidation chemistry and coupling reactions. A study by Ananikov and Zalessky¹³⁵ has described that the decomposition of [Pd⁰₂(dba)₃·dba] cannot be completely avoided. Large Pd particles (sized from 10-200 nm, analyzed by TEM) have been found in commercial batches of [Pd⁰₂(dba)₃·dba]. The authors also proposed the utilization of [Pd⁰₂(dba)₃·dba] of unknown purity, *i.e.* presence of large Pd particles, may be a problem for catalysis. However, despite highlighting this potential problem, the authors did not investigate a way to measure the real and active catalytic species and therefore the implication of the impurities was not determined.

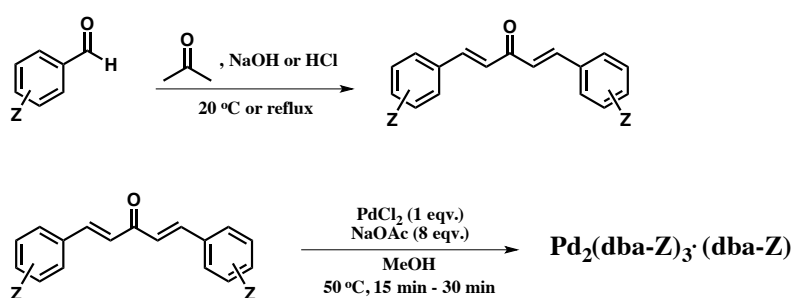


Figure 2.2 Target synthesis of ligands and Pd catalysts for 8-modified fluorescent nucleosides.

With one eye on conducting cross-coupling reactions on biomolecules (*e.g.* nucleosides), it was envisaged that reactions in water would be useful to develop. Therefore, different Pd catalysts based on hydroxylated and alkyloxy dba framework ligands were initially investigated. The target ligands and Pd complexes for synthesis are shown in Figure 2.2.

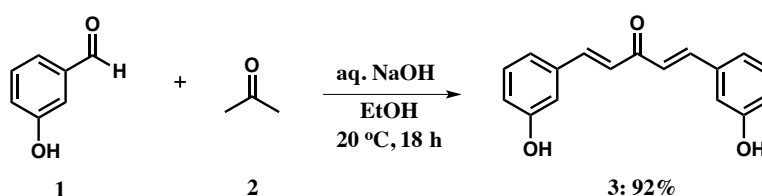
In terms of the ligand synthesis, symmetrical and unsymmetrical dba-frameworks may be accessed by a number of methods, the most simple of which involves Claisen-Schmidt condensation.¹³⁶ The Pd complexes were generally accessed by the first published methodology for synthesis of $[\text{Pd}^0_2(\text{dba})_3\cdot\text{dba}]$, where the excess of dba was dissolved in a hot methanolic solution (*ca.* 50 °C) with sodium acetate in the presence of PdCl_2 .¹³⁷

2.2 Synthesis of hydroxylated-dba Pd complexes

In the first part of this study, hydroxylated-dba Pd complexes were investigated, some of which are novel. This research builds on studies conducted within our group and those later reported by Goodson *et al.*¹³²

2.2.1 Synthesis of the ligand for $\text{Pd}_2(3\text{-OH-dba})_3\cdot(3\text{-OH-dba})$

Initially it was proposed that hydroxy-substituted aryl aldehyde **1** could be used to synthesise the hydroxylated-dba ligands. It was decided to investigate the Claisen-Schmidt condensation reaction between two molecules of aldehyde **1** and acetone **2**, which is mediated by base (NaOH) (Scheme 2.2). The acidic α -proton of **2** is removed by NaOH, resulting in the formation of an enolate anion, which is made relatively stable by the delocalization of electrons. Next, the carbonyl carbon of **1** is attacked by the enolate anion to give an intermediate alkoxide. Loss of water delivers product **3**.



Scheme 2.2 Synthesis of ligand **3**.

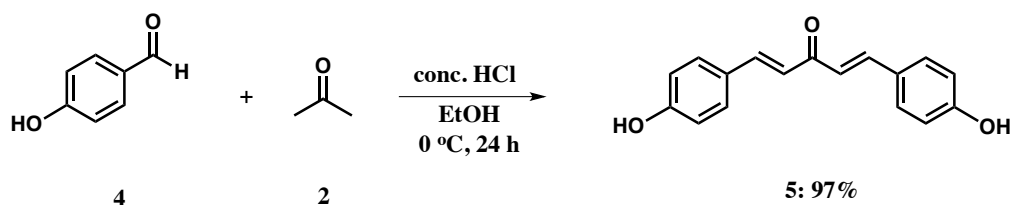
Product **3** simply precipitates from the reaction mixture. However, in the case of these hydroxylated-dba compounds it is necessary to adjust the pH of the reaction medium. This is achieved by addition of solid CO_2 (dry ice), which increases the acidity of the reaction media, leading to product precipitation, *i.e.* a yellow solid which can be easily filtered and dried in air, and does not require column chromatography. Using this work-up procedure an excellent yield (92%) of compound **3** was recorded, and the yield was much higher than previously reported (15%).¹³⁸ The ^1H NMR spectrum of this compound (in CD_3OD , 400 MHz) exhibits the following key proton attributes: as a *trans*-alkene is formed, two protons at 7.69 and 7.16 ppm are observed with a $^3J_{\text{HH}}$ coupling constant of

16.2 Hz, which is expected for this type of enone product. The ^{13}C NMR spectrum exhibits 9 carbon signals. For example, the C=O is seen at 191.5 ppm, and a range of aromatic signals between 120-150 ppm. The IR spectrum of this compound shows OH and C=O groups at 3389 cm^{-1} and 1619 cm^{-1} , respectively. The mass spectrum shows the expected mass ion at m/z 267.1012 (MH^+) by ESI-MS. The melting point range of the product was found to be $196\text{-}198\text{ }^\circ\text{C}$, which compares well with the literature ($198\text{-}200\text{ }^\circ\text{C}$).¹³⁹

2.2.2 Synthesis of the ligand for $\text{Pd}_2(4\text{-OH-dba})_3\cdot(4\text{-OH-dba})$

The ligand for $[\text{Pd}_2(4\text{-OH-dba})_3\cdot(4\text{-OH-dba})]$ was prepared by treatment of hydroxysubstituted **4** with acetone at ambient temperature using the method of Goodson *et al.*¹³² The reaction of NaOH in an ethanol/water solvent system gave low yields of the product, which can be explained by a poor conversion to product (and recovery of a large amount of starting material). The reactions were then tested under different conditions. For example, increasing the reaction temperature from room temperature (*ca.* $20\text{ }^\circ\text{C}$) to $40\text{ }^\circ\text{C}$, using HCl instead of NaOH,¹⁴⁰ altering the solvent from ethanol to methanol, or increasing the number of equivalents of **4**. In all cases, low product yields were recorded. These practical difficulties therefore meant the approach was unfeasible. A second approach was therefore evaluated using conc. HCl to mediate the transformation (Scheme 2.3).

Unlike the base-catalysed Claisen-Schmidt condensation, the acid-catalysed reaction begins with tautomerisation of **2** to form the enol. The enol adds to the protonated carbonyl group of aldehyde **4**, which activates the carbon towards electrophilic attack. Finally, proton transfer and dehydration gives neutral product **5**.

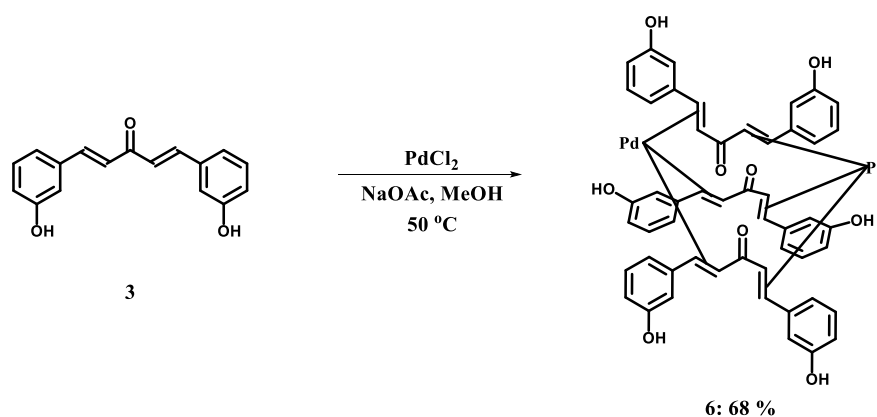


Scheme 2.3 Acid-catalysed synthesis of ligand **5**.

It was necessary to add conc. HCl dropwise with cooling (ice bath), and indeed the product yields increased. The product was isolated in high yield as an air stable yellow solid, which could be purified by recrystallization from ethanol (note a small amount of starting material was present in the crude material). The ^1H NMR spectrum of the recrystallised material (in CD_3OD) exhibits the following key proton attributes – as a *trans*-alkene is formed, two protons at 7.70 and 7.05 ppm are observed with a $^3J_{\text{HH}}$ coupling constant of 16 Hz. The mass spectrum shows the expected pseudomolecular mass ion at m/z 267.1022 (MH^+) by ESI-MS. The melting point range of the product was found to be 241-243 $^\circ\text{C}$, which compares well with the literature (243-245 $^\circ\text{C}$).¹⁴¹

2.2.3 Synthesis of the complex $[\text{Pd}_2(\text{dba-3-OH})_3\cdot\text{dba-3-OH}]$

Preparation of the novel $[\text{Pd}_2(\text{dba-3-OH})_3\cdot\text{dba-3-OH}]$ (**6**) complex was first attempted by reaction of the dba-3-OH ligand **3** with PdCl_2 in the presence of NaOAc in MeOH at 50 $^\circ\text{C}$ over 15 min (Scheme 2.4). The reaction was attempted several times under varying reaction conditions. For example, NaOAc was added first, then the ligand, to a mixture of PdCl_2 with **3** in MeOH at 3.94×10^{-2} M concentration. This reaction quickly turned a green colour and after heating at 50 $^\circ\text{C}$ for 19 h afforded Pd nanoparticles, which precipitated from solution. It is proposed that the long reaction time led to the product complex decomposing to form Pd nanoparticles (PdNPs, as there is a kinetic and thermodynamic driving force for this). According to Ananikov *et al.*¹³⁵ the *s-cis,s-cis* conformation should be thermodynamically more preferred due to minimised steric repulsions in the ligands. However, from research from our group it was found that *s-trans, s-cis* is the preferred conformation in the dinuclear Pd^0 complex.¹⁴² Also, the decomposition of the complex may take place either due to intrinsic instability or initiated by reaction with trace acid and other impurities in the solvent, which may involve ligand dynamics and exchange.



Scheme 2.4 Synthesis of $[\text{Pd}_2(\text{dba-3-OH})_3\cdot\text{dba-3-OH}]$ **6**. The coordination mode about each alkene moiety is determined later.

In a second attempt the reaction time was reduced to 4 h, although large Pd nanoparticles (uncharacterised) were found to be the exclusive product. Subsequently it was determined that the concentration of the reactions affected the outcome of the reaction. At a higher concentration of PdCl₂ (4.68×10^{-2} M), and conducting the reaction for 40 mins, afforded a purple complex in 68% yield. The UV-vis spectrum (MeOH) showed a band for the Pd complex ($\lambda_{\text{max}} = 540$ nm), which is associated with the d-d transition. This compares well with Pd₂(dba)₃ ($\lambda_{\text{max}} = 520$ nm).¹⁴³ The ¹H NMR spectrum of this complex (in CD₃OD) shows that 12 protons are visible (as doublets), which can be correlated by ¹H COSY (Figure 2.3). The ¹H-¹H COSY spectrum of [Pd₂(dba-3-OH)₃·dba-3-OH] showed that H-1 coupled with H-7 and that H-2 correlated with H-11. H-3 coupled with H-4 and H-5 coupled with H-6. H-8 coupled with H-12 and H-9 coupled with H-10. This confirms the presence of 12 alkene protons (in two different Pd environments). The free ligand is also observed, so the following formulation is proposed - [Pd₂(dba-3-OH)₃·(dba-3-OH)_n]. The ratio of free ligand to Pd calculated from NMR ¹H integration is ~3.6:1.

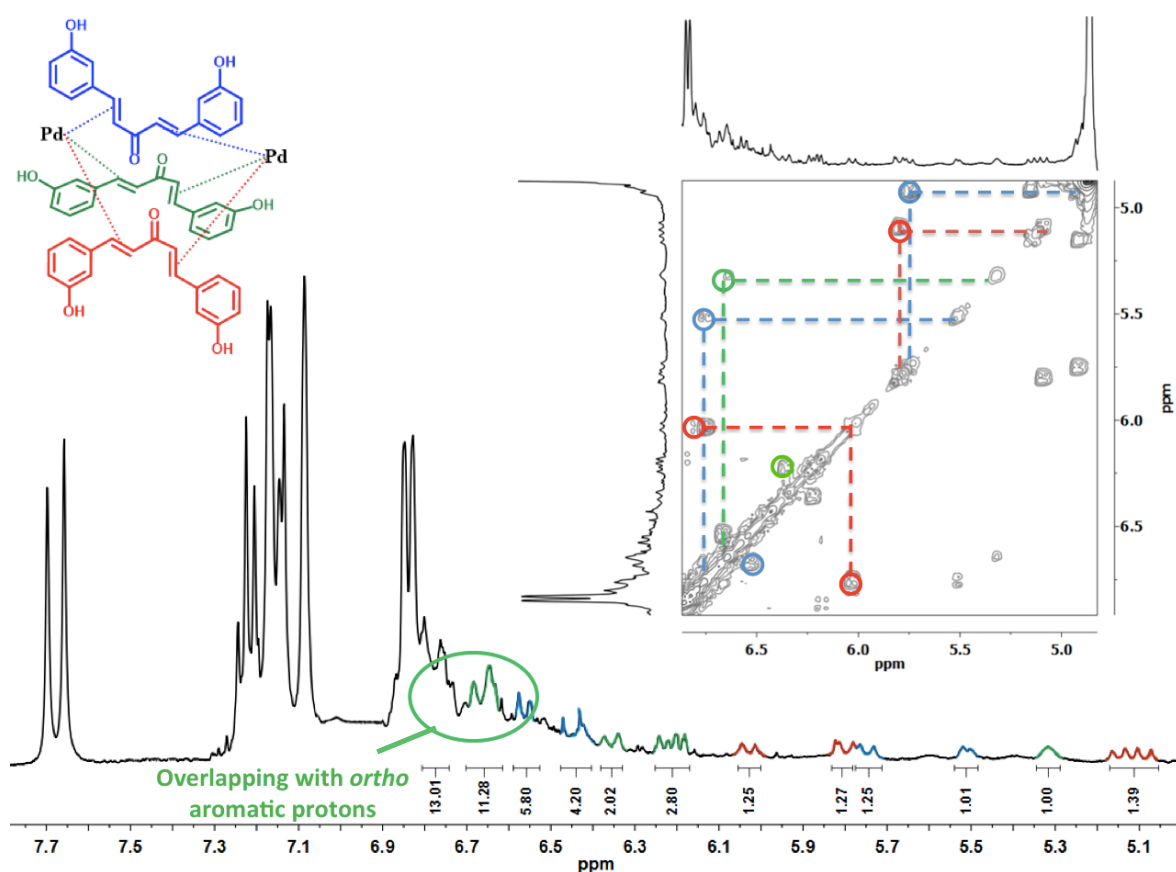


Figure 2.3 ¹H NMR spectrum and ¹H-¹H COSY spectrum of [Pd₂(dba-3-OH)₃·dba-3-OH] **6** (in CD₃OD, 400 MHz at 300 K).

The microanalytical data for this complex is different on hydrogen and carbon, compared to the theoretical values. Expected for the calculated chemical formula of $C_{68}H_{56}O_{12}Pd_2$ is C 63.91%, H 4.42%, whereas C 40.71%, H 6.63% was recorded for the product synthesised. The data indicates that some PdNPs are present in the sample (low carbon content), which was later confirmed (see Section 2.6). The high hydrogen content suggests that solvent is also present. An approximate calculation can be made – $[Pd_2(dba-3-OH)_3 \cdot dba-3-OH] \cdot Pd_6(CH_3OH)_{35}$, which gives theoretical values of C, 40.72, H, 6.50, which is closer to the experimental values obtained. The presence of Pd clusters with the Pd complex are therefore present.

The Kawazura study relied on key information in the chemical shift difference between X- and Y- protons within individual olefins (Figure 2.4), which derives from the enone conformation in dba. In the non-coordinated dba, the *s-cis* form has a minimum $\Delta\delta_{X1-Y1}$ value of 0.5 ppm and in the *s-trans* form a maximum value of 1.5 ppm. By extrapolation-coordinated olefins with the range of $\Delta\delta_{X1-Y1}$ value between δ 0.069-0.186 ppm was assumed to be the *s-cis* form, while between δ 0.631-0.965 was proposed to be in a *s-trans* form.¹⁴² According to the figure above, H3 and H4, H5 and H6, H9 and H10 were *s-cis* and the others were *s-trans*.

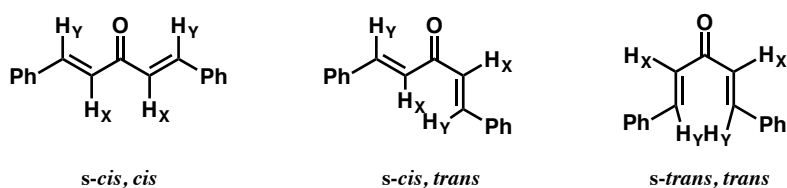


Figure 2.4 Three conformations in dba.

Table 2.1 1H NMR data for $[Pd_2(dba-3-OH)_3 \cdot dba-3-OH]$ (CD_3OD , 400 MHz).

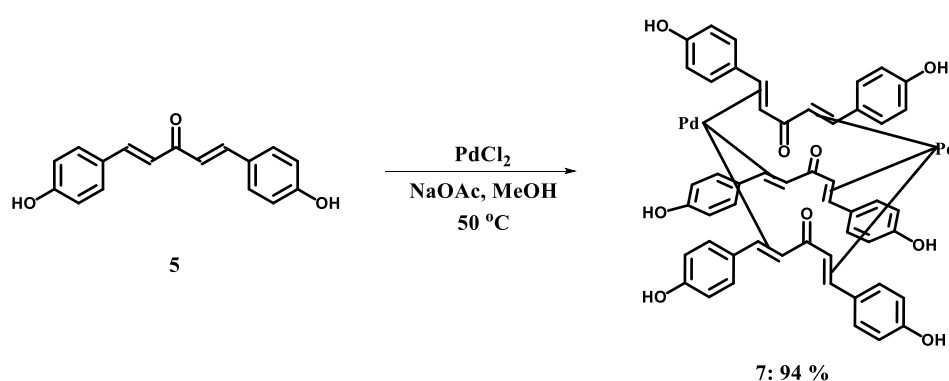
No.	δ_X / ppm	J / Hz ^a	No.	δ_Y / ppm	J / Hz	$\Delta\delta_{X1-Y1}$ / ppm	<i>s-cis</i> or <i>s-trans</i>
H1	6.78	-	H7	6.03	12.1	0.75	<i>s-trans</i>
H2	6.65	14.2	H11	5.32	-	1.33	<i>s-trans</i>
H3	6.56	10.5	H4	6.45	10.5	0.13	<i>s-cis</i>
H5	6.36	12.2	H6	6.21	-	0.14	<i>s-cis</i>
H8	5.80	12.1	H12	5.10	12.1	0.7	<i>s-trans</i>
H9	5.73	13.0	H10	5.52	-	0.21	<i>s-cis</i>

^a Where a coupling constant is not specified it is due to poor resolution deriving from overlapping isomeric structures or exchange processes. In each case the protons are correlated by 1H COSY.

Twelve protons were shown to be coupled to each other by ^1H COSY NMR. Among these, the coupling constant for each olefin should be the same which indicate the Pd is moderately coordinated to the olefin (H3 and H4, H8 and H12), whereas, if the coupling constant cannot be measured (not a clear doublet signal) due to the conformation of olefin which coordinated with Pd changing between *trans* and *cis* (H1 and H7, H2 and H11, H5 and H6, H9 and H10) (Table 2.1).

2.2.4 Synthesis of the complex $\text{Pd}_2(\text{4-OH-dba})_3 \cdot (\text{4-OH-dba})$

The preparation of $\text{Pd}_2(\text{dba-4-OH})_3 \cdot \text{dba-4-OH}$ complexes (**7**) was first attempted by reaction of the ligand **5** with PdCl_2 in the presence of reducing agent (NaOAc), in MeOH at 50 °C, again by the method of Goodson *et al.* (Scheme 2.5).¹³²



Scheme 2.5 Synthesis of $[\text{Pd}_2(\text{dba-4-OH})_3 \cdot \text{dba-4-OH}]$ **7**.

The reaction was attempted several times under varying reaction conditions. For example, NaOAc was added first to a mixture of PdCl_2 with dba-4-OH in MeOH at 2.11×10^{-2} M concentration. This reaction turned a green colour, which after heating at 50 °C for 1.5 h (shorter than the literature)¹³² afforded Pd nanoparticles, which precipitated from solution. The reaction turned from purple to green and took 2.5 h (less than the literature time of 4 h)¹³² to undergo this change. It is proposed that the long reaction time may have led to the product complex decomposing to form Pd, which is similar to $[\text{Pd}_2(\text{dba-3-OH})_3 \cdot \text{dba-3-OH}]$ described earlier. It was found that the reaction time again affected the yield of the reaction. At a concentration of PdCl_2 (2.11×10^{-2} M), over 30 mins, afforded a purple complex in 54% yield. The UV-vis spectrum (MeOH) showed a band for the Pd complex ($\lambda_{\text{max}} = 552$ nm), which is associated with the d-d transition. This compares well with $\text{Pd}_2(\text{dba})_3$ ($\lambda_{\text{max}} = 520$ nm).¹⁴³ The ^1H NMR spectrum of this complex (in CD_3OD) shows that 12 protons are visible (as doublets), which can be correlated by ^1H COSY (Figure 2.5).

The ^1H COSY spectrum of Pd complex showed that H-1 coupled with H-6 and that H-2 significantly correlated with H-3, and H-4 coupled with H-5, H-7 coupled with H-9, and H-8 coupled with H-9 (Figure 2.5). This confirms the presence of 12 alkene protons (two different Pd environments). A free ligand is also observed, so the following formulation is proposed - $\text{Pd}_2(\text{dba-4-OH})_3\cdot(\text{dba-4-OH})_n$. The ratio of free ligand to Pd calculated from NMR ^1H integration is 3.2: 1.

For the coupling constants of each olefin was the same which gives resolved signals (Table 2.2). According to the $\Delta\delta_{\text{X1-Y1}}$ value, the *s-trans* conformations were H1/H6 and H8/H9 olefins.

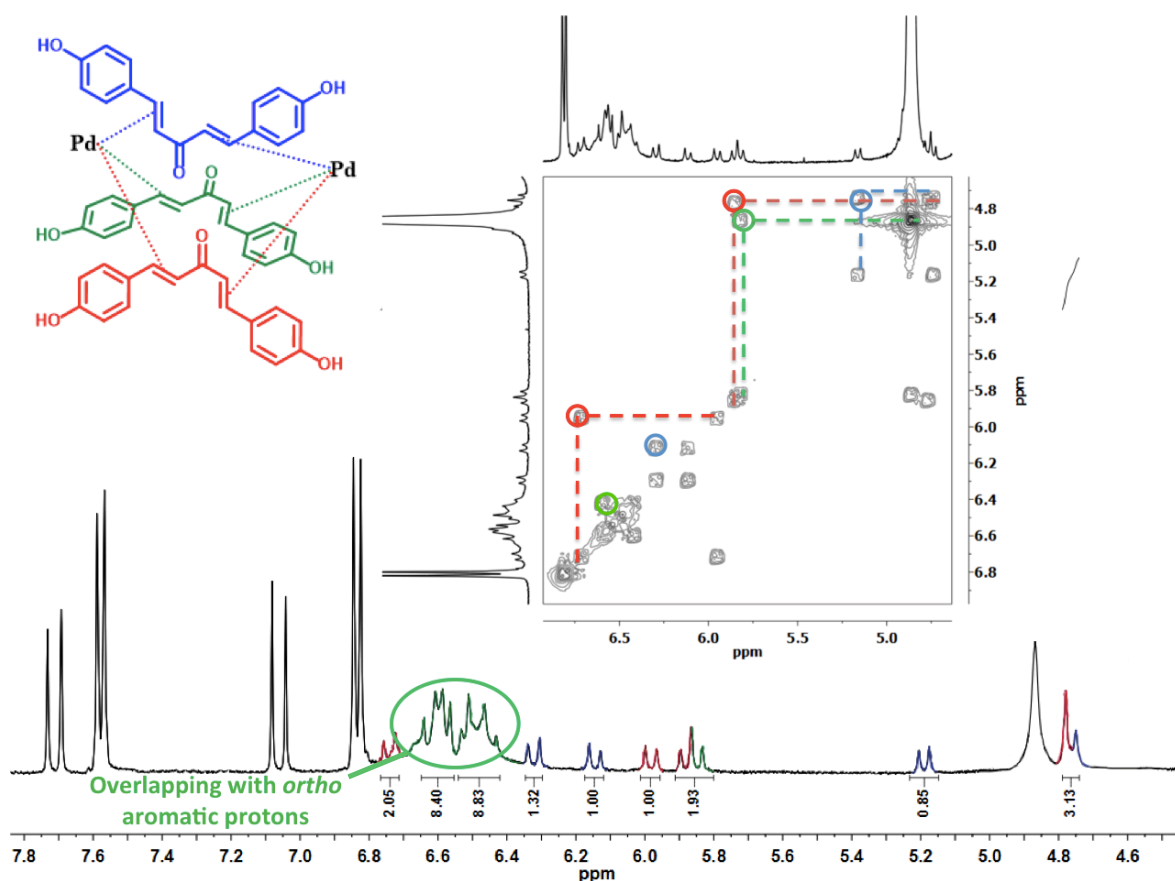


Figure 2.5 ^1H NMR spectrum and ^1H - ^1H COSY of $[\text{Pd}_2(\text{dba-4-OH})_3\cdot\text{dba-4-OH}]$ **7** (in CD_3OD , 400 MHz, 300 K).

The microanalytical data for this complex is different on hydrogen and carbon from the theoretical values. Expected for the chemical formula $\text{C}_{68}\text{H}_{56}\text{O}_{12}\text{Pd}_2$ is C 63.91%, H 4.42%. However, C 56.63%, H 4.65% was obtained. The data indicate that some PdNPs are present in the sample (suggested by low carbon content), which was later confirmed. An approximation can be made – $[\text{Pd}_2(\text{dba-4-OH})_3\cdot\text{dba-4-OH}]\cdot\text{Pd}_3(\text{CH}_3\text{OH})_{35}\cdot 3\text{H}_2\text{O}$, which gives theoretical values of C, 56.63%, H, 4.62%, closer to the experimental values obtained. No attempt was made to dry this material further, as it is known that the solvent can aid the stabilisation of Pd nanoparticles.¹⁴²

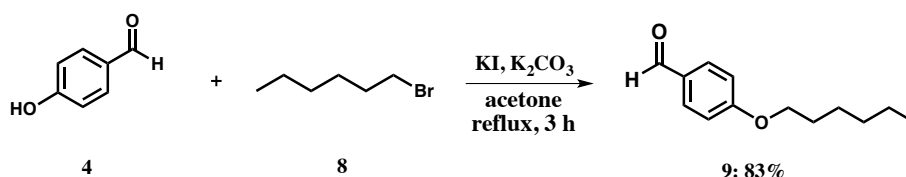
Table 2.2 ^1H NMR spectroscopic data for $[\text{Pd}_2(\text{dba-4-OH})_3\text{-dba-4-OH}]$ (CD_3OD , 400 MHz).

No.	δ_x / ppm	J / Hz	No.	δ_y / ppm	J / Hz	$\Delta\delta_{x1-y1}$ / ppm	<i>s-cis</i> or <i>s-trans</i>
H1	6.74	13.5	H6	5.99	13.5	0.75	<i>s-trans</i>
H10	6.63	13.4	H11	6.45	13.4	0.18	<i>s-cis</i>
H2	6.60	8.3	H3	6.49	8.3	0.15	<i>s-cis</i>
H4	6.33	12.9	H5	6.15	12.9	0.18	<i>s-cis</i>
H7	5.87	11.8	H9	4.77	11.8	0.10	<i>s-cis</i>
H8	5.19	11.8	H9	4.77	11.8	0.42	<i>s-trans</i>

2.3 Synthesis of hydroxylated– and alkyloxy–dba Pd complexes

2.3.1 Synthesis of the ligand for $[\text{Pd}_2(4\text{-OH},4'\text{-alkyloxy-dba})_3\cdot(4\text{-OH},4'\text{-alkyloxy-dba})]$

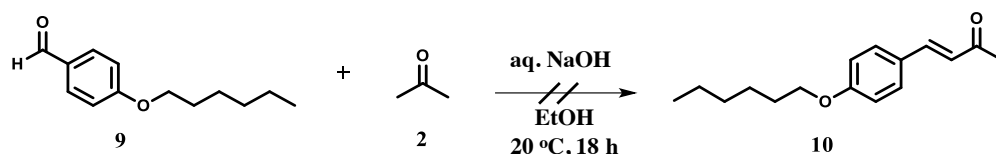
The synthesis of 4-hexylbenzaldehyde **9** was achieved by the reaction of commercially available **4** and 1-bromohexane **8**, mediated by the base, K_2CO_3 , under refluxing conditions for 6 h, using the method described.¹⁴⁴ The product **9** was isolated in 83% yield (after chromatography on silica gel) (Scheme 2.6).



Scheme 2.6 Synthesis of compound **9**.

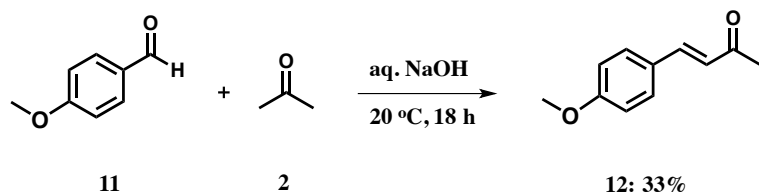
The ^1H NMR spectrum of the recrystallised material of **9** (in CDCl_3) exhibits the following key proton attributes – the aldehyde proton appears at 9.84 ppm as a singlet. The hexyl protons were observed at 3.92 (2H), 1.71 (2H), 1.43 (4H), 1.31 (2H) and 0.86 (3H) ppm. To improve the product conversion of the reaction, the solubility of the starting materials was found to be an issue. Changing the solvent to DMF increased the yield to 96%, which did not require column chromatography (residual DMF could be seen in the ^1H NMR spectrum of this product). Other conditions examined include: a) increasing the reaction temperature to 80 °C, where the yield dropped (53%); b) increasing the number of equivalents of 1-bromohexane (from 1.1 eqv. to 2 eqv.), although no improvement in product conversion was recorded (57%).

The Claisen-Schmidt condensation reaction between 4-hexoxybenzaldehyde **9** and acetone **2**, mediated by the NaOH, to give **10** was examined (Scheme 2.7). The reaction gave low yields of **10**, which can be explained by recovery of significant starting material **9**.

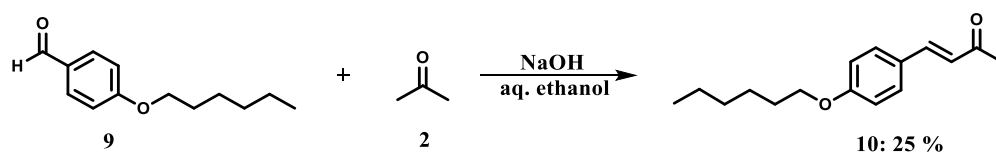


Scheme 2.7 Attempted synthesis of compound **10**.

In order to exploit the reactivity of the initial method for synthesis of **10**, the reaction was attempted using commercially available 4-methoxybenzaldehyde **11**, instead of **9** (Scheme 2.8). The results showed the method was feasible for the synthesis of **12**. There was no obvious change from the previous attempt. The product **12** was isolated in 33% yield by column chromatography. The ^1H NMR spectrum of **12** (in CDCl_3 , 400 MHz) exhibits the following key proton attributes: as a *trans*-alkene is formed, a proton at 6.60 ppm is observed with a $^3J_{\text{HH}}$ coupling constant of 16.2 Hz. The ^{13}C NMR spectrum exhibits 9 carbon signals. For example the C=O is seen at 198 ppm, along with the expected aromatic signals between 162-125 ppm.



Scheme 2.8 Synthesis of compound **12**.

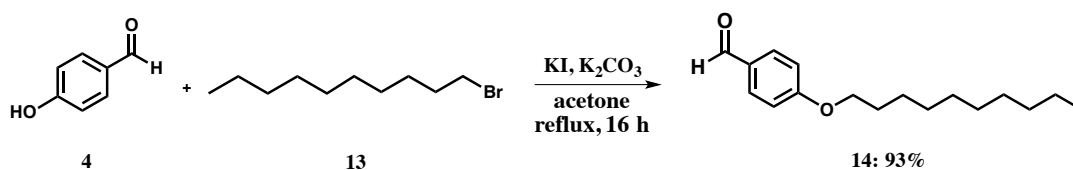


Scheme 2.9 Synthesis of compound **10**.

With the synthesis of compound **12** in hand, a similar approach was applied to **10**. Initial attempts afforded only low yields of the desired product **10**. The reactions were then tested under different conditions to improve the product yield. For example, increasing the reaction temperature from room temperature (*ca.* 18 °C) to 40 °C, or increasing the number of equivalents of NaOH, adding THF to the solvent system, or using EtOH-toluene- H_2O at different temperatures (70 °C and 50 °C).¹⁴⁵ In all cases, only low product yields were recorded (10%). Therefore, these practical difficulties meant this

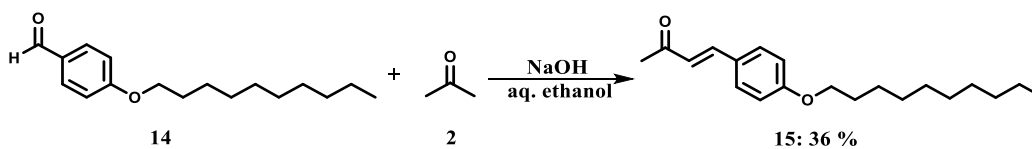
approach was deemed unfeasible. A second approach was therefore evaluated. A reaction was tested with ethanol as the solvent system (Scheme 2.9). The conversion was slightly increased after the product was purified by recrystallisation from ethanol (25% yield). A modified version of work-up was developed: recrystallised from hot ethanol with warm water in the flask, adding H₂O dropwise with cooling precipitated small crystals – the product was then isolated in 34% yield by column chromatography on silica gel. The ¹H NMR spectrum of **10** (in CDCl₃, 400 MHz) exhibits the following key proton attributes: as a *trans*-alkene is formed, one of protons at 6.60 ppm is observed with a ³J_{HH} coupling constant of 16.2 Hz. The other proton (δ 7.47) is overlapped with the *ortho*-aromatic protons. The ¹³C NMR spectrum exhibits 16 carbon signals. For example, the C=O group is seen at 162 ppm, and a range of aromatic signals between 125-145 ppm. The IR spectrum of compound **10** exhibits a band at 1607 cm⁻¹ which is assigned to ν(C=O), whereas the band at 1592 cm⁻¹ corresponds to ν(C=C).

The synthesis of 4-(decyloxy)benzaldehyde **14** was attempted by reacting **4** and 1-bromodecane **13**, mediated by K₂CO₃, under refluxing conditions for 36 h, using the method described in the literature (Scheme 2.10).¹⁴⁴



Scheme 2.10 Synthesis of decane compound **14**.

This allowed isolation of product **14** as a liquid in 93% yield, after column chromatography on silica gel. The ¹H NMR spectrum of the recrystallised material (in CDCl₃) exhibits the following key proton attributes – the aldehyde signal appears as a singlet at δ 9.80 ppm. The hexyl signals were observed at δ 4.05 (2H), δ 1.75 (2H), δ 1.30-1.60 (14H), δ 0.82 (3H) ppm. The mass spectrum shows the expected mass ion at *m/z* 263.2008 (MH⁺) and *m/z* 285.1832 (MNa⁺) by ESI-MS.

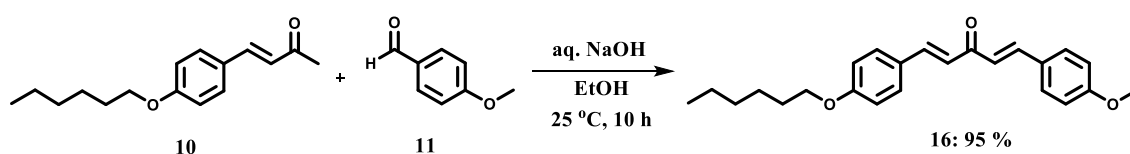


Scheme 2.11 Synthesis of target compound **15**.

Following the same procedure for the synthesis of **10** in NaOH at room temperature, target compound **15** was synthesised, where similar problems were noted. The product was contaminated by a mixture of unknown by-products, which were difficult to separate by column chromatography. The product was isolated in 36% yield. The ¹H NMR spectrum of **15** (in CDCl₃, 400 MHz) exhibits the following

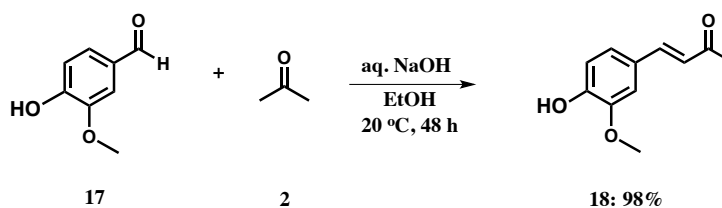
key proton attributes: as a *trans*-alkene is formed, protons at 6.60 and 7.45 ppm (with ArH overlapped) are observed with a $^3J_{\text{HH}}$ coupling constant of 16.2 Hz. The IR spectrum of **15** exhibits a band at 1667 cm^{-1} , is assigned to $\nu(\text{C}=\text{O})$. The mass spectrum shows the expected pseudomolecular mass ion at m/z 303.2316 (MH^+) and sodiated molecular ion m/z 325.2138 (MNa^+) by ESI-MS.

The novel 4-OH,4'-hexyloxy-dba ligand **16** was synthesised in a similar way to that described for **10** (Scheme 2.12). The product precipitates from the reaction mixture and was isolated in high yield (95%), as an air stable white solid. The ^1H NMR spectrum of **16** (in CDCl_3 , 400 MHz) exhibits the following key proton attributes: as a *trans*-alkene is formed, two protons at 7.70 and 6.95 ppm are observed with a $^3J_{\text{HH}}$ coupling constant of 16.2 Hz. The IR spectrum of **16** exhibits a band at 1689 cm^{-1} assigned to $\nu(\text{C}=\text{O})$. The ^{13}C NMR spectrum exhibits 9 carbon signals. For example, the $\text{C}=\text{O}$ is seen at 189.9 ppm, along with the expected aromatic signals between 124-162 ppm.



Scheme 2.12 Synthesis of compound **16**.

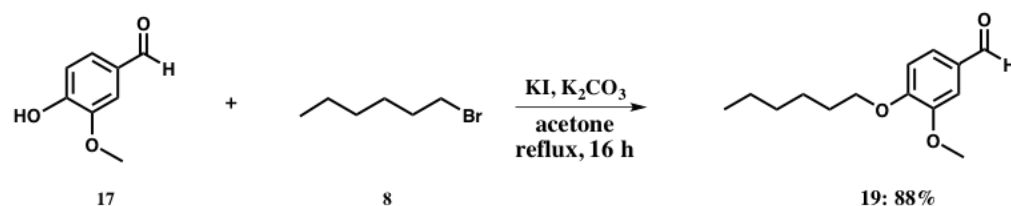
In order to bring the hydroxyl group into the dba framework, the synthesis of **18** was attempted from commercially available **17** (vanillin), follow a one-step reaction procedure, using the method of Kuo-Hsiung Lee *et al.*¹⁴⁶ The product was isolated in high yield (98 %) *via* simple purification involving extraction of the aqueous solution with CHCl_3 (Scheme 2.13).



Scheme 2.13 Synthesis of compound **18**.

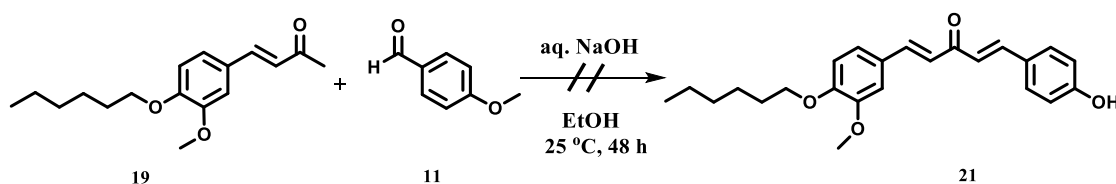
The ^1H NMR spectrum of **18** (in CDCl_3 , 400 MHz) exhibits the following key proton attributes: as a *trans*-alkene is formed, protons at 7.42 and 6.58 ppm are observed with a $^3J_{\text{HH}}$ coupling constant of 16.2 Hz. The IR spectrum of **18** exhibits a band at 1668 cm^{-1} , which is assigned to $\nu(\text{C}=\text{O})$, whereas the band at 1581 cm^{-1} which is assigned to $\nu(\text{C}=\text{C})$. The ^{13}C NMR spectrum reveals the $\text{C}=\text{O}$ group at 199 ppm, along with a range of aromatic signals between 150-125 ppm.

Following these encouraging results, the synthesis of **19** was attempted from **17** and **8**, mediated by K_2CO_3 , under refluxing conditions for 24 h.¹⁴⁴ The product was isolated as a liquid in 88% yield (Scheme 2.14). The ^1H NMR spectrum of **19** (in CDCl_3 , 400 MHz) exhibits the following key proton attributes: as a *trans*-alkene is formed, protons at δ 7.41 ppm and δ 6.55 ppm are observed with a $^3J_{\text{HH}}$ coupling constant of 16.2 Hz. The hexane signal could be observed at δ 1.84-1.71(2H), δ 1.46-1.22 (6H), δ 0.88-0.82 ppm. The ^{13}C NMR spectrum exhibits 16 carbon signals. For example the $\text{C}=\text{O}$ is seen at δ 149.6 ppm, along with the expected aromatic signals between δ 110-125 ppm.



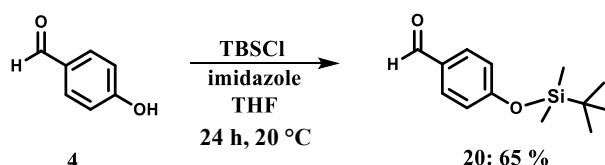
Scheme 2.14 Synthesis of compound **19**.

With both components in hand, synthesis of the dba ligand **21** was first attempted by the same method as compound **9** (Scheme 2.15). Unfortunately, no reaction was observed, as the starting material **19** decomposed slowly under the reaction conditions.



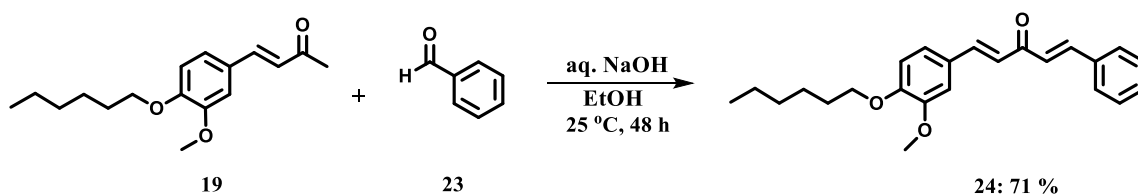
Scheme 2.15 Attempted synthesis of compound **21**.

The TBS group is bulky enough to selectively protect primary alcohols.¹⁴⁷⁻¹⁴⁹ Therefore, protected silyl ether compound **20** was synthesized using a catalytic amount of imidazole in THF (Scheme 2.16).¹⁵⁰ The product was isolated as a liquid in 65% yield, after chromatography on silica gel. Compound **20** was recrystallised from ethyl acetate. ^1H NMR spectrum of the **20** (in CDCl_3) exhibits the following key proton attributes – the aldehyde signal appears as a singlet at δ 9.86 ppm; the signals where the two methyl groups are connected to the Si could be observed at δ 0.22 ppm (6 H) as a single peak. The signals for the *tert*-butyl group could be observed at δ 0.97 ppm (9 H) as a singlet.



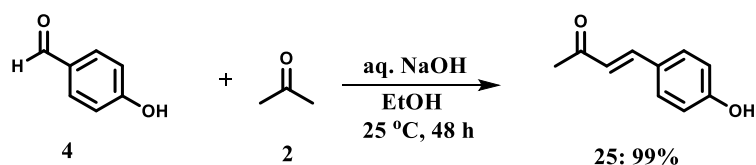
Scheme 2.16 Synthesis of compound 20.

In order to exploit the activity of the **19**, the synthesis of **24** was attempted (Scheme 2.17). The product was isolated as a liquid in 71% yield (after chromatography on silica gel). The ^1H NMR spectrum of **24** (in CD_3OD , 400 MHz) exhibits the following key proton attributes: as a *trans*-alkene is formed, two proton signals at 7.82 - 7.75 and 7.16 ppm are observed with a $^3J_{\text{HH}}$ coupling constant of 16.2 Hz, which is expected for an enone. The other proton signal (7.79) was overlapped with the *ortho* aromatic protons. ^{13}C NMR spectrum exhibits 17 carbon signals. For example, the C=O group is seen at 193.5 ppm, along with a range of aromatic signals between 162-124 ppm. The IR spectrum of compound **24** exhibits a band at 1667 cm^{-1} is assigned to $\nu(\text{C}=\text{O})$, whereas the band at 1595 cm^{-1} is assigned to $\nu(\text{C}=\text{C})$.



Scheme 2.17 Synthesis of compound 24.

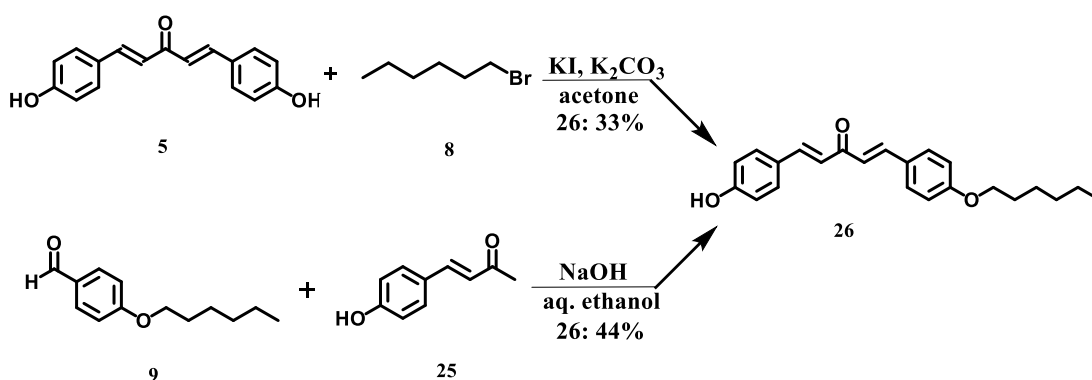
When the synthesis of dba-4-OH **5** (see page 57) was tested under various conditions, an intriguing result was obtained and it is not immediately obvious why the results are different to the expected result. Due to excess acetone being used in the reaction, the product obtained was not the desired one, instead it was hydroxyl compound **25**. To test the reproducibility of the reaction, as in the case of the hydroxylated dba compound **3**, it is also necessary to adjust the pH of the reaction medium. This was achieved by addition of solid CO_2 (dry ice), which increased acidity leading to product precipitation as a yellow solid which can easily filtered and dried in air, and did not require further purification. Using this work-up procedure a yield of **25** of 99% was recorded (Scheme 2.18).



Scheme 2.18 Synthesis of compound 25.

The ^1H NMR spectrum of compound **25** (in CDCl_3 , 400 MHz) exhibits the following key proton attributes: a *trans*-alkene with proton signals at δ 7.85 and 6.62 ppm and $^3J_{\text{HH}}$ coupling constant of 16.2 Hz. The ^{13}C NMR spectrum exhibits 17 carbon signals. For example, the C=O is seen at 193.5 ppm, and a range of aromatic signals between 118-155 ppm. The mass spectrum shows the expected protonated mass ion at m/z 163.0754 (MH^+) by ESI-MS.

The novel 4-OH, 4'-alkyloxy dba ligand **26**, was synthesised from dba-4-OH **5** and 1-bromohexane **8**. The reaction of **5** and **8** in the presence of K_2CO_3 and KI and acetone under reflux for 24 h gave low yields of the product (33%), which can be explained by a poor conversion to product (and recovery of a large amount of starting material) and difficulty in separating side-products by chromatography (Scheme 2.19). The reaction gave four components (see Experiment Section), which allowed compound **25** to be tested in the Claisen-Schmidt condensation.



Scheme 2.19 Synthesis of 4-OH, 4'-OHexyl dba compound **26**.

A second approach was therefore evaluated, with having the promising hydroxyl compound **25** in hand. A Claisen-Schmidt condensation reaction between **9** and **25**, mediated by base (NaOH), was tested. However, in the case of these hydroxylated dba compounds it was necessary to adjust the pH of the reaction medium. This was achieved by addition of solid CO_2 (dry ice), leading to product precipitation. Pleasingly, the product was isolated as a dark yellow solid in 44% yield (after chromatography on silica gel) (Scheme 2.19). The by-product was 4-alkyloxy dba **35** (see p78) isolated, in 48% yield (after chromatography on silica gel). The ^1H NMR spectrum of the **26** (in CDCl_3) exhibits the following key proton attributes – as a *trans*-alkene is formed, two protons at 7.69 and 6.90 ppm are observed with a $^3J_{\text{HH}}$ coupling constant of 16.0 Hz (Figure 2.6). The signal of

hydroxyl group is singlet at 8.09 ppm. The mass spectrum shows the expected mass ion at m/z 351.1943 (MH^+) by ESI-MS. ^{13}C NMR spectrum exhibits 22 carbon signals. For example, the $C=O$ is seen at 189.6 ppm, along with the expected aromatic signals between 162-125 ppm. The IR spectrum of compound **24** exhibits a band at 1598 cm^{-1} , which is assigned to $\nu(C=C)$. For by-product **35**, the 1H NMR spectrum of the material (in $CDCl_3$) exhibits the following key proton attributes – as a *trans*-alkene is formed, two protons at 7.71 and 6.91 ppm are observed with a $^3J_{HH}$ coupling constant of 16.1 Hz. The mass spectrum shows the expected mass ion at m/z 435.2889 (MH^+) by ESI-MS. ^{13}C NMR spectrum exhibits 13 carbon signals. For example, the $C=O$ is seen at 186.7 ppm, along with a range of aromatic signals between 161-124 ppm. The IR spectrum of compound **24** exhibits a band at 1595 cm^{-1} assigned to $\nu(C=C)$. All data was exactly the same as using an alternative method for synthesis of **35**.

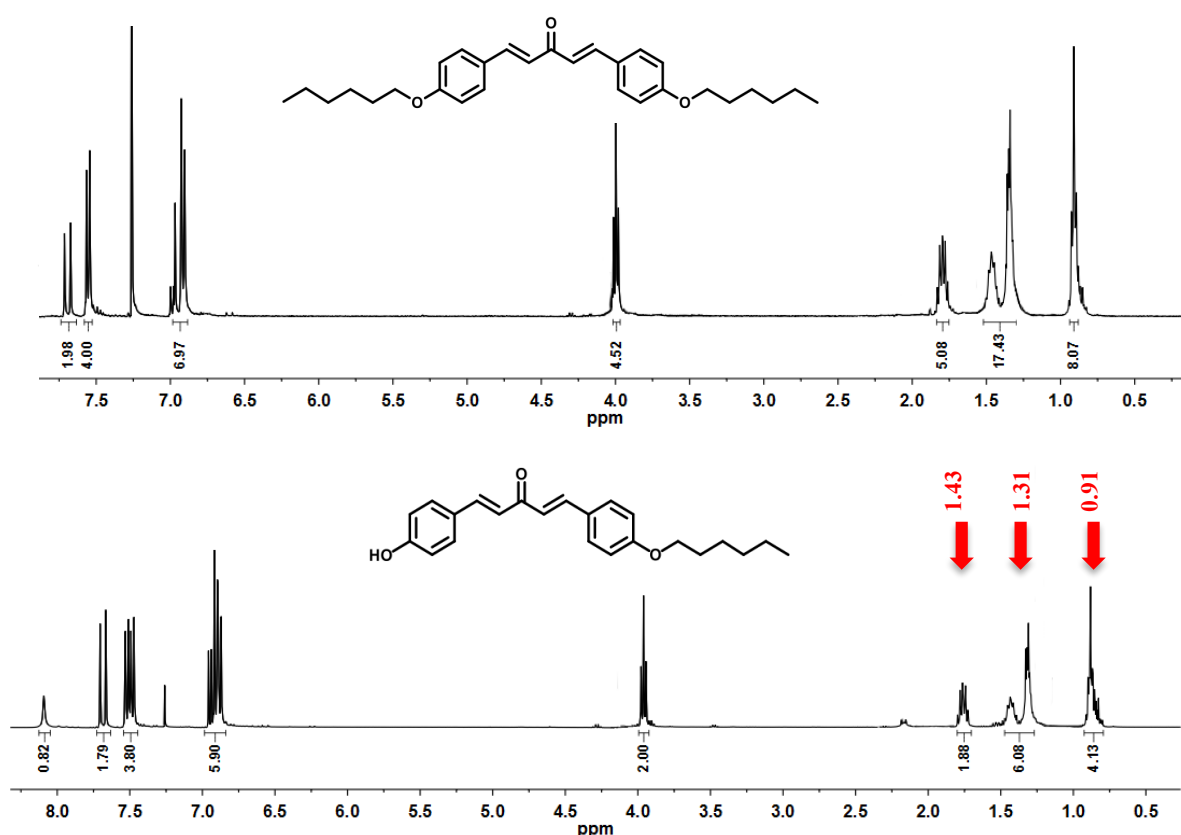
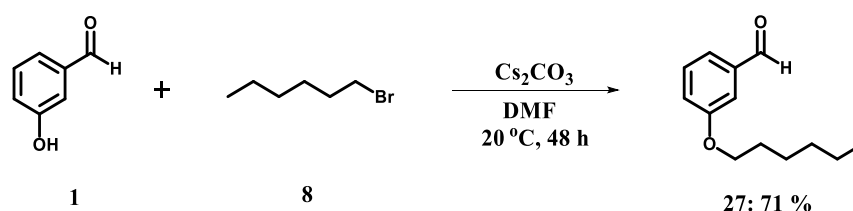


Figure 2.6 1H NMR spectrum of **26** and by-product of **26** (**35**) (in $CDCl_3$, ref. δ 7.26, 400 MHz).

2.3.2 Synthesis of the ligand for $Pd_2(4-OH, 3'-alkyloxy\ dba)_3 \cdot (4-OH, 3'-alkyloxy\ dba)$

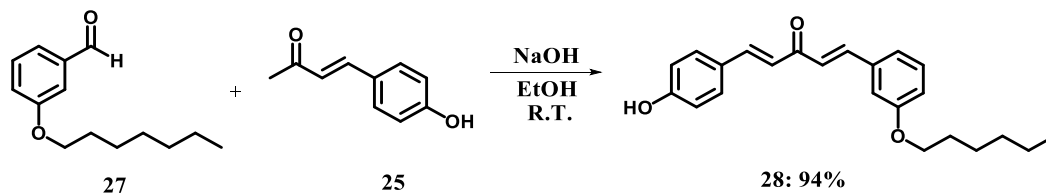
Initially it was proposed that 3-hydroxybenzaldehyde **1** and 1-bromohexane **8** could be used to synthesize **27**, mediated by KOH.¹⁵¹ The reaction of KOH in DMSO gave low yields of the product, which can be explained by poor product conversion (and recovery of a large amount of starting material, 82% of starting material). The reactions were then tested under different conditions. For

example, increasing the reaction temperature from room temperature (*ca.* 18 °C) to 50 °C, and altering the solvent from DMSO to DMSO/water. In all cases, only low product yields were recorded. This approach was therefore deemed unfeasible. A second approach was therefore evaluated: using Cs₂CO₃ as the base in DMF.¹⁵² Although the reaction did not reach full conversion, the product was isolated as a liquid in 71% yield (after chromatography on silica gel). This approach proved more successful (Scheme 2.20). The ¹H NMR spectrum of the recrystallised material (in CDCl₃) exhibits the following key proton attributes – the aldehyde signal appears as a singlet at 9.95 ppm. The hexyl group was observed at 3.99 (CH₂), 1.78 (CH₂), 1.47 – 1.28 (3 × CH₂), and 0.89 (CH₃) ppm.



Scheme 2.20 Synthesis of compound 27.

The novel 4-OH, 3'-alkyloxy dba ligand, **28**, was synthesised from aldehyde **27** and hydroxyl motif **25**. It was decided to investigate the Claisen-Schmidt condensation reaction, which is mediated by the base (NaOH) in ethanol (Scheme 2.21).



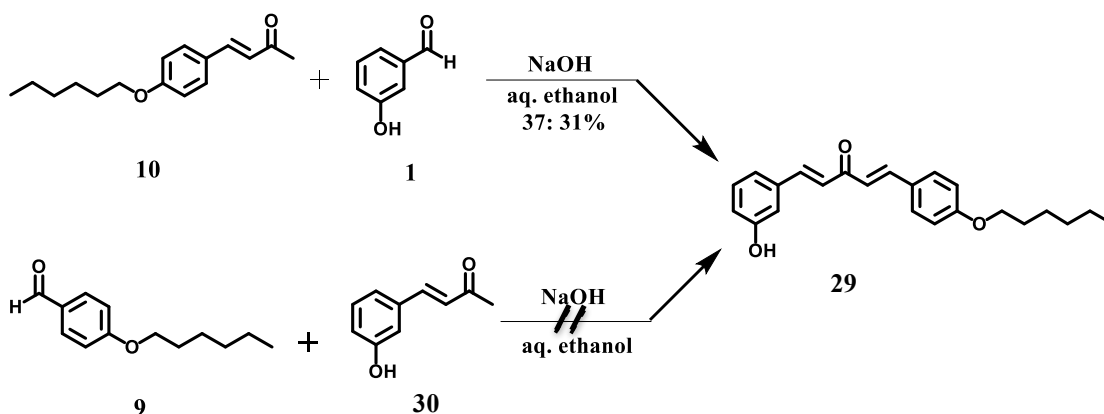
Scheme 2.21 Synthesis 4-OH, 3'-OHexyl dba compound **28**.

In the synthesis of unsubstituted dba the product simply precipitates from the reaction mixture. However in the case of **28** it was necessary to adjust the pH of the reaction medium. This was achieved by addition of solid CO₂ (dry ice), which increases the acidity leading to product precipitation as a yellow solid, which can be easily filtered, and does not require column chromatography. However, unlike the symmetrical hydroxylated dba ligands **3** and **5**, compound **28** was sticky even after drying in air. Nevertheless, an excellent yield (94%) was recorded. The ¹H NMR spectrum of this compound (in CDCl₃, 400 MHz) exhibits the following key proton attributes: as a *trans*-alkene is formed, two protons at 7.69 and 6.55 ppm are observed with a ³J_{HH} coupling constant of 16.2 Hz, which is expected for this type of enone product. The hexyl group signals were confirmed with signals at 3.98 (OCH₂), 1.85 – 1.29 (4×CH₂), 0.91 (CH₃) ppm. The ¹³C NMR spectrum exhibits 18 carbon signals. For example, the C=O is seen at 190.4 ppm, along with the

expected aromatic signals between 161-124 ppm. The IR spectrum of compound **24** exhibits a band at 1596 cm^{-1} which is assigned to $\nu(\text{C}=\text{C})$. The mass spectrum shows the expected mass ion at m/z 351.1939 (MH^+) by ESI-MS.

2.3.3 Synthesis of the ligand for $\text{Pd}_2(3\text{-OH, 4'-alkyloxy dba})_3 \cdot (3\text{-OH, 4'-alkyloxy dba})$

From the previous experience, the hydroxyl group caused problems with synthesis (as it also showed for synthesis of dba ligand with 4-hydroxy group motif), so the reaction of synthesis of **30** by benzylidene acetone **29** and **1** at room temperature was first attempted (Scheme 2.22). The novel 3'-OH, 4-alkyloxy dba ligand **29** was synthesised and contaminated by unknown by-products, which was purified by column chromatography. The reaction mixture then was purified, and gave four separable compounds, *i.e.* starting material, target product **29**, **34**, and a mixture of **29** and **34**. The product **29** was isolated as a liquid in 31% yield (after chromatography on silica gel) (Scheme 2.22).



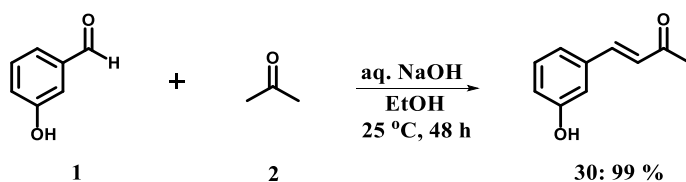
Scheme 2.22 Synthesis of 3'-OH, 4-alkyloxy dba compound **29**.

The ^1H NMR spectrum of **29** (in CDCl_3 , 400 MHz) exhibits the following key proton attributes: as a *trans*-alkene is formed, one of protons at 7.76 ppm is observed with a $^3J_{\text{HH}}$ coupling constant of 16.2 Hz. The other proton is overlapped with *ortho* aromatic protons. The hexyl group signals could be observed at 4.04 (2H), 1.83 – 1.75 (2H), 1.54 – 1.31 (6H), 0.94 (3H) ppm. The ^{13}C NMR spectrum exhibits 16 carbon signals. For example, the $\text{C}=\text{O}$ is seen at 188.3 ppm, along with a range of aromatic signals between 160-125 ppm. The IR spectrum of **29** exhibits a band at 1596 cm^{-1} , assigned to $\nu(\text{C}=\text{C})$. The mass spectrum shows the expected mass ion at m/z 351.1945 (MH^+) by ESI-MS.

2.3.4 Preparation of the ligand and complex for Pd₂(3-OH, 3'-alkyloxy dba)₃

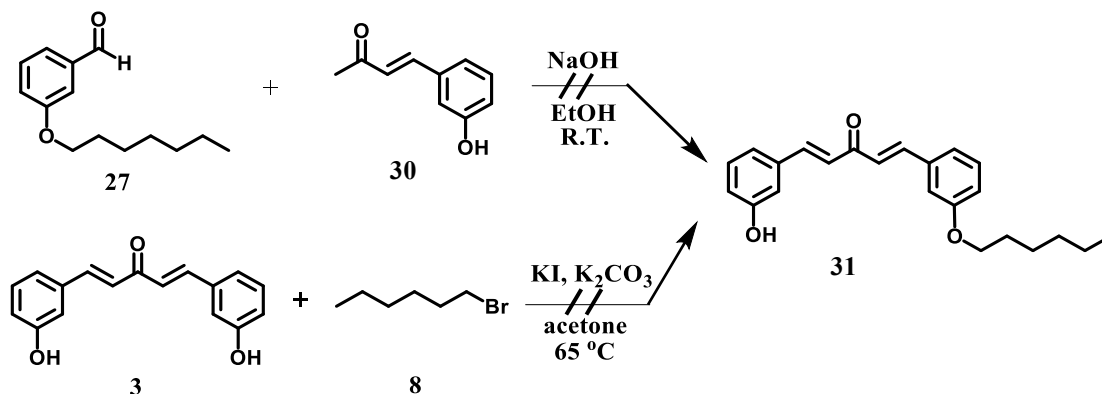
2.3.4.1 Preparation of the ligand for Pd₂(3'-OH, 3-alkyloxy dba)₃

The same approach was followed as for the synthesis of **25**. The product was isolated in high yield as an air-stable yellow solid *via* simple work-up (99%, Scheme 2.23). The ¹H NMR spectrum of **30** (in CD₃OD, 400 MHz) exhibits the following key proton attributes: a *trans*-alkene formed, with protons at 7.57 and 6.11 ppm, with a ³J_{HH} coupling constant of 16.2 Hz, which is expected for this type of enone product. The ¹³C NMR spectrum exhibits 9 carbon signals. For example, the C=O is seen at 198.2 ppm, and the expected aromatic signals between 118-150 ppm.



Scheme 2.23 Synthesis of 3-hydroxy compound **30**.

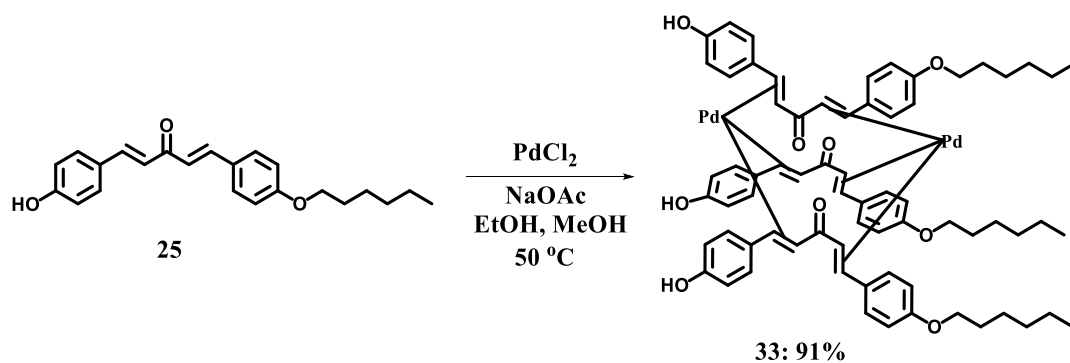
The 3'-OH, 3-alkyloxy dba ligand, **31**, could be prepared by reaction of **3** and **8** (Scheme 2.24). The reaction of K₂CO₃ in KI and acetone system reflux for 40 h gave low yields of the product. However, under a variety of conditions, including altering the equivalents of 1-bromohexane, or high temperature, no reaction was found to occur.



Scheme 2.24 Synthesis of 3'-OH, 3'-alkyloxy dba compound **31**.

2.3.4 Synthesis of the complex of Pd₂(4-OH, 4'-alkyloxy dba)₃•(4-OH, 4'-alkyloxy dba)

The preparation of complex **33** was first attempted by reaction of the dba ligand **25** with PdCl₂ in the presence of reducing agent (NaOAc) in MeOH and EtOH (3:2, v/v). This reaction turned a green colour after heating at 50 °C for 2 h at 1.78×10⁻² M concentration afforded Pd nanoparticles (uncharacterised), which precipitated from solution (Scheme 2.25).



Scheme 2.25 Synthesis of Pd complex 33.

The reaction time was reduced to 20 min, which led to less Pd nanoparticle formation. It is proposed that the longer reaction times aids complex decomposition to form Pd nanoparticles. Subsequently it was determined that the concentration of the reactions affects the outcome of the reaction. At a higher concentration of PdCl_2 ($2.33 \times 10^{-2} \text{ M}$), for 20 mins, gave a purple complex in 91% yield. The UV-vis spectrum (MeOH) showed a band for the Pd complex ($\lambda_{\text{max}} = 552 \text{ nm}$), which is associated with the d-d transition, comparing well with $\text{Pd}_2(\text{dba})_3$ ($\lambda_{\text{max}} = 520 \text{ nm}$).¹⁴³ The ^1H NMR spectrum of this complex (in CD_3OD) shows that 12 alkenic protons are visible (as doublets), which were correlated by ^1H COSY (Figure 2.7).

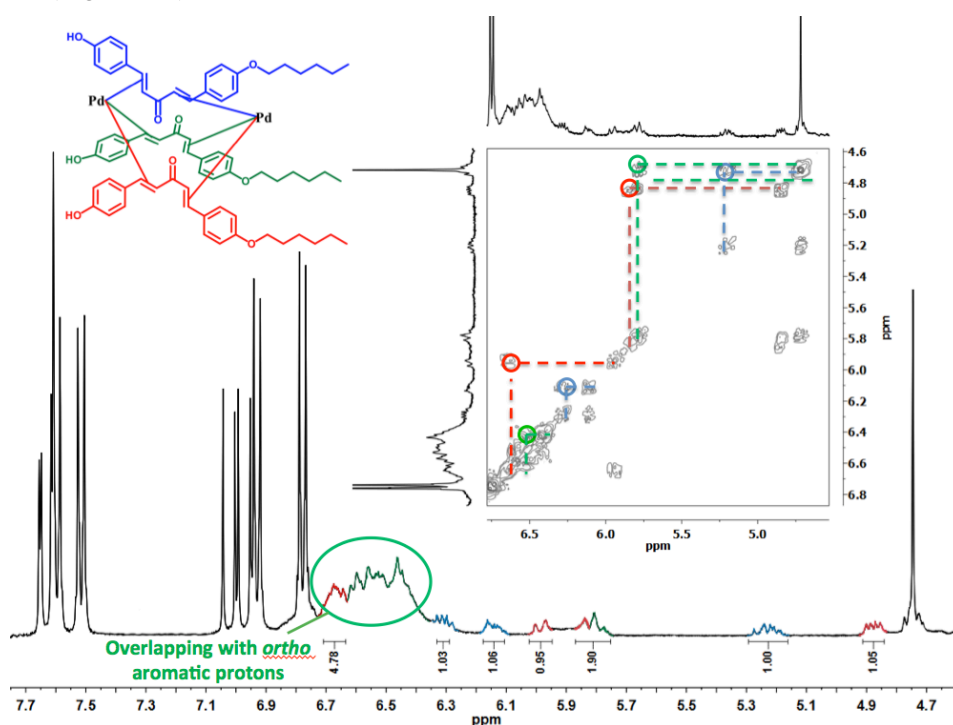


Figure 2.7 ^1H NMR and ^1H - ^1H COSY spectrum of Pd complex 33 (in THF-d_8 , ref. δ 3.58, 1.72, 400 MHz).

The ^1H - ^1H COSY spectrum of the Pd complex **33** showed that H-1 coupled with H-6 and that H-2 significantly correlated with H-3, and H-4 coupled with H-5, H-7 coupled with H-9, and H-8 coupled with H-10, H-7 coupled with H-10 from ^1H - ^1H COSY spectrum (Table 2.2). This confirms the presence of 12 alkene protons (two different Pd environments). A free ligand was also observed, so the following formulation has been proposed - $\text{Pd}_2(4\text{-OH},4'\text{-alkyloxy-dba})_3\cdot 4\text{-OH},4'\text{-alkyloxy-dba}$.

The microanalytical data for complex **33** does not match expected chemical formula on hydrogen and carbon, based on the theoretical values. The expected for the chemical formula $\text{C}_{92}\text{H}_{102}\text{O}_{12}\text{Pd}_2$ is C 68.44%, H 6.49%. However, C 62.46%, H 6.64% was obtained. The data indicate that PdNPs are present in the sample (low carbon content), which was later confirmed (see section 2.5). The high hydrogen content suggests that solvent is also present. An approximation calculation can be made – $[\text{Pd}_2(\text{dba-4-OH},4'\text{-OHhexyl})_3\cdot\text{dba-4-OH},4'\text{-OHhexyl}]\cdot\text{Pd}_4(\text{CH}_3\text{OH})_3$, which gives theoretical values of C, 63.31%, H, 6.61%, which is closer to the experimental values obtained.

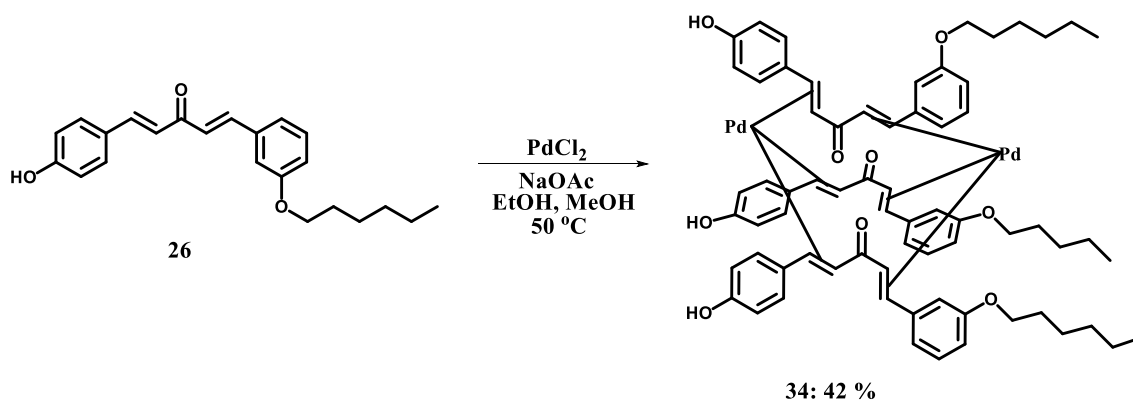
Due to the ligand **26** is being as symmetrical, and contained hydroxyl group and hexyl group, ligand **26** gives rise to increased conformational possibility and isomeric preferences (Table 2.3). As a result, some couplings are not clear (*i.e.* couplings at 6.56 and 6.31 ppm). According to the $\Delta\delta_{\text{X1-Y1}}$ value, a *s-cis* conformation was deduced for H2 and H3, H4 and H5, H7 and H9.

Table 2.3 ^1H NMR spectroscopic data for complex **33**.

No.	δ_{X} / ppm	J / Hz	No.	δ_{Y} / ppm	J / Hz	$\Delta\delta_{\text{X1-Y1}}$ / ppm	<i>s-cis</i> or <i>s-trans</i>
H1	6.68	13.5	H6	5.98	13.5	0.7	<i>s-trans</i>
H2	6.56	-	H3	6.46	-	0.1	<i>s-cis</i>
H4	6.31	13.5	H5	6.15	13.5	0.16	<i>s-cis</i>
H7	5.81	12.4	H9	4.87	12.4	0.06	<i>s-cis</i>
H8	5.22	12.9	H10	12.59	12.9	0.47	<i>s-trans</i>
H7	5.73	12.9	H10	4.75	12.9	0.98	<i>s-trans</i>

2.3.6 Synthesis of the complex of $\text{Pd}_2(4\text{-OH}, 3'\text{-alkyloxy dba})_3\cdot(4\text{-OH}, 3'\text{-alkyloxy dba})$

Preparation of complex **34** was first attempted by reaction of **26** with PdCl_2 in the presence of NaOAc in MeOH and EtOH (3:2, v/v). At a higher concentration of PdCl_2 (2.27×10^{-2} M), and conducting the reaction for 20 mins, afforded a purple complex in 42% yield (Scheme 2.26). The UV-vis spectrum (MeOH) showed a band for the Pd complex ($\lambda_{\text{max}} = 544$ nm), which compares well with $\text{Pd}_2(\text{dba})_3$ ($\lambda_{\text{max}} = 520$ nm).¹⁴³ The ^1H NMR spectrum of complex **34** (in CD_3OD) shows that the 12 alkene protons are visible (as doublets) (Table 2.4).



Scheme 2.26 Synthesis of Pd complex 34.

Table 2.4 ^1H NMR data for complex 34.

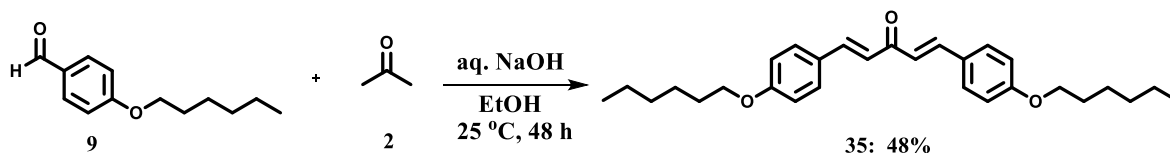
No.	δ (complex 45) / ppm	No.	δ (complex 45) / ppm
1	6.47	7	5.82
2	6.40	8	5.67
3	6.33	9	5.46
4	6.29	10	5.23
5	6.16	11	4.98
6	6.01	12	4.82

The microanalytical data for this complex is good on carbon. The expected data, based on the chemical formula $\text{C}_{91}\text{H}_{102}\text{O}_{12}\text{Pd}_2$ is C 62.87%, H 6.42%. C 62.56%, H 8.61% were obtained. The high hydrogen content suggests that solvent is present. An approximate calculation can be made – $[\text{Pd}_2(\text{dba-4-OH,3'-OHHexyl})_3\text{-dba-4-OH,3'-OHHexyl}] \cdot \text{Pd}_2(\text{CH}_3\text{OH})_{16} \cdot \text{H}_2\text{O}$, gives theoretical values of C, 62.85%, H, 8.59%, which is closer to the experimental values obtained.

2.4 Synthesis of alkyloxy dba Pd complexes

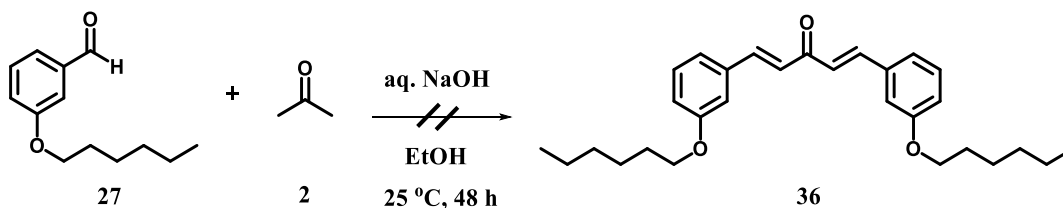
2.4.1 Synthesis of the ligand for $\text{Pd}_2(4,4'\text{-alkyloxy-dba})_3 \cdot (4,4'\text{-alkyloxy-dba})$

The novel 4'-alkyloxy dba ligand **35** was synthesised from **9** and acetone **2**. It was decided to investigate the Claisen-Schmidt condensation reaction between two 4-hexoxybenzaldehydes and acetone, mediated by NaOH, which gave the product in 48% yield (Scheme 2.27).



Scheme 2.27 Synthesis of symmetrical hexane-dba 35.

2.4.2 Synthesis of the ligand for $\text{Pd}_2(3, 3'\text{-alkyloxy dba})_3 \cdot (3, 3'\text{-alkyloxy dba})$

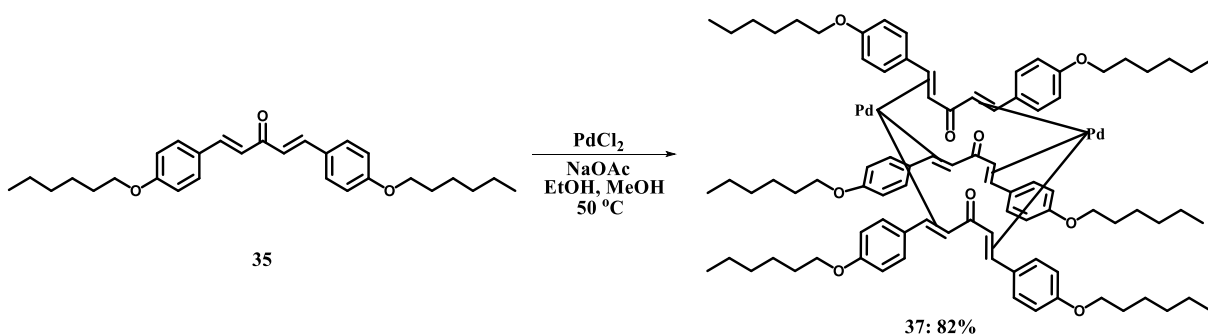


Scheme 2.28 Synthesis of ligand 36.

A similar method for the synthesis of **36** was used (Scheme 2.28), although no reaction was observed, which may be a result of starting material **27** decomposing under the reaction conditions.

2.4.3 Synthesis of the complex of $\text{Pd}_2(4\text{-alkyloxy-dba})_3 \cdot (4\text{-alkyloxy-dba})$

Preparation of $\text{Pd}_2(4\text{-alkyloxy-dba})_3 \cdot 4\text{-alkyloxy-dba}$ complexes was first attempted by reaction of the 4-alkyloxy-dba ligand with PdCl_2 in the presence of NaOAc in MeOH and EtOH (3:2, v/v) (Scheme 2.29). This reaction turned a green colour, which after heating at 60 °C for 4 h at 1.75×10^{-2} M concentration afforded Pd nanoparticles (uncharacterised), which precipitated from solution. The reaction was attempted under other conditions: the reaction time was reduced to 10 min, and less nanoparticle formation was observed. It is proposed that the longer reaction time may have led to the product complex decomposing to form Pd nanoparticles; in a second attempt, the concentration of PdCl_2 was increased. Subsequently it was determined that the concentration of the reactions seemed to affect the outcome of the reaction. At a higher concentration of PdCl_2 (2.33×10^{-2} M) for 10 mins, afforded a purple complex in 82% yield.



Scheme 2.29 Synthesis of complex Pd complex 37.

The UV-vis spectrum (chloroform) showed a band for the Pd complex ($\lambda_{\text{max}} = 540 \text{ nm}$), associated with the d-d transitions, comparing well with $\text{Pd}_2(\text{dba})_3$ ($\lambda_{\text{max}} = 520 \text{ nm}$).¹⁴³ The ^1H NMR spectrum of complex 37 (in CDCl_3) shows that the 12 protons of the alkene are visible (as doublets), which were correlated by ^1H COSY (Figure 2.8).

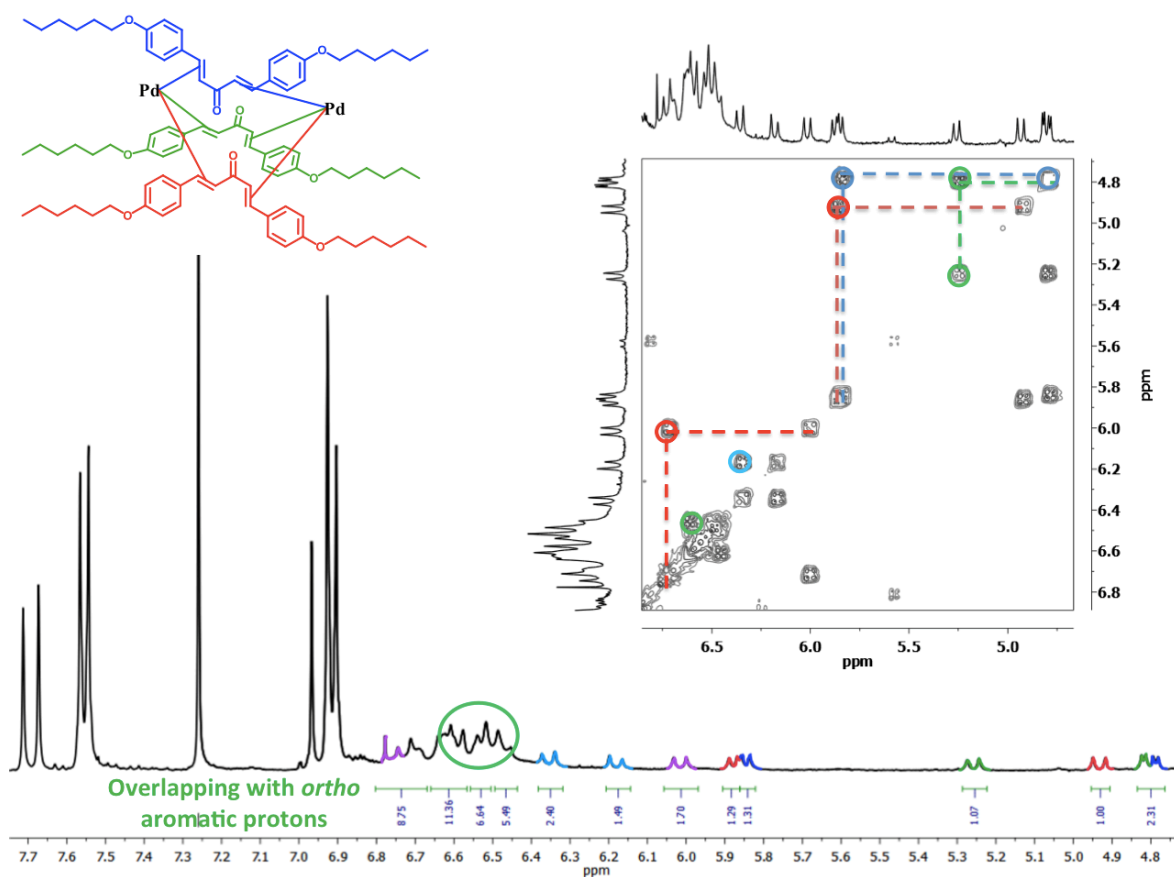


Figure 2.8 ^1H NMR and ^1H - ^1H COSY spectrum of Pd complex 37 (in CDCl_3 , ref. δ 7.26, 400 MHz).

The microanalytical data for this complex is in good agreement on hydrogen and carbon with theoretical values, based on the chemical formula $C_{116}H_{152}O_{12}Pd_2$, C 71.40%, H 7.85%. Values of 71.61%, H 7.76% were obtained, which showed the material to be pure. The 1H COSY spectrum of Pd complex **37** showed that H-2 coupled with H-3 and that H-4 significantly correlated with H-5, and H-8 coupled with H-12, and H-6 coupled with H-1, and H-7 coupled with H-10, and H-9 coupled with H-11 in 1H - 1H COSY spectrum (Table 2.4). This confirms the presence of 12 alkenic protons (and two different Pd environments). A free ligand is also observed, so the following formulation is proposed $Pd_2(4\text{-alkyloxy-dba})_3 \cdot 4\text{-alkyloxy-dba}$. Twelve protons have been coupled with each other from results of 1H - 1H COSY NMR. Among these, the entire coupling constant for each olefin should be the same, which indicate the Pd steadily, coordinated to the alkene (Table 2.5).

Table 2.5 1H NMR data for complex **37**.

No.	δ_X / ppm	J / Hz	No.	δ_Y / ppm	J / Hz	$\Delta\delta_{X1-Y1}$ / ppm	<i>s-cis</i> or <i>s-trans</i>
H1	6.63	13.2	H6	6.12	13.2	0.51	unclear
H2	6.58	-	H3	6.52	-	0.06	<i>s-cis</i>
H4	6.43	13.2	H5	6.27	13.2	0.16	<i>s-cis</i>
H7	5.96	13.2	H10	5.23	13.2	0.73	<i>s-trans</i>
H8	5.81	12.7	H12	4.83	12.7	0.98	<i>s-trans</i>
H9	5.78	12.0	H11	5.18	12.0	0.6	<i>s-trans</i>

2.5 Transmission electron microscopy (TEM) analysis

Transmission electron microscopy (TEM) uses high-energy electrons to penetrate through a thin sample. It used widely to characterization of the metal-containing nanoparticles or particles.^{153,154} Due to the difference in size in each species, some of the TEM images have to focus on the particle shapes rather than a whole window viewing. Therefore, the manual measurements for each complex are different, depending on the numbers of particle shown in each image. Visual inspection of the histograms (Figure 2.9-2.12, see insets) reveals a number of outlying sizes. The particles from the reaction of **6** in methanol showed the largest diameters about 200 nm (Figure 2.9); the particles from the reaction of **7** in methanol showed large clusters with diameters of *ca.* 200 nm (Figure 2.10). Reaction of **33** in methanol exhibited more particles than the pure hydroxyl Pd complex (**6** and **7**). The diameters of the particles were found to between 3 - 6 nm (Figure 2.11). The particles from the reaction **37** showed little evidence of particle formation (Figure 2.12). This is in-keeping with the good results obtained by elemental analysis. The slight difference in particle sizes of these four Pd complexes is interesting, as the ligand clearly affects the stability of these Pd^0 complexes.

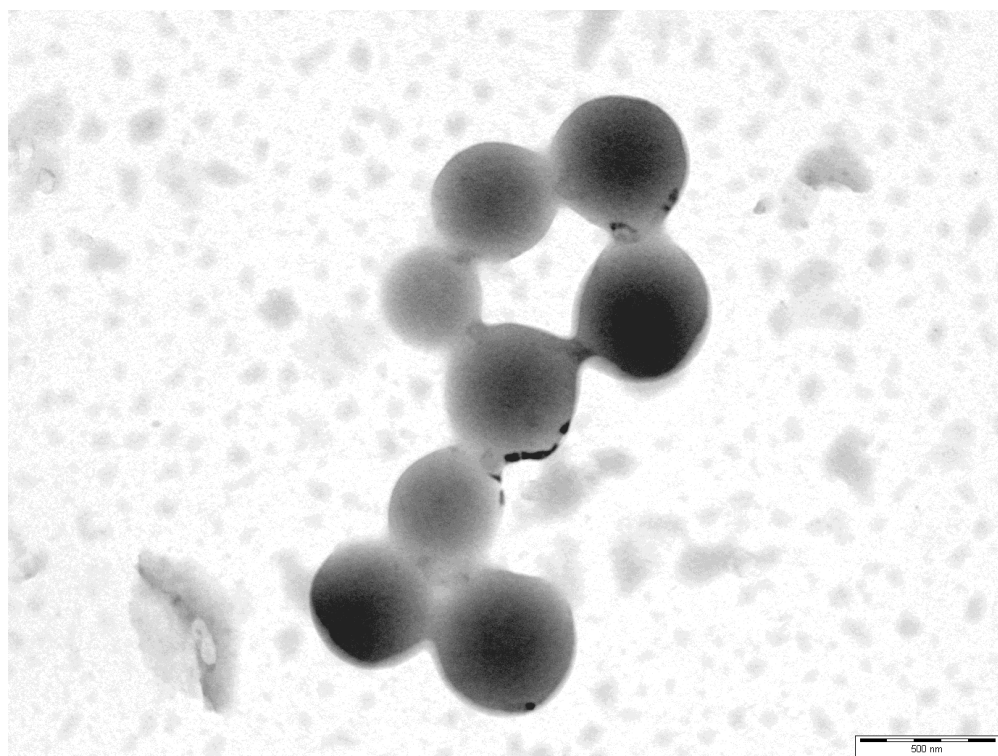


Figure 2.9 Example electron micrograph of large Pd particles derived complex **6**, approx. 200nm.

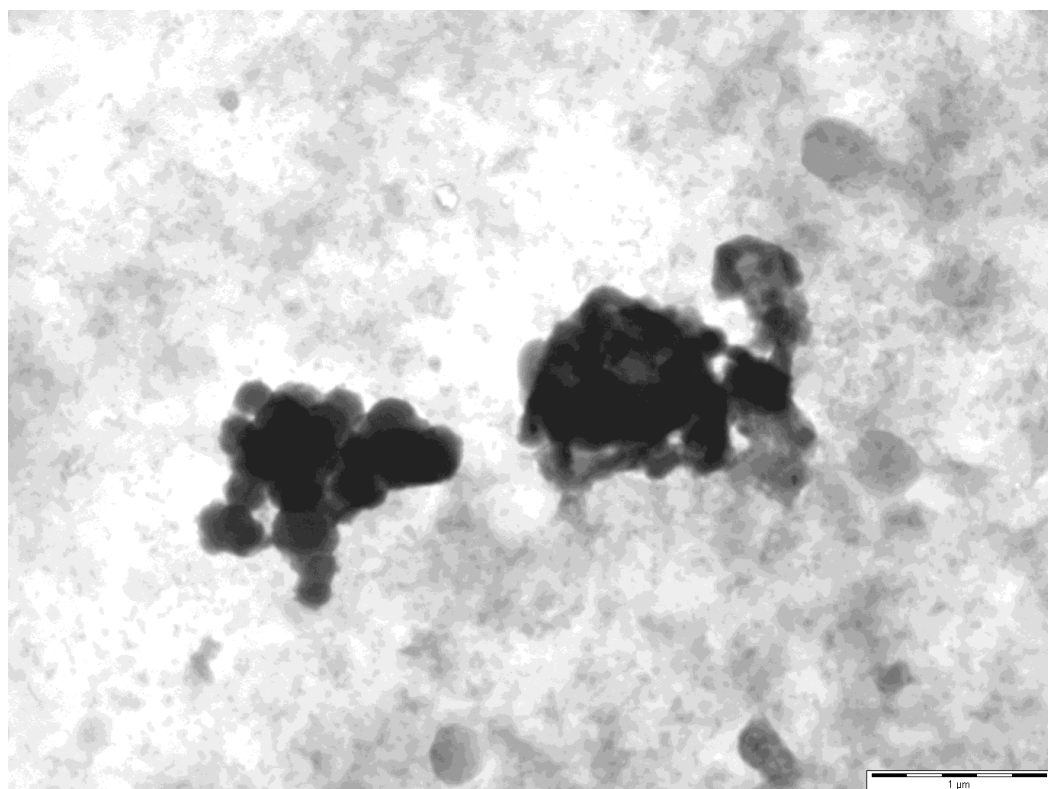


Figure 2.10 Example electron micrograph of Pd particles derived from complex **7**.

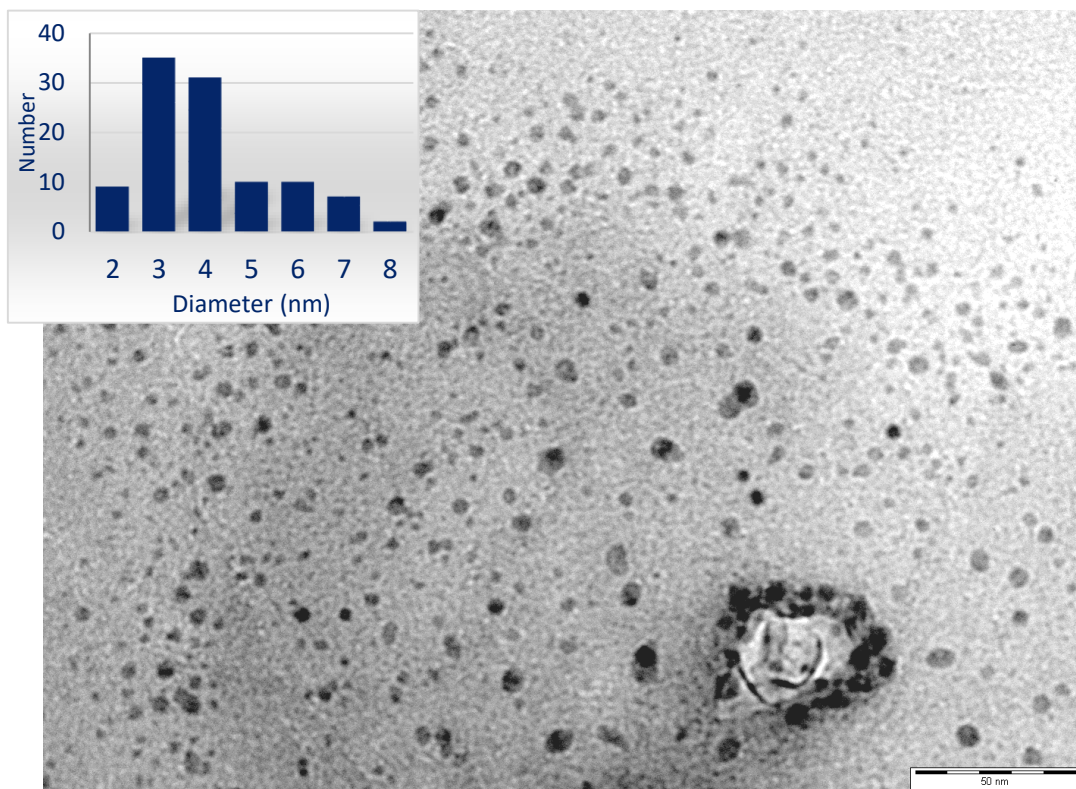


Figure 2.11 Example electron micrograph of a Pd particle of complex **33**. Inset shows histogram of particle diameter (nm), approx. 5-10 nm, across a sample of nanoparticles ($n = 104$).

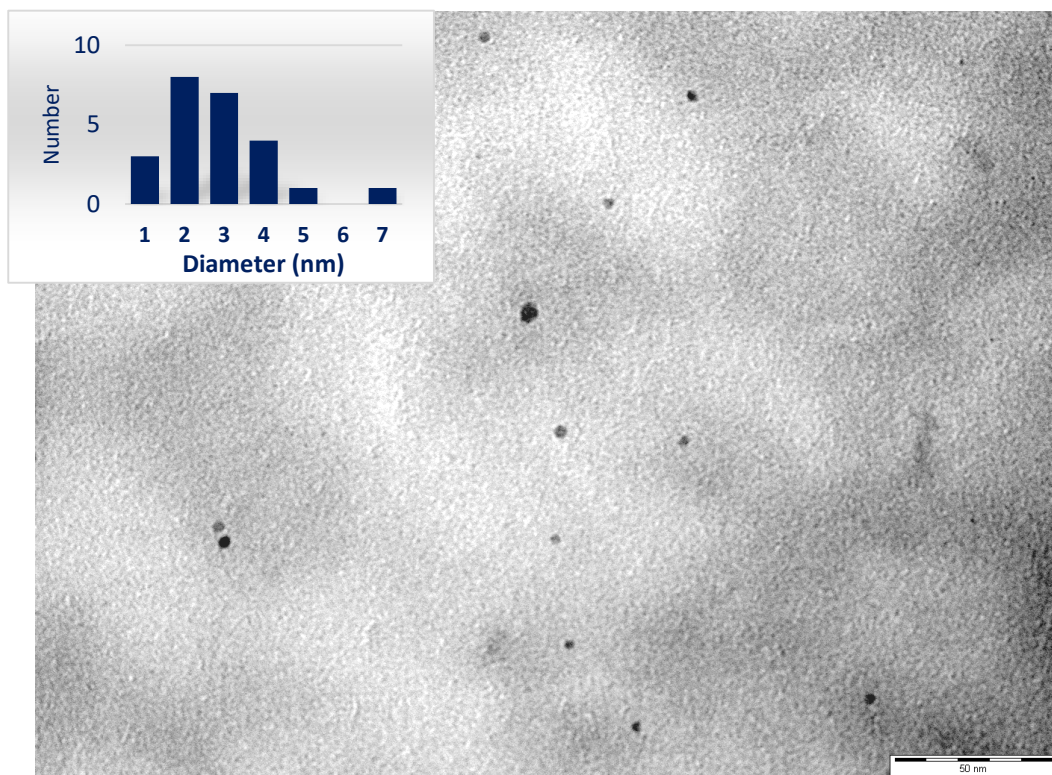
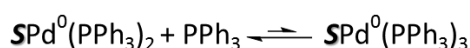
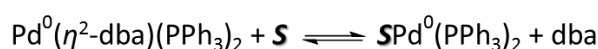
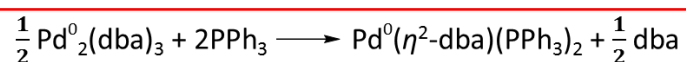


Figure 2.12 Example electron micrograph of a Pd particle of complex **37**. Inset shows histogram of particle diameter (nm) across a sample of nanoparticles ($n = 24$).

2.6 Active Pd ratio from the [Pd₂(dba)₃] complexes

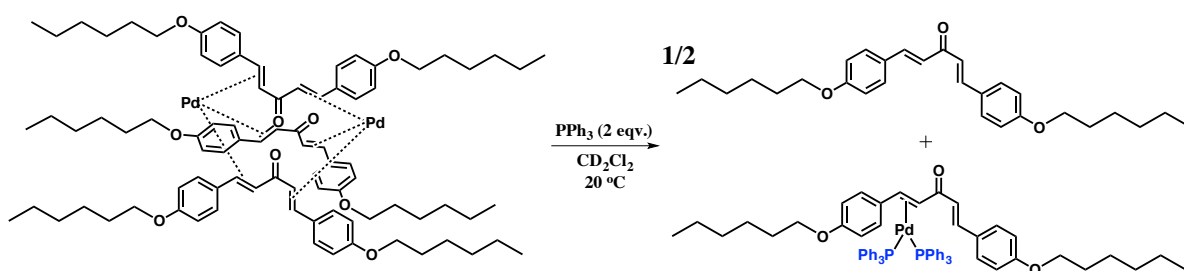
From the synthesis of the Pd complexes, there were some interesting points that should not be ignored: a) Increasing the concentration of Pd complexes, the formation of PdNPs was strongly affected by this – too low or high concentration could favor PdNP formation; b) Increasing the reaction temperature, favored PdNP formation. c) Increasing the reaction times, also favored PdNP formation.

The compositions of mixtures of Pd₂(dba)₃ were studied by Jutand and co-workers,¹³³ who established the following formulate for monodentate ligands such as triphenylphosphine (PPh₃) in DMF and THF (solvent noted *S* hereafter, Scheme 2.30).



Scheme 2.30 The kinetic equilibrium processes of {Pd⁰(dba)₂ + *n*L} in oxidative addition reactions.

The hypothesis detailed above prompted an investigation into determining the purity of the ‘Pd-dba’ complexes in a reaction with PPh₃. For calculating the purity of the Pd complexes, the methodology is described in Scheme 2.31. All reactions were conducted in a glove box, using 2 eqv. of triethyl phosphate, as a reference. The ³¹P NMR integrations of the reference peak and complex phosphine signals, allowed the purity to be estimated.



Scheme 2.31 Addition of PPh₃ to ‘Pd-dba-Z’ complex **37**.

All the ‘Pd-dba-Z’ complexes (**6**, **7**, **33** and **37**) were subjected to the same investigation. The ¹H NMR spectrum of Pd complex **37** in CDCl₃ showed Pd, *ca.* 29% of proton ratio (calculated from integration of free ligand and Pd complex by ¹H NMR) (Figure 2.13); elemental analysis showed that it was 98% pure; the active Pd calculated here = 71% (total active Pd, calculated from the

methodology above). For $[\text{Pd}_2(\text{dba})_3, \text{dba}]$, ^1H NMR of $\text{Pd}_2(\text{dba})_3, \text{dba}$ in CDCl_3 showed *ca.* 25% purity (Figure 2.14); elemental analysis of $\text{Pd}_2(\text{dba})_3$ showed that it was 94% pure; the real purity was found to be 67% (total active Pd). The results from these have been shown that the new methodology to calculate active Pd species has potential for determining the purity of the Pd complexes.

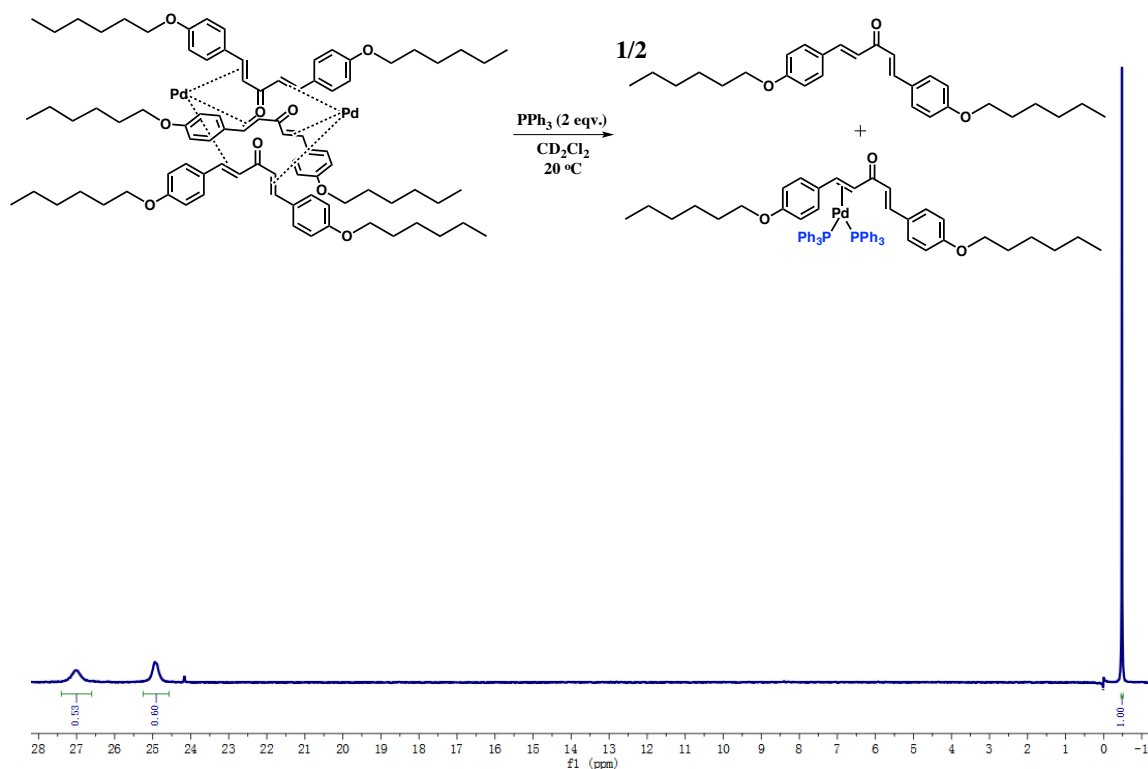


Figure 2.13 ^{31}P NMR spectrum of ‘Pd-dba-Z’ complex **37** in R.T. (CD_2Cl_2).

At room temperature, ‘Pd-dba-Z’ complex **37** indicates that the ^{31}P signals are exchanging (two broad ^{31}P signals), thus the integrations may not be reliable (Figure 2.13). However, compared to the reference peak, they are broad and the reference peak sharp. It indicated the reference is reliable and the ^{31}P signal of the test compound (**48**) are not exchanging with reference, so there can be reasonable confidence in these data, certainly enough to give an estimation of purity.

A similar situation occurs for $\text{Pd}_2(\text{dba})_3$ at room temperature (Figure 2.14). For example, the low temperature experiment at $-35\text{ }^\circ\text{C}$ showed little phosphorus ligand exchange (Figure 2.15).

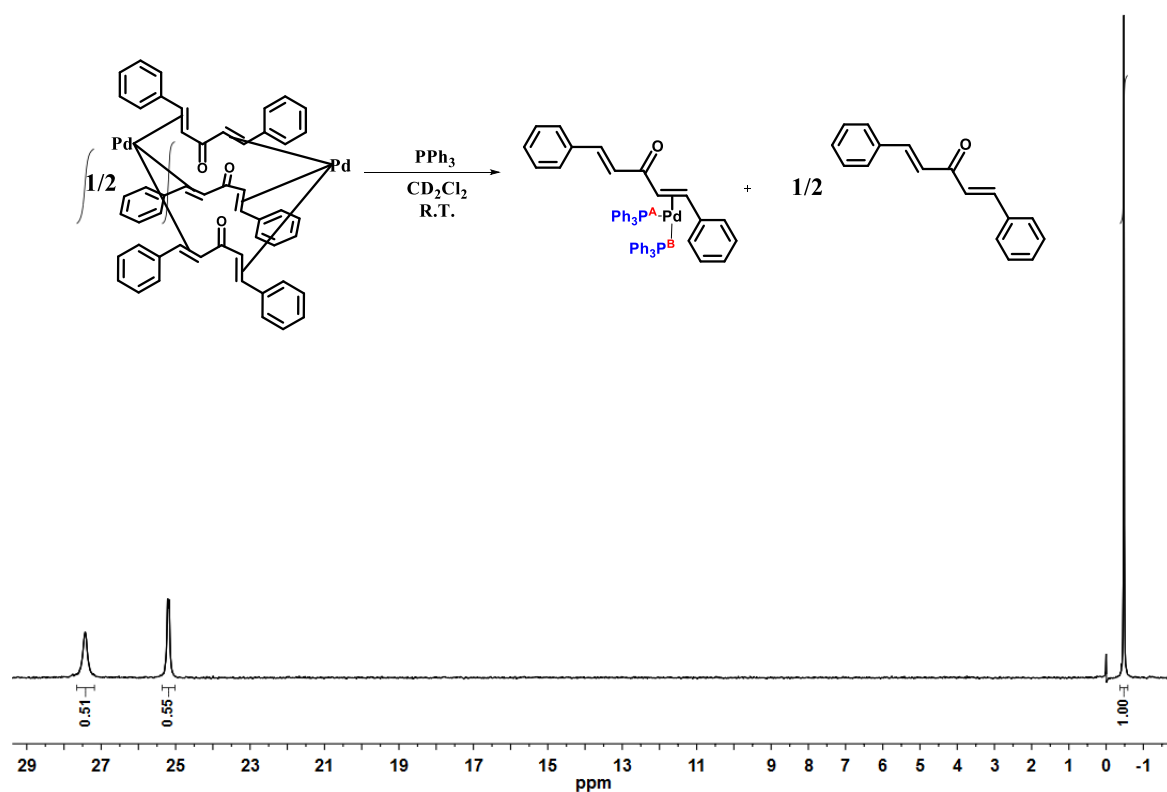


Figure 2.14 ³¹P NMR spectrum of the [Pd⁰₂(dba)₃·dba] at R.T. (CD₂Cl₂).

Table 2.6 Active Pd ratio of ‘Pd-dba-Z’ complexes determined by NMR and elemental analysis.

Catalysts	Integration of P ^A	Integration of P ^B	Calculated from integration of ¹ H NMR	Calculated from elemental analysis	Active Pd (calculated from integration of ³¹ P NMR)
6 (THF-d ₆)	0.39	0.43	28 %	97 %	52 %
7 (THF-d ₆)	0.47	0.52	31 %	98 %	63 %
33 (CDCl ₃)	0.46	0.52	19 %	99 %	62 %
37 (CDCl ₃)	0.53	0.60	29 %	98 %	71 %
Pd ₂ (dba) ₃ ·dba (CDCl ₃)	0.51	0.55	25 %	94 %	67 %

With the same method, the purity of the ‘Pd-dba’ complexes were tested and compared with [Pd₂(dba)₃·dba]. As there display different solubilities, different deuterated NMR solvents were required for these studies. Furthermore, the method was compared with other methods, *i.e.*

integration of ^1H NMR spectra and comparison of elemental analysis data (Table 2.6). The highest active Pd catalyst is complex **37**, and the poorest active Pd catalyst was found to be complex **6**.

As each Pd complex possess two phosphorus environments, A and B, which are in exchange, we can expect for complex **33** that there are two complexes, are where $\text{Pd}(\text{PPh}_2)_2$ is attached to the dba-olefin nearest to the OH group and another $\text{Pd}(\text{PPh}_2)_2$ attached to the dba-olefin nearest the O-hexyl group. Therefore, the Pd complex **33** was tested at two different temperatures. At low temperature ($-35\text{ }^\circ\text{C}$), two sets of phosphorus signals were observed as major and minor signals in a ratio of approximated 2:1. Whereas at room temperature only broad phosphorus signals were observed. The experiment confirms the asymmetric coordination mode of the unsymmetrical dba ligand containing OH and O-hexyl groups

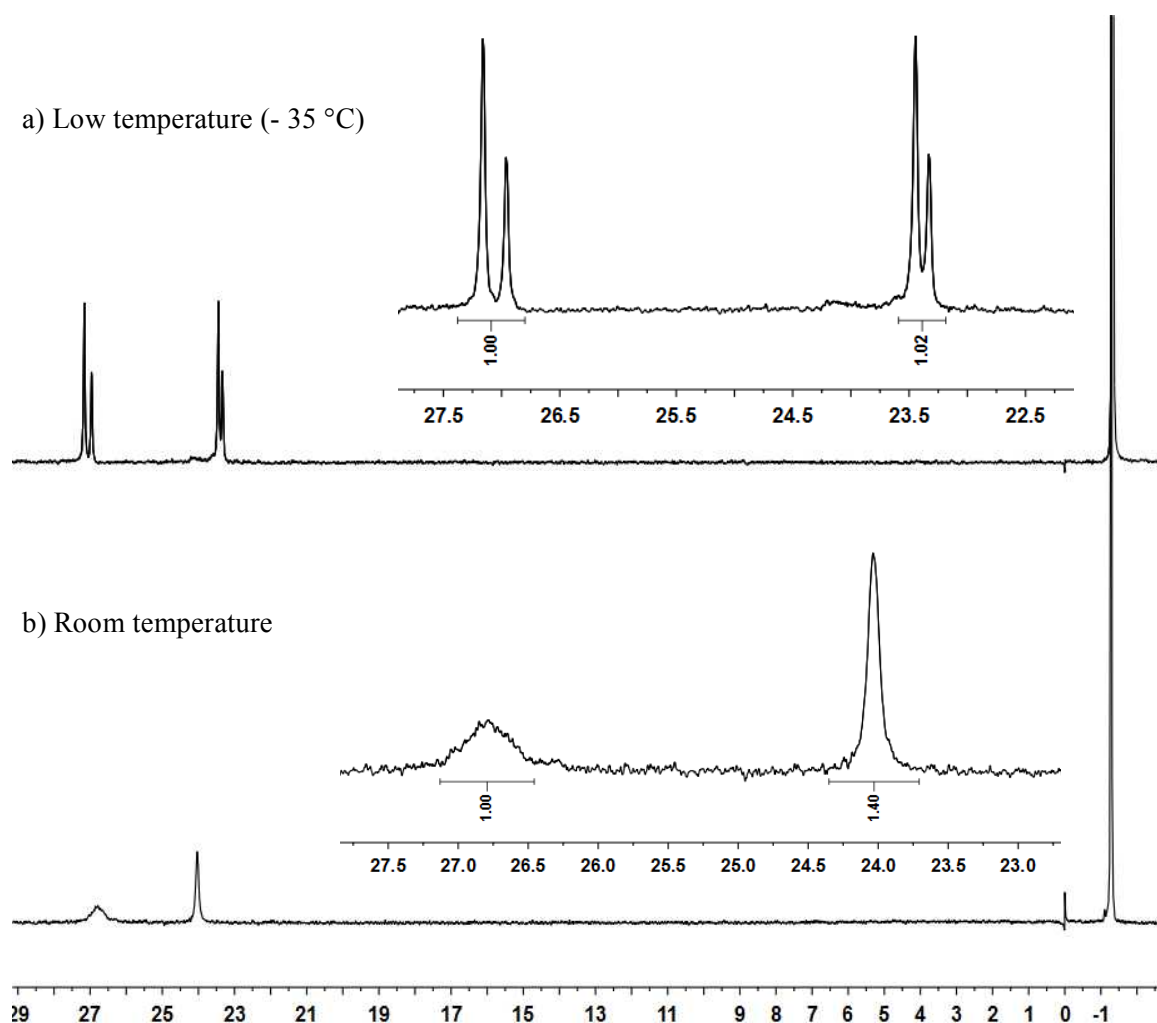


Figure 2.15 ^{31}P NMR of Pd complex **33** under different temperatures (CD_2Cl_2).

In summary, elemental analysis is not the optimal way for testing the purity of the 'Pd-dba' complexes, although it does often give satisfactory Pd/dba ratios. The methodology described above

can be used as a helpful tool to measure the real Pd/L ratio (L = dba or phosphine), which is ultimately important for Pd-mediated cross-coupling reactions.

2.7 Conclusion

- A novel class of dba-ligands and their Pd complexes were designed and synthesised using Claisen-Schmidt condensation reactions and traditional synthetic methods for $[\text{Pd}_2(\text{dba})_3.\text{dba}]$ and derivatives, respectively.
- Adjustment of the pH of the hydroxylated dba compounds during reaction work-up was achieved by addition of solid dry ice, which increases acidity, promoting product precipitation.
- Use of HCl instead of NaOH in the synthesis of the 4-OH-dba ligand dramatically improved the yield of the product.
- Triethyl phosphate was used as reference to investigate the total active Pd derived from 'Pd-dba' complexes. NMR spectroscopic analysis revealed ligand exchange, as shown by room temperature and low temperature measurements.
- PdNPs are formed during the synthesis of 'Pd-dba' complexes. Their formation appears to relate to the structure of the dba ligands. Acid catalysis can aid their degradation.
- NMR and IR spectroscopy, UV-vis spectroscopy, TEM, and mass spectrometry, were used to analyse the structures of the Pd complexes.

2.8 Experimental

General Details

Chemical reagents were purchased from Sigma Aldrich[®], Alfa Aesar[®], Acros[®] or Fluorochem[®] and used as received. Pd(OAc)₂ was purchased from Precious Metals Online. All reactions were carried out under a nitrogen atmosphere unless otherwise stated. Petroleum ether refers to the fraction of petroleum that is collected at 40 – 60 °C. Reactions requiring anhydrous or air-free conditions were carried out in dry solvent under an argon or nitrogen atmosphere using oven- or flame-dried glassware. Filtration was performed under gravity through fluted filter paper unless otherwise stated. Inorganic solutions used were prepared using deionized water. TLC analysis was carried out using Merck 5554 aluminum backed silica plates, and visualised using UV light at 254 and 365 nm. Retention factors (*R_f*) are reported along with the solvent system used in parenthesis. All column chromatography was carried out using Merck silica gel 60 (particle size 40-63 μm) purchased from Sigma Aldrich.

Nuclear Magnetic Resonance Spectroscopy (NMR Spectroscopy)

Proton (¹H), carbon (¹³C) spectra were recorded on a Jeol ECS400 and Bruker AV500/AV600/AV700 spectrometers. All chemical shifts in ¹H NMR spectra are reported in parts per million (ppm, δ) relative to tetramethylsilane, using residual NMR solvent as an internal standard (CDCl₃: 7.26 ppm, DMSO-d₆: 2.50 ppm, MeOD-d₄: 3.31 ppm, CD₂Cl₂: 5.32 ppm). Multiplicities are described as singlet (s), doublet (d), triplet (t), quartet (q), multiplet (m), apparent (app.) and broad (br). ¹³C spectra were referenced to deuterated solvent. The spectra were processed in MestreNova[®] software and, where required, exported as JPEG images into the appropriate document. All chemical shifts in ¹³C NMR spectra are reported in ppm (δ) and are referenced to the NMR solvent (CDCl₃: 77.36 ppm, DMSO-d₆: 39.52 ppm, MeOD-d₄: 49.00 ppm, CD₂Cl₂: 53.49 ppm). Chemical shifts are reported in parts per million and were referenced to residual non-deuterated solvent. Coupling constants have been quoted to ±0.2 Hz. ¹H NMR chemical shift are given to 2 decimal places; ¹³C NMR chemical shift are given to 2 decimal places. Spectra were typically recorded at 298 K.

Mass Spectrometry (MS)

Mass spectrometry was performed using a Bruker daltronics microTOF spectrometer, an Agilent series 1200 LC, or a Thermo LCQ using electrospray ionization (ESI), with less than 5 ppm error for all HRMS. Liquid injection field desorption ionization (LIFDI) mass spectrometry was performed using a Wasters GCT Premier mass spectrometer. All data were acquired in positive ion mode using ESI or LIFDI ionisation. All LIFDI data reported is within 120 ppm error.

Infrared Spectroscopy (IR)

IR spectroscopy was carried out on Thermo-Nicolet Avatar-370 FT-IR spectrometer, or a PerkinElmer Spectrum Two spectrometer. Spectra were taken in either solid state (KBr disc), or in solution, thin film.

Melting Points (m.p.)

Melting points were obtained on a Stuart SMP3 machine. Experiments were run using a ramp rate of 3 °C min⁻¹ to above the required melting temperature. The melting point was taken as the onset of the observed endothermic peak. The machine was calibrated using an indium standard.

Transmission electron microscopy (TEM)

Transmission electron microscopy was performed at the University of York Department of Biology Technology Facility using a FEI Technai 12 G2 BioTWIN microscope, operated at 120 kV. The images were enlarged, and particle sizes measured manually, captured using SIS Megaview III camera. Samples were suspended in methanol or chloroform and applied to a TEM grid with a Formvar/carbon film. Statistical analyses were performed and histograms drawn using Microsoft Excel.

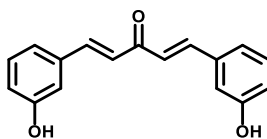
UV-Vis Spectroscopy

UV-Vis spectroscopy was performed on a JASCO V-560 spectrometer. The UV-Vis spectrophotometer was temperature controlled at 20 °C using a water bath; spectra were recorded using matched quartz cuvettes (λ_{max} is reported). The UV-Vis spectra of 5 solutions at different concentrations were measured (all absorbance values were below 2 OD). The UV-Vis spectra were plotted for each analogue (absorbance *vs.* wavelength) at the different concentrations. The molar absorption coefficients were obtained by plotting UV absorbance *vs.* analogue concentration, and applying the Beer-Lambert law. A baseline in the required solvent was carried out prior to starting an assay.

Elemental Analysis

Elemental analysis was carried out using an Exeter Analytical CE-440 Elemental Analyser, with the percentages reported as an average of two runs.

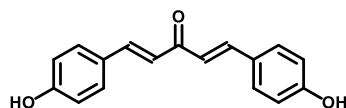
(1E,4E)-1,5-Bis(3-hydroxyphenyl)penta-1,4-dien-3-one (3)



Aqueous NaOH (4.91 g, 0.123 mol) in water (24.6 ml) was added dropwise to a stirred solution of 3-hydroxybenzaldehyde (10 g, 81.9 mmol, 2.05 eqv.) and acetone (2.9 ml, 2.316 g, 40 mmol) in abs ethanol (33 ml), and stirred at room temperature 25 °C for 18 h. Then water (120 ml) and dry ice were added, yellow solid started to form on the side of round-bottomed flask about 2 min. After 20 min, water (50 ml) was added, then most of the precipitated out. If the precipitation was not come out, 2 M of HCl was added (pH likely about 6). Filtered on a bucher filter funnel (paper), washed with a small amount of water (10 ml). Dried in air to give a yellow powder (9.75 g, 92%).

MP 196–198 °C; ¹H NMR (400 MHz, CD₃OD) δ: 7.69 (d, *J* = 16.2 Hz, 2H, COCH=CH), 7.24-7.18 (m, 2H, ArH), 7.16 (d, *J* = 16.2 Hz, 2H, COCH=CH), 7.16-7.11 (m, 4H, ArH), 7.11-7.06 (m, 2H, ArH), 6.89-6.83 (m, 2H, ArH); ¹³C NMR (100 MHz, CD₃OD) δ: 191.54, 159.09, 145.32, 137.83, 131.52, 126.53, 121.27, 119.58, 115.83; Elemental Analysis (CHN) C: 76.24% H: 5.62% (Calculated: C: 76.68% H: 5.30%); ESI-MS *m/z* = 267 (100), 91 (25), 194 (15)[M+H]; ESI-HRMS *m/z* = 267.1012 [M+H]⁺ (calc. for C₁₇H₁₄O₃ = 267.1016); IR (Pressed KBr disc): 3389, 3242, 1619, 1581, 984, 864, 784, 668 cm⁻¹.

(1E,4E)-1,5-bis(4-hydroxyphenyl)penta-1,4-dien-3-one (5)¹⁴¹

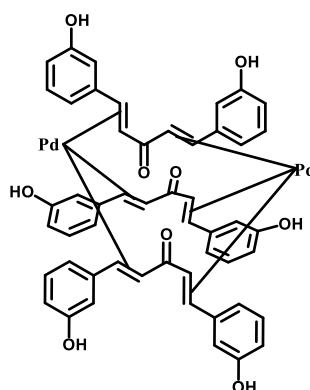


In a 250-mL three-neck flask equipped with a mechanical stirrer 4-hydroxybenzaldehyde (6.1 g, 2 eqv., 0.05 mmol) ethanol (20ml), and acetone (1.84 ml, 1 eqv., 0.025 mol) were introduced. The contents of the flask were cooled to 0 °C and then conc. HCl (2.0 mL) was added dropwise in 5 min. Stirring was continued at 0 °C for 24 h. After standing for 7 days, the mixture was treated with ice water (the colour became dark green), the precipitate was filtered off, washed with ice-water in order to eliminate the acid as completely as possible and dried in vacuum. The crude material was recrystallised from ethanol to afford yellow solid (6.44 g, 97%).

TLC *R_f* 0.50 (30 % EtOAc/Pet.); MP 241–243 °C; ¹H NMR (400 MHz, CD₃OD) δ: 7.70 (d, *J* = 16 Hz, 2H, COCH=CH), 7.56 (d, *J* = 8.7 Hz, 4H, ArH), 7.05 (d, *J* = 16 Hz, 2H, COCH=CH), 6.84 (d, *J* = 8.7 Hz, 4H, ArH); ¹³C NMR (100 MHz, CD₃OD) δ: 201.59, 161.45, 146.44, 131.71, 127.11, 124.72, 117.02. ESI-MS *m/z* = 267.3040 [M+H]⁺ (calc. for C₁₇H₁₄O₃ = 266.0943); Elemental Analysis (CHN)

C: 77.04% H: 5.32% (Calculated: C: 76.68% H: 5.30%); ESI-MS m/z = 267 (100), 90 (50), 123 (10)[MH⁺]; 289 (40)[MNa⁺]; ESI-HRMS m/z = 267.1022 [M+H]⁺ (calc. for C₁₇H₁₅O₃= 267.1016), m/z = 289.0838 [M+Na]⁺ (calc. for C₁₇H₁₄NaO₃= 289.0835); IR (Pressed KBr disc): 3390, 3243, 1618, 1580, 1453, 1216, 1106, 983, 865, 785, 669 cm⁻¹.

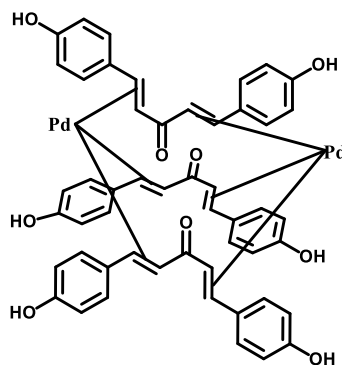
Pd₂(3-OH-dba)₃ complex (6)



A 100 ml round-bottomed flask was charged with anhydrous sodium acetate NaOAc (0.1856 g, 2.26 mmol, 8.01 eqv.), (1*E*,4*E*)-1,5-bis(3-hydroxyphenyl)penta-1,4-dien-3-one, **3** (0.248 g, 0.932 mmol, 3.3 eqv.) and methanol (6 ml) and a magnetic stir bar. The flask was placed in a 50 °C oil bath, and a condenser placed on top of the flask. After 15 min, PdCl₂ (0.05 g, 0.282 mmol, 1 eqv.) was added. The mixture was stirred at 50 °C for 15 min and then allowed to cool. The crude product was cooled, dried on a Bucher filter, and washed with water (50 ml), to give a purple solid (0.15 g, 89%).

MP 220–221 °C; ¹H NMR (400 MHz, CD₃OD, 20 °C) δ: 7.69 (d, J = 16 Hz, 2H; CH=CHCO), 7.25-7.21 (m, 2H, ArH), 7.16 (d, J = 16.2 Hz, 2H, COCH=CH), 7.16-7.11 (m, 4H, ArH), 7.12-7.06 (m, 2H, ArH), 6.89-6.83 (m, 2H, ArH), 6.78-6.74 (m, 1H; Pd-alkene), 6.65 (d, 1H; Pd-alkene), 6.56 (d, 1H, Pd-alkene), 6.47-6.41 (m, 1H; Pd-alkene), 6.39-6.33 (m, 1H; Pd-alkene), 6.22-6.17 (m, 2H; Pd-alkene), 6.06-6.01 (m, 1H; Pd-alkene), 5.83-5.76 (m, 1H; Pd-alkene), 5.76-5.69 (m, 1H; Pd-alkene), 5.54-5.49 (m, 1H; Pd-alkene), 5.36-5.31 (m, 1H; Pd-alkene), 5.11-5.05 (m, 1H; Pd-alkene); Elemental Analysis (CHN) C: 63.91%, H: 4.42% (Calculated : 40.69%, H 6.63%)

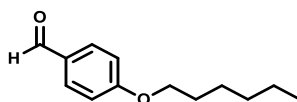
Pd₂(4-OH-dba)₃ complex (7)



A 100 ml round-bottomed flask was charged with anhydrous sodium acetate (0.1856 g, 2.26 mmol, 8.01 eqv.), (1E,4E)-1,5-bis(4-hydroxyphenyl)penta-1,4-dien-3-one (0.248 g, 0.932 mmol, 3.3 eqv.) and 7 ml of methanol and a magnetic stir bar. The flask was placed in a 50 °C oil bath, and use a condenser on the top of flask, and after 15 min, PdCl₂ (0.025 g, 0.141 mmol, 1 eqv.) was added. The mixture was allowed to stir at 50 °C for 30 min. The crude product was cooled, dried on a Bucher filter, and washed with water (50 ml) to give a purple solid (0.12 g, 94%).

MP 233–234 °C; ¹H NMR (400 MHz, CDCl₃) δ: 7.70 (d, *J* = *J* = 16 Hz, 2H, COCH=CH), 7.58 (d, *J* = 8.7 Hz, 4H, ArH), 7.05 (d, *J* = 16 Hz, 2H, COCH=CH), 6.84 (d, *J* = 8.7 Hz, 4H, ArH), 6.74 (d, 2H, Pd-alkene), 6.64–6.58 (m, 1H, Pd-alkene), 6.58 – 6.45 (m, 1H, Pd-alkene), 6.33 (d, *J* = 13.2 Hz, 1H, Pd-alkene), 6.15 (d, *J* = 13.2 Hz, 1H, Pd-alkene), 5.99 (d, *J* = 13.2 Hz, 1H, Pd-alkene), 5.87 (d, *J* = 13.5 Hz, 1H, Pd-alkene), 5.19 (d, *J* = 12.1 Hz, 1H, Pd-alkene), 4.77 (d, 2H, Pd-alkene); Elemental Analysis (CHN) C 63.91%, H 4.42% (Calculated: 56.631%, H 4.646%).

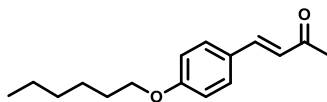
4-(4'-(Hexyloxy)phenyl)but-3-en-2-one (9)¹⁵⁵



4-hydroxybenzaldehyde (3.66 g, 1 eqv., 0.030 mol), KI (4.98 g, 1 eqv., 0.030 mol), and powdered K₂CO₃ (8.28 g, 2 eqv., 0.060 mol) were taken in acetone (50.0 mL) and refluxed for 2 h. 1-bromohexane (6.8 mL, 1.1 eqv., 0.033 mol) was added dropwise to the above reaction mixture over 3 min. The reaction mixture was further refluxed under an inert atmosphere for 3 h at 58 °C, then the reaction mixture was cooled, acetone was removed under vacuum, and the residue was poured into water (100 mL). It was extracted into dichloromethane (DCM) and washed with NaOH (50 mL, 2 % solution) and with brine (20 mL). The organic layer was dried over anhydrous MgSO₄, filtered and concentrated *in vacuo* to give a pale yellow liquid as product. Rapid column chromatography on silica (eluent: petrol/ethyl acetate 3:97 → 10:90, v/v). gave the title compounds as a liquid (1.98 g, 83%).

TLC R_f 0.50 (20 % EtOAc/Pet.); MP 85–87 °C; ^1H NMR (400 MHz, CDCl_3 , 20 °C) δ : 9.84 (s, 1H; CHO), 7.06 (dt, 2H; $J = 8.8, 2.3$ Hz; H2+H6), 6.94 (dt, 2H, $J = 8.8, 2.3$ Hz; H3+H5), 3.92 (t, 2H, $J = 6.6$ Hz; H1'), 1.74-1.66 (m, 2H, $J = 6.6$ Hz; H2'), 1.52-1.31 (m, 4H, $J = 6.6$ Hz; H3'-H4'), 1.29-1.22 (m, 2H, $J = 6.6$ Hz; H5'), 0.88-0.83 (m, 3H, $J = 6.6$ Hz; H6'); ^{13}C NMR (100 MHz, CDCl_3 , 20 °C) δ : 190.8 (CHO), 164.2, 131.9, 130.1, 128.6, 114.8, 114.2, 68.2, 31.6, 29.1, 25.6, 22.7, 14.1; Elemental Analysis (CHN) C: 75.46% H: 8.87% (Calculated: C: 75.69% H: 8.79%); ESI-MS m/z 206(100)[MH^+] and m/z 228(15)[MNa^+]; ESI-HRMS m/z 206.1378 [$\text{M}+\text{H}$] (calc. for $\text{C}_{13}\text{H}_{19}\text{O}_2 = 206.1361$); IR (Solution: DCM): 2929, 2856, 1690, 1251 cm^{-1} .

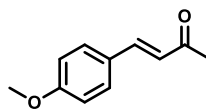
(E)-4-(4-(Hexyloxy)phenyl)but-3-en-2-one (10)



A cooled solution of aqueous sodium hydroxide (0.5 g, 5 eqv. 0.005 mol) dissolved in water (10 ml) was added to a solution of 4-(4-(hexyloxy)phenyl)but-3-en-2-one (0.5 g, 1 eqv. 0.00226 mol) in 5 ml of ethanol solution stirred at 0 °C. Acetone (0.9 ml, 5 eqv. 0.0113 mol) was added and the mixture was stirred at 35 °C for 10 h, then filtered on a bucher filter funnel, recrystallised from hot ethanol with warm water under the flask (putting on the heater). Add H_2O dropwise and cooled it down to recrystallize the crude product. The extract was purified by rapid column chromatography on silica (eluent: petrol/ethyl acetate 93:7 \rightarrow 88:12, v/v). Collected fractions were evaporated *in vacuo* to yield liquid product (0.57 g, 62%).

MP 103–105 °C; TLC R_f 0.50 (30 % EtOAc/Pet.); ^1H NMR (400 MHz, CDCl_3) δ : 7.51-7.44 (m, 3H, $\text{CH}=\text{CHCOCH}_3$ and ArH), 6.90 (d, $J = 8.8$ Hz, 2H, ArH), 6.60 (d, $J = 16.2$ Hz, 1H, $\text{CH}=\text{CHCOCH}_3$), 3.88 (t, 2H, $J = 6.6$ Hz; H1'), 2.36 (s, 2H, H2'), 1.83 – 1.74 (m, 2H, H3'), 1.51 – 1.42 (m, 2H, H4'), 1.36-1.31 (m, 4H, H5'), 1.94-0.87 (m, 3H, H6'). ^{13}C NMR (100 MHz, CDCl_3 , 20 °C) δ : 198.8, 161.4, 143.3, 130.3, 127.1, 115.1, 68.3, 31.5, 29.4, 27.5, 25.7, 22.9, 14.0; ESI-MS $m/z = 247$ (100), 89 (50)[MH^+]; 269 (30)[MNa^+]; ESI-HRMS $m/z = 247.1689$ [$\text{M}+\text{H}$] $^+$ (calc. for $\text{C}_{17}\text{H}_{15}\text{O}_3 = 247.1693$), $m/z = 269.1506$ [$\text{M}+\text{Na}$] $^+$ (calc. for $\text{C}_{17}\text{H}_{14}\text{NaO}_3 = 269.1512$); IR (Pressed KBr disc): 2937, 2866, 1607, 1592, 1510, 1452, 1255, 1117, 1026, 984, 834 cm^{-1} .

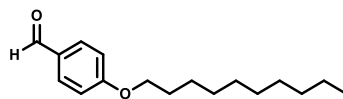
4-(4-(Hexyloxy)phenyl)but-3-en-2-one (12)



To a solution of aqueous sodium hydroxide (1 g, 2.5 eqv. 0.025 mol) dissolved in water (10 ml) at 10 °C, acetone (2.9 ml, 4 eqv., 0.04 mol) was added followed by the 4-methoxybenzaldehyde (1 ml, 1 eqv., 0.01 mol). The mixture was then stirred once every 15 min for 2 h before being 18 h. The reaction mixture was extracted with ethyl acetate (20 ml) and the extracts were purified by rapid column chromatography on silica (eluent: petrol/ethyl acetate 80:20 → 50:50, v/v). Collected fractions were evaporated *in vacuo* to yield product, white solid (0.59 g, 33%).

MP 73–75 °C, lit.⁴⁶ MP 74–76 °C; TLC R_f 0.30 (30 % EtOAc/Pet.); ^1H NMR (400 MHz, CDCl_3) δ : 7.51–7.44 (m, 3H), 6.91 (d, 2H, $J = 8.7$ Hz), 6.60 (d, 1H, $J = 16.2$ Hz), 3.84 (s, 3H), 2.36 (s, 3H); ^{13}C NMR (100 MHz, CDCl_3) δ : 197.9, 161.8, 144.1, 130.2, 126.9, 124.9, 114.3, 55.1, 28.6; ESI-MS m/z 177(100)[MH^+] and m/z 199(30)[MNa^+]; ESI-HRMS m/z 177.0906 [$\text{M}+\text{H}$]($\text{C}_{11}\text{H}_{13}\text{O}_2 = 177.0916$), 199.0723 [MNa^+] (calc. for $\text{C}_{11}\text{H}_{12}\text{NaO}_2 = 199.0730$).

4-(Decyloxy)benzaldehyde (14)

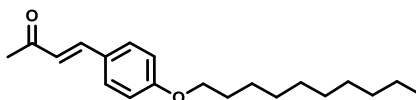


4-hydroxybenzaldehyde (7.32 g, 1 eqv., 0.06 mol), KI (9.96 g, 1 eqv., 0.06 mol), and powdered K_2CO_3 (16.56 g, 2 eqv., 0.12 mol) were taken in dry acetone (120.0 mL) and refluxed for 2 h under air. 1-bromodecane (13.6 mL, 1.1 eqv., 0.066 mol) was added dropwise to the above reaction mixture over 3 min. The reaction mixture was further refluxed for 16 h under air. It was cooled, the residue was poured into water (100 mL), and the acetone was removed under vacuum. The residue was extracted from dichloromethane (DCM) and washed with NaOH (150 mL, 2 % solution) and with brine (100 mL). The organic layer extracts were combined, dried (MgSO_4), and filtered. The reaction mixture was extracted with ethyl acetate (20 ml) and the extract was purified by rapid column chromatography on silica (eluent: petrol/ethyl acetate 100:0 → 3:1, v/v), dry-load the product with silica. Collected fractions were evaporated *in vacuo* to yield product to give the yellow liquid (14.65 g, 93%).

TLC R_f 0.50 (20 % EtOAc/Pet.); ^1H NMR (400 MHz, CDCl_3) δ : 9.80 (s, 1H, CHO), 7.75 (dt, $J = 8.6$ Hz, 2.2 Hz, 2H, ArH), 6.92 (dt, $J = 8.6$ Hz, 2.2 Hz, 2H, ArH), 4.05 (t, $J = 6.6$ Hz, 2H, H1'), 1.78–1.71 (m, $J = 6.6$ Hz, 2H, H2'), 1.60–1.36 (m, 14H, H3' – H9'), 0.82 (t, $J = 6.6$ Hz, 3H, H10'); ^{13}C

NMR (100 MHz, CDCl₃) δ : 190.6 (CHO), 164.2, 131.8, 129.7, 114.7, 68.3, 31.9, 30.7, 29.4, 29.0, 26.0, 22.7, 14.1; ESI-MS m/z 263(100)[MH⁺] and m/z 285(20)[MNa⁺]; ESI-HRMS m/z 263.2008 [M+H] (C₁₇H₂₇O₂= 263.2006), 285.1832 [MNa⁺] (calc. for C₁₇H₂₆NaO₂= 285.1825).; IR (Solution: DCM): 2926, 2852, 1688, 1256, 1112, 1022, 975, 826 cm⁻¹.

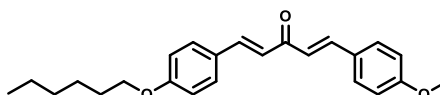
(E)-4-(4-(Decyloxy)phenyl)but-3-en-2-one (15)



A cooled solution of aqueous sodium hydroxide (0.5 g, 5 eqv. 0.01 mol) dissolved in water (10 ml) was added to a solution of 4-(decyloxy)benzaldehyde (0.5 g, 1 eqv. 0.002 mol) in 4 ml of ethanol solution stirred at 0 °C. Acetone (0.9 ml, 5 eqv. 0.01 mol) was added and stirred at 25 °C. The extract was purified by rapid column chromatography on silica (eluent: ethyl acetate/petrol. 1: 12, v/v). Collected fractions were evaporated *in vacuo* to yield product to give the yellow liquid (0.22 g, 36%).

TLC R_f 0.50 (10 % EtOAc/Pet.); ¹H NMR (400 MHz, CDCl₃) δ : 7.50-7.43 (m, 3H, CH=CHCOCH₃ and ArH), 6.90 (d, J = 8.6, 2H, ArH), 6.61 (d, J = 16.2, 1H, CH=CHCOCH₃), 3.98 (t, 3H, H1'), 2.35 (s, 3H, CH=CHCOCH₃), 1.82-1.75 (m, 2H, H2'), 1.58-1.49 (m, 2H, H3'), 1.41-1.07 (m, 14H, H3' – H9'), 0.94-0.76 (m, 3H, H10'); ¹³C NMR (100 MHz, CDCl₃) δ : 190.3, 165.1, 143.8, 131.7, 129.8, 114.5, 69.1, 31.7, 30.8, 29.3, 29.1, 26.0, 22.5, 14.2; ESI-MS m/z 89(100), 303(30)[MH⁺]; m/z 325(5)[MNa⁺]; ESI-HRMS m/z 303.2316 [M+H] (C₂₀H₃₁O₂= 303.2319), 325.2143 [MNa⁺] (calc. for C₂₀H₃₀NaO₂= 325.2138); IR (Solution: DCM): 2931, 2861, 1691, 1667, 1262, 1131, 1027, 983, 837 cm⁻¹.

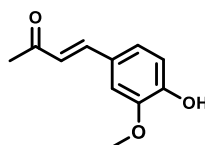
(1E,4E)-1-(4-(Hexyloxy)phenyl)-5-(4-methoxyphenyl)penta-1,4-dien-3-one (16)



A cooled solution of aqueous sodium hydroxide (3.692 mg, 5 eqv. 0.0923 mmol) dissolved in water (0.01 ml) was added to a solution of (E)-4-(4-(hexyloxy)phenyl)but-3-en-2-one (5.0 mg, 1.1 eqv. 0.02 mmol) in 3 ml of ethanol solution stirred at 0 °C. 4-Methoxybenzaldehyde (2.25 μ l, 1 eqv. 0.0185 mmol) was added and the mixture was stirred at 25 °C for 10 h, then washed with 50 ml water. The precipitate was filtered off to give the silver and white solid (6.94 mg, 95%).

TLC R_f 0.40 (30 % EtOAc/Pet.); MP 155–157 °C; ^1H NMR (400 MHz, CDCl_3) δ : 7.70 (d, $J = 16.2$ Hz, 2H, $\text{COCH}=\text{CH}$), 7.58–7.49 (m, 4H, ArH), 7.01–6.92 (m, 6H, $\text{COCH}=\text{CH}$ and ArH), 3.96 (t, 2H, $\text{H1}'$), 3.86 (s, 3H, OCH_3), 1.83–1.75 (m, 2H, $\text{H2}'$), 1.36–1.23 (m, 4H, $\text{H3}' - \text{H5}'$), 0.91 (m, 3H, $\text{H6}'$); ^{13}C NMR (100 MHz, CDCl_3) δ : 189.9, 162.1, 143.9, 130.1, 126.6, 124.5, 115.1, 61.8, 55.6, 31.7, 28.9, 27.3, 25.7, 22.6, 13.1; ESI-MS m/z 91(100), 159(30), 227(40), 365(50)[MH^+]; m/z 387(50)[MNa^+]; ESI-HRMS m/z 365.2019 [MH^+] (calc. for $\text{C}_{24}\text{H}_{29}\text{O}_3 = 364.2033$), 387.1974 [MNa^+] (calc. for $\text{C}_{24}\text{H}_{28}\text{NaO}_3 = 364.2033$); IR (Pressed KBr disc): 2942, 2864, 1689, 1264, 1174, 1114, 1027, 985, 834 cm^{-1} .

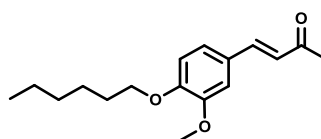
(E)-4-(4-Hydroxy-3-methoxyphenyl)but-3-en-2-one (18)



3-Ethoxy-4-hydroxybenzaldehyde (10 g, 60 mmol), acetone (80 mL), and 1 N NaOH (100 mL), were dissolved in acetone, and 1 N sodium hydroxide was added to the solution with continuous stirring. Stirring was continued 48 h. Excess acetone was removed under reduced pressure. Upon acidification with 1 N HCl, the reaction mixture was extracted with CHCl_3 , and then solution was organic extracts were dried over anhydrous MgSO_4 . The solvent was removed *in vacuo* and the resulting yellow solid was recrystallised from EtOAc to give yellow solid (11.37 g, 99%).

TLC R_f 0.30 (20 % EtOAc/Pet.); MP 123–125 °C; ^1H NMR (400 MHz, CDCl_3) δ : 7.42 (d, $J = 16.2$, 1H, $\text{CH}_3\text{COCH}=\text{CH}$), 7.15–7.06 (m, 1H, ArH), 7.05–6.97 (m, 2H, ArH), 6.92 (d, $J = 8.1$, 1H, ArH), 6.58 (d, $J = 16.2$, 1H, $\text{CH}_3\text{COCH}=\text{CH}$), 6.10 (s, 1H, ArH), 3.92 (s, 3H, OCH_3), 2.36 (s, 3H, $\text{CH}_3\text{COCH}=\text{CH}$); ^{13}C NMR (100 MHz, CDCl_3) δ : 199.0, 148.8, 146.9, 130.8, 125.5, 124.8, 48.7, 25.8; ESI-MS m/z 207(100)[MH^+]; m/z 229(50)[MNa^+]; ESI-HRMS m/z 207.1736 [MH^+] (calc. for $\text{C}_{11}\text{H}_{13}\text{O}_3 = 207.1729$), 229.0221 [MNa^+] (calc. for $\text{C}_{11}\text{H}_{12}\text{NaO}_3 = 229.0224$); IR (Pressed KBr disc): 3261, 3000, 1668, 1581, 1259, 1022, 978.

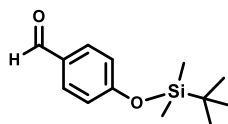
(E)-4-(4-(Hexyloxy)-3-methoxyphenyl)but-3-en-2-one (19)



(1*E*,4*E*)-1-(4-(hexyloxy)phenyl)-5-(4-methoxyphenyl)penta-1,4-dien-3-one (5 g, 1 eqv., 26 mmol), KI (4.316 g, 1 eqv., 26 mmol), and powdered K₂CO₃ (7.186 g, 2 eqv., 52 mmol) were taken in acetone (100.0 mL) and refluxed for 2 h under air. 1-Bromohexane (5.9 mL, 1.1 eqv., 28.6 mmol) was added dropwise to the above reaction mixture over 3 min. The reaction mixture was further refluxed for 16 h under air. It was cooled, the residue was poured into water (100 mL), and the acetone was removed under vacuum. Residue was extracted into dichloromethane (DCM) and washed with NaOH (100 mL, 2 % solution) and with brine (150 mL). The organic extracts were combined, dried (MgSO₄), and filtered. Collected fractions were evaporated *in vacuo* to yield product, yellow liquid (6.2908 g, 88%).

TLC *R_f* 0.50 (20 % EtOAc/Pet.); ¹H NMR (400 MHz, CDCl₃) δ: 7.41 (d, *J* = 16.2 Hz, 1H; CH₃COCH=CH), 7.12-7.01 (m, 2H; ArH), 6.82 (d, *J* = 8.2 Hz, 1H; ArH), 6.55 (d, *J* = 16.2 Hz, 1H; CH₃COCH=CH), 3.99 (t, 2H, *J* = 8.2 Hz; H1'), 3.84 (s, 3H; OCH₃), 2.31 (s, 3H; CH₃COCH=CH), 1.84 – 1.71 (m, 2H; H2'), 1.46 – 1.22 (m, 6H; H3' – H5'), 0.88 – 0.82 (m, 3H; H6'); ¹³C NMR (100 MHz, CDCl₃) δ: 196.8, 151.2, 149.6, 125.1, 123.1, 122.7, 112.4, 110.2, 69.1, 56.4, 31.7, 29.3, 27.4, 26.1, 22.6, 14.1; ESI-MS *m/z* 277(100)[MH⁺]; ESI-HRMS *m/z* 277.1793 [MH⁺] (calc. for C₁₇H₂₅O₃= 277.1798); IR (Solution: DCM): 2933, 2871, 1666, 1547, 1264, 1024, 972, 833.

4-((*tert*-Butyldimethylsilyl)oxy)benzaldehyde (20)

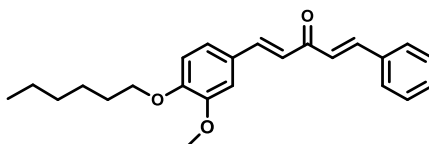


To a stirred solution of 4-hydroxybenzaldehyde (2.00 g, 1 eqv., 16.35 mmol) in THF (40 ml) was added imidazole (2.45 g, 2.2 eqv., 36.03 mmol) and *tert*-butyldimethylsilyl chloride (3.70 g, 1.5 eqv., 24.54 mmol) at rt. After 24 h water (40 ml) was added, and the mixture was diluted with DCM (40 ml). The layers were separated, and the aqueous layer was extracted with DCM (40 ml × 3). The combined organic layers were washed with brine (50 ml × 1), dried (MgSO₄), filtered and concentrated. The crude product was filtered with a pad of silica, washed with diethyl ether, then purification by flash chromatography, purified by rapid column chromatography on silica (eluent: ethyl acetate/petrol 3: 97 → 5: 95, v/v). Collected fractions were evaporated *in vacuo* to yield product to give the colorless liquid (2.813 g, 65%).

¹H NMR (400 MHz, CDCl₃) δ: 9.86 (s, 1H, CHO), 7.76 (d, *J* = 8.4 Hz, 2H, ArH), 6.92 (d, *J* = 8.4 Hz, 2H, ArH), 0.97 (s, 9H, C(CH₃)₃), 0.22 (s, 6H, Si(CH₃)₂); ¹³C NMR (100 MHz, CDCl₃) δ: 188.8, 161.5, 130.5, 124.5, 114.9, 32.3, 25.7; ESI-MS *m/z* 237(100)[MH⁺]; ESI-HRMS *m/z* 237.1304 [MH⁺]

(calc. for $C_{13}H_{21}O_2Si$ = 237.1306); IR (Solution: DCM): 3385, 2932, 2859, 1690, 1599, 1508, 1273, 1155, 909 cm^{-1} .

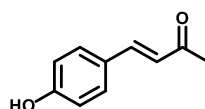
(1E,4E)-1-(4-(Hexyloxy)-3-methoxyphenyl)-5-phenylpenta-1,4-dien-3-one (24)



To a cooled solution of sodium hydroxide (0.3289 g, 5 eqv., 8.22 mmol) in H_2O (2 ml) was added to a solution of (E)-4-(4-(hexyloxy)-3-methoxyphenyl)but-3-en-2-one (0.5 g, 1.1 eqv., 1.81 mmol) in EtOH (4 ml) solution stirred at 0 °C, 4-benzaldehyde (0.1676 g, 1 eqv., 1.65 mmol) was added and stirred at 25 °C for 48 hours. The mixture was diluted with 1 M HCl (pH likely 6), then extracted it with DCM for three times. The combined organic phases (DCM-bottom layers) were washed with brine and dried over anhydrous $MgSO_4$, then filtered. The filtrate was concentrated *in vacuo* to give the crude product. The compound was purified by rapid column chromatography on silica (eluent: ethyl acetate/petrol 1: 6, v/v). Collected fractions were evaporated *in vacuo* to yield product (0.4283 g, 71%).

TLC R_f 0.50 (30 % EtOAc/Pet.); MP 134 – 137 °C; 1H NMR (400 MHz, CD_3OD) δ : 7.82 – 7.75 (m, 2H; $COCH=CH$), 7.48-7.39 (m, 4H; ArH), 7.31-7.24 (m, 3H; ArH), 7.16 (d, J = 16.2 Hz, 2H; $COCH=CH$), 6.99 (d, J = 8.2 Hz, 1H; ArH), 4.14-4.02 (m, 2H; $H1'$), 3.91 (s, 3H; OCH_3), 1.84-1.78 (m, 2H; $H2'$), 1.55-1.36 (m, 6H; $H3' - H5'$), 0.94-0.85 (m, 3H; $H6'$); ^{13}C NMR (100 MHz, CD_3OD) δ : 193.5, 151.8, 143.4, 131.3, 129.1, 127.8, 123.4, 122.3, 118.5, 111.7, 72.7, 63.3, 31.9, 29.2, 27.8, 20.1, 14.6; ESI-MS m/z 89(30), 235(30), 365(100)[MH^+]; ESI-HRMS m/z 365.2095 [MH^+] (calc. for $C_{24}H_{29}O_3$ = 365.2111); IR (Pressed KBr disc): 2935, 2864, 1667, 1595, 1258, 1118, 1021, 976, 835 cm^{-1} .

(E)-4-(4-Hydroxyphenyl)but-3-en-2-one (25)

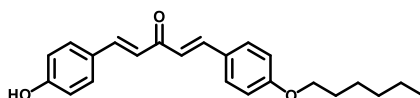


Aqueous NaOH (4.91 g, 0.123 mol) in water (24.6 ml) was added dropwise to a stirred solution of 4-hydroxybenzaldehyde (10 g, 81.9 mmol, 1 eqv.) and continually add acetone (15 ml, 0.2043 mol) in abs ethanol (55 ml), stirred at room temperature 25 °C for 48 h. Then water (120 ml) and dry ice

were added, yellow solid started to form on the side of round-bottomed flask about 2 min. After 20 min, water (50 ml) was added, then most of the precipitated out. If the precipitation was not come out, 2 M of HCl was added (pH likely about 6), then filtered on a bucher filter funnel (paper), washed with a small amount of water (10 ml). Dried in air to give a light yellow powder (14.70 g, 99%).

TLC R_f 0.30 (30 % EtOAc/Pet.); MP 73–75 °C; ^1H NMR (400 MHz, CD_3OD) δ : 7.85 (d, $J = 16.2$ Hz, 1H; ArCH=CHCOCH₃), 7.50 (d, 2H, $J = 8.6$ Hz; ArH), 6.82 (d, 2H, $J = 8.6$ Hz; ArH), 6.62 (d, 1H, $J = 16.2$ Hz; ArCH=CHCOCH₃), 2.34 (s, 3H; COCH₃); ^{13}C NMR (100 MHz, CDCl_3) δ : 201.5, 161.6, 146.4, 131.5, 127.2, 124.7, 116.9, 27.1; ESI-MS m/z 162 (60), 147 (100), 119 (40), 43 (17) [MH^+]; ESI-HRMS m/z 163.0754 [$\text{M}+\text{H}$](calc. for $\text{C}_{10}\text{H}_{11}\text{O}_2 = 163.0754$).

(1E,4E)-1-(4-(Hexyloxy)phenyl)-5-(4-hydroxyphenyl)penta-1,4-dien-3-one (26)



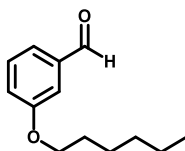
METHOD A: (1E,4E)-1,5-bis(4-hydroxyphenyl)penta-1,4-dien-3-one (0.1667 g, 1.05 eqv., 0.6259 mmol), KI (0.0989 g, 1 eqv., 0.6259 mmol), and powdered K_2CO_3 (0.1648 g, 2 eqv., 1.1922 mmol) were taken in acetone (13 mL) and refluxed for 2 h under air. 1-Bromohexane (0.1667 mL, 2 eqv., 1.7882 mmol) was added dropwise to the above reaction mixture over 3 min. The reaction mixture was further refluxed for 48 h under air, cooled, the residue was poured into water (100 mL), and the acetone was removed under vacuum. The reaction mixture was extracted into dichloromethane (DCM) and washed with brine (100 mL). The organic layer extracts were combined, dried (MgSO_4), and filtered. The compound was purified by column chromatography on silica (eluent: ethyl acetate/petrol 1: 4, v/v). Collected fractions were evaporated *in vacuo*. The results from column chromatography separated four parts: (1) symmetrical hexane-dba (0.0031 g); (2) start material and mono hexane-dba overlapped (0.0098 g); (3) mono hexane-dba (0.0072 g, 33%); (4) start material (0.0072 g).

METHOD B: Aqueous NaOH (0.3878 g, 0.009695 mol, 5 eqv.) in water (2.3 ml) was added dropwise to a stirred solution of the appropriate 4-(4-(hexyloxy)phenyl)but-3-en-2-one (0.4 g, 0.001939 mol, 1 eqv.) and (E)-4-(4-hydroxyphenyl)but-3-en-2-one (0.31426 g, 0.001939 mol, 1 eqv.) in abs ethanol (6 ml), stirred at room temperature 0 °C and then reacted at 25 °C for 48 h. Then water (50 ml) and dry ice were added, yellow solid started to form on the side of round-bottomed flask about 2 min. After 20 min, water (10 ml) was added, then most of the precipitated out. If the precipitation was not come out, 2 M of HCl was added (pH likely about 6), then filtered on a bucher filter funnel (paper),

washed with a small amount of water (10 ml). Dried in air to give a yellow powder as crude product. The crude compound was purified by rapid column chromatography on silica (eluent: ethyl acetate/petrol 1: 4 → 1: 2, v/v). Collected fractions were evaporated *in vacuo* to give the product as yellow solid and by-product as lighter yellow solid (0.30 g, 44%).

TLC R_f 0.50 (20 % EtOAc/Pet.); MP 131–132 °C; ^1H NMR (400 MHz, CDCl_3 , 20 °C) δ : 8.09 (s, 1H, OH), 7.69 (d, $J = 16.0$ Hz, 2H, $\text{CH}=\text{CHCO}$), 7.59–7.43 (m, 4H; ArH), 6.98–6.92 (d, $J = 16.0$ Hz, 2H; $\text{CH}=\text{CHCO}$), 6.94 (dt, 2H, $J = 8.8, 2.3$ Hz; ArH), 3.92 (t, 2H, $J = 6.6$ Hz; $\text{H1}'$), 1.76–1.72 (m, 2H, $J = 6.6$ Hz; $\text{H2}'$), 1.43–1.32 (m, 2H, $J = 6.6$ Hz; $\text{H3}'$ – $\text{H4}'$), 1.31–1.26 (m, 4H; $\text{H5}'$), 0.87–0.83 (m, 3H, $J = 6.6$ Hz; $\text{H6}'$); ^{13}C NMR (100 MHz, CDCl_3 , 20 °C) δ : 189.6, 161.3, 159.4, 143.5, 142.9, 130.8, 130.4, 129.8, 129.6, 127.1, 123.1, 122.9, 116.2, 115.9, 114.1, 113.9, 68.3, 31.6, 29.2, 25.7, 22.8, 14.5; Elemental Analysis (CHN) C: 77.46% H: 7.88% (Calculated: C: 78.83% H: 7.48%); ESI-MS m/z 351(100), 172 (15) [M+H]; ESI-HRMS m/z 351.1943 [M+H] (calc. for $\text{C}_{23}\text{H}_{26}\text{O}_3 = 351.1955$); IR (Pressed KBr disc): 3277, 2936, 2854, 1598, 1509, 1443, 1257, 1169, 1111, 1032, 991, 835, 577, 518 cm^{-1} .

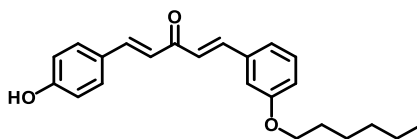
3-(Hexyloxy)benzaldehyde (27)¹⁵²



3-Hydroxybenzaldehyde (5.00 g, 41 mmol, 1.5185 eqv.), 1-bromohexane (4.455 g, 27 mmol, 1 eqv.) and Cs_2CO_3 (14.4 g, 44 mmol, 1.0732 eqv.) were stirred in DMF (36 mL) under air for 48 h at RT. Water (50 mL) was added to the dark suspension, which was extracted with Et_2O (2 × 100 mL). The combined extracts were washed with brine (30 mL), dried (MgSO_4) and evaporated to give orange oil. The compound was purified by column chromatography on silica (eluent: ethyl acetate/petrol 1: 5, v/v). Collected fractions were evaporated *in vacuo*. Collected two fractions, the first fraction was the desired product (5.41 g, 71%).

TLC R_f 0.50 (20 % EtOAc/Pet.); ^1H NMR (400 MHz, CDCl_3) δ : 9.95 (s, 1H, CHO), 7.48–7.39 (m, 2H, ArH), 7.41–7.34 (m, 1H, ArH), 3.99 (t, 2H, $J = 6.6$ Hz; $\text{H1}'$), 1.78 (m, 2H, $J = 6.6$ Hz; $\text{H2}'$), 1.47–1.28 (m, 6H, $\text{H3}' - \text{H5}'$), 0.89 (t, 3H, $J = 7.4$ Hz; $\text{H6}'$); ^{13}C NMR (100 MHz, CDCl_3) δ : 192.4 (CHO), 159.2, 137.4, 129.9, 123.4, 121.8, 112.6, 68.5, 31.3, 29.1, 25.6, 22.6, 14.0; ESI-MS m/z 207(100)[M+H], 229(15)[M+Na]; ESI-HRMS m/z 207.1371 [M+H] (calc. for $\text{C}_{13}\text{H}_{19}\text{O}_2 = 207.1380$), m/z 229.1190 [M+Na] (calc. for $\text{C}_{13}\text{H}_{18}\text{NaO}_2 = 229.1199$).

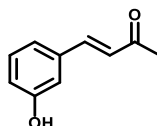
(1E,4E)-1-(3-(hexyloxy)phenyl)-5-(4-hydroxyphenyl)penta-1,4-dien-3-one (28)



NaOH (1.1634 g, 0.0909 mol, 5 eqv.) in water (6.8 ml) was added dropwise to a stirred solution of the appropriate 3-(hexyloxy)benzaldehyde (1.2 g, 0.00582 mol, 1 eqv.) and (1E,4E)-1,5-bis(4-hydroxyphenyl)penta-1,4-dien-3-one (0.9429 g, 0.00582 mol, 1 eqv.) in abs ethanol (18 ml). The mixture was stirred at room temperature 0 °C for 1 h and then at 25 °C for 48 h. Then water (50 ml) and dry ice were added, yellow solid started to form on the side of round-bottomed flask about 2 min. After 20 min, water (10 ml) was added, then most of the precipitated out. If the precipitation was not come out, 2 M of HCl was added (pH likely about 6) to the mixture, then filtered on a bucher filter funnel (paper), washed with a small amount of water (10 ml). The product was dried in air to give a yellow powder, which was a sticky yellow compound (0.50 g, 76%).

TLC R_f 0.50 (10% EtOAc/Pet.); $^1\text{H NMR}$ (400 MHz, CDCl_3) δ : 7.69 (d, $J = 16.2$ Hz, 2H, $\text{COCH}=\text{CH}$), 7.50-7.42 (m, 1H, ArH), 7.45-7.34 (m, 2H, ArH), 7.31-7.25 (m, 1H, ArH), 7.17 (d, $J = 8.2$ Hz, 2H, $\text{COCH}=\text{CH}$), 7.11-7.02 (m, 1H, ArH), 6.98-6.77 (m, 1H, ArH), 6.55 (d, $J = 16.2$ Hz, 1H, $\text{COCH}=\text{CH}$), 3.98 (t, 2H, $J = 6.6$ Hz; $\text{H}1'$), 1.85-1.29 (m, 8H, $\text{H}2' - \text{H}5'$), 0.91 (m, 3H, $\text{H}6'$); $^{13}\text{C NMR}$ (100 MHz, CDCl_3 , 20 °C) δ : 190.4, 161.1, 159.7, 142.9, 131.0, 129.7, 129.6, 127.1, 123.8, 123.7, 116.3, 115.9, 62.4, 32.1, 29.4, 25.5, 22.4, 14.2; ESI-MS m/z 90(20), 257(10), 351(100)[$\text{M}+\text{H}$]; ESI-HRMS m/z 351.1949 [MH^+] (calc. for $\text{C}_{23}\text{H}_{27}\text{O}_3 = 351.1955$); IR (Pressed KBr disc): 3269, 2933, 2862, 1596, 1512, 1464, 1261, 1173, 1027, 994 cm^{-1} .

(E)-4-(4-Hydroxyphenyl)but-3-en-2-one (30)

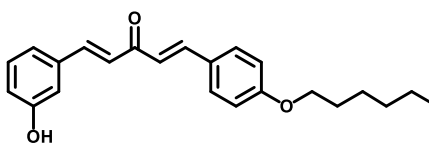


NaOH (4.91 g, 0.123 mol) in water (24.6 ml) was added dropwise to a stirred solution of 4-hydroxybenzaldehyde (10 g, 81.9 mmol, 2.05 eqv.) and continually add acetone (100 ml, 1.638 mol) in abs ethanol (33 ml), stirred at room temperature 25 °C for 48 h. Then water (150 ml) and dry ice were added, yellow solid started to form on the side of round-bottomed flask about 2 min. After 20 min, water (50 ml) was added, then most of the precipitated out. If the precipitation was not come out, 2 M of HCl was added (pH likely about 6) to the mixture, then filtered on a bucher filter funnel

(paper), washed with a small amount of water (10 ml), and then dried in air to give a yellow powder (15.79 g, 99%).

MP 87–88 °C; ¹H NMR (400 MHz, CD₃OD) δ: 7.57 (d, *J* = 16.2 Hz, 1H, CH₂COCH=CH), 7.19 (dd, *J* = 8.1 Hz, 2H, ArH), 7.04 (d, *J* = 8.1 Hz, 2H, ArH), 6.11 (d, *J* = 16.2 Hz, 1H, CH₂COCH=CH), 2.37 (s, 3H, COCH₃); ¹³C NMR (100 MHz, CD₃OD) δ: 198.2, 161.4, 146.2, 132.2, 126.1, 118.7, 116.9, 115.8, 28.3; ESI-MS *m/z* 163(80)[M+H], 185(100)[M+Na]; ESI-HRMS *m/z* 163.0762 [MH⁺] (calc. for C₁₀H₁₁O₂ = 163.0782), *m/z* 185.0581 [MH⁺] (calc. for C₁₀H₁₀NaO₂ = 185.0673).

(1*E*,4*E*)-1-(4-(Hexyloxy)phenyl)-5-(3-hydroxyphenyl)penta-1,4-dien-3-one (29)

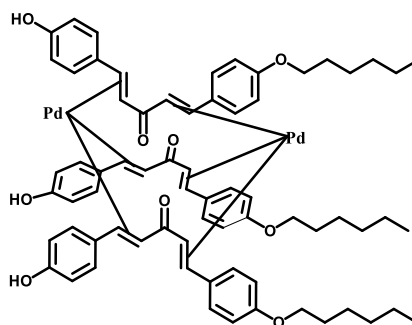


METHOD A: NaOH (0.1939 g, 4.8475 mmol, 5 eqv.) in water (1.1 ml) was added dropwise to a stirred solution of 4-hexoxybenzaldehyde (0.2 g, 0.9695 mmol, 1 eqv.) and (E)-4-(4-hydroxyphenyl)but-3-en-2-one (0.1572 g, 0.9695 mmol, 1 eqv.) in abs ethanol (4 ml), stirred at room temperature 0 °C for 1 h and then at 25 °C for 24 h. Then water (50 ml) and dry ice were added, yellow solid started to form on the side of round-bottomed flask about 2 min. After 20 min, water (10 ml) was added, then most of the precipitated out. If the precipitation was not come out, 2 M of HCl was added (pH likely about 6) to the mixture, then filtered on a bucher filter funnel (paper), washed with a small amount of water (10 ml), then dried in air to give a yellow powder.

METHOD B: aqueous NaOH (0.1546 g, 3.866 mol) in water (0.94 ml) was added dropwise to a stirred solution of 3-hydroxybenzaldehyde (0.0944 g, 0.7732 mmol, 1 eqv.) and (E)-4-(4-(hexyloxy)-3-methoxyphenyl)but-3-en-2-one (0.2 g, 0.812 mmol, 1.05 eqv.) in abs ethanol (2 ml), stirred at room temperature 0 °C for 1 h and then at 25 °C. Then water (50 ml) and dry ice were added, yellow solid started to form on the side of round-bottomed flask about 2 min. After 20 min, water (10 ml) was added, then most of the precipitated out. If the precipitation was not come out, 2 M of HCl was added (pH likely about 6) to the mixture, then filtered on a bucher filter funnel (paper), washed with a small amount of water (10 ml), then dried in air to give a yellow powder. The crude compound was purified by rapid column chromatography on silica (eluent: ethyl acetate/petrol 1:12 → 1:5, v/v), separating four compounds. Collected fractions were evaporated *in vacuo* to give the yellow solid (0.10 g, 31%).

TLC R_f 0.50 (20% EtOAc/Pet.); m.p. 134–135 °C; ^1H NMR (400 MHz, CD_3OD) δ : 7.76 (d, $J = 16.1$ Hz, 1H, $\text{COCH}=\text{CH}$), 7.71-7.66 (m, 3H, ArH), 7.33-7.21 (m, 1H, ArH), 7.19-7.11 (m, 4H, ArH), 6.99 (d, $J = 8.6$ Hz, 2H, $\text{COCH}=\text{CH}$), 6.91-6.84 (m, 1H, ArH), 4.04 (t, 2H, $J = 6.6$ Hz; $\text{H1}'$), 1.83-1.75 (m, 2H, $\text{H2}'$), 1.54-1.31 (m, 6H, $\text{H3}' - \text{H5}'$), 0.94 (m, 3H, $\text{H6}'$); ^{13}C NMR (100 MHz, CDCl_3) δ : 188.3, 159.2, 144.5, 134.8, 130.9, 127.3, 123.7, 121.1, 116.3, 114.8, 68.3, 32.6, 28.7, 26.2, 21.1, 14.7; ESI-MS m/z 150(100), 172(20), 351(30)[$\text{M}+\text{H}$]; ESI-HRMS m/z 351.1945 [MH^+] (calc. for $\text{C}_{23}\text{H}_{27}\text{O}_3 = 351.1955$); IR (Pressed KBr disc): 3274, 2936, 2850, 1596, 1512, 1447, 1249, 1161, 1037, 991, 836 cm^{-1} .

$\text{Pd}_2(4\text{-OH}, 4'\text{-alkyloxy dba})_3$ complex (33)

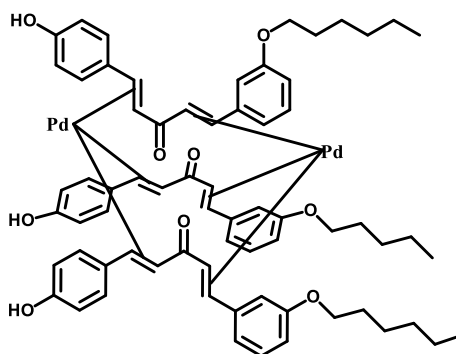


To a 100 ml round bottom flask a solution of sodium acetate (0.1822 g, 20 eqv., 2.2722 mmol), and (1*E*,4*E*)-1-(4-(hexyloxy)phenyl)-5-(4-hydroxyphenyl)penta-1,4-dien-3-one (0.1193 g, 3 eqv., 0.3408 mmol) in methanol (3 ml) and ethanol (2 ml) was stirred at 60 °C until all solid showed dissolved. PdCl_2 (0.0206 g, 1 eqv., 0.1136 mmol) was added and the mixture was heated at 50 °C for 20 min. The crude product was cooled, dried on a Bucher filter, and washed with water (50 ml) to give a purple solid (0.10 g, 73%).

MP 159–161 °C; ^1H NMR (400 MHz, THF-d_8 , 20 °C) δ : 8.81 (s, OH), 7.73-6.64 (m, $J = 8.1$ Hz, 2H; $\text{CH}=\text{CHCO}$, and ArH), 7.51 (d, $J = 8.1$ Hz, ArH), 7.04 – 6.92 (m, 2H, $\text{CH}=\text{CHCO}$ and ArH), 6.78 (d, $J = 8.1$ Hz, 2H, ArH), 6.71 – 6.36 (m, 4H, ArH), 6.86 (m, 2H, ArH), 6.71-6.65 (m, 1H; Pd-alkene), 6.59-6.53 (m, 1H; Pd-alkene), 6.48-6.42 (m, 1H, Pd-alkene), 6.36-6.29 (m, 1H; Pd-alkene), 6.19-6.12 (m, 1H; Pd-alkene), 6.03-5.95 (m, 2H; Pd-alkene), 5.88-5.80 (m, 1H; Pd-alkene), 5.27-5.21 (m, 1H; Pd-alkene), 4.91-4.85 (m, 1H; Pd-alkene), 4.75 (s, 1H; Pd-alkene), 4.00 (t, 2H, $J = 6.6$ Hz; $\text{H1}'$), 1.82-1.76 (m, 2H; $\text{H2}'$), 1.52-1.41 (m, 2H; $\text{H3}'\text{-H4}'$), 1.38-1.31 (m, 4H; $\text{H5}'$), 0.96-0.93 (m, 3H, $J = 6.6$ Hz; $\text{H6}'$); ^{13}C NMR (100 MHz, THF-d_8 , 20 °C) δ : 192.4, 166.1, 159.8, 145.9, 149.4, 137.4, 133.5,

133.1, 132.4, 128.3, 125.7, 125.3, 121.4, 118.5, 115.7, 114.7, 69.9, 34.3, 29.7, 26.2, 23.1, 15.7;
Elemental Analysis (CHN) C 62.46 %, H 6.04 % (Calculated: 68.44 %, H 6.49 %).

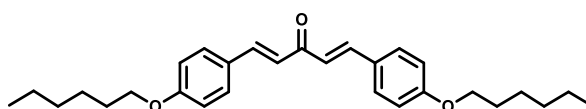
Pd₂(4-OH, 3'-alkyloxy dba)₃ complex (34)



To a 100 ml round bottom flask a solution of sodium acetate (0.1822 g, 20 eqv., 2.2722 mmol), and (1*E*,4*E*)-1-(3-(hexyloxy)phenyl)-5-(4-hydroxyphenyl)penta-1,4-dien-3-one (0.1193 g, 3 eqv., 0.3408 mmol) in methanol (3 ml) and ethanol (2 ml) was stirred at 60 °C until all solid dissolved. PdCl₂ (0.0206 g, 1 eqv., 0.1136 mmol) was added and heated at 50 °C for 20 min. The crude product was cooled, dried on a Bucher filter, and washed with water (50 ml) to give a purple solid (0.05 g, 42%).

MP 128–129 °C; ¹H NMR (400 MHz, THF-d₈, 20 °C) δ: 7.66 – 7.59 (m, 1H, ArH), 7.50 (d, *J* = 8.1 Hz, 1H; ArH), 7.27 – 7.20 (m, 2H, ArH), 7.16 (d, *J* = 16.2 Hz, 1H, CH=CHCO), 7.01 (d, *J* = 16.2 Hz, 1H, CH=CHCO), 6.99-6.91 (m, 1H, ArH), 6.79 (d, *J* = 8.1 Hz, 1H, ArH), 6.75-6.53 (m, 6H, ArH, Pd-alkene), 6.46-6.40 (m, 1H, Pd-alkene), 6.35-6.29 (m, 1H; Pd-alkene), 6.15-6.10 (m, 1H; Pd-alkene), 6.02-5.93 (m, 2H; Pd-alkene), 5.87-5.83 (m, 1H; Pd-alkene), 5.24-5.20 (m, 1H; Pd-alkene), 4.89-4.82 (m, 1H; Pd-alkene), 4.71 (s, 1H; Pd-alkene), 4.01 (t, 2H, *J* = 6.6 Hz; H1'), 1.83-1.75 (m, 2H; H2'), 1.51-1.42 (m, 2H; H3'-H4'), 1.36-1.32 (m, 4H; H5'), 0.95-0.92 (m, 3H, *J* = 6.6 Hz; H6'); ¹³C NMR (100 MHz, THF-d₈, 20 °C) δ: 191.7, 160.4, 146.6, 137.2, 133.1, 129.7, 125.1, 124.2, 118.8, 117.4, 115.9, 69.8, 35.1, 29.8, 28.0, 23.3, 16.4; Elemental Analysis (CHN) C 62.56%, H 8.61% (Calculated: 68.44%, H 6.49%).

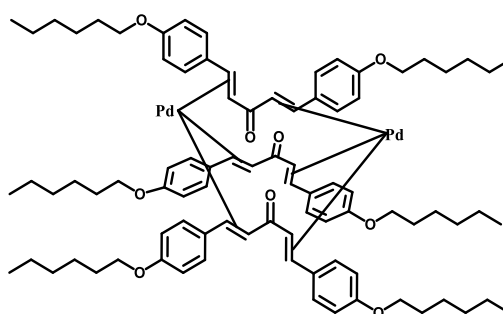
(1*E*,4*E*)-1-(3-(Hexyloxy)phenyl)-5-(3-hydroxyphenyl)penta-1,4-dien-3-one (35)



The successful procedure is followed by the same reaction of synthesis of **26** (0.41 g, 48%).

TLC R_f 0.50 (10 % EtOAc/Pet.); m.p. 127–128 °C; ^1H NMR (400 MHz, CDCl_3) δ : 7.71(d, J = 16.1 Hz, 2H; $\text{COCH}=\text{CH}$), 7.52 (d, J = 8.2 Hz, 4H; ArH), 7.06-6.93 (m, 4H, ArH), 6.91(d, 2H, J = 16.1 Hz, 2H; $\text{COCH}=\text{CH}$), 4.00(t, 4H, J = 6.6 Hz; $\text{H1}'$), 1.88-1.79 (m, 4H, $\text{H2}'$), 1.48-1.29 (m, 12H, $\text{H3}'$ – $\text{H5}'$), 0.91(m, 6H, $\text{H6}'$); ^{13}C NMR (100 MHz, CDCl_3) δ : 186.7, 160.9, 142.8, 130.1, 128.9, 123.2, 114.9, 68.0, 31.7, 28.9, 25.8, 22.5, 14.6; ESI-MS m/z 207(15), 435(100)[$\text{M}+\text{H}$]; ESI-HRMS m/z 435.2889 [MH^+] (calc. for $\text{C}_{29}\text{H}_{39}\text{O}_3$ = 435.2895); IR (Pressed KBr disc): 2937, 2872, 2361, 1595, 1511, 1263, 1177, 1028, 980, 836 cm^{-1} .

$\text{Pd}_2(4\text{-hexyloxy dba})_3$ complex (37)



To a 100 ml round bottom flask a solution of sodium acetate (0.1822 g, 20 eqv., 2.2722 mmol), and (*1E,4E*)-1-(4-(hexyloxy)phenyl)-5-(4-hydroxyphenyl)penta-1,4-dien-3-one (0.1193 g, 3 eqv., 0.3408 mmol) in methanol (3 ml) and ethanol (2 ml) was stirred at 60 °C until all solid dissolved.) PdCl_2 (0.0206 g, 1 eqv., 0.1136 mmol) was added and heated at 50 °C for 20 min. The crude product was cooled, dried on a Bucher filter, and washed with water (50 ml) to give a purple solid (0.13 g, 91%).

MP 159–161 °C; ^1H NMR (400 MHz, CDCl_3 , 20 °C) δ : 7.71(d, J = 16.1 Hz, 2H; $\text{COCH}=\text{CH}$), 7.52 (d, J = 8.2 Hz, 4H; ArH), 7.08-6.94 (m, 4H, ArH), 6.91(d, 2H, J = 16.1 Hz, 2H; $\text{COCH}=\text{CH}$), 6.63 (d, 1H; Pd-alkene), 6.58 (d, 1H; Pd-alkene), 6.52 (d, 1H, Pd-alkene), 6.43 (d, 1H; Pd-alkene), 6.27 (d, 1H; Pd-alkene), 6.12 (d, 1H; Pd-alkene), 5.96 (d, 1H; Pd-alkene), 5.81 (d, 1H; Pd-alkene), 5.78 (d, 1H; Pd-alkene), 5.23 (d, 1H; Pd-alkene), 5.18 (d, 1H; Pd-alkene), 4.83 (d, 1H; Pd-alkene), 4.00(t, 4H, $\text{H1}'$), 1.83-1.75 (m, 4H, $\text{H2}'$), 1.48-1.29 (m, 12H, $\text{H3}'$ – $\text{H5}'$), 0.95-0.90 (m, 6H, $\text{H6}'$); ^{13}C NMR (100 MHz, CDCl_3) δ : 186.6, 160.4, 142.8, 130.3, 128.6, 123.7, 114.3, 67.6, 31.5, 28.8, 26.0, 22.3, 14.4; Elemental Analysis (CHN) C 62.46%, H 6.04% (Calculated: 68.44%, H 6.49%).

General procedure for 'Pd-dba' complex purity determinations

The 'Pd-dba' complex (0.004355 mmol, 1 eqv.) was mixed with PPh₃ (0.01742 mmol, 4 eqv. – Pd/PPh₃ theoretical ratio = 1:2) in CD₂Cl₂ (0.5 ml, dry). Triethyl phosphate in CD₂Cl₂ (0.316 ml, see below for calculation of stock solution concentration) was added to the mixture, which was subsequently transferred to a Young's NMR tube (all operations performed in the glove box). ³¹P and ¹H NMR spectra were then measured.

Stock solution preparation

Triethyl phosphate (0.10452 mmol, 24 eqv.) was dissolved CD₂Cl₂ (3 ml, dry).

Calculation methodology for Pd purity research

$$\frac{n(\text{ref.}) \times (P^A + P^B)}{n(\text{PPh}_3) \times 1}$$

n: molar concentration (mmol);

ref: triethyl phosphate;

P^A, P^B: integration of A and B phosphorus from ³¹P NMR spectrum;

The integration of triethyl phosphate phosphorus was set as 1.

CHAPTER 3

SYNTHESIS OF HIGHLY CONJUGATED LINEAR ETHYNYL NUCLEOSIDES

3 Synthesis of highly conjugated linear ethynyl nucleosides

3.1 Introduction

The assembly of modified nucleosides *via* metal-catalysed cross-coupling has attracted growing interest due to various applications ranging from therapeutics to catalysis. To expand the scope of these applications, modified fluorescent nucleosides are highly sought after.^{156–160} Donor-acceptor phenylene-ethynyl substituted π -conjugated organic derivatives, which push low-lying charge-transfer excited states, can be used as relatively small fluorescent nucleoside analogues.^{161–164} The low-lying charge transfer states of alkynyl or aryl groups in these analogues can be tuned by altering the substituents on the aryl ring, in essence allowing one to tailor-make analogues for specific applications. Specifically, the low-lying charge transfer energy states of the alkynyl or aryl groups can be tuned through alteration of the *para*-substituent to modulate the fluorescent properties while minimising the degree of steric changes to the phenylene-ethynyl purine compound. The synthesis of linear *p*-conjugated 8-alkynylated adenosines and guanosines will be discussed in this chapter.

Protection of both the sugar hydroxyl groups and the reactive heteroaromatic substituents was considered necessary until some researchers developed reaction conditions showing unprotected halogenated nucleosides can be effectively cross-coupled with various nucleophilic components.^{165–167} Previous work by the Fairlamb group has concerned a practical Sonogashira alkylation protocol for unprotected 8-alkynylated adenosines and guanosines catalysed by Pd^{II} precatalyst, PdCl₂(PPh₃)₂ (Figure 3.1). Furthermore, a preliminary fluorescence study involving changes to the substituent on the phenylene ring has been reported.⁹⁷

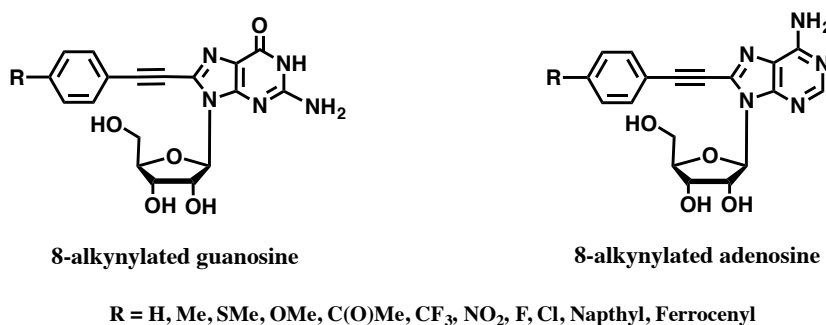


Figure 3.1 Previous work on the synthesis of 8-alkynylated guanosine and adenosine derivatives.

It was decided to focus primarily on the alkylation of purine nucleosides. The second part of the study would then involve trying to understand the fluorescent properties of the synthesised compounds. The global aim was to develop fluorescent base analogues—possessing conjugation with appropriate photophysical properties for studying mismatching DNA or RNA duplexes. The key

design principles rely on the physical characteristics of the conjugated 8-modified purine base. Attention was focussed on C8-modified adenosine and guanosine analogues.

3.2 Sonogashira alkylation of unprotected 8-modified fluorescent nucleosides

3.2.1 Sonogashira alkylation of unprotected 8-bromoguanosine and adenosine

On a general note, Pd-catalysed cross-coupling reactions have proven efficient for synthesis of substituted nucleosides.^{168,169} Furthermore, the Pd-mediated processes appear to be more facile with adenosine derivatives.⁹⁰ Guanine can coordinate to Pd through different modes – at nitrogen or oxygen. A hindrance for the cross-coupling of haloguanosines is the inherent binding affinity of Pd ions to guanine moieties *vide infra* (through N7 and O6, or N1 and O6 to both Pd⁰ and Pd^{II}; Figure 3.2). The problem has been described by Shaughnessy and co-workers, providing evidence for the inhibitory effects of the guanine moiety in Suzuki cross-couplings of unprotected halonucleosides under aqueous conditions (at *ca.* pH = 10).⁹⁰ Therefore, adenosines act as monodentate ligands for Pd, via N7 or N3, respectively, and guanosine behaves as a bidentate ligand, the Pd atom being firmly bound at N7 and weakly via O6.^{170–172}

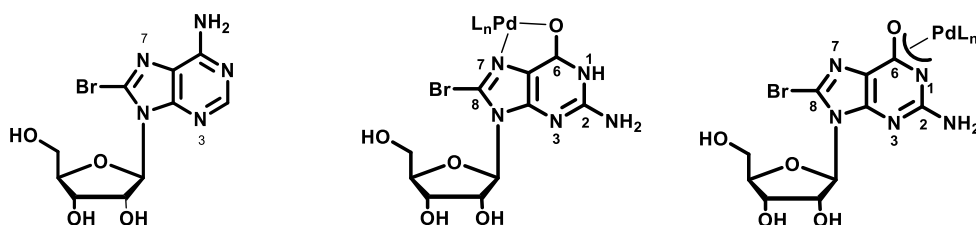


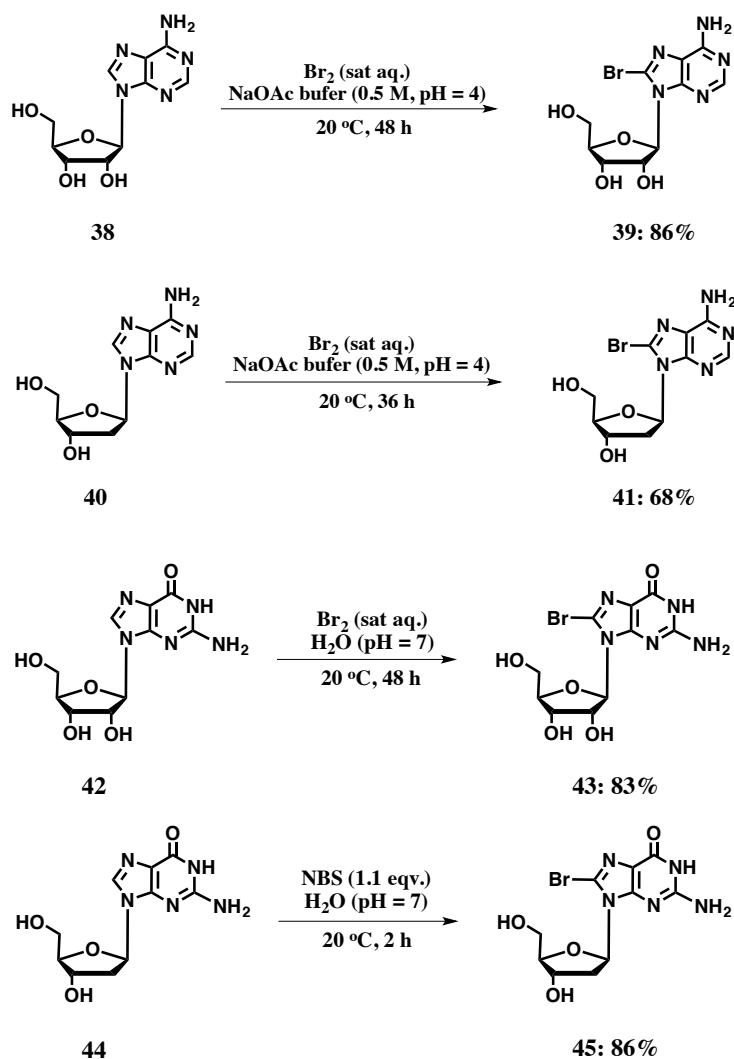
Figure 3.2 Possible coordination of 8-BrG to Pd under basic conditions compared with 8-BrA.

However, there were no literature examples involving the alkylation of unprotected-8-bromoguanosine with terminal acetylenes until our group's first work.¹²⁰ The Sonogashira alkylation was utilised for the synthesis of π -conjugated adenosine and guanosine systems. Flasche and Crisp found that the protection of hydroxyl or amino substituents in guanosines was required for efficient Sonogashira cross-coupling and solubilisation of guanosine into organic solvents.^{173,174} The problem may come from the hindrance of guanosine derivatives, generally, in Pd-catalysed cross-couplings.

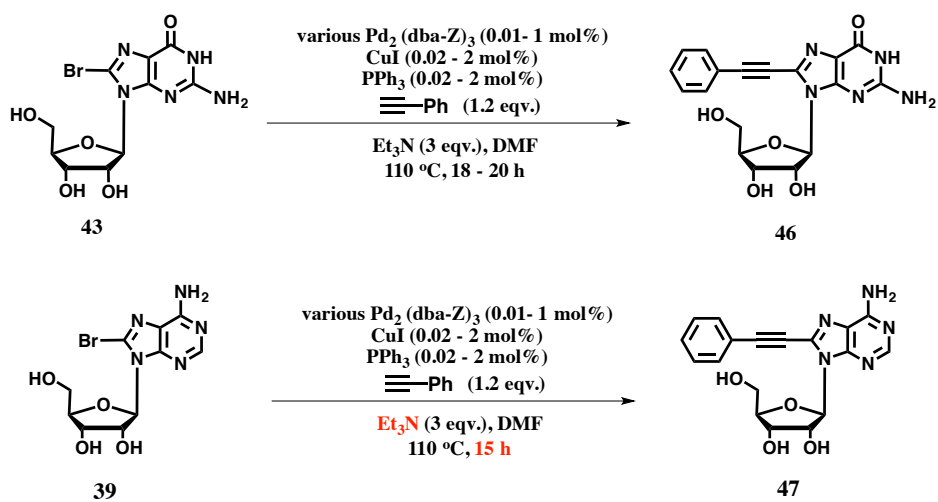
It is interesting to note that C-8 alkynylation required more rigorous conditions for adenosine than guanosine. This does not mean or prove that complexation of the Pd catalyst by interaction through guanosine N7 and O6 explains the poor reactivity of guanosine generally in Pd-catalysed cross-coupling reactions, from a mechanistic point of view. The pre-functionalisation step was carried out on adenosine and guanosine, using Br₂. The first attempts for preparation of brominated adenosine and guanosine involved the use of NBS (*N*-Bromosuccinimide).¹⁷⁵ For the synthesis of 8-bromo-(deoxy)adenosine (**39** and **41**), the reaction was low-yielding in the first experiments. It was found that slow dropwise addition of saturated Br₂ was required to give the product in good yield (Scheme 3.1).¹⁷⁶ Key to the success of the synthesis of **41** was to maintain the pH of the reaction mixture at 6.5 (no higher than 7). It is also noteworthy that water, which was used for the synthesis of **43** and **45**, needed to be deionised and at pH <7.

The Sonogashira alkynylation of 8-bromoguanosine **43** with phenylacetylene was undertaken using standard conditions (Scheme 3.2).⁴² Interestingly, it was found that there was no need to protect compound **43** at the O6 position to inhibit the complexation of Pd/Cu by guanosine derivatives. A focus was directed towards the 'Pd-dba' complexes as novel catalysts for these types of transformations. The synthesis of catalysts, **6**, **7**, **33**, and **37**, was detailed in Chapter 2.

Cross-couplings with adenosine **39** required use of freshly-distilled trimethylamine and reduced reaction times, as the β-glycosyl bond was found to be much more sensitive than cross-couplings employing guanosine.



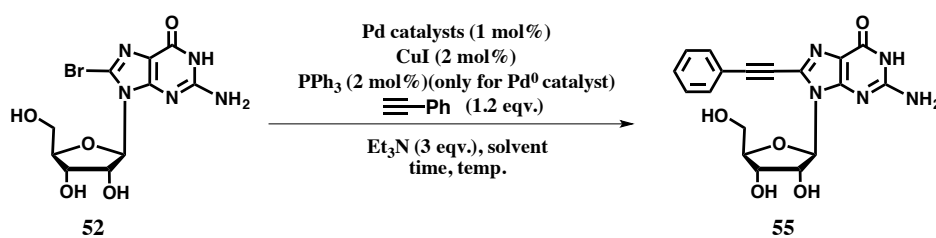
Scheme 3.1 Synthesis of 8-bromo-(deoxy)adenosine **39(41)** and 8-bromo-(deoxy)guanosine **43(45)**.



Scheme 3.2 Sonogashira alkynylations of unprotected 8-bromoguanosine/adenosine **46** and **47** with phenylacetylene.

Several reaction conditions using the different Pd catalysts, reaction times, solvents and temperatures were examined and the results are summarized in Table 3.1. In addition to DMF, other less hazardous solvents were utilised with these Sonogashira reactions. The need to replace DMF solvents is due to its designation as a reproductive toxin.¹⁷⁷ However, without DMF, there are often solubility problems which also pose a challenge. Acetonitrile is a good first choice replacement solvent, which is easily dried by distillation over calcium hydride. Besides DMF, solvent mixtures were tested, e.g. 1:1 mixture of acetonitrile:water and 1:3 mixture of Et₃N:acetonitrile.¹¹⁸ Ethylene carbonate was also investigated. However, due to the solubility issues, no product was formed from the reaction using both PdCl₂(PPh₃)₂ and Pd⁰₂(dba)₃·dba precatalysts (Entries 1 and 2). The reaction proceeded in acetonitrile: water = 1:1 solvent system using Pd⁰₂(dba)₃·dba catalyst at lower temperature, while the Pd^{II} precatalyst did not work for the reaction under the same conditions (Entries 3–5). Meanwhile, Et₃N: acetonitrile = 1:3 solvent system was found to give only poor yields for both Pd catalysts (Entries 6 and 7).

Table 3.1 Various attempts to affect the cross-coupling of 8-bromoguanosine **43**.

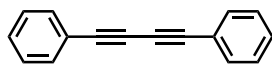


Entry	Pd catalysts	Time (h)	Solvent	Temp (°C)	Reaction outcome ^a
1	PdCl ₂ (PPh ₃) ₂	18	ethylene carbonate	110	N.R. ^b
2	Pd ⁰ ₂ (dba) ₃ ·dba	18	ethylene carbonate	110	N.R. ^b
3	PdCl ₂ (PPh ₃) ₂	18	MeCN: H ₂ O = 1:1	110	N.R. ^b
4	PdCl ₂ (PPh ₃) ₂	22	MeCN: H ₂ O = 1:1	60	N.R. ^b
5	Pd ⁰ ₂ (dba) ₃ ·dba	22	MeCN: H ₂ O = 1:1	60	52%
6	PdCl ₂ (PPh ₃) ₂	18	Et ₃ N: MeCN = 1:3	80	9%
7	Pd ⁰ ₂ (dba) ₃ ·dba	18	Et ₃ N: MeCN = 1:3	80	7%

^a As determined by ¹H NMR spectroscopy and mass spectrometry (ESI, +ve mode), isolated following purification by silica gel chromatography. ^b Recovery of starting material confirmed by ¹H NMR spectroscopy.

For reactions giving products **46**, **47** and other modified nucleosides, a column-free protocol was used. The purification required DMF removal at 40–50 °C *in vacuo*, which afforded dark coloured solids. The purity of the products could be improved by washing with boiling water (removing Et₃N·HCl salts and unreacted **39** and **43**). The process was found to be more efficient using a fluted

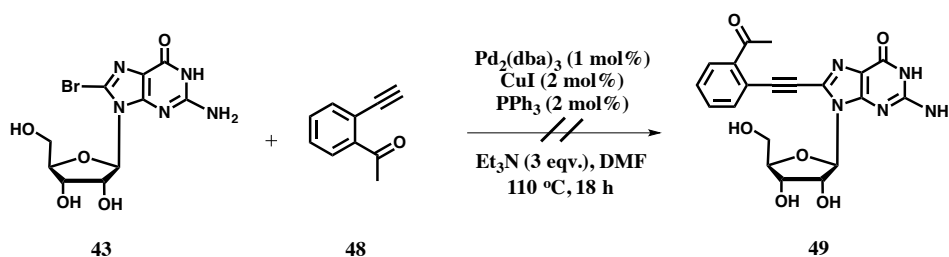
filter paper and glass funnel, rather than filtration through a glass sinter. The solids were also washed with small quantities of EtOAc and Et₂O to remove any traces of homocoupled 1,4-diyne side-product (Figure 3.3), which was formed from the reduction of PhCl₂(PPh₃)₂ with 2 equivalents of the *in situ* generated alkynecuprate (by Glaser-type coupling).



homocoupled product

Figure 3.3 Homocoupled product from reaction of Sonogashira alkylation of unprotected 8-bromoguanosines/adenosines.

At one stage in the project, we were keen to use *in-situ* FT-IR instrument (ReactIRTM) for tracking reaction progress. The carbonyl signals in the alkyne **48** and the product **49** were hypothesised by provide characteristic IR signals to follow (Scheme 3.3). Unfortunately, it was not possible to form the desired product **49**. Only starting material was recovered from these reactions.



Scheme 3.3 Attempted synthesis of compound **49** for use in ReactIRTM studies.

3.2.2 Pd catalyst activity towards Heck and Sonogashira cross-coupling reactions

3.2.2.1 Pd(0)-mediated Sonogashira cross-coupling reactions

The activity of the Pd catalysts against the Sonogashira cross-coupling reactions of 8-bromoguanosine and 8-bromoadenosine with terminal alkynes under optimised conditions were evaluated (Figure 3.4 and 3.5). Pd catalysts **6**, **7**, **33**, and **37** (at different catalyst loadings) were tested. High concentrations of Pd (*ca.* 10 mol%) may cause low yields due to rapid Pd agglomeration and precipitation.¹⁷⁸ The complex [Pd⁰₂(dba)₃·CHCl₃] can be made by recrystallization of [Pd⁰₂(dba)₃·dba] from CHCl₃ solution, which is thought to be generally of higher purity.^{135,142} This complex was the benchmark ‘control’ catalyst, allowing a comparison of activity with the new Pd catalysts **6**, **7**, **33** and **37**.

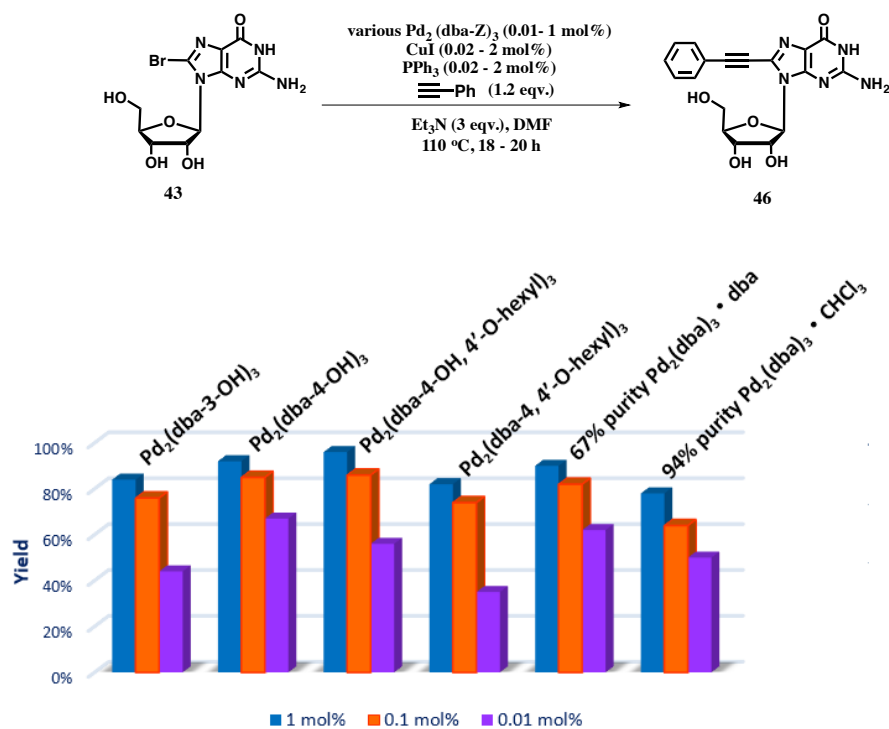


Figure 3.4 Screening the activity of novel Pd catalysts 1 mol% against the Sonogashira cross-coupling reaction of 8-bromoguanosine **43** to give **46**.

From the above figures, as the Pd catalyst loading decreased from 1 mol% to 0.01 mol%, the yield dropped significantly. For the adenosine reactions, the new Pd catalysts exhibited slightly improved yields, relative to both [Pd⁰₂(dba)₃•dba] and [Pd⁰₂(dba)₃•CHCl₃]. The best Pd catalyst was Pd₂(dba-4-OH, 4'-O-hexyl)₃ (**33**) for both guanosine and adenosine reactions. For both types of reaction, the yield reduced dramatically using 0.01 mol% catalyst loading. The optimised reaction conditions for C8-modification was found using 1 mol% of catalyst **33**.

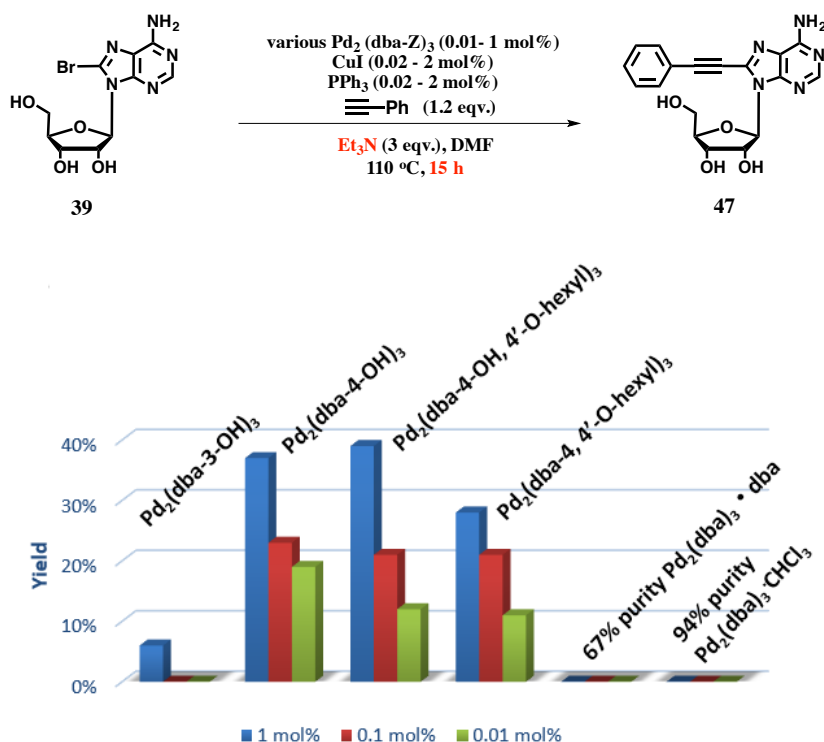


Figure 3.5 Screening the activity of novel Pd catalysts against the Sonogashira cross-coupling reaction of 8-bromoadenosine **39** to give **47**.

3.2.2.2 Pd(0)-mediated Heck alkenylation of 5-iodo-2'-deoxyuridine

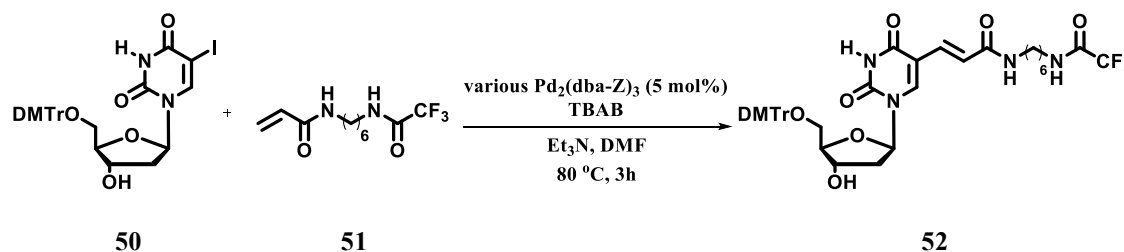
Fu and co-workers have shown the intramolecular effect on Heck reactions of unactivated alkyl halides. They used Pd₂(dba-4-OMe)₃ as catalyst instead of Pd₂(dba-4-H)₃, which provided improved product selectivity in intermolecular Heck cyclisation reactions.¹⁷⁹ Therefore we anticipated seeing dba-Z ligand effects in Heck cross-coupling reactions.

The modified 2'-deoxyuridine has become a valuable alternative to the classical synthetic methodology due to its wide application on post-synthesis conjugation of diagnostic biomolecules, utilised in the research field of fluorescent probe.¹⁸⁰ Modified molecule **52** has been reported via a Heck cross-coupling assisted by toxic organomercurial salts and K₂PdCl₄ in low yield (24%).¹⁸¹ In the meanwhile, the Sanghvi group investigated [Pd₂(dba-4-OMe)₃] as the catalyst.¹⁸² The Sanghvi group questioned that Pd₂(dba-4-OMe)₃ may accelerate the reaction due to the presence of PdNPs, which are catalytically active.

Pd catalysts were screened against the Heck cross-coupling reaction of DMT protected uridine **50** with **51** (Table 3.1). Compared to Pd₂(dba-4-OMe)₃, the best performing catalysts were found to be

7 and **33**. In this study, no evidence for PdNPs was found in the Pd₂(dba-4-OMe)₃ material, which was confirmed by TEM measurements.

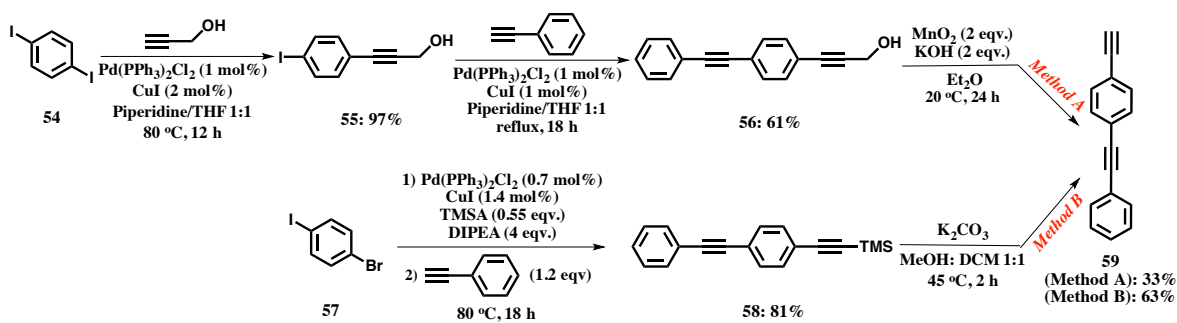
Table 3.2 Pd catalyst activity toward a Heck cross-coupling reaction of a pyrimidine nucleoside **50** and alkene **51**.



Pd catalysts	Isolated Yield (52) /%
Pd ₂ (dba-3-OH) ₃ (6)	87
Pd ₂ (dba-4-OH) ₃ (7)	91
Pd ₂ (dba-4-OH,4'-OHHexyl) ₃ (33)	89
Pd ₂ (dba-4-OHexyl) ₃ (37)	72
Pd ₂ (dba-4-OMe) ₃ (53)	80

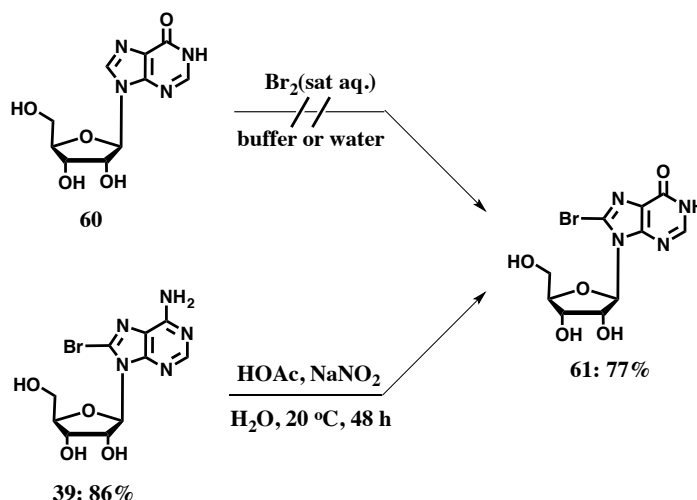
3.2.3 Modification of multiple alkyne motif on C8 nucleosides

The synthesis of highly conjugated linear ethynyl purines has been investigated as part of this project. The synthesis of target motif **59** can be accessed by two approaches detailed within the literature – Method A¹⁸³ and Method B¹⁸⁴ (Scheme 3.4). Method B is more traditional and more practical than Method A, which contains two Sonogashira cross-coupling steps, whereas Method B, involves a one-pot reaction of **57**. Moreover, silyl alkyne **58** is more stable than propargyl alcohol **56**. Nevertheless, both methods A and B were tested. For Method A, the overall yield of **59** was much lower than Method B (33% versus 63% respectively). The product also appeared to suffer from decomposition using Method A, which perhaps indicates an impurity being present. In summary, Method B was more feasible for the synthesis of compound **59**.



Scheme 3.4 Comparison of two routes for synthesising target compound **59**.

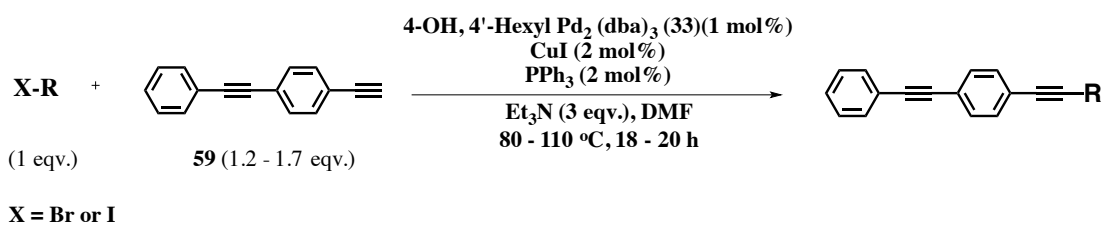
Inosine can form a base pair with adenine, cytosine, or uracil. Little work has been done on inosine fluorescent probes thus far. Therefore, a C8 modified alkyne with potential fluorescent characteristics was identified for synthesis. A variety of reaction conditions were tried,¹⁸⁵ but unlike the synthesis of **39** or **43**, the synthesis of 8-Br-inosine could not be achieved directly from inosine. The target compound **61** was synthesised from 8-bromo-adenosine **39** using NaNO₂, under acidic conditions, in good yield (77%).

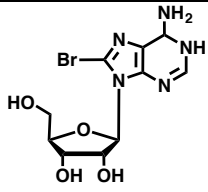
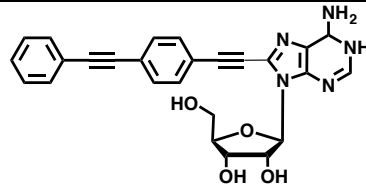
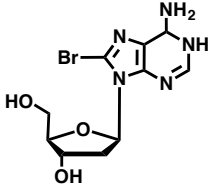
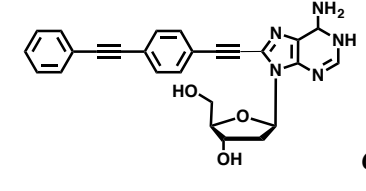
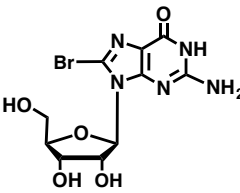
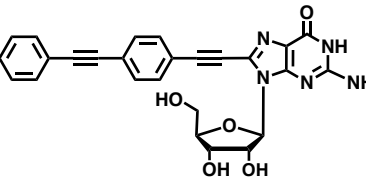
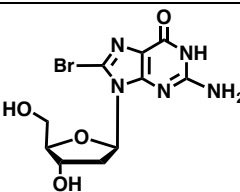
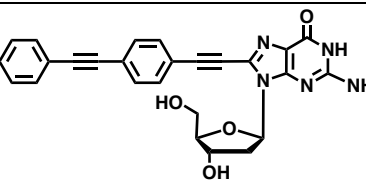
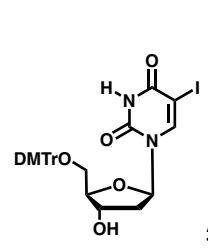
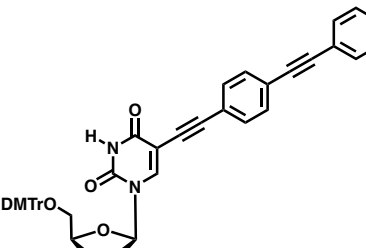
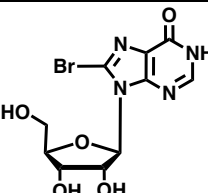
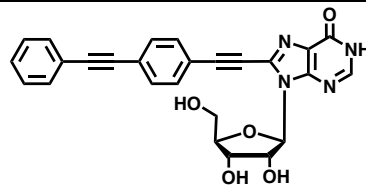


Scheme 3.5 Synthesis of 8-Bromoinosine **61**.

With the desired multiple alkyne ‘Ph–CC–Ph–CC–’ motif **59** and optimised reaction conditions in hand, **59** was reacted with purine and other nucleosides, using Sonogashira cross-coupling reactions. The modification at C8 of adenosines, guanosines, and uridines with **59** have been shown to be a useful way of introducing fluorescent labels to nucleosides in addition to showing interesting properties (Table 3.32). For the reaction with deoxyadenosine and inosine as the starting materials, the PhCCPhCCH **59** needed to be used in excess (1.8 equivalents). The reaction solvent for the syntheses detailed in Table 3.3 were freshly prepared and distilled. These nucleosides were characterised by NMR spectroscopy, taking compound **65** for example (Figure 3.6). The UV/Vis and fluorescence properties of the modified analogues have been investigated to determine their suitability for use as biological probes (See Chapter 4).

Table 3.3 Modification at C8 of adenosines/guanosines/uredines/inosines.



Entry	Brominated nucleosides	Product	Yield
1	 39	 62	89% ^{a,c,f}
2	 41	 63	95% ^{b,d,f}
3	 43	 64	92% ^{a,c,e}
4	 45	 65	96% ^{b,c,e}
5	 50	 66	96% ^{b,d,f}
6	 61	 67	80% ^{b,c,f}

^a Reaction conducted at 110 °C. ^b Reaction conducted at 80 °C. ^c Reaction time 18 h. ^d Reaction time 22 h. ^e Reaction carried out with 1.2 eqv. of **59**. ^f Reaction carried out with 1.7 eqv. of **59**.

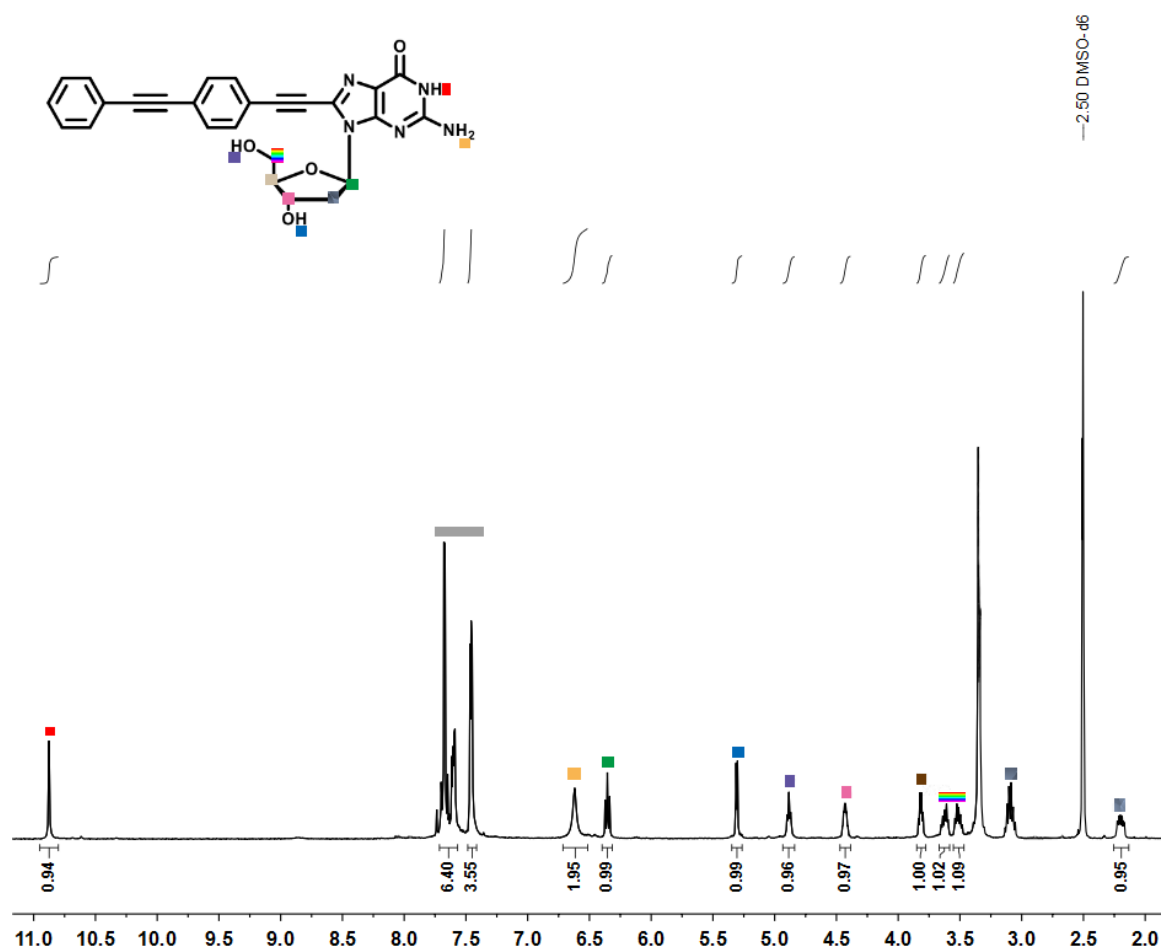


Figure 3.6 ¹H NMR spectrum of compound 65.

3.2.3.1 Greener solvent investigation

Propylene carbonate (PC) is a polar aprotic solvent, seen as greener than DMF, and it has been used as an alternative solvent for cross-coupling reactions (Table 3.4).¹⁸⁶ Degassed PC was obtained using “freeze-pump-thaw” cycles. PC (B.P. = 242 °C) has a higher boiling point than DMF (B.P. 154 °C). The melting point of PC is -49 °C, while ethylene carbonate (EC) is +37 °C. In addition, PC can be used without EC or other co-solvent.¹⁷⁷ It was found that the starting materials were only partially soluble in PC between 25-80 °C. Therefore, reaction mixtures were sonicated with occasional stirring for 20 mins before adding Pd catalyst, as sonication may have effects on the catalyst activation. The reaction temperature in PC was set at 135 °C for better dissolution. Longer reaction times were also found necessary when using PC and the yields were generally lower than when using DMF, especially for compound **62** (Entry 3). Interestingly, 2'-deoxyguanosines **64** and **65** displayed a similar cross-coupled product yield when using either PC or DMF (Entries 1 and 2).

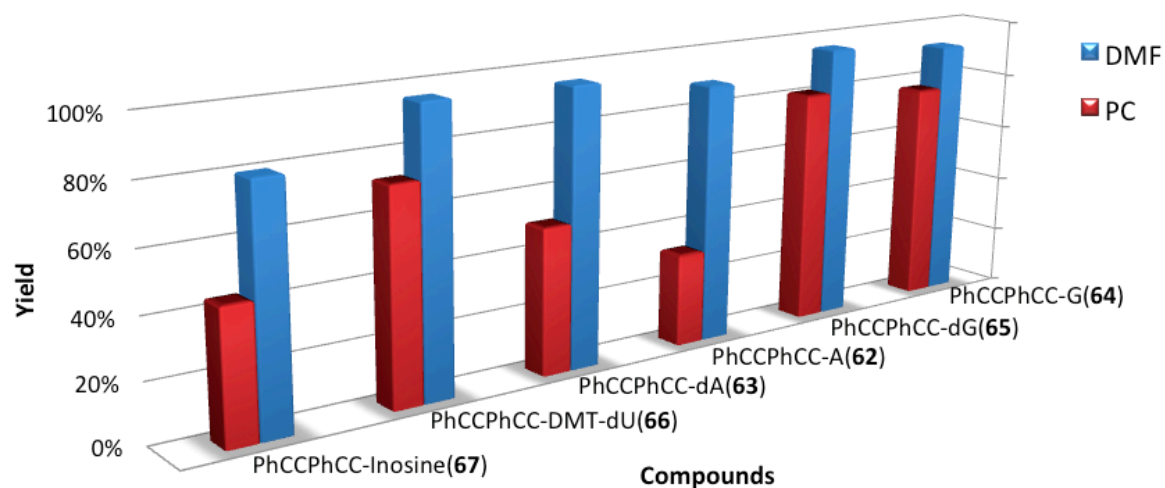
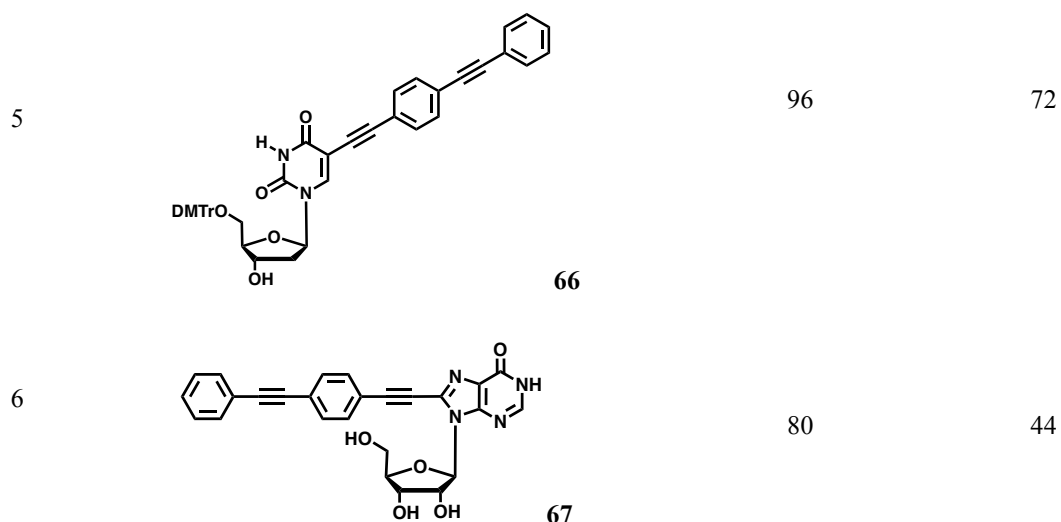


Table 3.4 Yield comparison for the cross-coupling reaction in PC and DMF.

Entry	Product	Yield in DMF %	Yield in PC %
1	 67	92	77
2	 63	96	81
3	 65	89	32
4	 62	95	50



3.2.3.2 NMR spectroscopic analysis of nucleosides derivatives and insights into their preferred conformations

A common problem that emerges for modified nucleosides is that substrate affinity and specificity are affected. Even minor modifications can lead to a loss in activity towards the target enzyme. One factor that dictates the activity of a synthetic nucleoside is the conformation of the sugar moiety.¹⁸⁷ Sugar conformations can be locked using appropriately designed nucleosides.¹⁸⁸ It is important to consider how structural modifications to the purine nucleoside can affect the conformational preference of the sugar unit.

NMR spectroscopy is a powerful tool for determining structural information about nucleosides.¹⁸⁹ NMR spectra were recorded in $(\text{CD}_3)_2\text{SO}$ since the nucleosides were only partially soluble in other polar solvent including methanol. There are two conformations that are found in nucleosides, *syn* and *anti*, which are defined by the torsion angle shown in Figure 3.8. The *anti-syn* equilibrium is based on relationship between nucleobase and sugar, brought about by glycosyl bond rotation. A hydrogen bond is often seen between the 5'-hydroxyl group and the N6.

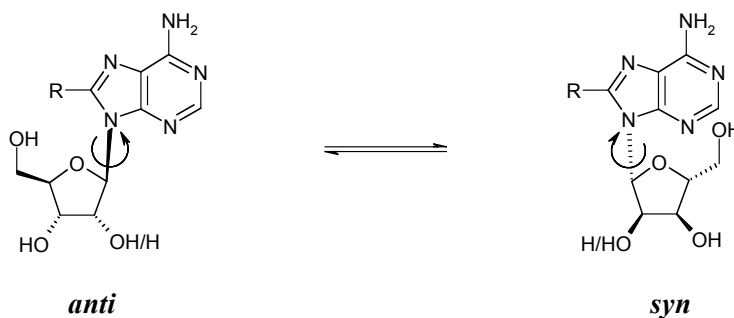


Figure 3.8 Conformation flip from *anti* to *syn*.

The *anti-syn* relationship is an equilibrium, which favours the *anti*-conformation at room temperature for natural nucleosides (*syn* is disfavoured by up to 6 kcal mol⁻¹),¹⁹⁰ although the presence of purine substituents can tip the balance of this equilibrium (Figure 3.9). The natural *anti*-conformer can be pushed into the *syn*-conformer by added steric bulk. There are a number of characteristic changes which occur in the ¹³C and ¹H NMR spectra, which are directly associated with the *anti-syn* conformational shift. By comparison of the chemical shifts, the conformer adopted in solution can be identified. Analysis of furanose carbon chemical shifts and the C2'-H to that of the natural nucleoside occurring during an *anti* to *syn* flip, allows the following changes in chemical shift to occur.⁸

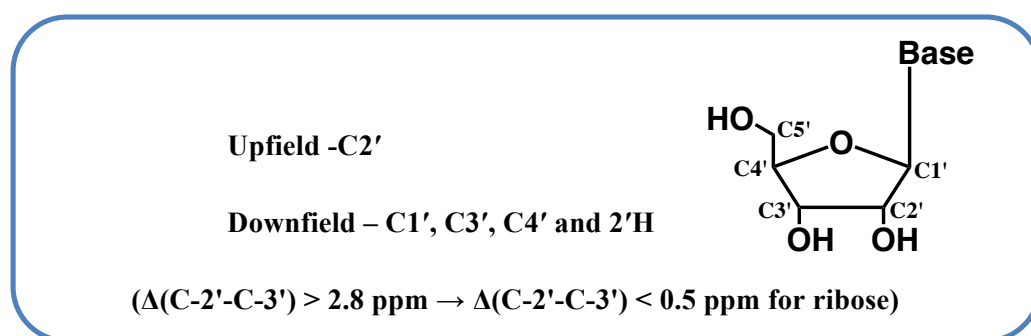


Figure 3.9 Equilibrium of the *anti-syn* relationship.

The torsion angle around the nucleoside glycosyl bond $\chi(O4'-C1'-N9-C4)$ gives rise to the *syn* and *anti*-conformers. The *anti*-conformer happens in both A-type and B-type nucleic acid secondary structures.¹⁹⁰ Modifications on nucleosides can cause an exchange in the preferred conformer from *anti* to *syn*. Usually, the exchange from *anti* to *syn* is related an upfield shift of $\delta(C2')$ and a downfield shift of $\delta(C1')$, $\delta(C3')$ and $\delta(C4')$ in the ¹³C NMR spectrum. The chemical shift of the C2'-H in ¹H NMR spectra can also determine the conformation of *syn/anti*.¹⁹⁰ Although this method does not take into account of the impact of other conformational changes on $\delta(C2'-H)$, it is still an indication of the predominant species. The nucleosides NMR data were shown in Table 3.5, with comparison to other natural nucleosides.

Table 3.5 ^1H and ^{13}C NMR chemical shift data of natural^a and modified nucleosides.^b

Entry	Nucleoside	C1'	C2'	C3'	C4'	C2'- H	Major conformer
1	A (38) ^a	86.7	74.3	71.4	88.8	4.64	<i>anti</i>
2	8-Br-A (39)	86.7	71.1	70.9	90.4	5.08	<i>syn</i>
3	8-(Ph)-A (47)	86.7	71.2	71.1	89.0	5.04	<i>syn</i>
4	62	86.8	74.6	70.7	89.1	5.02	<i>anti</i>
5	dA (40) ^a	83.8	39.7	71.8	88.7	2.73	<i>anti</i>
6	8-Br-dA (41)	83.8	40.0	71.7	88.9	3.24	<i>anti</i>
7	63	84.2	46.2	70.2	89.1	3.16	<i>anti</i>
8	G (42) ^a	85.1	73.6	70.3	86.3	4.37	<i>anti</i>
9	8-Br-G (43)	85.6	70.2	70.4	88.9	5.01	<i>syn</i>
10	8-(Ph)-G (46)	85.7	70.5	70.2	88.9	4.95	<i>syn</i>
11	64	85.9	70.8	70.5	86.9	4.95	<i>syn</i>
12	dG (44)	82.5	39.5	70.7	87.5	2.50	<i>anti</i>
13	8-Br-dG (45)	85.0	71.6	70.9	87.8	3.16	<i>anti</i>
14	65	86.5	71.3	70.1	89.6	3.05	<i>anti</i>
15	I ^a	85.6	74.0	70.2	87.4	4.46	<i>anti</i>
16	8-Br-I (61)	86.6	71.3	70.2	88.3	5.52	<i>anti</i>
17	67	86.1	76.4	71.4	87.9	4.21	<i>anti</i>
18	dU ^a	87.4	71.1	76.1	85.0	3.79	<i>anti</i>
19	66	87.3	76.9	72.8	89.7	3.21	<i>anti</i>
20	70	80.6	74.1	73.8	85.7	4.55	<i>syn</i>
21	71	84.3	75.8	74.1	86.5	4.18	<i>syn</i>

^a Data obtained from literature sources.^{191–193} ^b Data obtained in DMSO-d⁶ at 298 K at 400 MHz.

The pucker of the ribose ring is the second principal conformational variation of a nucleoside. There are twenty possible sugar conformations. The most currently observed and biologically important conformers are C2'-*endo* and C3'-*endo* conformations. C2'-*endo* conformations are associated with B-type DNA, whereas C3'-*endo* conformations are associated with A-type DNA. According to the Karplus equation on the ^1H coupling constants of the nucleosides, the ratio of C2'-*endo* to C3'-*endo* are able to determined.¹⁹⁴ This methodology assumes that only C2'-*endo* and C3'-*endo* conformations are present. The coupling constants relevant to the sugar pucker are $J_{3'4'}$ and $J_{1'2'}$, due to the C4'-H signal does not have resolved coupling constants, therefore $J_{3'4'}$ was measured from the C3'-H signal. The conformation of sugar in modified C8 nucleosides and natural nucleosides is slightly different. This methodology is a well indicator to determine the modifications introduced will not considerably disrupt the secondary structure of duplexes containing these modified nucleosides or change their biological properties through changing in conformation of sugar.

Because the two conformations are substantially different in terms of their spectroscopic properties, NMR data can be used to calculate the relative populations of 2E and 3E structures by utilising proton-proton coupling constants. On the NMR timescale the two conformers cannot be resolved and an averaged signal is observed. From the coupling constants observed ($J_{1'2'}$ and $J_{3'4'}$), a value for the percentage population of each conformer can be calculated (Figure 3.10).¹⁹⁵ The following equation can be used to give a reasonably reliable indication to the sugar pucker equilibrium:

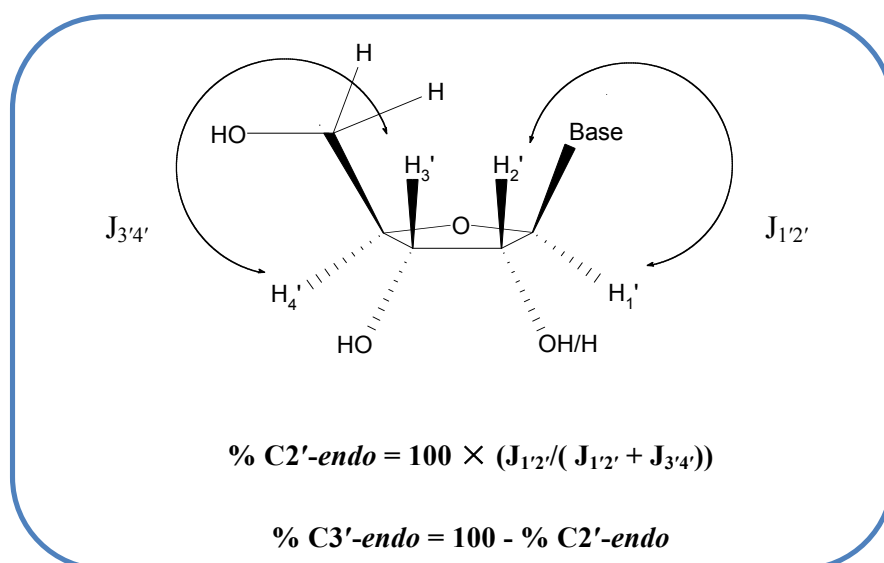


Figure 3.10 ^1H - ^1H coupling constants between the proton signals on the furanose ring.

This was applied to selected compounds from the C8-modified nucleosides. The results are shown in Table 3.6.

Table 3.6 NMR ^1H - ^1H spin-spin coupling constants and ratio of C2'-*endo* to C3'-*endo* of nucleosides from data given in Table 3.5^b.

Entry	Nucleoside	$J_{1'2'}$	$J_{3'4'}$	%C2'- <i>endo</i>	%C3'- <i>endo</i>
1	A (38) ^a	6.2	3.0	67	33
2	8-Br-A (41)	6.9	2.3	75	25
3	8-(Ph)-A (47)	6.9	1.9	78	22
4	62	6.5	m	n.d.	n.d.
5	dA (40) ^a	7.9	2.6	75	25
6	8-Br-dA (41)	6.9	1.7	80	20
7	63	7.1	3.0	70	30
8	G (42) ^a	5.9	3.3	64	36
9	8-Br-G (43)	6.4	3.4	65	35
10	8-(Ph)-G (46)	6.5	3.1	68	32
11	64	6.3	3.9	62	38
12	dG (44) ^a	6.0	2.7	69	31
13	8-Br-dG (45)	7.3	3.1	70	30
14	65	7.5	3.0	71	29
15	I ^a	5.9	3.9	60	40
16	8-Br-I (61)	5.9	3.1	65	35
17	67	6.7	3.2	68	32
18	dU ^a	6.6	3.4	66	34
19	65	6.7	3.8	64	36
20	70	6.6	3.5	65	35
21	71	6.5	3.5	65	35

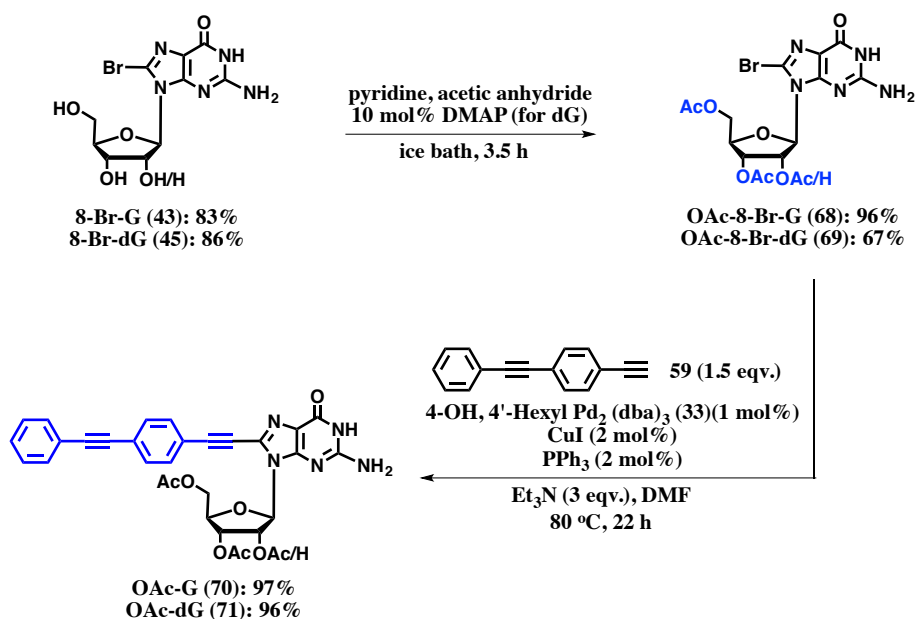
^a Data obtained from literature sources.¹⁹¹⁻¹⁹³ ^b Data obtained in DMSO-d₆ at 298 K.

3.4 Guanine-quartet study involving 8-alkynylated purines

3.4.1 Synthesis alkylation of 8-modified for G-quartet study

The crucial requirement for making guanine-quartet (G-quartet) is the preservation of high structural similarity to the natural nucleobases, including the retention of the Watson and Crick and Hoogsteen's base pairing faces. So far, few fluorescent guanosine mimics have been studied, but they are imperfect and consist of destabilized G-quartet structures. Some have also resulted in non-emissive fluorescent probes.¹⁹⁶⁻²⁰⁴ For these reasons, the development of new guanosine analogues which contain the multiple alkyne 'Ph-CC-Ph-CC-' motif **59**, is highly desirable for attempting a G-quartet study.

It was recognised that the assembly behaviour of G-quartets could be examined (*e.g.* OAc-protected guanosines **70** and **71** Scheme 3.7) by an NMR spectroscopic study, using variable concentration and temperature with and without addition of a cation.



Scheme 3.6 Synthesis of acetate-protected (deoxy)guanosine derivatives **70** and **71**.

The reaction began by bromination of 2'-(deoxy)guanosine **42**(**44**) using saturated bromine to give 8-bromo-(deoxy)guanosines **43**(**45**). The synthesis of acetate-protected 8-bromoguanosine **68** was straightforward,²⁰⁵ with excellent yield. The synthesis of acetate protected 8-bromodeoxyguanosine **69** posed a considerable challenge. Several reaction conditions were attempted and it was found that DMAP was important for **69**. The reason is the high basicity of DMAP for acetate, which is able to drive the dehydration of carboxylic group. The work-up for both reactions giving products **70** and **71** were simple and for the multiple alkyne 'Ph-CC-Ph-CC-' motif functionalization reactions, a

similar methodology was used as for other functionalised purines. However, for the work-up procedure, it was necessary to use Et₂O for removing the traces of homocoupled product. Acetonitrile also has been investigated for the acetoxylation reactions instead of DMF. However, no product was obtained from the reactions.

3.4.2 NMR study

The G-quartets study started with different concentrations of nucleosides at room temperature without cations, before varying the temperature. The G-quartets with cation study used a protocol in which the solution was prepared by dissolving PhCCPhCC-O(d)G in freshly distilled CDCl₃ and this solution was washed with aqueous solution containing cation.²⁰⁶⁻²⁰⁸ The CDCl₃ and aqueous layers were separated, and the CDCl₃ was centrifuged to remove residual water. Several methods were used to study the assembly behaviour of G-quartets, but no conclusive evidence of peak shifting or new peaks was observed, suggesting a lack of self-assembly (Table 3.7). The problem could possibly be due to trace water from the cation solution, which allowed for the proton to shift between –OH and –NH groups.

Table 3.7 G-Quartets study with various conditions.

Compound in Solvent	CDCl ₃		CD ₂ Cl ₂	
	Cations		Concentration (R. T.)	Temperature (at 700 MHz)
OAc-G (70)	N/A	10 mM K ⁺ 10 mM Ca ²⁺	7 mM, 14mM,	-60 °C – 25 °C
		50 mM K ⁺ 50 mM Ca ²⁺	29 mM, 58 mM	
OAc-dG (71)	N/A	10 mM K ⁺ 10 mM Ca ²⁺	7 mM, 14mM,	-60 °C – 25 °C
			29 mM, 58 mM	

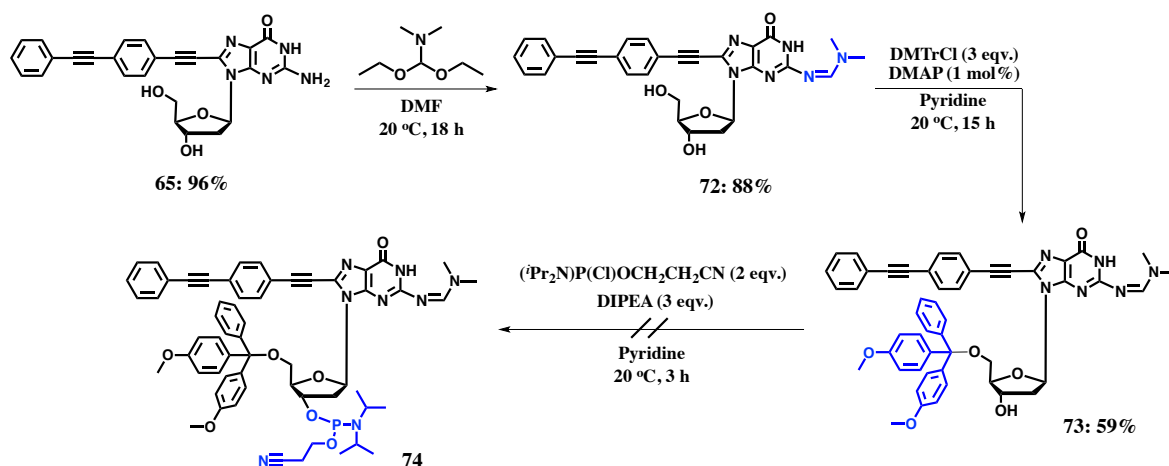
3.5 Attempts to synthesise precursor compounds for solid-phase synthesis

In order to incorporate the modified nucleosides into nucleic acids, a solid-phase synthesis was required. Hence 3'-O-phosphorochloridates reacted rapidly with the corresponding 3'-protected nucleoside and produce subsequent oxidation of phosphite. Nevertheless, the phosphorochloridites could neither be isolated nor stored due to their high reactivity. Therefore, they needed to be protected by phosphitylation from 5'-O-protected nucleosides. To avoid undesirable side reactions, exocyclic amino groups of adenine and guanine must be temporarily blocked during the synthesis.

In order to allow the automation of solid-phase synthesis, protected phosphoramidites have been developed.^{209–212} The most commonly used protecting group for the exocyclic amine of adenosine nucleosides prior to solid phase synthesis is benzoyl. However, the best protecting group for the exocyclic amine of guanosine nucleosides, prior to solid phase synthesis, is *N,N*-dimethylformamide (DMF). The most common 5'-hydroxyl protection is DMTr group, as it can offer a good balance between nucleoside stability and ease of trityl group removal. The most widely used protecting group for oligosynthesis on phosphate is 2-cyanoethyl group, due to the ease of phosphate cleavage with ammonia. This method has been used for the hydrolysis of ester bonds releasing oligonucleotides from a solid support.²¹³

As mentioned Chapter 1, the naturally occurring nucleotides (nucleoside-3'- or 5'-phosphates) are insufficiently reactive to afford an expedite synthetic preparation of oligonucleotides. The selectivity and the rate of the formation of internucleosidic linkages is extremely enhanced by using 3'-*O*-(*N,N*-diisopropyl phosphoramidite) of nucleosides. The synthesis of the protected phosphoramidite of guanosine was undertaken from the parent compound **65** (Scheme 3.8).²¹⁴

The formamidine **72** was formed quantitatively, the crude mixture was washed with ethyl acetate and dried *in vacuo*, to remove the trace of starting material which bound to the product. The 5'-OH protection step was achieved with a dimethoxytrityl (DMTr) protecting group from the respective DMTr-chloride. Installation of the 5'-hydroxyl with DMTrCl was also successful, after reaction optimisation in pyridine, giving **73** in modest isolated 59% yield. A catalytic amount of DMAP (0.1 mol%) is essential for this reaction, without it, the reaction did not work. The protected guanosine was then converted to the phosphoramidite, **74**. Unfortunately, the pure desired product for **74** could not be isolated. The mass spectrum showed the product; ¹H NMR showed the product contained an unknown impurity, which could not be separated by column chromatography on silica gel due to the high polarity of product and its instability on silica gel.



Scheme 3.7 Protection of **74** for solid-phase synthesis.

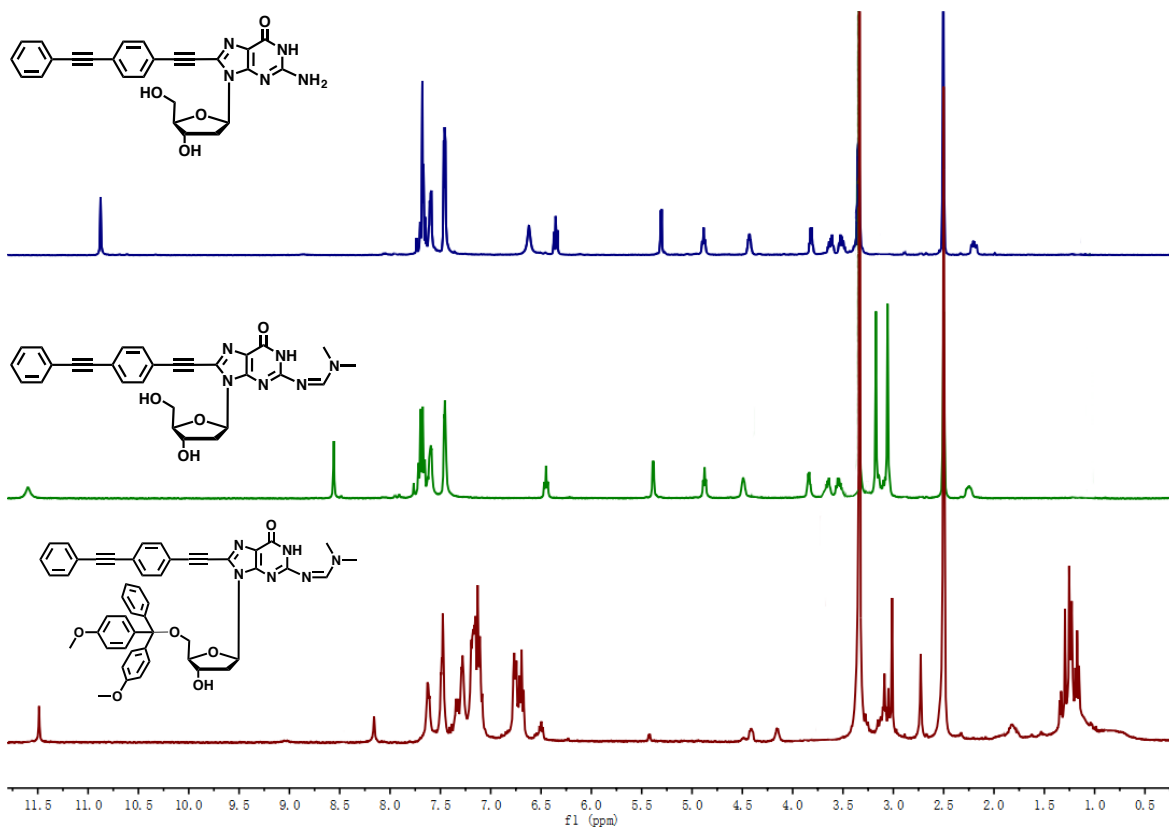
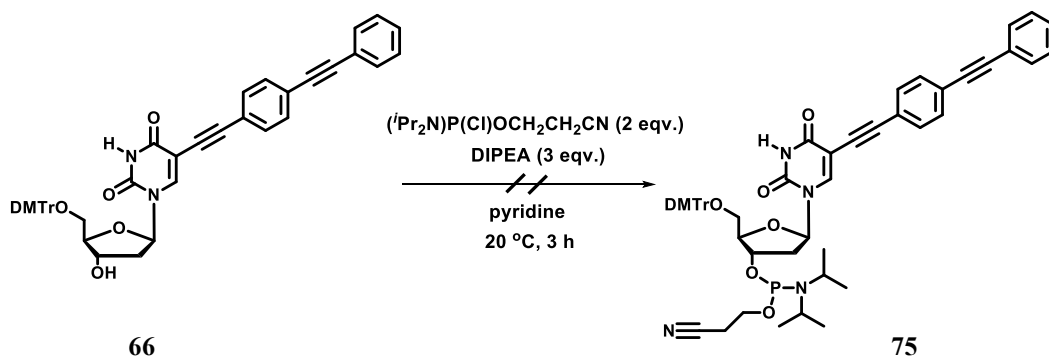


Figure 3.11 Stack ^1H NMR spectra for synthesise precursor PhCCPhCC-dG for solid-phase synthesis.

Stacked ^1H NMR spectra of **65**, **72** and **73** are shown in Figure 3.11. The peaks from each protecting group became obvious. Protons from deoxyguanosine were slightly changed.

Due to the unclear result from protection of phosphoramidite guanosine, the same synthetic scheme to phosphoramidite uridine was subsequently used (Scheme 3.9) to check the compatibility of the

protecting groups for solid-phase synthesis. Unfortunately, the pure desired product for **75** could not be isolated by this method.



Scheme 3.8 Synthesis of uridine phosphoramidite **75**.

3.6 Conclusion

- The crucial point for the synthesis of 8-bromo-2'-deoxyadenosine was using deionised water and pH of 6.5-7. Freshly distilled triethylamine and shorter reaction times were necessary for Sonogashira cross-couplings of adenosines. Guanosine derivatives were found to be less sensitive, despite the guanine ring being a known hinderance and interfering group in Pd-catalysis, especially Suzuki-Miyaura and direct arylation proceses.
- The synthesis of 8-modified nucleosides has been successfully carried out by Pd-catalysed Sonogashira alkynylation reactions.
- Yields of the “PhCCPhCC-” analogues were improved by focusing on the reaction work-up procedures, specifically how the compounds were filtered – this is a practical but key point which aids their isolation.
- The library of Pd catalysts, described within Chapter 2, was applied in the Sonagashira and Heck cross-coupling reactions, by altering Pd catalyst loadings. The optimised Pd catalyst, which gave the highest yield was $\text{Pd}_2(4\text{-OH}, 4'\text{-OHexyl dba})_3$ (**33**).
- The greener solvent, propylene carbonate was compared with DMF in Sonogashira cross-coupling chenmistry, which is a viable alternative.
- NMR spectroscopic analysis allowed the preferred conformations of the new nucleosides derivatives to be determined.
- A preliminary G-quartet study revealed that acetate derivatives of the C8-alkynylated guanosine and deoxyguanosine showed no evidence of self-assembly.

3.7 Experimental

General Details

Chemical reagents were purchased from Sigma Aldrich[®], Alfa Aesar[®], Acros[®] or Fluorochem[®] and used as received. Pd(OAc)₂ was purchased from Precious Metals Online. All reactions were carried out under a nitrogen atmosphere unless otherwise stated. Dry THF, CH₂Cl₂, hexane, toluene and acetonitrile were obtained from a Pure Solv MD-7 solvent system and stored under nitrogen. Dry methanol was obtained by drying over 3 Å molecular sieves. Ether and THF were degassed by bubbling nitrogen gas through the solvent during sonication. Dry pyridine, triethylamine and TMEDA were obtained by distillation from KOH and stored under nitrogen. Dry acetone and cyclohexane were obtained by distillation from CaH₂ and stored under nitrogen. Dry DMF and DMSO were obtained from Acros[®], DMF was degassed by N₂ bubbling while sonication; DMSO was used as received. Dry deuterated solvents were distilled (under static vacuum) from Na. Petroleum ether refers to the fraction of petroleum that is collected at 40 – 60 °C. Air sensitive procedures were performed using standard Schlenk line techniques. Nitrogen gas was oxygen free and dried immediately prior to use by passing through a column of sodium hydroxide pellets and silica. Reactions requiring anhydrous or air-free conditions but without using Schlenk line techniques were carried out in dry solvent under an argon or nitrogen atmosphere using oven- or flame-dried glassware. Where indicated, a Braun[®] Unilab glove (dry) box was used (<0.5 ppm O₂). Filtration was performed under gravity through fluted filter paper unless otherwise stated. Inorganic solutions used were prepared using deionized water. TLC analysis was carried out using Merck 5554 aluminium backed silica plates, and visualised using UV light at 254 and 365 nm. Retention factors (*R_f*) are reported along with the solvent system used in parenthesis. All column chromatography was carried out using Merck silica gel 60 (particle size 40-63 µm) purchased from Sigma Aldrich. Preparatory TLC was carried out using Analtech UNIPLATE glass-backed silica plates.

Nuclear Magnetic Resonance Spectroscopy (NMR Spectroscopy)

Proton (¹H), carbon (¹³C), phosphorus (³¹P) NMR spectra were recorded on a Jeol ECS400 and Bruker AV500/AV600/AV700 spectrometers. All chemical shifts in ¹H NMR spectra are reported in parts per million (ppm, δ) of tetramethylsilane using residual NMR solvent as an internal standard (CDCl₃: 7.26 ppm, DMSO-d₆: 2.50 ppm, MeOD-d₄: 3.31 ppm, CD₂Cl₂: 5.32 ppm). Multiplicities are described as singlet (s), doublet (d), triplet (t), quartet (q), multiplet (m), apparent (app.) and broad (br). ¹³C spectra were referenced to deuterated solvent. The spectra were processed in MestreNova[®] software and, where required, exported as JPEG images into the appropriate document. All chemical shifts in ¹³C NMR spectra are reported in ppm (δ) and are referenced to the NMR solvent (CDCl₃: 77.36 ppm, DMSO-d₆: 39.52 ppm, MeOD-d₄: 49.00 ppm, CD₂Cl₂: 53.49 ppm). Chemical shifts are

reported in parts per million and were referenced to residual undeuterated solvent. Coupling constants have been quoted to ± 0.2 Hz. ^1H NMR chemical shifts are given to 2 decimal places; ^{13}C NMR chemical shifts are given to 1 decimal place. Spectra were typically recorded at 298 K. ^{31}P spectra were externally referenced to H_3PO_4 .

Mass Spectrometry (MS)

Mass spectrometry was performed using a Bruker Daltonics micrOTOF spectrometer, an Agilent series 1200 LC, or a Thermo LCQ using electrospray ionization (ESI), with less than 5 ppm error for all HRMS. Liquid injection field desorption ionization (LIFDI) mass spectrometry was performed using a Waters GCT Premier mass spectrometer. All data were acquired in positive ion mode using ESI or LIFDI ionisation. All LIFDI data reported is within 120 ppm error.

Infrared Spectroscopy (IR)

IR spectroscopy was carried out on Thermo-Nicolet Avatar-370 FT-IR spectrometer, or a PerkinElmer Spectrum Two spectrometer. Spectra were taken in either solid state (KBr disc), or in solution, thin film.

Melting Points (m.p.)

Melting points were obtained on a Stuart SMP3 machine. Experiments were run using a ramp rate of $3\text{ }^\circ\text{C min}^{-1}$ to the required melting temperature. The melting point was taken as the onset of the observed endothermic peak. The machine was calibrated using an indium standard.

UV-Vis Spectroscopy

UV-Vis spectroscopy was performed on a JASCO V-560 spectrometer. The UV-Vis spectrophotometer was temperature controlled at $20\text{ }^\circ\text{C}$ using a H_2O bath; spectra were recorded using matched quartz cuvettes (λ_{max} is reported). The UV-Vis spectra of 5 solutions at different concentrations were measured (all absorbance values were below 2 OD). The UV-Vis spectra were plotted for each analogue (absorbance vs. wavelength) at the different concentrations. The molar absorption coefficients were obtained by plotting UV absorbance vs. analogue concentration, and applying the Beer-Lambert law. A baseline in the required solvent was carried out prior to starting an assay.

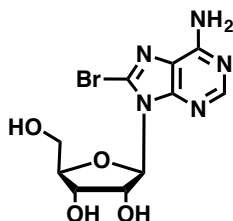
Elemental Analysis

Elemental analysis was carried out using an Exeter Analytical CE-440 Elemental Analyser, with the percentages reported as an average of two runs.

Stock Solutions

Stock solutions for each Sonogashira reaction which contained Pd catalysts, CuI, and PPh₃ or PdCl₂(PPh₃)₂, were prepared typically by dissolving in 50 to 60 μL of dry DMF.

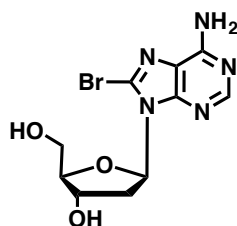
(2*R*,3*R*,4*S*,5*R*)-2-(6-Amino-8-bromo-9*H*-purin-9-yl)-5-(hydroxymethyl)tetrahydrofuran-3,4-diol (39)



Adenosine (1.05 g, 3.92 mmol, 1.0 eqv.) was dissolved in NaOAc buffer (0.5 M, pH 4, 20 ml) with heating to 40 °C and stirring. The solution was cooled to 20 °C and a saturated solution of Br₂ (sat aq, 30 ml water and 6 ml bromine) was added dropwise (cautiously) over 6 h. The mixture was left to stir for 3 d at 20 °C. The colour of the solution was discharged by the addition of Na₂S₂O₃ (5 M, 20 ml) and the pH of the solution was adjusted to 7 with NaOH (5 M). The solution was left to recrystallise for 16 h. The product was filtered, washed with H₂O (30 ml), cold acetone (10 ml), and air-dried to afford the product as a yellow crystalline solid (1.15 g, 86%).

TLC R_f 0.50 (25% MeOH/CHCl₃); MP 212–213 °C (dec.); ¹H NMR (400 MHz, *d*₆-DMSO, 20 °C): δ = 8.12 (s, 1H; C2-H), 7.60 (br s, 2H; NH₂), 5.84 (d, *J* = 6.9, 1H; C1'-H), 5.55 (br s, 1H; C5'-OH), 5.48 (br s, 1H; C2'-OH), 5.25 (s, 1H; C3'-OH), 5.12-5.06 (m, 1H; C2'-H), 4.22-4.18 (m, 1H; C3'-H), 3.99-3.97 (m, 1H; C4'-H), 3.67-3.63 (m, 1H; C5'-H₁), 3.53-3.49 (m, 1H; C5'-H₂); ¹³C NMR (100.6 MHz, *d*₆-DMSO, 20 °C): δ = 155.7, 152.8, 150.2, 128.1, 119.2, 91.1, 85.9, 71.3, 70.6, 62.8; ESI-MS *m/z* (%): 141(90), 162(50), 346 (100) [⁷⁹BrM], 348 (95) [⁸¹BrM]; ESI-HRMS *m/z* 346.0142 [M+H](calc. for C₂₀H₁₃BrN₅O₄ = 346.0145); IR (DMSO Solution): 3325 cm⁻¹ (OH), 3088 cm⁻¹ (NH).

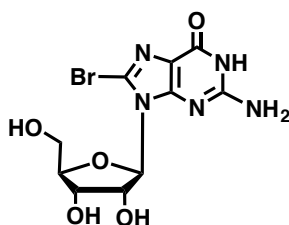
**(2R,3S,5R)-5-(6-Amino-8-bromo-9H-purin-9-yl)-2-(hydroxymethyl)tetrahydrofuran-3-ol
(41)**¹⁷⁶



Saturated bromine was dissolved in freshly prepared acetate buffer, pH 4.0 (8 ml) and stirred for 1–2 h until fully dissolved. The bromine solution was added in portions over 10 min to a slurry of 2'-deoxyadenosine (1.2 g, 6.696 mmol, 1 eqv.) in acetate buffer (18 ml). The reaction was complete by TLC after 36 h in the dark. The reaction was quenched by gradual addition of a saturated aqueous solution of Na₂S₂O₃ until the red colour of Br₂ had disappeared, then the reaction mixture was neutralized with 2M NaOH. The solution was left to recrystallise for 16 h, then washed with cold water and dried. The compound was purified by column chromatography on silica (eluent: ethyl acetate/methanol 85%: 15%, v/v). Collected fractions were evaporated *in vacuo* to give a beige solid was 0.0532 g (63%).

TLC Rf 0.55 (25% MeOH/CHCl₃); MP 209-211 °C (dec.); ¹H NMR (400 MHz, *d*₆-DMSO, 20 °C): δ = 8.11 (s, 1H, 2-H), 7.53 (br s, 2H, 6-NH₂), 6.29 (t, 1H, *J* = 6.90 Hz; C1'-H), 5.36 (s, 1H, C3'-OH), 5.34-5.26 (m, 1H, C5'-OH), 4.54-5.47 (m, 1H, C4'-H), 3.93-3.86 (m, 1H, C3'-H), 3.65-3.63 (m, 1H, C5'-H₁), 3.49-3.45 (m, 1H, C5'-H₂), 3.27-3.21 (m, 1H, C2'-H₁), 2.23-2.16 (m, 1H, C2'-H₂). ESI-MS *m/z* (%): 162(50), 329(100) [⁷⁹BrM], 331(95) [⁸¹BrM]; ESI-HRMS *m/z* 329.01 [M+H](calc. for C₁₀H₁₂BrN₅O₃ = 329.04); IR (DMSO Solution): 3455 cm⁻¹ (OH), 3348 cm⁻¹ (NH).

2-Amino-8-bromo-9-((2R,3R,4S,5R)-3,4-dihydroxy-5-(hydroxymethyl)tetrahydrofuran-2-yl)-1,9-dihydro-6H-purin-6-one (43)

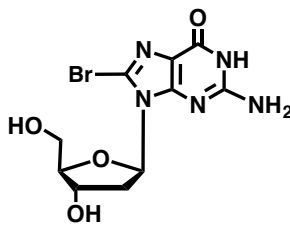


8-Bromoguanosine was prepared using guanosine (0.734 g, 2.6 mmol) suspended in doubly distilled water (4.4 mL) and saturated bromine (Aldrich) water (20 mL), then dropwise addition of the sat. bromine via glass drop funnel. The precipitated 8-bromoguanosine was recovered by

filtration, washed extensively with cold water, followed by cold acetone, and air-dried. Yield: 0.78 g (83 %).

TLC Rf 0.50 (33% MeOH/CHCl₃), MP 220-223 °C (dec.); ¹H NMR (400 MHz, *d*₆-DMSO, 20 °C): δ = 10.82 (s, 1H; NH), 6.51 (br s, 2H; NH₂), 5.69 (d, *J* = 6.4, 1H; C1'-H), 5.45 (d, *J* = 6.0, 1H; C2'-OH), 5.09 (d, *J* = 5.2, 1H; C3'-OH), 5.08-4.99 (m, 1H; C2'-H), 4.99-4.91 (m, 1H, C5'-OH), 4.14-4.12 (m, 1H; C3'-H), 3.86-3.84 (m, 1H; C4'-H), 3.63 (ddd, *J* = 5.2, 5.2, 12.0, 1H; C5'-H₁), 3.57-3.51 (m, 1H; C5'-H₂); ¹³C NMR (100.6 MHz, *d*₆-DMSO, 20 °C): δ = 154.2, 153.1, 151.9, 121.7, 116.3, 88.9, 85.6, 70.2, 69.4, 62.7; ESI-MS *m/z* (%): 150(50), 230(100)[⁷⁹BrM], 232(95)[⁸¹BrM]; ESI-HRMS *m/z* 361.0349 [M+H](calc. for C₁₀H₁₂BrN₅O₅ = 361.0351); IR (DMSO Solution): 3505 cm⁻¹(OH), 3421 cm⁻¹(NH), 3309 cm⁻¹(NH), 1696 cm⁻¹(CO).

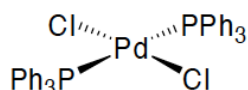
2-Amino-8-bromo-9-((2*R*,4*S*,5*R*)-4-hydroxy-5-(hydroxymethyl)tetrahydrofuran-2-yl)-1,9-dihydro-6*H*-purin-6-one (45)



NBS (*N*-Bromosuccinimide) (0.0733 g, 0.413 mmol, 1.1 eqv.) and 2'-deoxyguanosine (0.1 g, 0.373 mmol, 1 eqv.) in distilled water (5 ml) reacted within 15 min at room temperature. The precipitated solid was collected by filtration and washed with cold acetone and dried to give 8-bromo-2'-deoxyguanosine (0.109 g, 85%).

TLC Rf 0.45 (50% MeOH/CHCl₃); MP 215-217 °C (dec.); ¹H NMR (400 MHz, *d*₆-DMSO, 20 °C): δ = 10.81 (s, 1H, NH), 6.50 (s, 2H, NH₂), 6.15 (t, 1H, *J* = 7.3 Hz, C1'-H), 5.27 (d, 1H, *J* = 4.4 Hz, C3'-OH), 4.87 (t, 1H, *J* = 6 Hz, C5'-OH), 4.42-4.36 (m, 1H, C3'-H), 3.84-3.77 (m, 1H, C4'-H), 3.65-3.58 (m, 1H, C5'-H₁), 3.56-3.27 (m, 1H, C5'-H₂), 3.19-3.12 (m, 1H, C2'-H₁), 2.16-2.09 (m, 1H, C2'-H₂). ¹³C NMR (100.6 MHz, *d*₆-DMSO, 20 °C): δ = 155.3, 153.2, 151.9, 120.4, 117.4, 87.8, 45.0, 70.9, 61.9, 36.4; ESI-MS *m/z* (%): 136(40), 268(100)[⁷⁹BrM], 370(100)[⁸¹BrM]; ESI-HRMS *m/z* 367.9945 [M+H](calc. for C₁₀H₁₂BrN₅O₄ = 367.9970); IR (DMSO Solution): 3512 cm⁻¹(OH), 3436 cm⁻¹(NH), 3311 cm⁻¹(NH), 1694 cm⁻¹(CO).

Bis(triphenylphosphine)palladium(II)dichloride²¹⁵



Synthesis of PdCl₂(PPh₃)₂ was prepared from PdCl₂ (0.1773 g, 1 mmol, 1 eqv.) and PPh₃ (0.6295 g, 2.4 mmol, 2.4 eqv.) by dissolving both of the compounds in DMF (6.4 ml) at 150 °C under N₂ for 2 h. On cooling, PdCl₂(PPh₃)₂ crystallized out of the solution. After filtration, the crystals were rinsed with diethyl ether and dried at reduced pressure *in vacuo*. Further purification was by recrystallization from DCM to give yellow crystals (0.3053 g, 94 %).

MP 284 - 286 °C (dec.); ¹H NMR (400 MHz, CDCl₃, 20 °C): δ = 7.73-7.68 (m, 12H; ArH), 7.46-7.37 (m, 18H; ArH); ¹³C NMR (100 MHz, CDCl₃, 20 °C): δ = 135.0, 130.4, 129.6, 128.2; ³¹P NMR (162 MHz, CDCl₃, 20 °C): δ = 23.96; Elemental Analysis (CHN) C: 61.36% H: 4.98% (Calculated: C: 61.61% H: 4.31%); ESI-MS *m/z* 665 (20), 155 (100) [M+H]; ESI-HRMS *m/z* 665.1124 [M+H] (calc. for C₃₆H₃₀Cl₂P₂Pd 655.1458).

General procedure for Sonogashira cross-coupling of terminal alkynes reaction using PdCl₂(PPh₃)₂¹⁷⁰

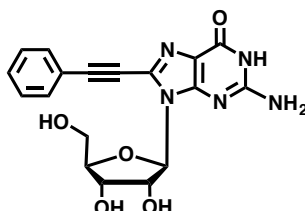
To a stirred suspension of brominated purine (0.1875 mmol, 1 equiv) in anhydrous DMF (2 mL) was added phenylacetylene (0.03 ml, 0.225 mmol, 1.2 equiv) and fresh distilled triethylamine (0.07 mL, 0.5625 mmol, 3 equiv) in a vacuum dried Schlenk tube. PdCl₂(PPh₃)₂ (0.0015 g, 0.00187 mmol, 1mol %) and CuI (0.0075 g, 0.00375 mmol, 2 mol %) were added and the reaction mixture was left to stir at 110 °C for 18 h, after which time it was allowed to cool to 40 °C and the DMF was removed *in vacuo* to leave a brown solid. The solid was transferred to a sintered glass filter and was washed with boiling water (5 × 10 mL), EtOAc (5 × 10 mL) and diethyl ether (3 × 10 mL) yielding the product as a light cream solid.

General procedure for the terminal alkynes Sonogashira cross-coupling reaction using Pd₂(dba-Z)₃ complexes¹⁷⁰

To a stirred suspension of brominated purine (0.1875 mmol, 1 equiv) in anhydrous DMF (2 mL) was added phenylacetylene (0.03 ml, 0.225 mmol, 1.2 equiv) and triethylamine (0.07 mL, 0.5625 mmol, 3 equiv) in a vacuum dried Schlenk tube. 1 mol% Pd₂(dba-Z)₃ (0.94 μmol, 1 mol%) and CuI (0.75 mg, 3.75 μmol, 2 mol%) and PPh₃ (0.99 mg, 3.75 μmol, 2 mol%) were added and the reaction mixture was left to stir at 110 °C for 15 h, after which time it was allowed to cool to 40 °C and the DMF

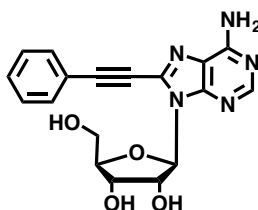
removed *in vacuo* to leave a brown solid. The solid was transferred to a sintered glass filter and was washed with boiling water (5×10 mL), EtOAc (5×10 mL) and diethyl ether (3×10 mL) yielding the product as a light cream solid.

2-Amino-9-((2*R*,3*R*,4*S*,5*R*)-3,4-dihydroxy-5-(hydroxymethyl)tetrahydrofuran-2-yl)-8-(phenylethynyl)-1,9-dihydro-6*H*-purin-6-one, 46



TLC Rf 0.30 (50% MeOH/CHCl₃); MP 236-238 °C (dec.); ¹H NMR (400 MHz, *d*₆-DMSO, 20 °C): δ = 10.88 (s, 1H; NH), 7.64-7.62 (m, 2H; Ar-H), 7.51-7.48 (m, 3H; Ar-H), 6.61 (br s, 2H; NH₂), 5.88 (d, *J* = 6.5, 1H; C1'-H), 5.49 (d, *J* = 6.5, 1H; C2'-OH), 5.12 (d, *J* = 5.2, 1H; C3'-OH) 5.01-4.97 (m, 2H; C2'-H, C5'-OH), 4.14-4.12 (m, 1H; C3'-H), 3.87-3.85 (m, 1H; C4'-H), 3.66-3.62 (m, 1H; C5'-H₁), 3.54-3.52 (m, 1H; C5'-H₂); ¹³C NMR (100.6 MHz, *d*₆-DMSO, 20 °C): δ = 156.3, 154.4, 151.6, 130.9, 129.2, 129.0, 128.9, 120.2, 117.1, 92.9, 88.5, 85.4, 79.2, 70.3, 70.1, 61.8; ESI-MS *m/z* (%): 185(100), 384(50)[MH⁺]; ESI-HRMS *m/z* 384.1302 (Calculated for C₁₈H₁₈N₅O₅ 384.1307); IR (DMSO Solution): 3425 cm⁻¹ (OH), 3331 cm⁻¹ (NH), 3115 cm⁻¹ (NH), 1694 cm⁻¹ (CO).

(2*R*,3*R*,4*S*,5*R*)-2-(6-Amino-8-(phenylethynyl)-9*H*-purin-9-yl)-5-(hydroxymethyl)tetrahydrofuran-3,4-diol, 47



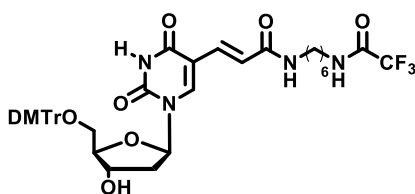
TLC Rf 0.25 (50% MeOH/CHCl₃); MP 171-173 °C (dec.); ¹H NMR (400 MHz, *d*₆-DMSO, 20 °C): δ = 8.16 (br s, 1H; C2-H), 7.69-7.66 (m, 2H; Ar-H), 7.62 (br s, 2H; NH₂), 7.56-7.49 (m, 3H; Ar-H), 6.06 (d, *J* = 6.9, 1H; C1'-H), 5.59-5.54 (m, 1H; C5'-OH), 5.48 (d, *J* = 2.4, 1H; C2'-OH), 5.26 (d, *J* = 4.7, 1H; C3'-OH), 5.02 (dd, 1H, *J* = 12.4, 6.9; C2'-H), 4.23 (br s, 1H; C3'-H), 4.01 (dd, *J* = 6.4, 1.9, 1H; C4'-H), 3.72-3.67 (m, 1H; C5'-H₁), 3.58-3.52 (m, 1H; C5'-H₂); ¹³C NMR (100.6 MHz, *d*₆-DMSO, 20 °C): δ = 156.2, 153.7, 148.4, 132.9, 132.3, 131.1, 129.2, 119.7, 94.1, 89.9, 86.8, 77.9, 71.5, 70.2, 62.8; ESI-MS *m/z* (%): 185(100), 273(20), 368(30)[MH⁺]; ESI-HRMS *m/z*

368.1363 (Calculated for C₁₈H₁₈N₅O₄ 368.1359); IR (DMSO Solution): 3433 cm⁻¹ (OH), 3326 cm⁻¹ (NH), 3164 cm⁻¹ (NH), 1657, 1314, 1053.

General procedure for the uridine Heck cross-coupling reaction using Pd₂(dba-Z)₃

A Schlenk tube equipped with magnetic stirrer was charged with [Pd₂(dba-Z)₃] (5 mol%) under N₂. This was flowed by the addition of DMT-5-I-dU (0.1312 g, 0.2 mmol, 1 eqv.), TBAB (0.0646 g, 0.2 mmol, 1 eqv.) and 0.1 ml DMF. The mixture was heated at 80 °C with stirring for 5 min when the colour changed to green. Then TFA-AA (0.0532 g, 0.2 mmol, 1 eqv.), Et₃N (0.07 ml, 0.4 mmol, 2 eqv.) and 0.1 ml DMF were added at R.T. The mixture was allowed to stir at 80 °C for 3 hours under N₂, TLC and the pH 7-8 was monitored, and cooled to R.T, then take 0.1 ml of the mixture for TEM measurement. The mixture was poured 10 ml ice water in remained material, and stirred for 10-15 min then white solid precipitates, then extracted the organic compound in 10 ml DCM and washed the DCM layer by brine water. Dried the organic layer over MgSO₄ and concentrated organic layer on rota evaporator up to 1 ml. The solution was slowly added toluene with scratching to precipitate out the desired product, which was recrystallised again with cooling (EtOH, 5 ml) to provide pure product. Filter the solid, dry it, white crystalline solid observed.

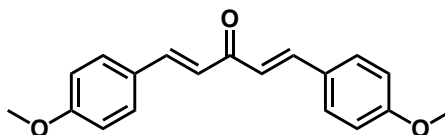
(*E*)-3-[1-(5-{[Bis(4-methoxyphenyl)(phenyl)methoxy]methyl}-4-hydroxytetrahydrofuran-2-yl)-2,4-dioxo-1,2,3,4-tetrahydropyrimidin-5-yl]-*N*-[6-(2,2,2-trifluoroacetamido)hexyl]acrylamide, 52



TLC Rf 0.40 (20% MeOH/CH₂Cl₂); mp 182-185 °C (dec.); ¹H NMR (400 MHz, d₆-DMSO, 20 °C): δ = 11.79 (s, 1H, CONHCO), 9.47 (s, 1H, CONHCH₂), 8.01–7.78 (m, 2H; CF₃CONH, C6' -H), 7.41–7.14 (m, 10H; CH=CHCO, ArH), 7.01–6.80 (m, 4H; ArH), 6.21–6.18 (m, 1H; C1' -H), 5.34 (m, 1H; CH=CHCO), 4.31 (s, 1H; C4' -H), 3.92–3.89 (m, 1H; C3' -H), 3.53 (s, 6H, OCH₃), 3.44 (s, 4H; C5' -H₁, C5' -H₂, C3''), 2.33–2.27 (m, 2H, C8''), 2.29–2.24 (m, 2H, C2' -H₁, C2' -H₂), 1.65–1.39 (m, 8H, C4'' - C7''); ¹³C NMR (100.6 MHz, d₆-DMSO, 20 °C): δ = 166.3, 162.7, 157.3, 155.2, 149.4, 145.7, 143.4, 136.4, 131.9, 129.3, 128.2, 127.5, 126.7, 125.9, 123.6, 117.1, 112.9, 109.4, 85.3, 84.7, 84.3, 69.7, 62.6, 53.6, 29.7, 28.3, 26.8, 26.1; APCI-MS *m/z* (%): 795(100)[MH⁺]; ESI-HRMS

m/z 795.3124 (Calculated for $C_{41}H_{46}F_3N_4O_9$ 795.3116); IR (DMSO Solution): 3422, 3078, 2932, 1711, 1605, 1502, 1256, 1178, 1031, 827 cm^{-1} .

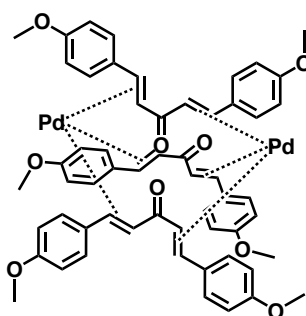
1, 5-Bis-(4-chlorophenyl)-penta-1,4-dien-3-one²¹⁶



To a 100ml round-bottle flask equipped with a magnetic stirrer was added a solution of sodium hydroxide (0.72 g, 0.018 mol, 2.5 eqv.) in water (7 mL). Ethanol (6 mL) was added with stirring and the solution was cooled in an ice-water bath. To the resultant solution, 4-methoxybenzaldehyde (1 g, 0.007 mol, 1 eqv.) and analytical grade acetone (0.208 g, 0.0036 mol, 0.5 eqv.) were added slowly over 15 minutes. On complete addition, the mixture was stirred for one hour at room temperature. A yellow solid appeared slowly, and after 1 h it was filtered *in vacuo* and then washed with ether (3×10 mL). The solid material was purified by flash chromatography using petroleum ether: ethyl acetate (4:1, v/v) to afford the title compound as a yellow solid (1.11 g, 94%).

MP 130–132 °C; ¹H NMR (400 MHz, CDCl₃, 20 °C): δ = 7.69 (d, 2H, J = 15.7), 7.56 (d, 4H; J = 8.4), 6.95 (d, 2H, J = 15.7), 6.92 (d, 4H, J = 8.4), 3.85 (s, 6H); ¹³C NMR (100.6 MHz, *d*₆-CDCl₃, 20 °C): δ = 188.7, 161.4, 142.5, 130.0, 127.4, 123.6, 114.2, 55.3; ESI-MS m/z (%): 294(100)[MH⁺], 161(40); ESI-HRMS m/z 294.1258 (Calculated for C₁₉H₁₈O₃ 294.1256); IR (CHCl₃ Solution): 1655 (C=O), 1631(C=C), 1605 (C=C aromatic), 1563 (C=C aromatic), 1175 cm^{-1} (CH trans).

Pd₂(dba-4-OMe)₃, 53¹³²

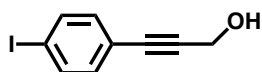


A 100 ml round-bottomed flask was charged with anhydrous sodium acetate (0.0928 g, 1.13 mmol, 8.01 eqv.), 1,5-bis-(4-chlorophenyl)-penta-1,4-dien-3-one (0.137 g, 0.466 mmol, 3.3 eqv.) and methanol (3.5 ml) and a magnetic stir bar. The flask was placed in a 50 °C oil bath, and use a condenser on the top of flask, and after 15 min, PdCl₂ (0.025 g, 0.141 mmol, 1 eqv.) was added. The

mixture was allowed to stir at 50 °C for 30 min. The crude product was dried with Buchner filtration, using water (50 ml) to wash to give the purple product (0.0336 g, 97%).

MP 138–140 °C; ¹H NMR (400 MHz, CDCl₃, 20 °C): δ = 7.69 (d, 2H, *J* = 15.7), 7.56 (d, 4H; *J* = 8.4), 6.95 (d, 2H, *J* = 15.7), 6.92 (d, 4H, *J* = 8.4), 3.85 (s, 6H); 6.76–6.70 (m, 1H; Pd-alkene), 6.68–6.61 (m, 1H; Pd-alkene), 6.59–6.51 (m, 1H, Pd-alkene), 6.42–6.36 (m, 1H; Pd-alkene), 6.24–6.17 (m, 1H; Pd-alkene), 5.89–5.81 (m, 2H; Pd-alkene), 5.34–5.28 (m, 1H; Pd-alkene), 4.97–4.91 (m, 1H; Pd-alkene), 4.86–4.79 (m, 1H; Pd-alkene), 3.52–3.46 (m, 1H; Pd-alkene), 3.85 (s, 6H); Elemental Analysis (CHN) C 61.62%, H 4.98% (Calculated for C₅₇H₅₄O₉Pd₂: C 62.47%, H 4.95%).

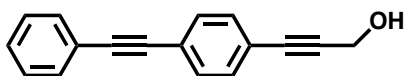
1-(4-Iodophenyl)propyn-3-ol, 55¹⁸³



A solution of 1,4-diiodobenzene (4 g, 12 mmol, 2 eqv.), PdCl₂(PPh₃)₂ (0.0423 g, 60 μmol), CuI (0.023 g, 0.12 mmol), and propargyl alcohol (0.34 g, 6.06 mmol) in 30 mL (1:1) distilled THF/*i*Pr₂NH solvent mixture, and the stirred reaction mixture was heated under reflux under nitrogen for 20 h at 80 °C. The mixture was diluted with ether (100 mL), washed with saturated ammonium chloride (100 mL), and DI water (100 mL). The solvent was removed under reduced pressure and the residue was subjected to column chromatography (20 % ethyl acetate / 80 % Pet., v/v) to afford product as yellow crystals (1.517 g, 97% yield).

TLC R_f 0.35 (20% EtOAc/Pet.); MP 100–102 °C; ¹H NMR (400 MHz, CDCl₃, 20 °C): δ = 7.66 (d, 2H, *J* = 8.65; Ar-H), 7.16 (d, 2H, *J* = 8.65; Ar-H), 4.48 (s, 2H, CH₂); ¹³C NMR (100.6 MHz, *d*₆-DMSO, 20 °C): δ = 137.1, 133.4, 122.2, 94.2 (Ar-C≡), 88.7 (≡C), 84.5, 50.9 (CH₂); ESI-MS *m/z* (%): 257(40)[MH⁺], 183(50), 143(100); ESI-HRMS *m/z* 257.1173 (Calculated for C₉H₇OI 257.1176); IR (Pressed KBr disc): 3319, 3219, 2925, 2865, 2237, 1578, 1486, 1026, 815 cm⁻¹.

1-(4-(Phenylethynyl)phenyl)propyn-3-ol, 56¹⁸³

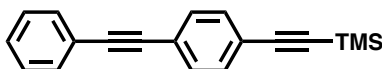


A solution of 1-(4-iodophenyl)propyn-3-ol (2.1233 g, 8.1792 mmol, 1 eqv.), PdCl₂(PPh₃)₂ (0.0576 g, 0.0818 mmol, 1 mol%), CuI (0.0154 g, 0.0818 mmol, 1 mol%) and

phenylacetylene (1.9 mL, 16.428 mmol) in 30 mL of a 1:1 (v/v) degassed mixture of THF/*i*Pr₂NH was stirred under argon reflux for 18 h. The mixture was diluted with Et₂O (20 mL), washed with saturated solution of NH₄Cl (20 mL) and DI water (20 mL). The solvent was removed under reduced pressure and the residue subjected to column chromatography (10 % ethyl acetate/90 % Pet., v/v) to afford **12** as yellow solid (0.94 g, 61% yield).

TLC Rf 0.30 (20% EtOAc/Pet.); MP 127-129 °C; ¹H NMR (400 MHz, CDCl₃, 20 °C): δ = 7.54-7.34 (m, 9H; Ar-H), 4.52 (s, 2H; CH₂); ¹³C NMR (100.6 MHz, *d*₆-DMSO, 20 °C): δ = 134.6, 133.1, 131.4, 131.2, 123.7, 121.9, 114.4, 114.1(Ar-C), 91.9, 88.7, 87.3, 85.2 (≡C), 68.4 (OCH₂); ESI-MS *m/z* (%): 233(100)[MH⁺], 209(45); ESI-HRMS *m/z* 233.0957 (Calculated for C₁₇H₁₃O 233.0961); IR (Pressed KBr disc): 3319, 2955, 2927, 2870, 1612, 1514, 1246, 1026, 835 cm⁻¹

4-Ethynylphenyl(trimethylsilyl)ethynylbenzene, **58**¹⁸⁴

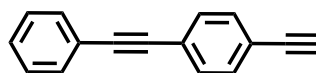


1-Bromo-4-iodobenzene (5.658g, 20.00 mmol), (trimethylsilyl) acetylene (TMSA) (2.96 mL, 11 mmol), bis(triphenylphosphine) palladium(II)chloride (0.28 g, 0.40 mmol), copper(I)iodide (0.152 g, 0.80 mmol), triphenylphosphine (0.262 mg, 1 mmol), Hünig's base (DIPEA, N,N-diisopropylethylamine) (14 mL, 80 mmol), and THF (35 mL) were reacted according to the following general coupling procedure. To an oven-dried glass sealed tube all solids including the aryl halide (bromide or iodide), alkyne, copper iodide, triphenylphosphine and palladium catalyst were added. The atmosphere was removed via vacuum and replaced with dry nitrogen (3 times). THF, remaining liquids, and Hünig's base or triethylamine were added and the reaction was heated in an oil bath while stirring. The reaction was allowed to stir at room temperature overnight. The liquid was then cannulated into a second screw cap tube under nitrogen, containing bistriphenylphosphinepalladium(II)chloride (0.28 g, 0.40 mmol) and copper(I)iodide (0.152 g, 0.80 mmol). Phenylacetylene (2.64 mL, 24.00 mmol) was added and the tube was capped and heated at 80 °C overnight. Upon cooling the reaction mixture was filtered via gravity filtration to remove solids and diluted with DCM. The reaction mixture was extracted with an aqueous solution of ammonium chloride (NH₄Cl) (3×50 ml). The organic layer was dried with magnesium sulfate and filtered. The solvent was then removed *in vacuo*. The crude product was purified via flash column chromatography (silica, ethyl acetate: petroleum ether = 0 % to 0.02 %, v/v) to yield 2.79 g (78%) of a white solid.

TLC Rf 0.40 (15% EtOAc/Pet.); MP 132 - 134 °C; ¹H NMR (400 MHz, CDCl₃, 20 °C): δ = 7.52-7.51 (m, 2H; Ar-H), 7.46-7.42 (m, 4H; Ar-H); 7.36-7.32 (m, 3H; Ar-H); 0.24 (s, 9H; ≡C-H); ¹³C NMR (100 MHz, CDCl₃, 20 °C): δ = 131.96, 131.66, 131.44, 128.56, 128.47, 123.36, 123.08, 122.97,

104.61, 96.23, 91.31, 89.06, 0.03; IR (KBr) 2200 cm^{-1} (w, $\text{C}\equiv\text{C}$), 2153 cm^{-1} (s, $\text{C}\equiv\text{C}-\text{Si}$); Elemental Analysis (CHN) C: 84.29% H: 5.43% (Calculated: C: 84.12% H: 5.57%); ESI-MS m/z 274 [M+H], 296 [M+Na]; ESI-HRMS m/z 274.1110 [M+H] (calc. for $\text{C}_{19}\text{H}_{15}\text{Si}$ 274.1124).

4-Ethynylphenylethynylbenzene, **59**¹⁸⁴

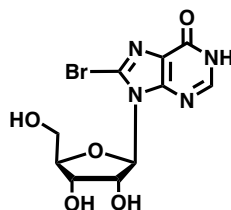


Method A: Manganese dioxide (0.6998 g, 8.0256 mmol), and potassium hydroxide (0.4511 g, 8.0256 mmol) were added in four separate portions to 1-(4-(phenylethynyl)phenyl)propyn-3-ol (0.9333 g, 4.0128 mmol) in Et_2O (20 mL) stirred at room temperature for 30 h. The reaction was diluted with Et_2O (50 mL) and filtered through a fritted funnel. The solvent was removed under reduced pressure and the residue was subjected to column chromatography (100 % Pet. to 2 % ethyl acetate/90 % Pet., v/v) to afford **68** as white solid (0.0412 g, 33% yield).

Method B: To a round bottom flask equipped with a stir bar were added compound 4-ethynylphenyl(trimethylsilyl)ethynylbenzene (2.635 g, 9.6 mmol, 1 eqv.), potassium carbonate (6.6336 g, 48 mmol, 5 eqv.), methanol (30 mL), and DCM (30 mL). The reaction was stirred for 2 h at 45 °C. The reaction was stirred, and upon completion the reaction mixture was diluted with DCM and washed with brine (3 times). The organic layer was dried over MgSO_4 , and the solvent was removed *in vacuo*. The crude product was purified by column chromatography on silica gel with 100 % hexane, yielding 1.1906 (57 %) of the desired white solid.

TLC Rf 0.50 (10% EtOAc/Pet.); MP 97–99 °C; ^1H NMR (400 MHz, CDCl_3 , 20 °C): δ = 7.55-7.58 (m, 2H; Ar-H), 7.43-7.51 (m, 4H; Ar-H); 7.38-7.40 (m, 3H; Ar-H); 3.20 (s, 1H; $\equiv\text{C}-\text{H}$); ^{13}C NMR (100 MHz, CDCl_3 , 20 °C): δ = 132.2, 132.1, 131.7, 129.0, 128.5, 124.1, 123.2, 122.4, 91.3, 89.1, 83.3, 79.2; IR (KBr) 3274, 3039, 2926, 2870, 2215, 1605, 1515, 1248, 1026, 826 cm^{-1} ; Elemental Analysis (CHN) C: 94.88% H: 4.91% (Calculated: C: 95.02% H: 4.98%); ESI-MS m/z 202 (100), 101 (15) [M+H]; ESI-HRMS m/z 202.0786 [M+H] (calc. for $\text{C}_{16}\text{H}_{10}$ 202.0782).

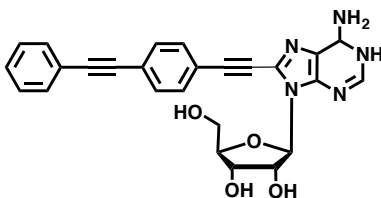
8-Bromo-9-((2*R*,3*R*,4*S*,5*R*)-3,4-dihydroxy-5-(hydroxymethyl)tetrahydrofuran-2-yl)-1,9-dihydro-6*H*-purin-6-one, 61



To a suspension of 8-bromoadenosine (0.25 g, 0.72 mmol, 1 eqv.) up in acetic acid–water (8 mL, 20:3 v/v), NaNO₂ (0.596 g, 8.637 mmol) was added in one portion and the resulting solution was stirred for 16 h. All solvents were evaporated and the residue taken up in EtOH and evaporated. The residue was partitioned between CHCl₃ and H₂O and the organic layer washed with sodium bicarbonate (20 ml, *sat.* aq) and then brine (20 ml), dried (MgSO₄), and evaporated to dryness. The residue was crystallized from aqueous EtOH (10 ml) to yield the title compound (0.211 g, 85%).

TLC R_f 0.40 (40% MeOH/DCM); MP 234–236 °C (dec.); ¹H NMR (400 MHz, DMSO-*d*₆, 20 °C) δ 8.09 (s, 1H; C2-H); 5.80 (d, 1H, *J* = 5.90; C1'-H), 5.57-5.50 (m, 1H; C2'-H), 5.31-5.23 (m, 1H; C2'-OH), 5.13-5.06 (m, 1H; C3'-OH), 5.07-5.01 (m, 1H; C5'-OH), 4.22-4.14 (m, 1H; C3'-H), 4.01-3.93 (m, 1H; C4'-H), 3.73-3.67 (m, 1H; C5'-H₁), 3.45-3.53 (m, 1H; C5'-H₂); ¹³C NMR (100 MHz, DMSO-*d*₆, 20 °C) δ: 155.7, 153.6, 151.9, 121.1, 116.9, 88.3, 86.6, 70.2, 70.3, 61.2; ESI-MS *m/z* 109(100), 157(10), 369[MNa⁺](10); ESI-HRMS *m/z* 368.9842 [M+H] (calc. for C₁₀H₁₁BrN₄NaO₅ = 368.9835); IR (DMSO Solution): 3505 cm⁻¹(OH), 3321 cm⁻¹(NH), 2926, 1683 (CO), 1527, 1369, 835 cm⁻¹.

Synthesis of (2*R*,3*R*,4*S*,5*R*)-2-(6-amino-8-((4-(phenylethynyl)phenyl)ethynyl)-1,6-dihydro-9*H*-purin-9-yl)-5-(hydroxymethyl)tetrahydrofuran-3,4-diol, 62

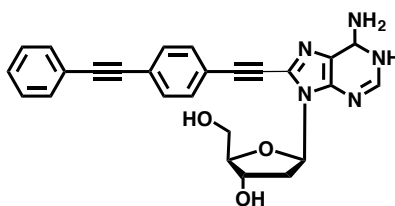


A solution of 8-bromoadenosine (0.0647 g, 0.1874 mmol, 1 equiv) in dry DMF (1.2 mL) was added to the (4-(phenylethynyl)phenyl)acetylene (0.0322 g, 0.1594 mmol, 1.7 equiv) and fresh distilled triethylamine (0.07 mL, 0.5626 mmol, 3 equiv) in a vacuum dried Schlenk tube. 4-OH, 4'-Hyxyl Pd₂(dba)₃ (2.64 g, 1.88 μmol, 1 mol %) and CuI (0.74 mg, 3.76 μmol, 2 mol %) and PPh₃ (0.001 g, 3.76 μmol, 2 mol %) added and the reaction mixture was left to stir at 110 °C for 18 h, after which

time it was allowed to cool to 40 °C and the DMF removed *in vacuo* to leave a brown solid. The solid was transferred to a sintered glass filter and washed with boiling water (5 × 20 mL), EtOAc (5 × 25 mL) and diethyl ether (2 × 25 mL) yielding the product as a light cream solid (0.0742 g, 86%).

TLC Rf 0.20 (40% MeOH/DCM); MP 182–184 °C; ¹H NMR (400 MHz, DMSO-*d*₆, 20 °C) δ 8.21 (br s, 1H; C2-H); 7.64 – 7.50 (m, 9H; ArH), 7.46 (s, 2H; NH₂), 6.11-6.04 (m, 1H; C1'-H), 5.65-5.56 (m, 1H; C5'-OH), 5.58-5.51 (m, 1H; C2'-OH), 5.33-5.26 (m, 1H; C3'-OH), 5.11-5.01 (m, 1H; C2'-H), 4.25-4.19 (m, 1H; C3'-H), 4.07-4.01 (m, 1H; C4'-H), 3.69-3.72 (m, 1H; C5'-H₁), 3.60- 3.51 (m, 1H; C5'-H₂); ¹³C NMR (100 MHz, DMSO-*d*₆, 20 °C) δ: 156.1, 153.0, 149.2, 147.5, 133.1, 131.9, 131.7, 128.6, 128.1, 127.3, 122.6, 122.4, 119.7, 101.1, 94.9, 89.6, 89.1, 87.0, 74.6, 70.7, 61.8; IR (Pressed KBr disc): 3308, 3169, 2918, 2221, 1649, 1331, 1095, 757; Elemental Analysis (CHN) C: 65.95 % H: 5.38% N: 13.84% (Calculated: C: 66.80 % H: 4.53% N: 14.98%); ESI-MS *m/z* 490[MNa⁺](52), 468 [MH⁺](100); ESI-HRMS *m/z* 490.1491 [M+Na] (calc. for C₂₆H₂₁N₅NaO₄=490.1495).

Synthesis of (2*R*,3*S*,5*R*)-5-(6-amino-8-((4-(phenylethynyl)phenyl)ethynyl)-1,6-dihydro-9H-purin-9-yl)-2-(hydroxymethyl)tetrahydrofuran-3-ol, 63

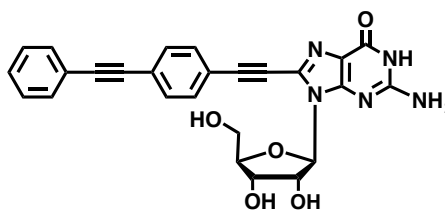


A solution of 8-bromodeoxyadenosine (0.0309 g, 0.0937 mmol, 1 equiv) in dry DMF (0.6 mL) was added to the (4-(phenylethynyl)phenyl)acetylene (0.0284 g, 0.1407 mmol, 1.5 equiv) and fresh distilled triethylamine (0.035 mL, 0.2813 mmol, 3 equiv) in a vacuum dried Schlenk tube. 1 mol% Pd₂(4-OH,4'-hexyl-dba)₃ (0.62 mg, 0.47 μmol, 1 mol %) and CuI (0.37 mg, 1.88 μmol, 2 mol%) and PPh₃ (0.5 mg, 3.75 μmol, 2 mol%) were added and the reaction mixture was left to stir at 80 °C for 22 h, after which time it was allowed to cool to 40 °C and the DMF removed *in vacuo* to leave a brown solid. The solid was transferred to a sintered glass filter and was washed with boiling water (5 × 20 mL), EtOAc (5 × 25 mL) and diethyl ether (2 × 25 mL) yielding the product as a light cream solid (0.04 g, 95%).

TLC Rf 0.20 (40% MeOH/DCM); MP 176–179 °C; ¹H NMR (400 MHz, DMSO-*d*₆, 20 °C) δ 8.24 (br s, 1H; C2-H); 7.78-7.55 (m, 9H; ArH), 7.48-7.43 (m, 1H; NH₂), 6.60-5.52 (m, 1H; C1'-H), 5.42-5.36 (m, 1H; C3'-OH), 5.35-5.29 (m, 1H; C5'-OH), 4.59-4.51 (m, 1H; C4'-H), 3.97-3.91 (m, 1H; C3'-H), 3.74-3.63 (m, 1H; C5'-H₁), 3.58-3.45 (m, 1H; C5'-H₂), 3.19-3.12 (m, 1H; C2'-H₁), 2.34-

2.27 (m, 1H; C2'-H₂); ¹³C NMR (100 MHz, DMSO-*d*₆, 20 °C) δ: 156.9, 152.2, 149.7, 147.4, 132.5, 131.7, 131.2, 128.4, 128.2, 127.9, 122.8, 119.1, 101.9, 89.9, 89.1, 89.0, 86.9, 70.2, 61.7, 39.4; IR (Pressed KBr disc): 3305, 3163, 2930, 2212, 1650, 1329, 1099, 754; Elemental Analysis (CHN) C: 68.85% H: 4.97% N: 14.35% (Calculated: C: 69.17% H: 4.53% N: 14.98%); ESI-MS *m/z* 452[MH⁺] (100); ESI-HRMS *m/z* 452.1717 [M+H] (calc. for C₂₆H₂₂N₅O₃= 452.1738).

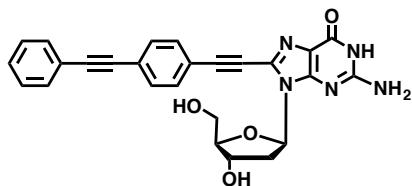
Synthesis of 2-amino-9-((2R,3R,4S,5R)-3,4-dihydroxy-5-(hydroxymethyl)tetrahydrofuran-2-yl)-8-((4-(phenylethynyl)phenyl)ethynyl)-1,9-dihydro-6H-purin-6-one, 64



A solution of 8-bromoguanosine (0.0338 g, 0.0937 mmol, 1 equiv) in dry DMF (0.6 mL) was added to the (4-(phenylethynyl)phenyl)acetylene (0.02275 g, 0.1125 mmol, 1.2 equiv) and fresh distilled triethylamine (0.035 mL, 0.2813 mmol, 3 equiv) in a vacuum dried Schlenk tube. 1 mol% 4-OH, 4'-Hyxyl Pd₂(dba)₃ (0.62 mg, 0.47 μmol, 1 mol%) and CuI (0.37 mg, 1.88 μmol, 2 mol%) and PPh₃ (0.5 g, 3.75 μmol, 2 mol%) were added and the reaction mixture was left to stir at 110 °C for 18 h, after which time it was allowed to cool to 40 °C and the DMF removed *in vacuo* to leave a brown solid. The solid was transferred to a sintered glass filter and was washed with boiling water (5 × 20 mL), EtOAc (5 × 25 mL) and diethyl ether (2 × 25 mL) yielding the product as a light cream solid (0.037 g, 82%).

TLC R_f 0.25 (40% MeOH/DCM); MP 234–236 °C (dec.); ¹H NMR (400 MHz, DMSO-*d*₆, 20 °C) δ 10.89 (s, 1H; NH); 7.67-7.59 (m, 6H; ArH), 7.52-7.46 (m, 3H; ArH), 6.62 (br s, 1H; NH₂), 5.93-5.85 (m, 1H; C1'-H), 5.54-5.47 (m, 1H; C2'-OH), 5.19-5.11 (m, 1H; C3'-OH), 5.03-4.91 (m, 1H; C2'-H, C5'-OH), 4.19-4.11 (m, 1H; C3'-H), 3.94-3.88 (m, 1H; C4'-H), 3.68-3.61 (m, 1H; C5'-H₁), 3.57-3.49 (m, 1H; C5'-H₂); ¹³C NMR (100 MHz, DMSO-*d*₆, 20 °C) δ: 156.7, 153.8, 148.8, 132.3, 132.1, 131.1, 129.5, 129.4, 129.2, 127.1, 121.1, 120.9, 120.7, 117.4, 101.6, 88.4, 88.1, 86.9, 86.5, 78.7, 70.8, 70.5, 61.2; IR (Pressed KBr disc): 3321, 2931, 1671, 1596, 1377, 837, 759, 682; Elemental Analysis (CHN) C: 63.66 % H: 5.13% N: 13.98% (Calculated: C: 64.59 % H: 4.53% N: 14.49%); ESI-MS *m/z* 484[MH⁺](100); ESI-HRMS *m/z* 484.1615 [M+H] (calc. for C₂₆H₂₂N₅O₅= 484.1618).

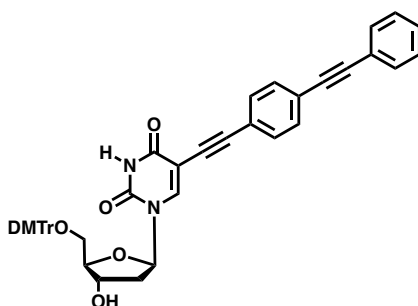
Synthesis of 2-amino-9-((2R,4S,5R)-4-hydroxy-5-(hydroxymethyl)tetrahydrofuran-2-yl)-8-((4-(phenylethynyl)phenyl)ethynyl)-1,9-dihydro-6H-purin-6-one, 65



A solution of 8-bromodeoxyguanosine (0.0338 g, 0.0937 mmol, 1 equiv) in dry DMF (0.6 mL) was added to the (4-(phenylethynyl)phenyl)acetylene (0.0284 g, 0.1407 mmol, 1.5 equiv) and triethylamine (0.035 mL, 0.2813 mmol, 3 equiv) in a vacuum dried Schlenk tube. 1 mol% 4-OH, 4'-Hyxyl Pd₂(dba)₃ (0.62 mg, 0.47 μmol, 1 mol%) and CuI (0.37 mg, 1.88 μmol, 2 mol%) and PPh₃ (0.5 mg, 3.75 μmol, 2 mol%) were added and the reaction mixture was left to stir at 80 °C for 18 h, after which time it was allowed to cool to 40 °C and the DMF removed *in vacuo* to leave a brown solid. The solid was transferred to a sintered glass filter and was washed with boiling water (5 × 20 mL), EtOAc (5 × 25 mL) and diethyl ether (2 × 25 mL) yielding the product as a light cream solid (0.043 g, 96%).

TLC Rf 0.20 (40% MeOH/DCM); MP 218–220 °C (dec.); ¹H NMR (400 MHz, DMSO-*d*₆, 20 °C) δ 10.84 (s, 1H; NH); 7.65-7.53 (m, 6H; ArH), 7.44-7.39 (m, 3H; ArH), 6.58 (br s, 1H; NH₂), 6.36-6.28 (m, 1H; C1'-H), 5.27 (d, 1H, *J* = 7.5 Hz; C3'-OH), 4.89-4.81 (m, 1H; C5'-OH), 4.45-4.37 (m, 1H; C3'-H), 3.82-3.76 (m, 1H; C4'-H), 3.62-3.55 (m, 1H; C5'-H₁), 3.48-3.44 (m, 1H; C5'-H₂), 3.11-3.04 (m, 1H; C2'-H₁), 2.22-2.16 (m, 1H; C2'-H₂); ¹³C NMR (100 MHz, DMSO-*d*₆, 20 °C) δ: 156.9, 153.1, 148.7, 132.4, 131.7, 131.9, 128.3, 128.1, 127.6, 122.7, 122.5, 117.9, 101.4, 94.7, 89.8, 89.6, 86.5, 81.3, 70.1, 61.2, 40.4; IR (Pressed KBr disc): 3319, 2930, 1682, 1592, 1364, 1045, 836, 756, 689; Elemental Analysis (CHN) C: 66.46% H: 4.98% N: 14.02% (Calculated: C: 66.80% H: 4.53% N: 14.98%); ESI-MS *m/z* 490 [MNa⁺](100), 465 (23), 413 (18), 363 (15); ESI-HRMS *m/z* 490.1486 [M+Na] (calc. for C₂₆H₂₁N₅NaO₄ = 490.1495).

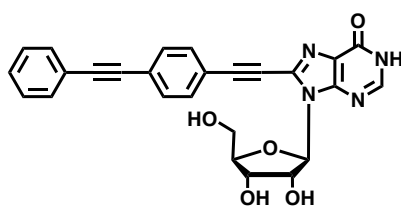
1-((2R,4S,5R)-5-((Bis(4-methoxyphenyl)(phenyl)methoxy)methyl)-4-hydroxytetrahydrofuran-2-yl)-5-((4-(phenylethynyl)phenyl)ethynyl)pyrimidine-2,4(1H,3H)-dione, 66



A solution of DMT-5-I-dU (0.0615 g, 0.0937 mmol, 1 equiv) in dry DMF (0.6 mL) was added to the (4-(phenylethynyl)phenyl)acetylene (0.0284 g, 0.1407 mmol, 1.5 equiv) and triethylamine (0.035 mL, 0.2813 mmol, 3 equiv) in a vacuum dried Schlenk tube. 1 mol% 4-OH, 4'-Hyxyl Pd₂(dba)₃ (0.62 mg, 0.47 μmol, 1 mol%) and CuI (0.37 mg, 1.88 μmol, 2 mol%) and PPh₃ (0.5 mg, 3.75 μmol, 2 mol%) were added and the reaction mixture was left to stir at 80 °C for 22 h, after which time it was allowed to cool to 40 °C and the DMF was removed *in vacuo* to leave a brown solid. The solid was transferred to a small filter funnel and was washed with boiling water (5 × 20 mL) and diethyl ether (2 × 25 mL) yielding the product as a light cream solid (0.0657 g, 96%).

TLC Rf 0.40 (30% MeOH/DCM); MP 184–186 °C (dec.); ¹H NMR (400 MHz, DMSO-*d*₆, 20 °C) δ 11.8 (br s, 1H; NH); 8.13 (s, 1H; C6-H), 7.60-7.53 (m, 3H; ArH), 7.48-7.40 (m, 9H; ArH), 7.10 (d, 1H, *J* = 8.15; ArH), 6.87-6.82 (m, 3H; ArH), 6.19-6.11 (m, 1H; C1'-H), 5.41-5.37 (m, 1H; C4'-H), 3.67 (s, 6H; OCH₃), 4.36-4.29 (m, 1H; C5'-H₁), 4.05-3.97 (m, 1H; C5'-H₂), 3.26-3.19 (m, 1H; C2'-H₁), 2.33-2.28 (m, 1H; C2'-H₂); ¹³C NMR (100 MHz, DMSO-*d*₆, 20 °C) δ: 165.8, 159.7, 157.4, 151.9, 143.8, 142.2, 136.8, 136.2, 128.7, 128.4, 128.3, 127.8, 127.4, 126.1, 122.4, 114.3, 100.9, 97.3, 95.5, 91.6, 89.7, 88.3, 86.9, 72.8, 64.5, 57.2, 40.3; IR (Pressed KBr disc): 3395, 2931, 2228, 1658, 1506, 1442, 1248, 1174, 1091, 1030, 826, 753, 690; Elemental Analysis (CHN) C: 74.97% H: 5.18% N: 3.18% (Calculated: C: 75.60 % H: 5.24% N: 3.83%); ESI-MS *m/z* 753[MNa⁺] (45), 684(50), 610(100), 536(70), 453(25); ESI-HRMS *m/z* 753.2571 [M+Na] (calc. for C₄₆H₃₈N₂NaO₇ = 753.2550).

9-((2*R*,3*R*,4*S*,5*R*)-3,4-Dihydroxy-5-(hydroxymethyl)tetrahydrofuran-2-yl)-8-((4-(phenylethynyl)phenyl)ethynyl)-1,9-dihydro-6*H*-purin-6-one, 67



A solution of 8-bromoinosine (0.065 g, 0.1874 mmol, 1 equiv) in dry DMF (1.2 mL) was added to the (4-(phenylethynyl)phenyl)acetylene (0.0643 g, 0.3186 mmol, 1.7 equiv) and fresh distilled triethylamine (0.07 mL, 0.5626 mmol, 3 equiv) in a vacuum dried Schlenk tube. 1 mol% 4-OH, 4'-Hyxyl Pd₂(dba)₃ (2.64 mg, 1.88 μmol, 1 mol%) and CuI (0.74 mg, 3.76 μmol, 2 mol%) and PPh₃ (10 mg, 3.6 μmol, 2 mol%) were added and the reaction mixture was left to stir at 110 °C for 18 h, after which time it was allowed to cool to 40 °C and the DMF removed *in vacuo* to leave a brown solid. The solid was transferred to a sintered glass filter and was washed with boiling water (5 × 20 mL),

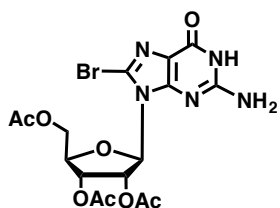
EtOAc (5 × 25 mL) and diethyl ether (2 × 25 mL) yielding the product as a light cream solid (0.0688 g, 80%).

TLC Rf 0.20 (40% MeOH/DCM); MP 185–188 °C (dec.); ¹H NMR (400 MHz, DMSO-*d*₆, 20 °C) δ 12.47 (br s, 1H; NH); 8.18 (s, 1H; C2-H), 7.78-7.69 (m, 2H; ArH), 7.63-7.54 (m, 3H; ArH), 7.49-7.41 (m, 4H; ArH), 6.04 (d, 1H, *J* = 6.7 Hz; C1'-H), 5.55 (d, 1H, *J* = 6.5 Hz; C2'-OH), 5.30 (d, 1H, *J* = 6.5 Hz; C3'-OH), 4.98 (d, 1H, *J* = 6.7 Hz; C5'-OH), 4.26-4.19 (m, 1H; C2'-H), 4.03-3.95 (m, 1H; C3'-H), 3.71-3.62 (m, 1H; C4'-H), 3.58-3.51 (m, 1H; C5'-H); ¹³C NMR (100 MHz, DMSO-*d*₆, 20 °C) δ: 156.9, 149.8, 147.6, 131.9, 129.5, 128.9, 128.7, 128.1, 127.3, 123.1, 122.8, 122.4, 117.3, 101.8, 89.1, 88.1, 87.9, 87.1, 86.5, 71.4, 61.9; IR (Pressed KBr disc): 3312, 3129, 2933, 1671, 1351, 1095, 838, 757; Elemental Analysis (CHN) C: 62.88 % H: 4.48% N: 11.84% (Calculated: C: 66.66 % H: 4.30% N: 11.49%); ESI-MS *m/z* 469[MH⁺](100), 417(35); ESI-HRMS *m/z* 469.1472 [M+H] (calc. for C₂₆H₂₁N₄O₅= 469.1498).

General procedure for the terminal alkynes Sonogashira cross-coupling reaction with optimized condition in propylene carbonate

To a stirred suspension of brominated purine (0.1875 mmol, 1 equiv) in anhydrous PC (2 mL) was added to the phenylacetylene (0.03 ml, 0.225 mmol, 1.2 equiv) and triethylamine (0.07 mL, 0.5625 mmol, 3 equiv) in a vacuum dried Schlenk tube. The reaction mixtures were sonicated with occasional stirring for 20 mins. The reaction temperature in PC needed to reach 135 °C for better dissolution. Then 1 mol% Pd₂(dba-Z)₃ (0.94 μmol, 1 mol %) and CuI (0.75 mg, 3.75 μmol, 2 mol %) and PPh₃ (0.99 mg, 3.75 μmol, 2 mol %) were added and the reaction mixture was left to stir at 90 °C for 24 h, after which time it was allowed to cool to 50 °C and the PC removed *in vacuo* to leave a brown solid. The solid was transferred to a sintered glass filter and was washed with boiling water (5 × 10 mL), EtOAc (5 × 10 mL) and diethyl ether (3 × 10 mL) yielding the product as a light cream solid.

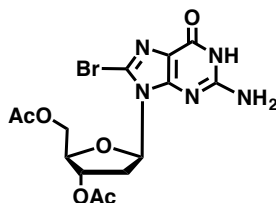
(2*R*,3*R*,4*R*,5*R*)-2-(Acetoxymethyl)-5-(2-amino-8-bromo-6-oxo-1,6-dihydro-9*H*-purin-9-yl)tetrahydrofuran-3,4-diyl diacetate, 68²⁰⁵



8-Bromoguanosine (2.015 g, 5.55 mmol) was dissolved in 5 mL of pyridine (Aldrich) and 3.5 mL of acetic anhydride. This mixture was stirred in an ice bath for 3.5 h after which 2,3,5-tri-Oacetyl-8-bromoguanosine precipitated. The precipitate was suspended in 25 mL of ice-cold water and filtered and the residue washed with 200 mL of ice-cold water and air-dried. Yield: 2.60 g (5.24 mmol, 96%).

TLC Rf 0.45 (10% MeOH/DCM); MP 217-219 °C (dec.); ¹H NMR (400 MHz, DMSO-*d*₆, 20 °C) δ 10.95 (s, 1H, NH), 6.62 (s, 2H; NH₂); 6.05-5.97 (m, 1H, C1'-H), 5.89 (d, 1H, *J* = 6.60; C2'-H), 5.71-5.65 (m, 1H; C3'-H), 4.46-4.39 (m, 1H; C4'-H), 4.38-4.27 (m, 1H; C5'-H₁), 4.26-4.18 (m, 1H; C5'-H₂), 2.12-1.99 (m, 9H; CH₃CO); ¹³C NMR (100 MHz, DMSO-*d*₆, 20 °C) δ: 171.8, 170.7, 170.3, 156.1, 154.4, 152.6, 120.8, 117.8, 88.3, 79.9, 71.9, 70.7, 63.4, 21.1, 20.8; ESI-MS *m/z* (%): 484(100)[⁷⁹BrM], 486(95)[⁸¹BrM]; ESI-HRMS *m/z* 486.4319 [M+H](calc. for C₁₆H₁₈BrN₅O₈ = 486.4322); IR (DMSO Solution): 3422 cm⁻¹(NH), 3307 cm⁻¹(NH), 1694 cm⁻¹(CO), 1606, 863.

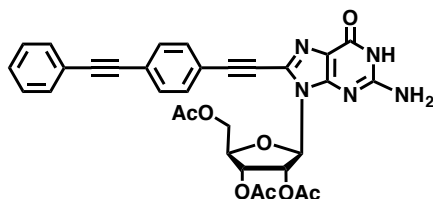
((2*R*,3*S*,5*R*)-3-Acetoxy-5-(2-amino-8-bromo-6-oxo-1,6-dihydro-9*H*-purin-9-yl)tetrahydrofuran-2-yl)methyl acetate, 69



2-Deoxy-8-bromoguanosine (0.056 g, 0.155 mmol, 1 eqv.), DMAP (*N,N*-dimethylamino-pyridine, 0.002 mg, 0.0155 mmol, 10 mol%) was dissolved in 0.2 mL of pyridine and 0.12 mL of acetic anhydride. This mixture was stirred in an ice bath for 3.5 h after which 2',3',5'-tri-Oacetyl-2-deoxy-8-bromoguanosine precipitated. The precipitate was suspended in 15 mL of ice-cold water and filtered and the residue washed with 200 mL of ice-cold water and air-dried (0.0446 g, 67%).

TLC Rf 0.40 (10% MeOH/DCM); MP 226-228 °C (dec.); ¹H NMR (400 MHz, DMSO-*d*₆, 20 °C) δ 10.86 (s, 1H, NH), 6.57 (s, 2H, NH₂), 6.17 (dd, 1H, *J*₁ = 8.7 Hz, *J*₂ = 5.9 Hz; C1'-H), 5.48-5.39 (m, 1H; C3'-H), 4.43-4.36 (m, 1H, C5'-H₁), 4.21-4.16 (m, 2H; C4'-H, C5'-H₂), 3.52-3.47 (m, 1H, C2'-H₁), 2.45-2.41 (m, 1H, C2'-H₂), 2.08 (s, 3H, COCH₃), 1.99 (s, 3H, COCH₃). ¹³C-NMR (101 MHz, DMSO-*d*₆): δ 171.1, 170.6, 156.3, 153.1, 151.6, 135.3, 116.5, 83.1, 81.3, 74.9, 62.9, 35.4, 20.8, 20.1; ESI-MS *m/z* (%): 349(70), 387(100), 452(20)[⁷⁹BrMNa], 454(20)[⁸¹BrMNa]; ESI-HRMS *m/z* 452.0172 [M+Na](calc. for C₁₄H₁₆BrN₅NaO₆ = 452.0176); IR (DMSO Solution): 3427 cm⁻¹(NH), 3314 cm⁻¹(NH), 1686 cm⁻¹(CO), 1617, 964.

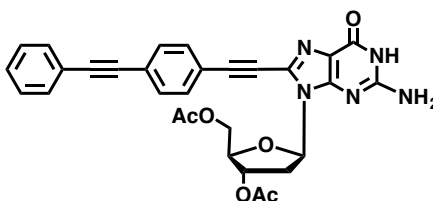
(2R,3R,4R,5R)-2-(Acetoxymethyl)-5-(2-amino-6-oxo-8-((4-(phenylethynyl)phenyl)ethynyl)-1,6-dihydro-9H-purin-9-yl)tetrahydrofuran-3,4-diyl diacetate, 70



A solution of acetylation of 8-bromoguanosine (0.3287 g, 0.6753 mmol, 1 equiv) in dry DMF (4 mL) was added to the (4-(phenylethynyl)phenyl)acetylene (0.2045 g, 1.013 mmol, 1.5 equiv) and triethylamine (0.28 mL, 2.0254 mmol, 3 equiv) in a vacuum dried Schlenk tube. 1 mol% 4-OH, 4'-Hyxyl Pd₂(dba)₃ (4.46 mg, 3.38 μmol, 1 mol %) and CuI (2.66 mg, 13.54 μmol, 2 mol %) and PPh₃ (3.6 mg, 13.54 μmol, 2 mol %) were added and the reaction mixture was left to stir at 80 °C for 22 h, after which time it was allowed to cool to 40 °C and the DMF removed *in vacuo* to leave a brown solid. The solid was transferred to a sintered glass filter and was washed with boiling water (5 × 20 mL), and diethyl ether (2 × 25 mL) yielding the product as a light cream solid (0.4053 g, 96%)

TLC Rf 0.25 (40% MeOH/DCM); MP 173-175 °C (dec.); ¹H NMR (400 MHz, CD₂Cl₂, 20 °C) δ 11.93 (br s, 1H, NH), 7.57-7.31 (m, 9H, ArH), 6.83 (br s, 2H; NH₂); 6.24-6.18 (m, 2H; C1'-H, C2'-H), 6.09-6.03 (m, 1H; C3'-H), 4.61-4.54 (m, 1H; C4'-H), 4.47-4.41 (m, 1H; C5'-H₁), 4.36-4.31 (m, 1H; C5'-H₂), 2.12-1.99 (m, 9H; CH₃CO); ¹³C NMR (100 MHz, CD₂Cl₂, 20 °C) δ: 170.9, 170.8, 157.1, 153.8, 149.6, 132.8, 132.1, 128.4, 128.3, 127.8, 122.7, 122.3, 120.8, 118.1, 117.8, 89.9, 85.7, 80.6, 74.1, 73.8, 62.6, 21.7, 20.9; Elemental Analysis (CHN) C, 62.88, H, 4.48, N, 11.84 (Calculated: C, 63.05, H, 4.46, N, 11.49); ESI-MS *m/z* (%): 632(52)[MNa⁺], 610(100)[MH⁺], 536(30); ESI-HRMS *m/z* [MNa⁺]: 632.1752 (calculated for C₃₂H₂₇N₅NaO₈ = 632.1744); IR (DMSO Solution): 3429, 3309, 2932, 2677, 2212, 1744, 1675, 1568, 1365, 1220, 1037, 834, 755, 689 cm⁻¹.

((2R,3S,5R)-3-Acetoxy-5-(2-amino-6-oxo-8-((4-(phenylethynyl)phenyl)ethynyl)-1,6-dihydro-9H-purin-9-yl)tetrahydrofuran-2-yl)methyl acetate, 71

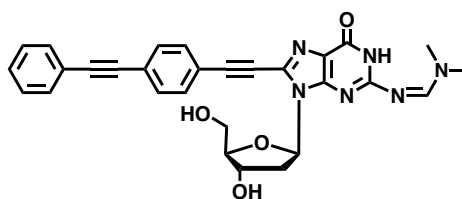


A solution of acetylation of 8-bromoguanosine (0.2896 g, 0.6753 mmol, 1 equiv) in dry DMF (4 mL) was added to the (4-(Phenylethynyl)phenyl)acetylene (0.2045 g, 1.013 mmol, 1.5 equiv) and

triethylamine (0.28 mL, 2.0254 mmol, 3 equiv) in a vacuum dried Schlenk tube. 1 mol% 4-OH, 4'-Hyxyl Pd₂(dba)₃ (4.46 mg, 3.38 μmol, 1 mol %) and CuI (2.66 mg, 13.54 μmol, 2 mol %) and PPh₃ (3.6 mg, 13.54 μmol, 2 mol %) were added and the reaction mixture was left to stir at 80 °C for 22 h, after which time it was allowed to cool to 40 °C and the DMF removed *in vacuo* to leave a brown solid. The solid was transferred to a sintered glass filter and was washed with boiling water (5 × 20 mL), and diethyl ether (2 × 25 mL) yielding the product as a light cream solid (0.7898 g, 97%).

TLC Rf 0.25 (40% MeOH/DCM); MP 158-161 °C (dec.); ¹H NMR (400 MHz, DMSO-d₆, 20 °C) δ 10.97 (s, 1H, NH), 7.68-7.39 (m, 9H; ArH), 6.72 (br s, 2H, NH₂), 6.11-6.05 (m, 1H, C1'-H), 6.04-5.97 (m, 1H; C3'-H), 5.69-5.62 (m, 1H, C4'-H), 4.47-4.39 (m, 1H; C5'-H₁), 4.38-4.31 (m, 1H; C5'-H₂), 4.23-4.17 (m, 1H, C2'-H₁), 3.14-3.09 (m, 1H, C2'-H₂), 2.12-2.08 (m, 6H, COCH₃); ¹³C-NMR (101 MHz, DMSO-d₆): δ 170.8, 170.7, 157.4, 153.6, 148.9 132.1, 132.1, 131.7, 128.4, 128.3, 127.8, 122.9, 122.2, 117.6, 102.4, 89.9, 86.7, 84.3, 81.9, 80.6, 74.1, 62.4, 36.9, 21.7, 20.0; Elemental Analysis (CHN) C, 66.17, H, 5.53, N, 13.25 (calculated: C, 65.33, H, 4.57, N, 12.70); ESI-MS *m/z* (%): 574(75)[MNa⁺], 552(100)[MH⁺]; ESI-HRMS *m/z* 574.1697[M+Na] (calculated for C₃₀H₂₅N₅NaO₆=574.1686); IR (DMSO Solution): 3425, 3307, 2936, 2677, 2206, 1738, 1676, 1591, 1363, 1230, 1035, 835, 756, 691.

(Z)-N'-((2R,4S,5R)-4-Hydroxy-5-(hydroxymethyl)tetrahydrofuran-2-yl)-6-oxo-8-((4-(phenylethynyl)phenyl)ethynyl)-6,9-dihydro-1H-purin-2-yl)-N,N-dimethylformimidamide, 72

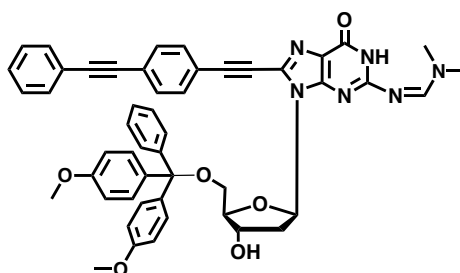


PhCCPhCC-deoxyguanosine **64** (0.6 g, 1.284 mmol, 1 eqv.) was placed in a Schlenk tube. Dry DMF (6 mL) was added, followed by dimethylformamide-diethyl-acetal (0.12 mL, 2.631 mmol, 4.1 eqv.), and the mixture was allowed to stir until completion overnight at room temperature. The reaction mixture was then evaporated to dryness, and the solid washed with EtOH and dried to yield product (0.59 g, 88%).

TLC Rf 0.30 (40% MeOH/DCM); MP 196–198 °C (dec.); ¹H NMR (400 MHz, DMSO-d₆, 20 °C) δ 11.56 (br s, 1H; NH); 8.56 (s, 1H; N=CH), 7.72-7.43 (m, 9H; ArH), 6.48-6.42 (m, 1H; C3'-OH), 5.42-5.35 (m, 1H; C2'-H), 4.93-4.87 (m, 1H; C5'-OH), 4.53-4.46 (m, 1H; C3'-H), 3.87-3.81 (m, 1H; C4'-H), 3.66-3.62 (m, 1H; C5'-H₁), 3.58-3.53 (m, 1H; C5'-H₂), 3.17-3.05 (m, 7H; C2'-H₁, N(CH₃)₂) 2.29-2.23 (m, 1H; C2'-H₂); ¹³C NMR (100 MHz, DMSO-d₆, 20 °C) δ: 158.8, 157.0, 156.9, 153.4,

148.7, 132.7, 131.6, 131.9, 128.6, 128.5, 127.6, 122.6, 122.5, 117.4, 101.8, 89.8, 89.7, 86.7, 81.7, 70.3, 61.2, 40.2, 35.9; IR (Pressed KBr disc): 3317, 2932, 1686, 1361, 1047, 837, 756; Elemental Analysis (CHN) C: 66.45% H: 5.52% N: 15.92% (Calculated: C, 66.66; H, 5.02; N, 16.08); ESI-MS m/z 523 $[MH^+]$ (100); ESI-HRMS m/z 523.0452 $[M+H]$ (calc. for $C_{29}H_{26}N_6O_4 = 523.0467$).

(Z)-N'-(9-((2R,4R,5R)-5-((Bis(4-methoxyphenyl)(phenyl)methoxy)methyl)-4-hydroxytetrahydrofuran-2-yl)-6-oxo-8-((4-(phenylethynyl)phenyl)ethynyl)-6,9-dihydro-1H-purin-2-yl)-N,N-dimethylformimidamide, 73



N_2 -PhCCPhCC-deoxyguanosine **81** (0.0783 g, 0.15 mmol, 1 eqv.) was dissolved in dry pyridine (1 ml). DMTrCl (0.18 g, 0.45 mmol, 3 eqv.) and DMAP (4-dimethylaminopyridine) (0.002 g, 0.015 mmol, 0.1 mol%) in dry pyridine (0.3 ml), cooled in an ice bath. DMAP was added dropwise into solution and the solution was stirred at RT for 19 hours. The reaction mixture was dissolved in EtOAc (10 ml), then washed with 2M of $CuSO_4$. The organic layer was dried with magnesium sulfate and filtered. The solvent was then removed *in vacuo* to afford the product (0.07 g, 59%).

MP 202–204 °C (dec.); 1H NMR (400 MHz, $DMSO-d_6$, 20 °C) δ 11.49 (br s, 1H; NH); 8.16 (s, 1H; $N=CH$), 7.62–6.62 (m, 22H; ArH), 6.55–6.46 (m, 1H; $C3'$ -OH), 5.47–5.43 (m, 1H; $C2'$ -H), 4.46–4.39 (m, 1H; $C5'$ - H_1), 4.17–4.12 (m, 1H; $C5'$ - H_2), 3.03–2.98 (m, 6H, OCH_3), 2.73 (s, 6H; $N(CH_3)_2$), 1.89–1.78 (m, 2H; $C2'$ - H_1 , $C2'$ - H_2); ^{13}C NMR (100 MHz, $DMSO-d_6$, 20 °C) δ : 159.2, 158.6, 157.1, 156.7, 153.3, 148.5, 143.8, 136.5, 132.7, 131.7, 131.6, 130.2, 128.9, 128.4, 128.3, 127.6, 127.5, 127.4, 127.2, 126.3, 122.1, 122.0, 117.6, 115.3, 101.8, 89.2, 89.1, 86.4, 81.7, 70.2, 61.7, 56.2, 40.3, 36.3; IR (Pressed KBr disc): 3324, 3309, 2930, 2659, 2216, 1747, 1682, 1364, 1022, 836, 752, 654 cm^{-1} ; ESI-MS m/z 407(100), 825(10) $[MH^+]$; ESI-HRMS m/z 825.3380 $[M+H]$ (calc. for $C_{50}H_{45}N_6O_6 = 825.3395$).

CHAPTER 4

PHOTOPHYSICAL CHARACTERISATION OF MODIFIED NUCLEOSIDES

4 Photophysical Characterisation of Modified Nucleosides

4.1 Introduction

Most information concerning the structure and dynamics of DNA and RNA can be gained via X-ray crystallography and NMR spectroscopy. These techniques, however, are limited regarding their resolution and timescale. Fluorescence offers a better approach for learning about the structure and dynamics of DNA and RNA, making real-time reporting of changes in microenvironment possible. Characterisation of real-time processes occurring within DNA and RNA allows mechanistic processes to be determined using an incorporated fluorescent probe at a certain target site.

To understand whether the synthesised C8-modified nucleosides can be used as fluorophores in a biological context, understanding their fundamental photophysical characteristics is of utmost importance. The full photophysical characterisation will be given, and the major properties and trends will be discussed. The photophysical data will be used to judge the potential applications and determine trends within the series of compounds synthesised from chapter 3.

4.1.1 Principles of fluorescence

The use of fluorescent molecules in biological research continues to increase due to their versatility, sensitivity and quantitative abilities.²¹⁷ Especially, for the fluorescent probes use, which is employed to detect protein location and activation, and conformational differences and monitor biological processes *in vivo*. Analogous compounds carrying detectable structural modifications that render the analogue fluorescent, could allow single-molecule detection using fluorescence microscopy techniques.^{218,219} These analogues could be used in biochemical studies of nucleic acid polymerases to reveal mechanistic information.^{220,221}

In photophysics, there are two observable emission types that can be detected. They are fluorescence and phosphorescence. Fluorescence is a form of luminescence when a fluorophore absorbs a photon of light, which raises the compound to an electronically excited state, S_1 . The fate of this species is varied, depending on the exact nature of the fluorophore and its environment, but the result is end with deactivation (loss energy) and then returns to the ground state without spin changing, with re-emission of a photon.²²² The main deactivation processes, which occur, are fluorescence. The spontaneous emission of light during transition of the system from its lowest vibrational energy level of an excited singlet state S_1 back to the ground state S_0 in room temperature (Figure 4.1). Thus, it is

a spin-allowed process, which follows the selection rule $\Delta S = 0$, in contrast to phosphorescence, where a forbidden non-radiative transition into an iso-energetic vibrational level of a triplet state T_1 with change of multiplicity occurs, which are labelled IC and ISC respectively.

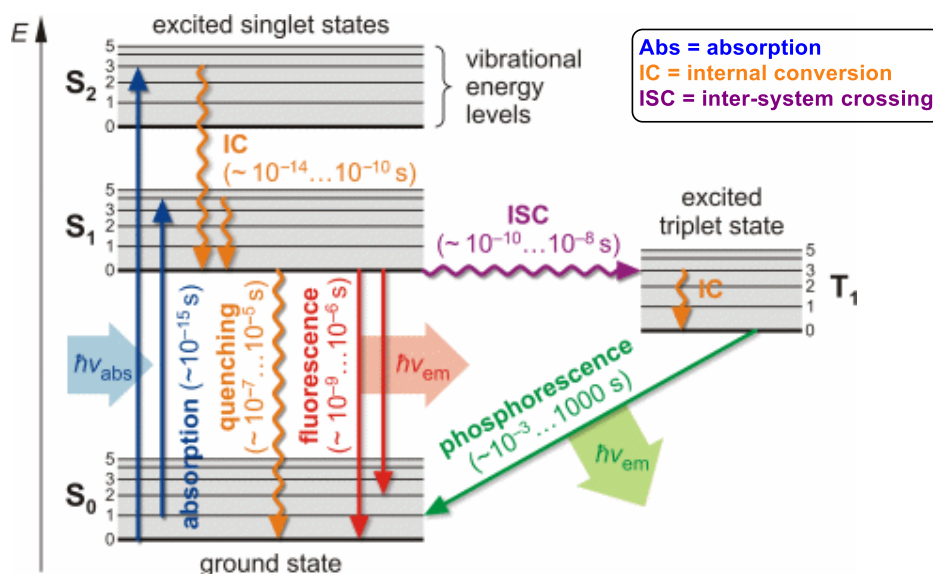


Figure 4.1 Jablonski (electronic transitions) diagram. Adapted image taken from website: <https://www.uni-leipzig.de/~pwm/web/?section=introduction&page=fluorescence>, accessed from 27/11/2015.

As illustrated in Figure 4.2, the sum of the quantum yield for fluorescence (Φ_F), phosphorescence (Φ_P), and non-radiative decay processes ($\Sigma\Phi_R$) is equal to one. Therefore, decreasing non-radiative decay can lead a higher efficient emission.

$$(\Phi_F) + (\Phi_P) + (\Sigma\Phi_R) = 1$$

Figure 4.2 Quantum yield equation.

Vibrational fine structure that could be detected *via* the absorption spectrum provides some indication of the degree of Frank-Condon overlap between electronic states (Figure 4.3). Both the ground and excited states are presented as energy outlines populated by vibrational energy states and rotational states. According to the Franck-Condon principle, excitation must happen by a vertical transition, resulting in the population of higher vibrational levels in the excited state. The vibrational energy may be lost as heat, and may be released the excited state to its zero vibrational level. Otherwise, the excited state may return to the ground state by emitting a photon (light green line). If this happens from the zero vibrational level the frequency or energy of the emitted light will be lower than that of the initially absorbed light, then generates the fluorescence.

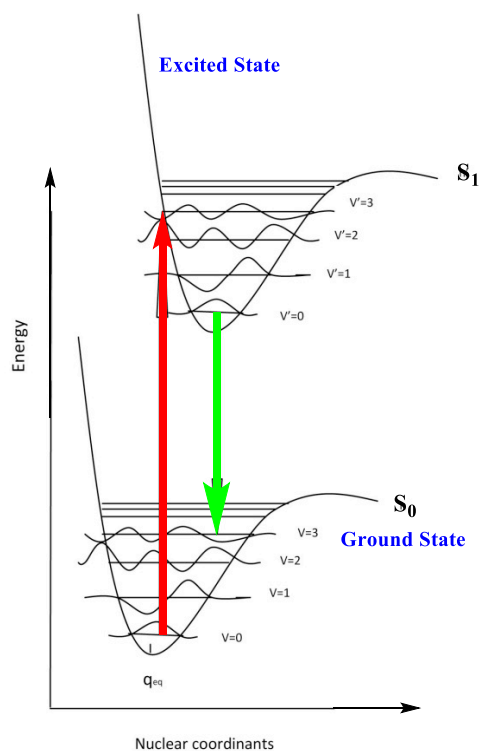


Figure 4.3 Jablonski (energy) diagram. Adapted image taken from website: <http://photobiology.info/Ilichev.html>, accessed from 25/11/2015.

Fluorophore-containing molecules are characterised by various photophysical properties: the molar absorption coefficient (determination of the efficiency of absorption from light at a particular wavelength relative to its molar concentration), the quantum yield (the efficiency of fluorescence emission for one photon) and fluorescence lifetime (a measure of the time a fluorophore spends in the excited state before returning to the ground state by emitting a photon). Fluorescence is a property possessed by the major of molecules, particularly with extended π -conjugated systems.

4.1.2 Fluorescent Nucleosides Analogues

The fluorescence properties of natural nucleic acids involved in replication are characterised by low quantum yields (Φ)⁹¹ due to fast decay from excited states.^{224,225} They range between 0.86×10^{-4} for adenosine and 1.32×10^{-4} for thymidine), associating with excited state lifetimes as picocseconds.^{67,69} Absorption measurements reveal as λ_{max} at around 260 nm, preferably in the visible range, whereby overlaps with the absorption spectrum of proteins (280 nm).²²⁶ The synthesis of fluorescent nucleoside analogues, which are sterically less bulky, but retain desired fluorescent properties, are valuable as fluorescent biological probes. The higher structural similarity to the natural nucleobases

to ensure the formation of W-C base pairs, the more valuable fluorescent nucleoside is. The shape, size, and hydrogen-bonding face all affect the modified fluorescence nucleoside. To be a suitable probe for the study of biological function, the fluorescent nucleoside analogues must have an easily observable emission ($\Phi_F > 1\%$) at physiological conditions: aqueous buffer, moderate salinity, and the pH range 6–8. Furthermore, the introduced fluorophore must absorb light at wavelengths away from proteins (280 nm) and nucleic acids (260 nm). It must possess a good fluorescence quantum yield ($\Phi > 0.1$) with the intrinsic fluorescence emission shifted away from tryptophan in proteins (300–350 nm). It is worth mentioning that the length and nature of the linker (usually alkyl chains) can also significantly affect the sensitivity of the probe for altering the nucleotide local environment.

4.1.3 Extinction coefficient and quantum yield

A number of key parameters are used to determine the fluorescence properties of the fluorescent analogues. The absorption maximum, λ_{\max} , is the wavelength of light where the greatest absorption occurs. It is determined by UV-vis spectroscopy. The extinction coefficient and quantum yield are two important properties of fluorophores, defining the effective brightness of the fluorophore. Extinction coefficients can be calculated using the Beer-Lambert Law (Figure 4.4). The Beer-Lambert law defines the relationship between the concentration of a solution and the amount of light absorbed by that solution:

$$A = \epsilon dC$$

Where:

A = Absorbance (optical density) at a particular wavelength ϵ = Molar

absorption coefficient ($\text{mol}^{-1} \text{dm}^{-3} \text{cm}^{-1}$)

d = Path length of the cuvette containing the sample (cm)

C = Concentration of the compound in the solution (mol dm^{-3})

Figure 4.4 Beer-Lambert Law.

ϵ is a measurement to understand the absorption at the λ_{\max} per mole of the fluorophore, for a given instrumental pathlength. Relatively, the wavelength of fluorescent of emission maxima, λ_{em} , is also measured. The difference between the λ_{\max} and λ_{em} in wavelength is known as the Stokes shift, the extent of which varies between fluorophores (quoted in cm^{-1}). The energy (wavelength) associated with emission is typically lower (higher) than the excitation light. The Stokes shift provides the

information of the fluorophore associated with the energy states of the excited and ground states of the chromophore. The quantum yield refers to the number of photons emitted relative to the number absorbed. The rate of radiative decay is much higher than the rate of non-radiative decay, therefore, the quantum yield might close to 1.0, and which also indicates that the fluorophore should exhibit strong emission. As the local chemical environment of the fluorophore affects it, the solvent conditions must be taken into consideration. The most reliable method for recording Φ_F is the comparative method,²²⁷ which is calculated in relation to other known (standard) fluorophores by using the following equation (Figure 4.5).

$$\Phi_X = \Phi_{ST} \left(\frac{Grad_x}{Grad_{ST}} \right) \left(\frac{\eta_X^2}{\eta_{ST}^2} \right)$$

Where:

ST = standard

X = test

Φ = fluorescence quantum yield

Grad = gradient from the plot of integrated fluorescence intensity vs absorbance

η = refractive index of solvent

Figure 4.5 Calculation of fluorescence quantum yields from acquired data.

In terms of the standard and test solution samples, with identical absorbance at the same excitation wavelength, can be expected to be absorbing the same number of photons. Hence, the ratio of the integrated fluorescence intensities of the two solutions, under identical conditions, can produce the ratio of the quantum yield values. It is important to use a wisely chosen concentration range and acquiring data at several different absorbance values, making sure a linearity across the concentration range. In order to minimise re-absorption effects (*i.e.* the inner filter effect),²²⁸ the concentration range should never exceed 0.1 abs at and above the excitation wavelength in a 10 mm fluorescence cuvette. This can avoid the presence of concentration effects, *e.g.* self-quenching. Applying a cross-calibration between a standard sample and test sample, ensuring both behave as expected, allows their Φ_F values to be used with confidence. This confirms the validity at using the standard sample and its quantum yield value.

As these 8-aryl-purine nucleosides were designed to be fluorophores, understanding their photophysical characteristics is of utmost importance. The full photophysical characterisation will be given, and the major properties and trends discussed. Ideally the compounds should have favourable absorption maxima (away from biomolecular absorption and emission bands) and possess high fluorescence quantum yields. It may be possible to link some of the trends to the structural parameters revealed by the conformational studies (*e.g.* NMR spectroscopic data, Chapter 3). The physical data will be used to judge the potential applications and determine trends within a given series/class.

4.2 UV-vis spectroscopy

Typically, a stock solution was prepared by dissolving 3.0 mg of C8 modified nucleosides in 3 ml of DMSO ($\sim 2 \times 10^{-3} \text{ mol dm}^{-3}$). Then a second stock solution was prepared, depending on the specific compound under study, to meet the range of required concentration. The λ_{max} values were obtained by measuring the UV-vis absorption spectrum for a given compound in a suitable solvent.

The UV-Vis spectra for five or six solutions at different concentrations were measured (all absorbance values were below 2 OD). These were performed in DMSO using accurate concentrations of the given compound under analysis. UV-vis spectroscopic analysis of the C8 modified nucleosides were recorded in DMSO over five concentrations between *ca.* 1×10^{-7} and 1×10^{-6} M at 20 °C. The UV-vis spectra were plotted (absorbance *vs.* wavelength) at different concentrations (Figure 4.5 and Figure 4.6). The molar absorption coefficients were obtained by plotting UV absorbance *vs.* analogue concentration, and calculated based on the Beer-Lambert law. DMSO was chosen for its good solvation to nucleosides at room temperature and to allow comparison with previously synthesised purine nucleosides.¹²⁰ Remarkably, at a higher concentration (*ca.* 1.0×10^{-3} M) in DMSO, nucleosides aggregate in solution and the intermolecular association becomes stable due to the hydrogen-bonding between purine bases.²²⁹ As a result, the properties of the chromophore may be changed relatively. The gradient of the graph corresponds to ϵ for a given compound. The spectroscopic analysis avoided noise from background and began from 270 nm to avoid the effect from solvent absorbance (at 268 nm for DMSO).²³⁰

Typically, C8 modified nucleosides exhibit a bathochromic shift: adenosine (260 nm),²³¹ guanosine (253 nm),²³² inosine (249 nm)²³³, uridine (263 nm),²³⁴ and phenylacetylene (233 nm)²³⁵ in MeOH. PhCCPhCC-(deoxy)adenosine exhibit absorbance maxima at (350 nm) 346 nm respectively (Figure 4.5). While PhCCPhCC-(deoxy)adenosine exhibits an absorbance maxima at 346 nm(**62**) and 358 nm(**63**), respectively (Figure 4.6).

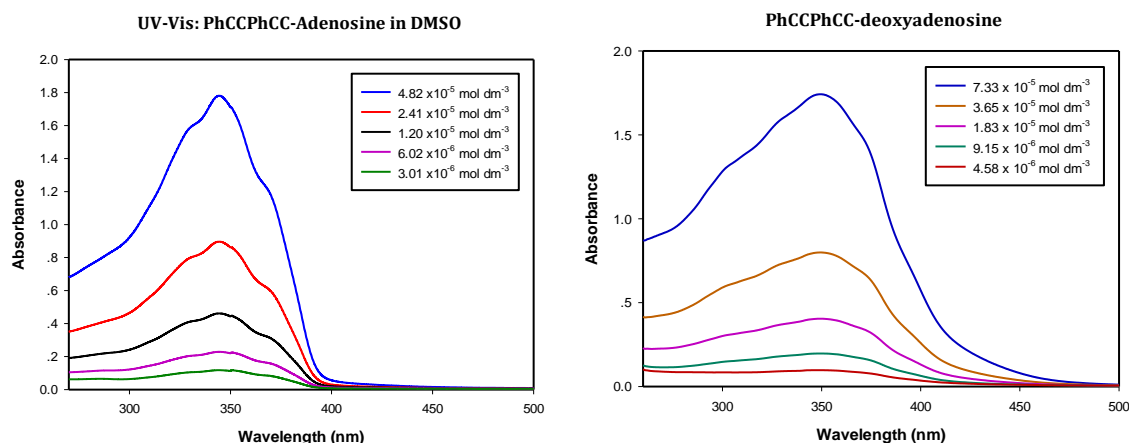


Figure 4.5 UV-vis spectra for varying concentrations of PhCCPhCC-(deoxy)adenosine **62(63)**, in DMSO at 20 °C.

PhCCPhCC-(deoxy)guanosine (**64** and **65**) both exhibited minor peaks on a shoulder (red arrow points to the main absorption peak, and the other arrows points to the minor absorption peaks) in the low energy region of the UV spectrum that is due to a hypsochromically shift with respect to the major peak (Figure 4.6). These two peaks arise from two different electronic transitions, most likely π - π^* and intramolecular charge transfer (ICT).^{236,237}

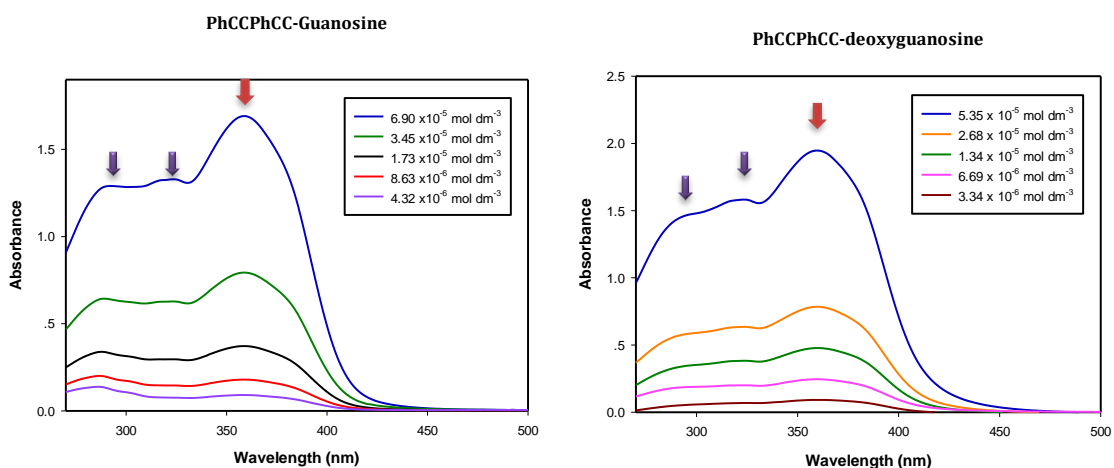


Figure 4.6 UV-vis spectra for varying concentrations of PhCCPhCC-(deoxy)guanosine, **64(65)**, in DMSO at 20 °C. The arrows show the absorption peaks.

The molar absorption coefficient for each analogue has been calculated from the absorbance and concentration based on the Beer-Lambert law (Figure 4.7). The results show a normal concentration for the absorbance measurement under 2 A.U.(Figure 4.7). This is also the case at

lower concentrations (Figure 4.7 inset) below 0.1 A.U., which were chosen to minimise inner filter effects.^{238,239} The spectra for C8-modified nucleosides analogues showed a linear decrease in absorption, with decreasing concentration indicating that aggregation of the nucleosides was unlikely at the concentrations tested. The molar absorption coefficient calculated from the absorbance and concentration (under 2 A.U.) was similar to that results at low concentration (under 0.1 A.U.).

PhCCPhCC-Guanosine in DMSO

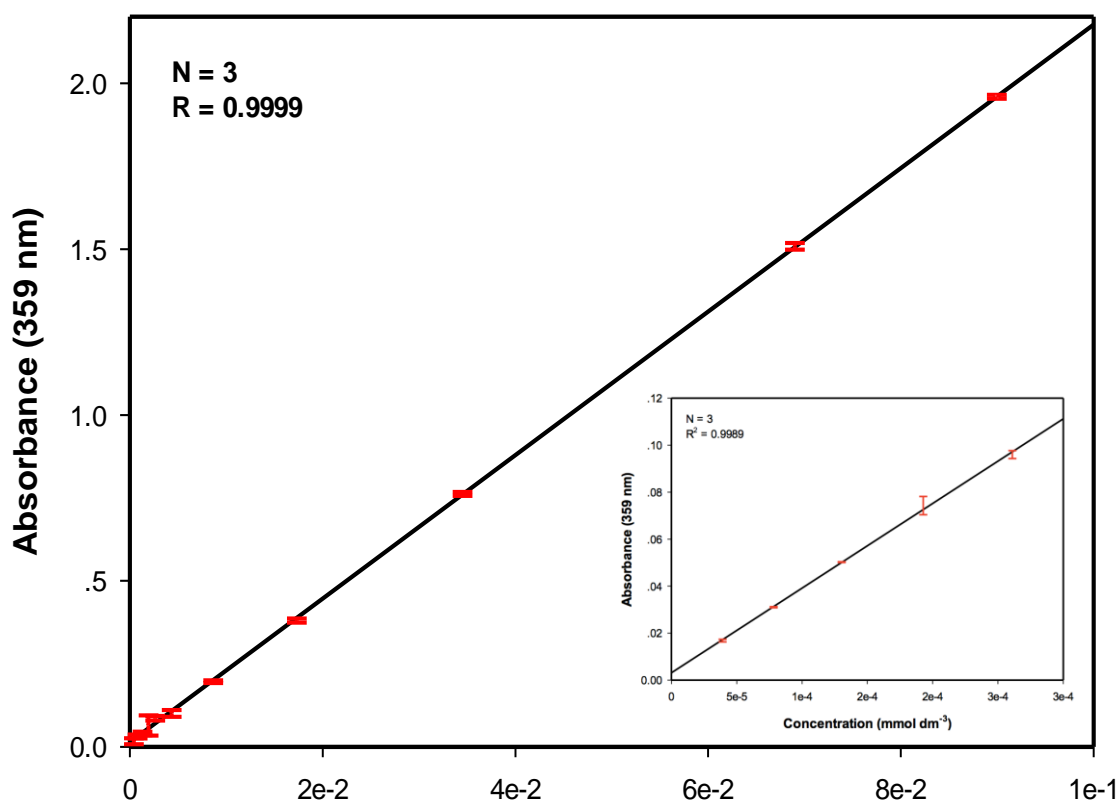


Figure 4.7 PhCCPhCC-guanosine **64** absorption concentration dependence (standard deviation of the mean is plotted).

4.3 Fluorescence spectroscopy

The fluorescence emission maxima, λ_{em} was determined using a fluorimeter, recorded in DMSO. The spectra were recorded at concentrations that gave a UV absorbance at or below 0.1 A.U., in order to minimise inner filter effects. The corrected fluorescence spectrum and the background are treated in the same way to obtain the emission value. The solvent background has been subtracted from the

entire fluorescence spectrum. All the measurements were repeated in triplicate and averaged. The variation in the wavelength of the λ_{em} of these nucleosides was much larger than the variation in λ_{max} . It may cause a huge variation in the Stokes shift value. In all cases, the instrument can only detect emission spectra, and is not able to show the excitation spectra.

The λ_{em} of guanosine analogues showed a red shift compared to adenosine analogues (Figure 4.8 and Figure 4.9). This indicated that the energy gap between the excited and ground states was smaller in guanosine analogues (lower energy) compared to the equivalent adenosine analogues (high energy). Inosine analogues showed a similar behaviour as guanosine analogues. Unlike the guanosine analogues, uridine and inosine analogues, showed blue shift.

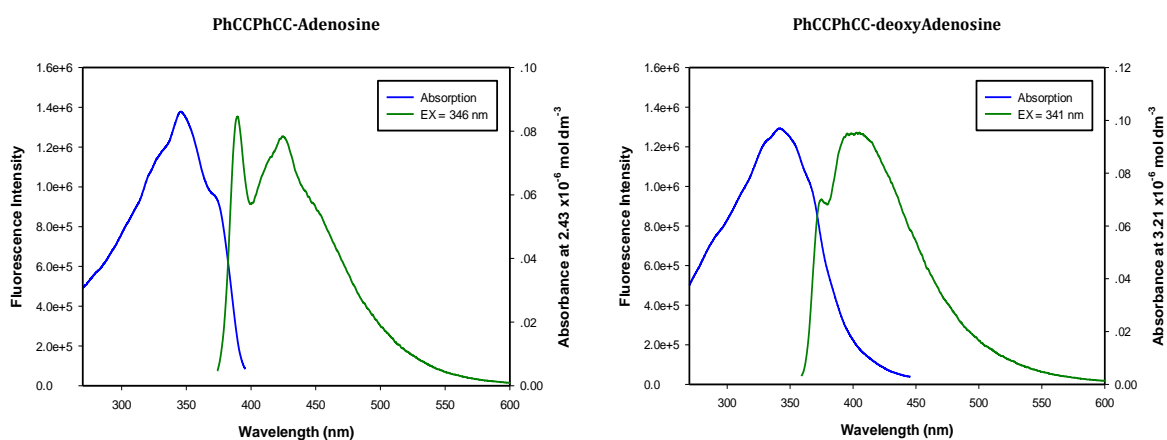


Figure 4.8 Absorption and emission spectra for PhCCPhCC-(deoxy)adenosine, **62(63)**, in DMSO at 20 °C.

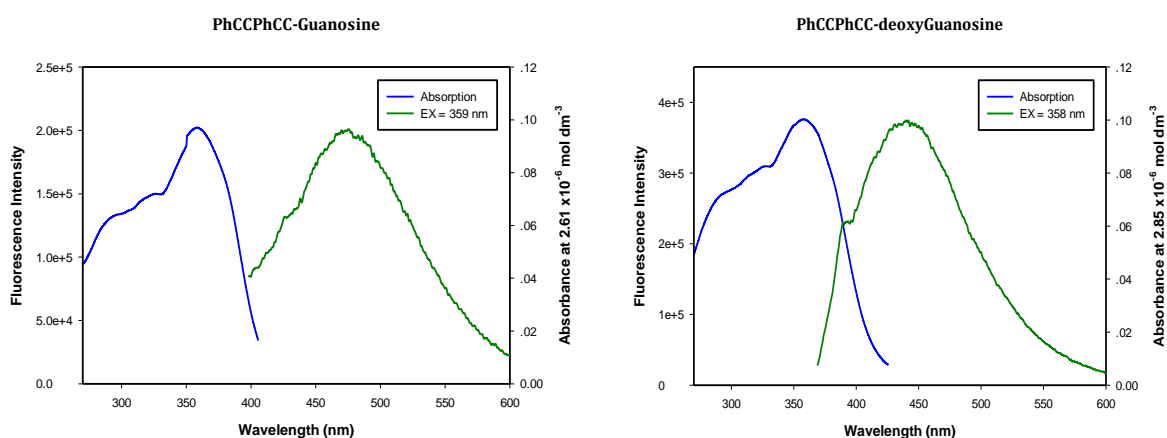


Figure 4.9 Absorption and emission spectra for PhCCPhCC-(deoxy)guanosine, **64(65)**, in DMSO at 20 °C.

UV-Vis experiments revealed that there is no concentration-dependent effect from the observation of linearity, due to its accuracy being less than 2. However, using the same concentrations for fluorescence excitation spectra, a concentration effect was observed, which could not be discerned

within the limits of detection for the instrument. Therefore, excitation spectra were recorded at varying concentrations between 2×10^{-6} - 2×10^{-7} M at 20 °C. The fluorescence excitation spectra were plotted (fluorescence intensity vs. wavelength) at different concentrations (Figure 4.10). Generally, the fluorescence emission spectra showed two maxima like the one shown in Figure 4.10. With one emission maxima in the region at ~ 370 nm (Peak 1) and one bathochromically shifted to ~ 450 nm (Peak 2).

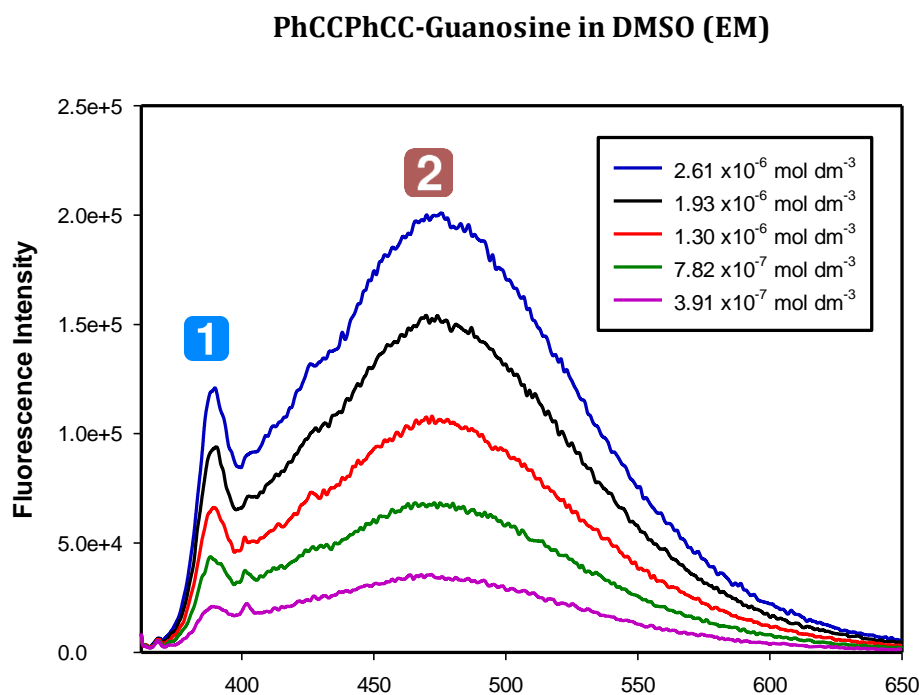


Figure 4.10 Concentration study of fluorescence excitation for PhCCPhCC-guanosine **64** in DMSO (emission = 476 nm).

Comparing λ_{\max} and λ_{em} of all the C8 modified compounds, (deoxy)guanosine analogues exhibit a longer absorbance wavelength than other analogues (Figure 4.11). While the inosine analogue appeared at a shorter absorbance wavelength.

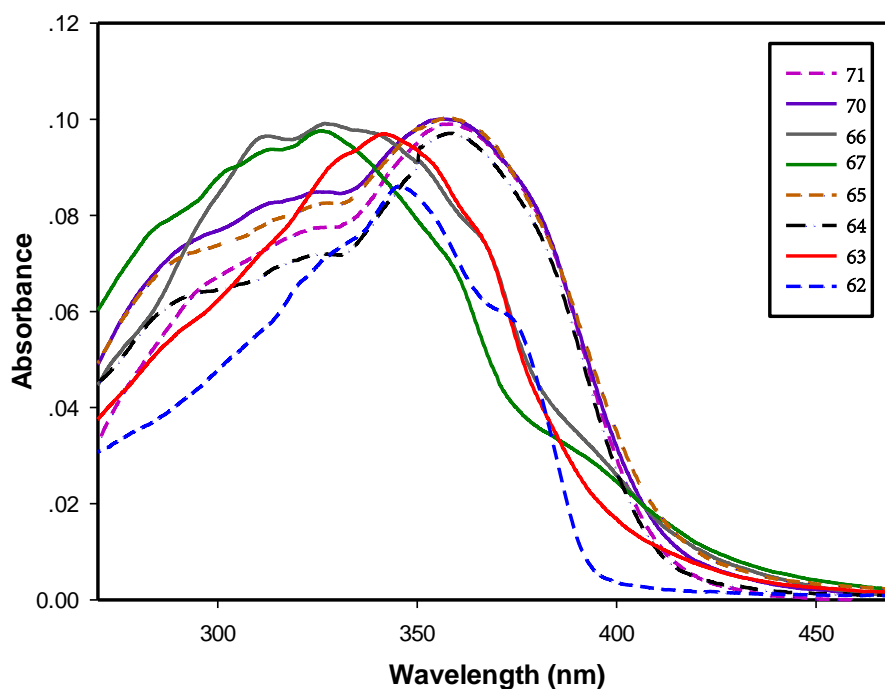


Figure 4.11 Absorption spectra of C8 modified nucleosides (approx. $C = 2.5 \times 10^{-6} \text{ M}$).

Comparing the λ_{em} of all the C8 modified nucleosides, although the (deoxy)guanosine appeared to possess a weaker fluorescence, the λ_{em} were longer emission wavelength than other analogues, especially for the PhCCPhCC-guanosine **64** compound (476 nm) (Figure 4.12). Fluorescence of PhCCPhCC-inosine **67** was almost as strong as the adenosine analogues and the emission wavelength

is also longer than the adenosine analogues. However, (deoxy)adenosine and deoxyuridine analogues showed strong fluorescence, with shorter emission wavelength.

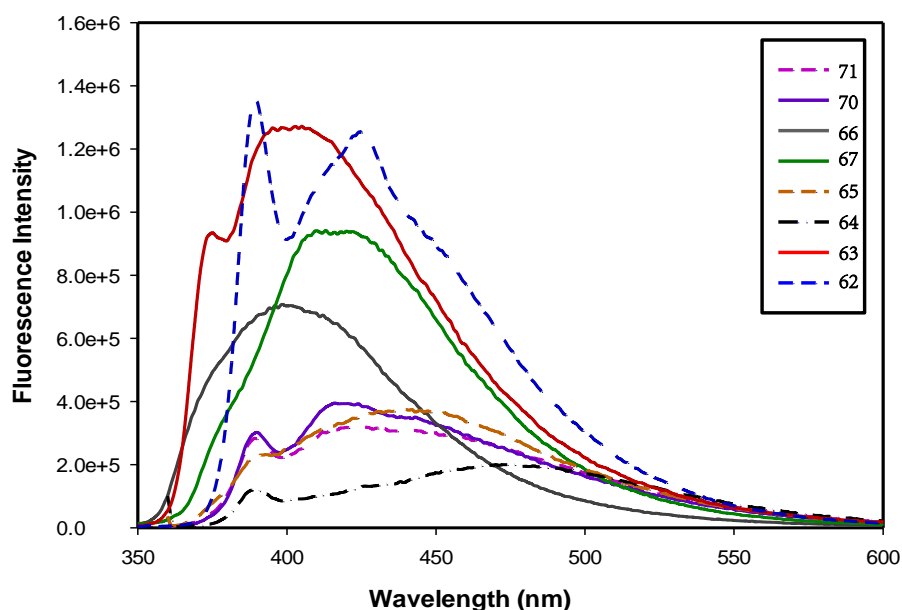


Figure 4.12 Emission spectra of C8 modified nucleosides (approx. $C = 2.5 \times 10^{-6} M$).

4.4 Photophysical characterisation of C-8 modified nucleosides

The synthesised C8 modified fluorescent analogues were analysed using UV-vis and fluorescence spectroscopy and their photophysical properties have been fully characterised. Important photophysical data are gathered in Table 4.1.

Table 4.1 Photophysical properties for 8-modified nucleosides.

Entry	Compound	Compound ID No.	λ_{max} (nm)	λ_{em} (nm)	$\epsilon / 10^4 M^{-1} cm^{-1}$	Standard Error ^a	Stokes shift (cm ⁻¹)
1	8-(Phenylethynyl)adenosine	47	321	392	2.19	0.0038	5642
2	8-(phenylethynyl)guanosine	46	330	429	5.77	0.0049	6993
3	PhCCPhCC-A	62	346	434	3.66	0.0021	5868
4	PhCCPhCC-G	64	358	476	2.18	0.0011	6024
5	PhCCPhCC-dA	63	350	462	2.34	0.0015	6926
6	PhCCPhCC-dG	65	358	445	3.64	0.0026	5461
7	PhCCPhCC-dU	66	326	411	4.08	0.0013	6344
8	PhCCPhCC-OG	70	357	448	4.48	0.0003	5690
9	PhCCPhCC-OdG	71	358	446	4.52	0.0018	5511
10	PhCCPhCC-I	67	327	415	3.72	0.0017	6485

^a Standard error was calculated by linear regression.

All of the C8 modified nucleosides showed that the UV absorption maxima were shifted away from the UV absorption bands of nucleic acids (260 nm) and proteins (280 nm). The C8-modified nucleoside analogues possess molar absorption coefficients of similar magnitude. They are also of high value (*ca.* $1 \times 10^4 \text{ mol}^{-1} \text{ dm}^3 \text{ cm}^{-1}$) suggesting they are effective chromophores. The λ_{max} observed for (deoxy)guanosine analogues were bathochromically shifted. The fluorescence for the (deoxy)guanosine analogues was much weaker than those observed for the (deoxy)adenosine analogues.

The novel modified purines showed longer absorption maxima than the phenylethynyl-modified purines (Entries 1-6). PhCCPhCC-guanosine appeared a the longest λ_{max} value and largest λ_{em} value (Entry 4). PhCCPhCC-dU **66** and inosine **67** showed a relatively short λ_{max} value and short λ_{em} (Entries 7 and 10). PhCCPhCC-deoxyadenosine appeared a largest Stokes shift (Entry 5). PhCCPhCC-(deoxy)guanosine analogues showed a relatively small Stokes shift compared to the other fluorescent nucleosides (Entries 4, 6, 8, 9).

4.5 Solvatochromism

Solvatochromism of fluorophores can provide information about the nature of the excited state and the electronic transitions.¹⁶⁴ When absorption spectra are investigated in solvents of different polarity, generally it is shown that not only the position but also the intensity of shape of the absorption band can vary, depending on the nature of the solvent. Solvatochromism is also utilised for biological applications, since a solvatochromic fluorescent probes can be used to assess the polarity of the local microenvironment. It is also important to determine how a fluorophore behaves in an aqueous environment. The solvatochromism of selected C8-modified nucleosides (PhCCPhCC-(deoxy)adenosine, PhCCPhCC-(deoxy)guanosine, and PhCCPhCC-inosine) was investigated by UV-Vis and fluorescent spectroscopy. In order to address applicability of these C8-modified nucleosides as fluorescent sensors, the effect of solvent polarity on fluorescence was studied. Solvents also influence fluorescence spectra due to the variety of solvation on the ground states and excited states.^{240,241} If the dipole moment of the excited state is greater than the dipole moment in the ground state, difference of solvation of these two states will appear. As a result, increasing the solvent polarity causes the increasing of the Stokes shift value. Furthermore, the excited state is usually stabilised by polar solvent, leading to a smaller energy gap between ground and excited states.

The UV-Vis spectral data revealed that the largest absorption λ_{max} values were obtained in DMF and DMSO. The reason is that these solvents are less polar, and the hypsochromically shift indicated the increased HOMO-LUMO energy gap. As the result, the dipole moment of the excited state in these two solvents is greater than the one in the ground state.^{240,241} The λ_{max} values were obtained in water were hypsochromically shifted compared to less polar solvents (MeOH, EtOH) for PhCCPhCC-(deoxy)guanosine.

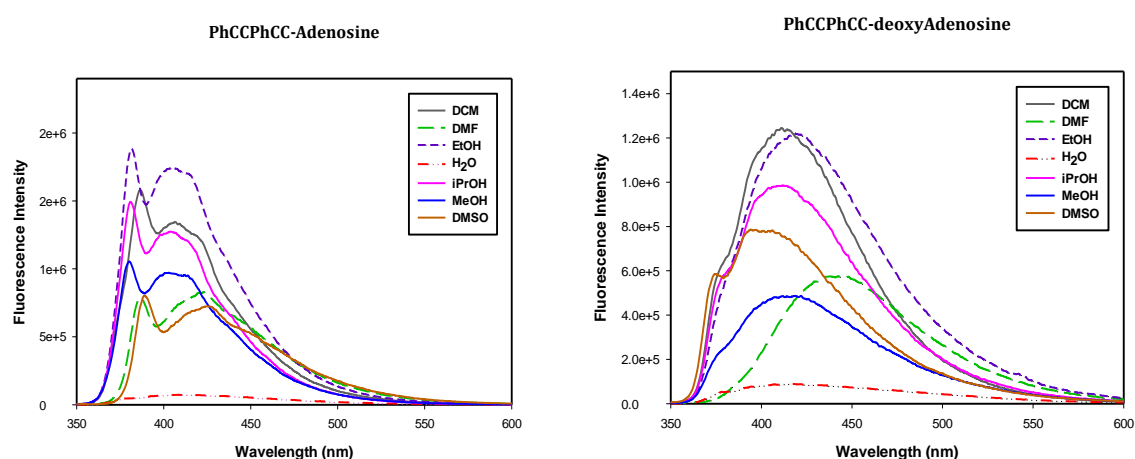


Figure 4.13 Solvatochromic effects on the fluorescence of PhCCPhCC-(deoxy)adenosine **62(63)** (1.5×10^{-6} M) at 20 °C.

Less polar solvents cannot be applied for these nucleosides due to their poor solubility. It was found that the guanosine analogues were more sensitive to solvatochromic property than equivalent analogues. From the data obtained (Figure 4.13, and 4.14), compounds were not fluorescent in water compared with the more non-polar solvents in all cases. EtOH and DCM obtained relatively high fluorescence in PhCCPhCC-(deoxy)adenosine analogues (Figure 4.13), while for PhCCPhCC-(deoxy)guanosine analogues, iPrOH and DCM obtained relatively high fluorescence (Figure 4.14). DMSO and DMF exhibit larger red shifts in all cases. A small bathochromic shift was observed from the emission maxima as the solvent polarity was increased (from DCM, 436 nm to H₂O, 461 nm) (PhCCPhCC-guansoine in Figure 4.14).

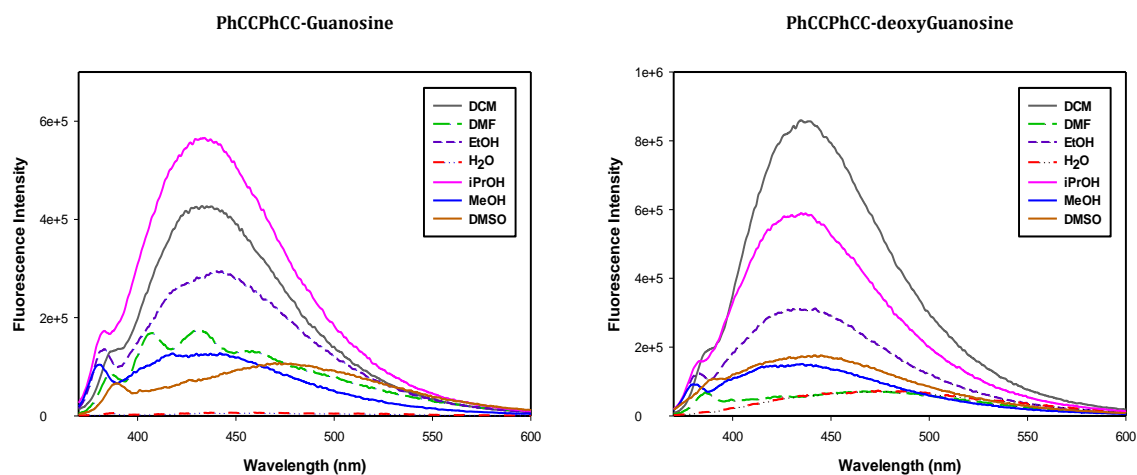


Figure 4.14 Solvatochromic effect on fluorescence of PhCCPhCC-(deoxy)guanosine (1.45×10^{-6} M) at 20 °C.

The quantum yields were firstly recorded from the UV-vis absorbance spectrum of the solvent background and sample solutions and record the fluorescence spectrum of the same solution in the 10 mm fluorescence cuvette. The experiments were repeated for five solutions with increasing concentrations of the selected sample. First, two standard compounds (quinine sulphate and anthracene, Figure 4.15) were cross-calibrated using the equation in Figure 4.5. This was achieved by calculating the quantum yield of each standard sample relative to one other. The standards were used to ensure the accuracy of the results obtained for the test samples. They were chosen because their absorption and emission wavelength are similar to test samples. Once the standard samples had been cross-calibrated and acceptable matches had been obtained, the quantum yield values for the test samples were calculated, using the same equation. The error associated with this method of quantum yield determination was previously estimated to be $\pm 10\%$.²⁴²

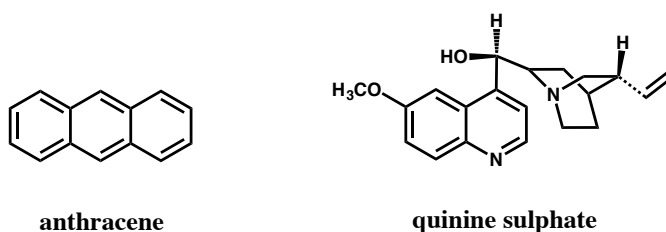


Figure 4.15 Anthracene and quinine sulphate – reference compounds.

The quantum yield can also be affected by the solvent polarity. The fluorescence λ_{em} obtained from all of the compounds were red shifted in polar solvents (DMSO and DMF), compared to more non-polar solvents (DCM) (Table 4.2). There are relatively small changes in the absorbance and emission maxima for these modified nucleosides as the solvent polarity changes. The biggest absorbance maximum varies between 335 nm (water) and 350 nm (DMSO), while the Stokes shift varies between 5876 cm^{-1} (water) and 6926 cm^{-1} (DMSO) for PhCCPhCCC-deoxyadenosine. Generally, in water,

the fluorescence emission was found to be very weak. The Stokes shifts calculated are shown in Table 4.3. The largest Stokes shift values were observed in water with a bathochromic shift.

Table 4.2 Solvent dependence of fluorescence emission for C8 modified nucleosides.

Entry	Compound	Compound ID No.	EtOH	^t PrOH	MeOH	DMF	H ₂ O	DCM	DMSO
			λ_{\max} (nm)	λ_{\max} (nm)	λ_{\max} (nm)	λ_{\max} (nm)	λ_{\max} (nm)	λ_{\max} (nm)	λ_{\max} (nm)
1	8-(phenylethynyl) adenosine	47	-	377 ^a	-	391 ^a	386 ^a	377 ^a	321
2	8-(phenylethynyl) guanosine	46	-	375 ^a	-	415 ^a	402 ^a	389 ^a	330
3	PhCCPhCC-A	62	340	340	339	343	334	341	346
4	PhCCPhCC-G	64	346	346	346	357	342	345	358
5	PhCCPhCC-dA	63	340	341	339	346	335	341	350
6	PhCCPhCC-dG	65	346	346	346	357	344	351	358
7	PhCCPhCC-I	67	323	325	323	311	316	326	327

^a Data taken from Andrew's Firth PhD thesis for comparison.²⁴³

Table 4.3 Stokes shifts for C8 modified nucleosides.

Entry	Compound	Compound ID No.	EtOH	^t PrOH	MeOH	DMF	H ₂ O	DCM	DMSO
			Stokes shift (cm ⁻¹)	Stokes shift (cm ⁻¹)	Stokes shift (cm ⁻¹)	Stokes shift (cm ⁻¹)	Stokes shift (cm ⁻¹)	Stokes shift (cm ⁻¹)	Stokes shift (cm ⁻¹)
1	8-(Phenylethynyl) adenosine	47	-	5221 ^a	-	5773 ^a	6042 ^a	5221 ^a	5642
2	8-(phenylethynyl) guanosine	46	-	4878 ^a	-	6207 ^a	6374 ^a	5157 ^a	6993
3	PhCCPhCC-A	62	3165	3165	3183	5514	6017	3486	5868
4	PhCCPhCC-G	64	6174	5860	6277	4863	7548	6050	6024
5	PhCCPhCC-dA	63	5488	5054	5802	6480	5870	5345	6926
6	PhCCPhCC-dG	65	6277	5913	5913	6644	8745	5607	5461
7	PhCCPhCC-I	67	5384	5062	5253	7764	6393	6044	6485

^a Data taken from Andrew's Firth PhD thesis for comparison.²⁴³

Table 4.4 Quantum yield of C8 modified nucleosides in different solvents.

Solvent	Compound	Compound ID No.	Quantum Yield ^A	Quantum Yield ^B	Quantum Yield ^{ave}
EtOH	PhCCPhCC-Adenosine	62	0.12	0.11	0.12
	PhCCPhCC-deoxyAdenosine	64	0.030	0.029	0.029
	PhCCPhCC-Guanosine	63	0.012	0.010	0.011
	PhCCPhCC-deoxyGuanosine	65	0.011	0.010	0.010
	PhCCPhCC-Inosine	67	0.031	0.029	0.030
^tPrOH	PhCCPhCC-Adenosine	62	0.12	0.11	0.12
	PhCCPhCC-deoxyAdenosine	64	0.060	0.052	0.056
	PhCCPhCC-Guanosine	63	0.024	0.021	0.022
	PhCCPhCC-deoxyGuanosine	65	0.036	0.031	0.033
	PhCCPhCC-Inosine	67	0.060	0.052	0.056
MeOH	PhCCPhCC-Adenosine	62	0.15	0.14	0.14
	PhCCPhCC-deoxyAdenosine	64	0.065	0.061	0.063
	PhCCPhCC-Guanosine	63	0.0072	0.0068	0.0070
	PhCCPhCC-deoxyGuanosine	65	0.0075	0.0071	0.0073
	PhCCPhCC-Inosine	67	0.072	0.068	0.070
DMF	PhCCPhCC-Adenosine	62	0.28	0.27	0.27
	PhCCPhCC-deoxyAdenosine	64	0.28	0.27	0.27
	PhCCPhCC-Guanosine	63	0.084	0.080	0.080
	PhCCPhCC-deoxyGuanosine	65	0.056	0.053	0.055
	PhCCPhCC-Inosine	67	0.17	0.16	0.16
H₂O	PhCCPhCC-Adenosine	62	0.069	0.067	0.068
	PhCCPhCC-deoxyAdenosine	64	0.035	0.033	0.034
	PhCCPhCC-Guanosine	63	0.028	0.027	0.027
	PhCCPhCC-deoxyGuanosine	65	0.027	0.026	0.027
	PhCCPhCC-Inosine	67	0.070	0.067	0.068
DCM	PhCCPhCC-Adenosine	62	0.30	0.30	0.30
	PhCCPhCC-deoxyAdenosine	64	0.30	0.30	0.30
	PhCCPhCC-Guanosine	63	0.11	0.10	0.11
	PhCCPhCC-deoxyGuanosine	65	0.12	0.12	0.12

PhCCPhCC-Inosine	67	0.15	0.15	0.15
------------------	----	------	------	------

A. Anthracene as standard; B. Quinine sulfate as standard.

Table 4.5 Effect on solvent on the fluorescence properties of PhCCPhCC-Adenosine.

Solvent	λ_{\max} (nm)	λ_{em} (nm)	$\epsilon/10^4 \text{ M}^{-1} \text{ cm}^{-1}$	Stokes shift (cm^{-1})	Φ	Solvent dielectric constant
EtOH	340	381	3.6	3165	0.1174	25.3
<i>i</i> PrOH	340	381	3.7	3165	0.1164	20.2
MeOH	339	380	3.6	3183	0.1399	33.0
DMF	343	423	3.5	5514	0.2724	38.3
H ₂ O	334	418	2.4	6017	0.0680	80.1
DCM	341	387	3.3	3486	0.2964	9.0
DMSO	346	434	3.6	5868	0.5113	47.2

Table 4.6 Effect on solvent on the fluorescence properties of PhCCPhCC-deoxyAdenosine

Solvent	λ_{\max} (nm)	λ_{em} (nm)	$\epsilon/10^4 \text{ M}^{-1} \text{ cm}^{-1}$	Stokes shift (cm^{-1})	Φ	Solvent dielectric constant
EtOH	340	418	3.0	5488	0.0294	25.3
<i>i</i> PrOH	341	412	3.0	5054	0.0558	20.2
MeOH	339	422	3.2	5802	0.0630	33.0
DMF	346	446	2.7	6480	0.2740	38.3
H ₂ O	335	417	2.2	5870	0.0340	80.1
DCM	341	387	2.6	5345	0.3008	9.0
DMSO	350	462	2.3	6926	0.5113	47.2

Table 4.7 Effect on solvent on the fluorescence properties of PhCCPhCC-Guanosine

Solvent	λ_{\max} (nm)	λ_{em} (nm)	$\epsilon/10^4 \text{ M}^{-1} \text{ cm}^{-1}$	Stokes shift (cm^{-1})	Φ	Solvent dielectric constant
EtOH	346	440	4.2	6174	0.0110	25.3
<i>i</i>PrOH	350	434	5.4	5530	0.0223	20.2
MeOH	346	442	4.8	6277	0.0070	33.0
DMF	357	432	3.9	4863	0.0816	38.3
H₂O	342	461	3.3	7548	0.0272	80.1
DCM	345	436	4.3	6050	0.1037	9.0
DMSO	358	476	3.2	6024	0.1171	47.2

Table 4.8 Effect on solvent on the fluorescence properties of PhCCPhCC-deoxyGuanosine

Solvent	λ_{\max} (nm)	λ_{em} (nm)	$\epsilon/10^4 \text{ M}^{-1} \text{ cm}^{-1}$	Stokes shift (cm^{-1})	Φ	Solvent dielectric constant
EtOH	346	442	5.3	6277	0.0104	25.3
<i>i</i>PrOH	350	435	5.2	5583	0.0334	20.2
MeOH	346	435	6.7	5913	0.0073	33.0
DMF	357	468	4.6	6644	0.0545	38.3
H₂O	350	492	3.7	8246	0.0269	80.1
DCM	351	437	4.0	5607	0.1202	9.0
DMSO	358	445	3.6	5461	0.1563	47.2

Table 4.9 Effect on solvent on the fluorescence properties of PhCCPhCC-Inosine.

Solvent	λ_{\max} (nm)	λ_{em} (nm)	$\epsilon/10^4 \text{ M}^{-1} \text{ cm}^{-1}$	Stokes shift (cm^{-1})	Φ	Solvent dielectric constant
EtOH	323	391	4.9	5384	0.0297	25.3
<i>i</i>PrOH	325	389	4.5	5062	0.0558	20.2
MeOH	323	389	4.2	5253	0.0700	33.0
DMF	311	410	4.4	7764	0.1635	38.3
H₂O	316	396	3.6	6393	0.0682	80.1
DCM	326	406	3.9	6044	0.1481	9.0
DMSO	327	415	3.7	6485	0.3018	47.2

From the above results, a large quantum yield for PhCCPhCC-adenosine was determined in DMSO. It had the lowest value in water, although a large Stokes shift was seen. Compared to adenosine, PhCCPhCC-deoxyadenosine was quite different – a large quantum yield and Stokes shift was seen in DMSO. The lowest quantum yield was recorded for ethanol. For PhCCPhCC-guansoine, a high Stokes shift and low quantum yield were found in water, whereas a large quantum yield was found in DMSO. Similar results were found for PhCCPhCC-deoxyguanosine. For the inosine derivative, the highest quantum yield was found in DMSO, whereas the lowest quantum yield was found in ethanol. The largest Stokes shift was found in DMF.

In summary, these nucleosides had low quantum yields (less than 2% in water), compared with the highest quantum yields showed for PhCCPhCC-(deoxy)adenosine (0.51) in DMSO. The slight change observed in different solvents may be due to the conformation of the nucleosides. Since the fluorescence of PhCCPhCC-(deoxy)adenosine was highly Solvatochromic. Thus, when the solvent polarity increases, the π - π^* level, which lies close to the n - π^* level, is lowered below the n - π^* level during the lifetime of the excited state by solvent relaxation. Thus, in polar solvents, the π - π^* state becomes a fluorescence-emitting state, and PhCCPhCC-(deoxy)adenosine showed strong fluorescence ($\Phi = 0.30$ in DCM).

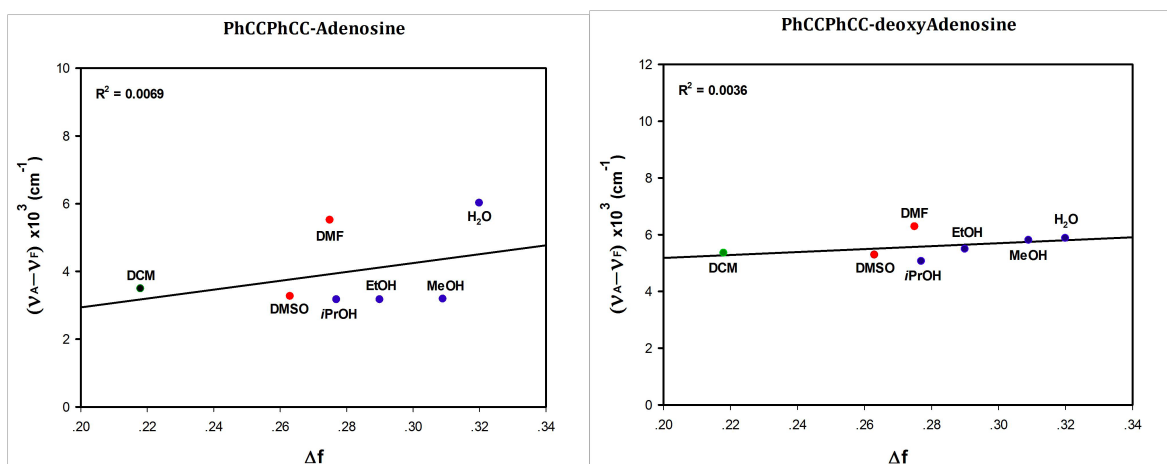


Figure 4.16 Lippert-Mataga plot for PhCCPhCC-(deoxy)adenosine.

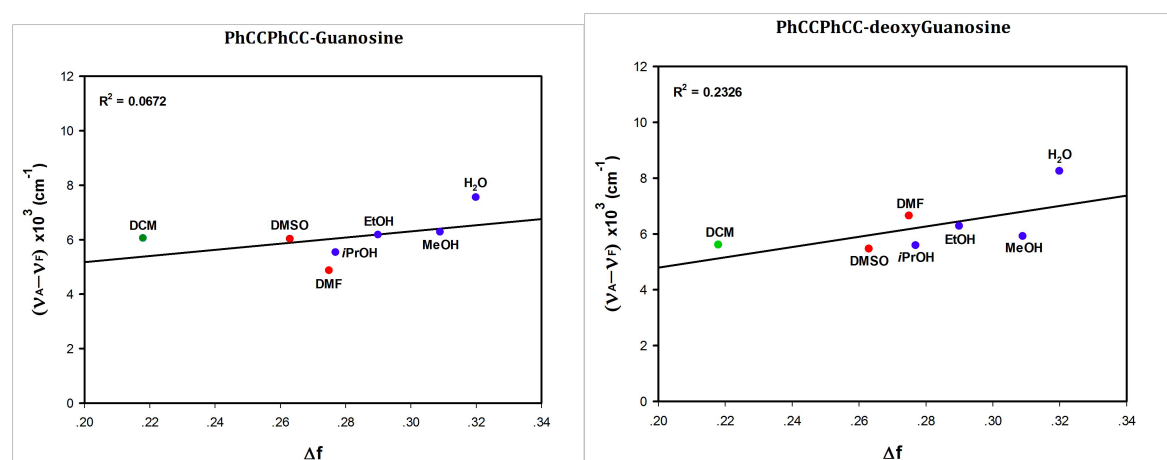


Figure 4.17 Lippert-Mataga plot for PhCCPhCC-(deoxy)guanosine.

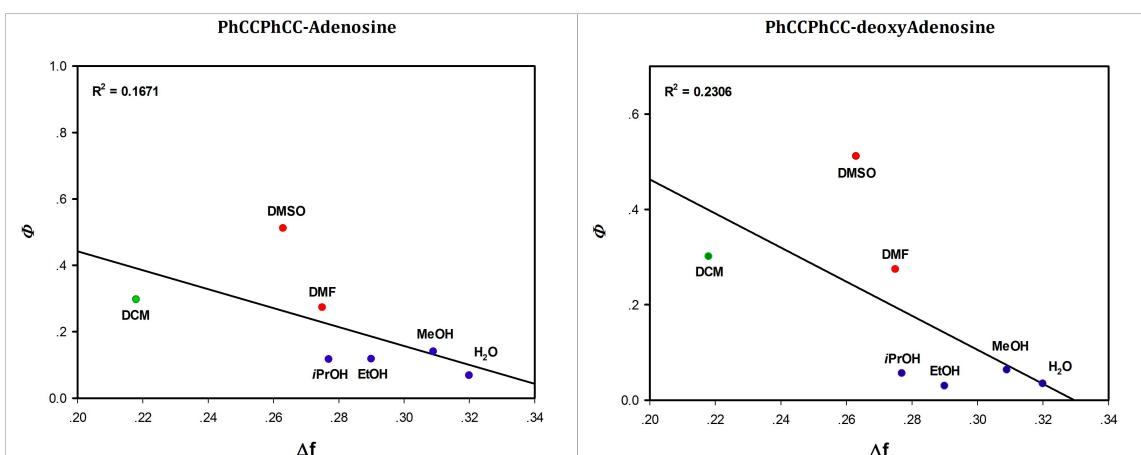


Figure 4.18 Attempted correlation between orientation polarizability (Δf) and quantum yield for PhCCPhCC-(deoxy)adenosine.

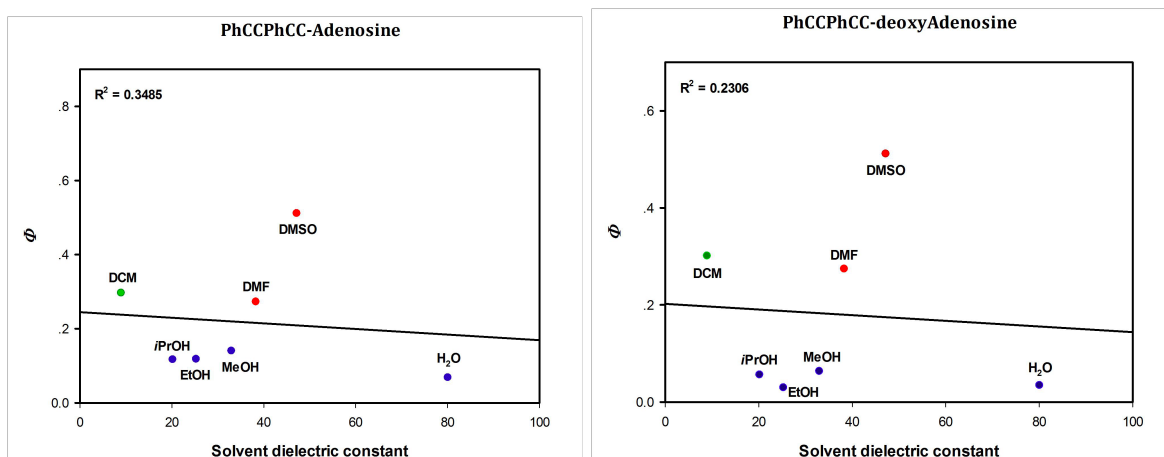


Figure 4.19 Attempted correlation between solvent dielectric and quantum yield for PhCCPhCC-(deoxy)adenosine.

Both the absorption and emission maxima vary slightly when the solvent was changed. When these changes in absorbance and emission maxima were plotted against solvent dielectric, there was no distinct correlation observed between ($\nu_A - \nu_F$) and the orientation polarizability (Δf) in a Lippert–Mataga plot (Figure 4.16 and 4.17), or quantum yield and Δf (Figure 4.18). The weak correlation was with quantum yield and solvent dielectric (Figure 4.19) for all the fluorescent analogues. There was no clear correlation between the absorbance wavelength and the solvent polarity, suggesting that the observed UV transitions are not due to ICT. Therefore, there may be other competing factors, such as preferential solvation of the ground or excited electronic states.^{244–246}

Solvent viscosity has also been investigated. Firstly, a photograph of solutions containing PhCCPhCC-Guanosine (5×10^{-5} M) dissolved in DMSO solution at 20 °C and 0 °C was taken using a UV transilluminator at 302 nm. Unfortunately, there was no visible increase in fluorescence at the lower temperature, *i.e.* where the local environment becomes more rigid. This suggested that PhCCPhCC-guanosine was not sensitive to local environment in DMSO and the formation of “PhCCPhCC-” motif did not slow down efficiency. DMSO was the only solvent that could fully dissolve the C8 modified nucleosides. For this solvent, the primary mechanism for decay from the excited state is not associated with solvent viscosity, thus for the compounds characterized here, rotational relaxation is not important.

4.6 Conclusion

- The spectroscopic properties of C8-modified nucleosides have been recorded.
- The UV-vis absorbance maxima and fluorescence emission maxima have been determined for the novel compounds, giving information about the Stokes shift, extinction coefficient, and quantum yield in each case.
- PhCCPhCC-guanosine revealed a large emission wavelength, and PhCCPhCC-(deoxy) adenosine analogues revealed a large Stokes shift value and quantum yield various solvents, including DMSO.
- Solvatochromism of the nucleosides has been also studied. It was found that the fluorescence emission was bathochromically shifted in polar solvents (DMSO and DMF).
- In DMSO, all the fluorescent compounds gave large quantum yields, especially PhCCPhCC-(deoxy) adenosine analogues. Large Stokes shift and characteristically low quantum yields were seen in water, which could be nevertheless useful in future biological studies.
- In DCM and *i*PrOH, the C8-modified fluorescent analogues exhibit strong emission.
- A poor correlation between the absorbance wavelength and the solvent polarity was determined, suggesting that the observed UV transitions are not primarily due to ICT.

4.7 Experimental

General Details

See previous Chapters for general synthesis details.

UV-Vis Spectroscopy

UV-Vis spectroscopy was performed on a JASCO V-560 spectrometer. The UV-Vis spectrophotometer was temperature controlled at 20 °C using a H₂O bath; spectra were recorded using matched quartz cuvettes (λ_{max} is reported). The UV-Vis spectra of 5 solutions at different concentrations were measured (all absorbance values were below 2 OD). The UV-Vis spectra were plotted for each analogue (absorbance *vs.* wavelength) at the different concentrations. The molar absorption coefficients were obtained by plotting UV absorbance *vs.* nucleosides analogue concentration, and applying the Beer-Lambert law. A baseline in the required solvent was carried out prior to starting an assay. The UV-Vis spectra were recorded for the sample within 1 h.

Fluorescence Excitation/Emission Spectra

Fluorescence excitation/emission spectra were recorded on a Jobin Yvon Fluoromax 3 spectrometer. The spectrometer was temperature controlled at 20 °C using a H₂O bath; spectra were recorded using matching quartz cuvettes. Fluorescence excitation and emission spectra were recorded at approximately $2 \times 10^{-4} \text{ mol dm}^{-3}$. The fluorescence excitation spectra were recorded with an emission wavelength set at 600 nm unless otherwise stated. The fluorescence excitation spectra usually displayed two wavelength maxima, which were subsequently used as the excitation wavelengths for the emission spectra. The fluorescence spectra were plotted for each analogue (fluorescence intensity *vs.* wavelength). Baselines were subtracted from the spectra.

Solvent Tests

UV-Vis spectra were recorded for analogues at $5 \times 10^{-5} \text{ mol dm}^{-3}$ in five or six different solvents. The UV-Vis spectra were plotted for each analogue (absorbance *vs.* wavelength) in the different solvents. Fluorescence emission spectra were recorded at a concentration of $5 \times 10^{-5} \text{ mol dm}^{-3}$. All fluorescence emission spectra were recorded using an excitation wavelength equal to the λ_{max} obtained from the UV-Vis spectrum. The fluorescence spectra were plotted for each analogue (fluorescence emission intensity *vs.* wavelength) in the different solvents.

Quantum Yields

The UV-Vis spectra of 5 solutions (in duplicate) were measured at different concentrations (all absorbance values were less than 0.1). The UV-Vis spectra were plotted for each analogue (absorbance vs. wavelength). All fluorescence emission spectra were recorded using an excitation wavelength equal to the λ_{max} obtained from the UV-Vis spectrum. The fluorescence spectra were plotted for each analogue (fluorescence emission intensity vs. wavelength). The area under the fluorescence spectra was measured at each concentration and plotted vs. absorbance. The gradient of the line fit to the data was used to calculate the quantum yield. For the standard compound, anthracene, was sonicated to get a better mixture for 30 min before its use.

Fluorescence Concentration Studies

Fluorescence excitation spectra were recorded for selected analogues at five or six different concentrations. All fluorescence excitation spectra were recorded using an emission wavelength equal to 500 nm (unless otherwise stated) and the excitation/emission monochromator slit widths set to 2 nm. The fluorescence emission spectra were plotted for each analogue (fluorescence emission intensity vs. wavelength). The intensity at λ_{max} (used λ_{max} at lowest concentration for all measurements) vs. concentration was plotted for each analogue.

Stock Solutions

DMSO stock solution

Stock solutions (A) for each analogue were prepared typically by dissolving 3.0 mg of analogue in 3 to 4 mL of DMSO. The solutions were stored in the dark at 20 °C.

DMSO and other solvents stock solution

Stock solutions for each analogue were prepared typically from 60 – 120 μL of the DMSO stock solution (A) in 3 ml of one of other solvents, making sure the sample concentration is no more than 5 % DMSO (v/v).

Parameters of Fluorometer and UV-vis spectrometer

JASCO V-560 spectrometer

Photometric: Abs. Response: Medium. Band Width: 1.0 nm. Scanning Speed: 400 nm/min. Start: 600 nm. End: 270 nm. Data Pitch: 0.5 nm

Jobin Yvon Fluoromax 3 spectrometer Emission Scan

Monochromator (1200 grooves/mm). Start Scan Initial wavelength: 270 nm. End Scan Final wavelength: 650 nm. Excitation λ = Variable. Increment = 0.5. Slits (bandpass): 2 nm. Detector (Signal S1). Integration time: 0.1 s. Units: CPS (counts per second). 3 scans averaged 20 °C.

Data Analysis

The data were baseline subtracted and downloaded into Excel. The fluorescence emission spectra were plotted in SigmaPlot 13.0 software.

CHAPTER 5

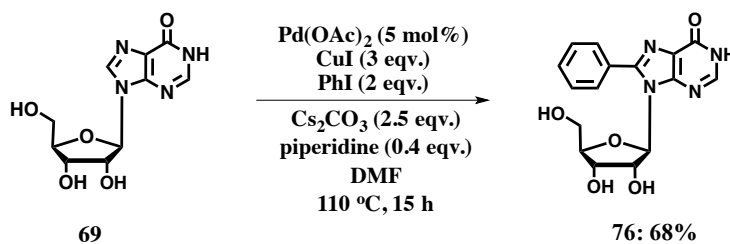
C-H DIRECT ARYLATION OF NUCLEOSIDES

5 C-H direct arylation of nucleosides

5.1 Introduction

Direct C–H bond arylation is one of the most efficient and useful methods for C–H bond activation.^{247,248} It has been used as an alternative methodology to classical cross-coupling reactions for aromatic and heteroaromatic compounds, which allows the potential for selective C-H bond functionalisation in nucleosides to be investigated.²⁴⁹

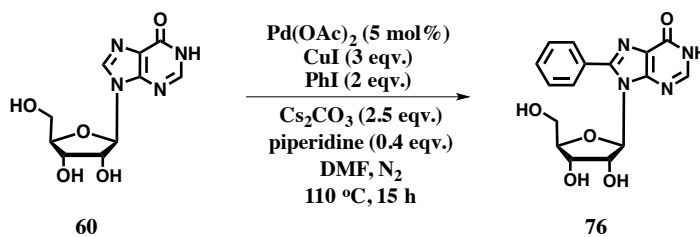
The motivation for the preliminary investigations of C-H bond direct arylation of nucleosides was a reported paper from Perez and co-workers.²⁵⁰ They proposed to apply the reaction conditions developed by Fairlamb¹²⁸ for adenosines to introduce a variety of differently substituted aryl groups at the 8-position of inosine (Scheme 5.1). However, only low conversion to the desired 8-aryl compound was detected, accompanied by difficulties to isolate the pure compound for biological testing. Therefore, there was a need to examine the C-H bond direct arylation protocol reported by Perez and co-workers (Scheme 5.1).²⁵⁰



Scheme 5.1 Synthesis of C-H bond direct arylation of inosine.

5.2 Direct arylation reactions of inosine

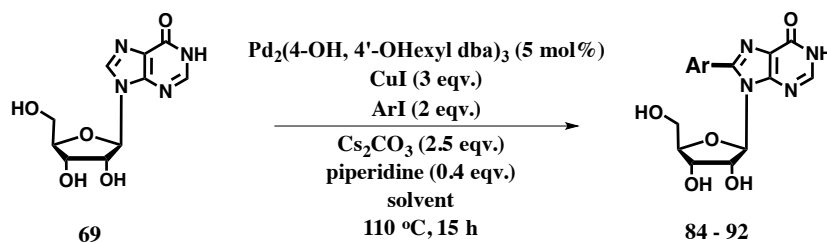
The first repeated reaction was C-H bond direct arylation with inosine using conditions similar to that from the Fairlamb group (5 mol% of Pd(OAc)₂, CuI), in the presence of Cs₂CO₃ and piperidine (as a dimethylamine mimic) in DMF at 110 °C for 15 h (Table 5.1, Entry 5). Whereas, under the same conditions *via* microwave under argon for 1 h, the yield dropped dramatically to 8% (Entry 6). Under argon atmosphere, similar results were obtained (Entry 7). Other Pd catalysts were tested at the same catalyst loading (5 mol%). The most efficient Pd catalyst was Pd₂(4-OH,4'-OHexyl-dba)₃, giving a 68% yield of **76**.

Table 5.1 Yields obtained for the direct arylation reaction of inosine using different Pd catalysts.

Entry	Pd catalysts	Isolated yield of 76 (%)
1	Pd ₂ (3-OH dba) ₃	19
2	Pd ₂ (4-OH dba) ₃	44
3	Pd ₂ (4-OH, 4'-OHexyl dba) ₃	68
4	Pd ₂ (4-OHexyl dba) ₃	17
5	Pd(OAc) ₂	57
6	Pd(OAc) ₂ (Microwave)	8
7	Pd(OAc) ₂ under Ar	59

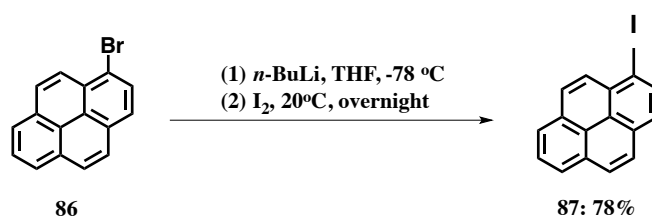
5.3 Substrate scope in the direct arylation reactions

With the optimised Pd catalyst for the direct arylation protocol applicable to inosine in hand, the substrate scope of a library of structurally diverse 8-arylinosine was evaluated, including *meta*- and *para*- substituted iodoarenes (Table 5.2). Unfortunately, only a few reactions worked under these reaction conditions. Electron-donating (Entries 1 and 2) substituents on the iodoarene, catalysed by Pd(OAc)₂, were well tolerated and coupled in modest yields under N₂ atmosphere. However, the same substituents catalysed by Pd₂(4-OH,4'-OHexyl-dba)₃ under N₂ atmosphere, gave similar yields compared to Pd(OAc)₂. Unfortunately, in PC solvent, the desired products could not be isolated. The solubility of inosine in PC may explain the origin of this problem. Only one of electron-withdrawing substituents on the iodoarene was tolerated (Entry 7). Others may be due to the steric hindrance around the metal centre impeding the reaction progress or the high sensitivity of these reactions to traces of air. A similar set of results was seen with the electron-donating substituents, with no reaction observed in PC solvent. It is worth mentioning that, the naphthyl substituent arylation worked for the reaction catalysed by Pd₂(4-OH,4'-OHexyl dba)₃. However, only a trace amount of product was isolated. All products were isolated using PrepTLC, following purification by chromatography on silica-gel.

Table 5.2 Substrate scope in the direct arylation of inosine using various aryl iodides.

Entry	Ar =	Compound ID number	$\text{Pd}(\text{OAc})_2$ in DMF under N_2 isolated yield (%)	$\text{Pd}(\text{OAc})_2$ in DMF under Ar isolated yield (%)	$\text{Pd}_2(4\text{-OH}, 4'\text{-OHexyl dba})_3$ in DMF under N_2 isolated yield (%)	$\text{Pd}_2(4\text{-OH}, 4'\text{-OHexyl dba})_3$ in PC isolated yield (%)
1		77	42	Trace	45	-
2		78	33	Trace	37	-
3		79	-	-	-	-
4		80	-	-	-	-
5		81	-	-	-	-
6		82	-	-	-	-
7		83	39	Trace	32	-
8		84	-	-	Trace	-
9		85	-	-	-	-

For Entry 9, the 1-iodopyrene substrate is not commercially available. Bromine-lithium exchange using *n*-BuLi and trapping with I_2 allowed the 1-iodopyrene to be prepared successfully (Scheme 5.2).²⁵¹



Scheme 5.2 Synthesis of 1-iodopyrene 87.

5.4 Conclusion

- The development of direct arylation conditions for the C8-arylation of unprotected inosine has been achieved in this study.
- The use of catalytic Pd(OAc)₂ and other [Pd⁰₂(dba-Z)₃] catalysts have been tested. For the limited number of reactions that were found to work well, Pd₂(4-OH, 4'-OHexyl-dba)₃ was the best catalyst, giving the highest yield of the product.
- The protocol was found to be effective with substituents (F and OMe) in DMF at 110 °C in N₂ atmosphere. Many other substituents were not tolerated under the reaction conditions tested as part of this study.

5.5 Experimental

General Details

Chemical reagents were purchased from Sigma Aldrich[®], Alfa Aesar[®], Acros[®] or Fluorochem[®] and used as received. Pd(OAc)₂ was purchased from Precious Metals Online. All reactions were carried out under a nitrogen atmosphere unless otherwise stated. Dry THF, CH₂Cl₂, hexane, toluene and acetonitrile were obtained from a Pure Solv MD-7 solvent system and stored under nitrogen. Dry methanol was obtained by drying over 3 Å molecular sieves. Ether and THF were degassed by bubbling nitrogen gas through the solvent during sonication. Dry pyridine, triethylamine and TMEDA were obtained by distillation from KOH and stored under nitrogen. Dry acetone and cyclohexane were obtained by distillation from CaH₂ and stored under nitrogen. Dry DMF and DMSO were obtained from Acros[®], DMF was degassed by N₂ bubbling while sonication; DMSO was used as received. Dry deuterated solvents were distilled (under static vacuum) from Na. Petroleum ether refers to the fraction of petroleum that is collected at 40 – 60 °C. Air sensitive procedures were performed using standard Schlenk line techniques. Nitrogen gas was oxygen free and dried immediately prior to use by passing through a column of sodium hydroxide pellets and silica. Reactions requiring anhydrous or air-free conditions but without using Schlenk line techniques were carried out in dry solvent under an argon or nitrogen atmosphere using oven- or flame-dried glassware. Where indicated, a Braun[®] Unilab glove (dry) box was used (<0.5 ppm O₂). Filtration was performed under gravity through fluted filter paper unless otherwise stated. Inorganic solutions used were prepared using deionized water. TLC analysis was carried out using Merck 5554 aluminium backed silica plates, and visualised using UV light at 254 and 365 nm. Retention factors (*R_f*) are reported along with the solvent system used in parenthesis. All column chromatography was carried out using Merck silica gel 60 (particle size 40-63 µm) purchased from Sigma Aldrich. Preparatory TLC was carried out using Analtech UNIPLATE glass-backed silica plates.

Nuclear Magnetic Resonance Spectroscopy (NMR Spectroscopy)

Proton (¹H), carbon (¹³C), phosphorus (³¹P) NMR spectra were recorded on a Jeol ECS400 and Bruker AV500/AV600/AV700 spectrometers. All chemical shifts in ¹H NMR spectra are reported in parts per million (ppm, δ) of tetramethylsilane using residual NMR solvent as an internal standard (CDCl₃: 7.26 ppm, DMSO-d₆: 2.50 ppm, MeOD-d₄: 3.31 ppm, CD₂Cl₂: 5.32 ppm). Multiplicities are described as singlet (s), doublet (d), triplet (t), quartet (q), multiplet (m), apparent (app.) and broad (br). ¹³C spectra were referenced to deuterated solvent. The spectra were processed in MestreNova[®] software and, where required, exported as JPEG images into the appropriate document. All chemical shifts in ¹³C NMR spectra are reported in ppm (δ) and are referenced to the NMR solvent (CDCl₃:

77.36 ppm, DMSO-d₆: 39.52 ppm, MeOD-d₄: 49.00 ppm, CD₂Cl₂: 53.49 ppm). Chemical shifts are reported in parts per million and were referenced to residual non-deuterated solvent. Coupling constants have been quoted to ± 0.2 Hz. ¹H NMR chemical shifts are given to 2 decimal places; ¹³C NMR chemical shifts are given to 1 decimal place. Spectra were typically recorded at 298 K. ³¹P spectra were externally referenced to H₃PO₄.

Mass Spectrometry (MS)

Mass spectrometry was performed using a Bruker daltronics micrOTOF spectrometer, an Agilent series 1200 LC, or a Thermo LCQ using electrospray ionization (ESI), with less than 5 ppm error for all HRMS. Liquid injection field desorption ionization (LIFDI) mass spectrometry was performed using a Wasters GCT Premier mass spectrometer. All data were acquired in positive ion mode using ESI or LIFDI ionisation. All LIFDI data reported is within 120 ppm error.

Infrared Spectroscopy (IR)

IR spectroscopy was carried out on Thermo-Nicolet Avatar-370 FT-IR spectrometer, or a PerkinElmer Spectrum Two spectrometer. Spectra were taken in either solid state (KBr disc), or in solution, thin film.

Melting Points (m.p.)

Melting points were obtained on a Stuart SMP3 machine. Experiments were run using a ramp rate of 3 °C min⁻¹ to the required melting temperature. The melting point was taken as the onset of the observed endothermic peak. The machine was calibrated using an indium standard.

Microwave

Microwave reactions were carried out in a CEM discovery labmate microwave with compressed air cooling.

Elemental Analysis

Elemental analysis was carried out using an Exeter Analytical CE-440 Elemental Analyser, with the percentages reported as an average of two runs.

General procedure for the direct arylation inosine using aryl iodide

To a vacuum-dried Schlenk tube was added inosine (0.0502 g, 0.1872 mmol, 1.0 eq), Cs₂CO₃ (0.153 g, 0.468 mmol, 2.5 eq), CuI (0.107 g, 0.561 mmol, 3.0 eq), Pd₂(dba-Z)₃ (0.005 mmol, 5 mol%) and the aryl iodide (0.0763 g, 0.374 mmol, 2.0 eq). The reaction vessel was evacuated under high vacuum at 25 °C with stirring, and then flushed with N₂ (three cycles). Dry distilled and degassed DMF (1 mL) or 'extra dry' DMF (Acros) was then added along with degassed piperidine (stored over 3Å molecular sieves, 7.4 µl, 0.75 mmol, 0.4 eq). The vessel was sealed and heated in an oil bath at 110 °C and stirred continuously for 15 h. The mixture was then allowed to cool to 25 °C and 1 M HCl solution (1 mL) was added. The pH was then adjusted to 6.5 with 1M NaOH and the aqueous solution was extracted with a *i*PrOH: EtOAc (1:9, v/v, 5 × 50 mL) mixture, by decanting from the reaction mixture. The organic extracts were combined, dried (MgSO₄), filtered and concentrated *in vacuo* to yield a thick gum, which was dried under high vacuum (ca. 0.8 mmHg). The crude mixture was re-dissolved/suspended in MeOH:CH₂Cl₂ (1:1, 20 mL) and adsorbed onto silica-gel (approximately 0.5 g) then concentrated *in vacuo*. A short silica-gel column (approximately 10 g) was eluted using MeOH: CH₂Cl₂ (2:98 v/v, moving in stepwise increments to 10:90 by gradient elution). The fractions containing the product were combined and the solvents were removed *in vacuo*, CH₂Cl₂ (10 ml) was added and then removed. The isolated product was then dried under high vacuum.

General procedure for the substrate scope in the direct arylation of inosine catalysed by Pd(OAc)₂

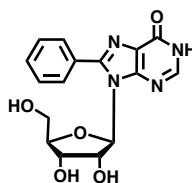
To a vacuum dried Schlenk tube was added inosine (0.1004 g, 0.3744 mmol, 1.0 eq), Cs₂CO₃ (0.306 g, 0.936 mmol, 2.5 eq), CuI (0.214 g, 1.122 mmol, 3.0 eq), Pd(OAc)₂ (0.004 g, 5 mol%) and the aryl iodide (0.748 mmol, 2.0 eq). The reaction vessel was evacuated under high vacuum at 25 °C with stirring, and then flushed with N₂ (three cycles). Dry distilled and degassed DMF (2 mL) or 'extra dry' DMF (Acros) was then added. The vessel was sealed and heated in an oil bath at 110 °C and stirred continuously for 15 h. The mixture was then allowed to cool to 25 °C and 1M HCl solution (2 mL) was added. The pH was then adjusted to 6.5 with 1 M NaOH and the aqueous solution was extracted with a *i*PrOH: EtOAc (1:9, v/v, 5 × 50 mL) mixture, by decanting from the reaction mixture. The organic extracts were combined, dried (MgSO₄), filtered and concentrated *in vacuo* to yield a thick gum, which was dried under high vacuum (ca. 0.8 mmHg). The crude mixture was re-dissolved/suspended in MeOH:CH₂Cl₂ (1:1, 20 mL) and adsorbed onto silica-gel (approximately 0.5 g) and concentrated *in vacuo*. A short silica-gel column (approximately 10 g) was eluted using MeOH: CH₂Cl₂ (2:98 v/v, moving in stepwise increments to 10:90 by gradient elution). The fractions

containing the product were combined and the solvents removed *in vacuo*, CH₂Cl₂ (10 ml) was added and then removed. The isolated product was then dried under high vacuum.

General procedure for the substrate scope in the direct arylation of inosine catalysed by Pd₂(4-OH, 4'-OHexyl dba)₃

To a vacuum dried Schlenk tube was added inosine (0.1004 g, 0.3744 mmol, 1.0 eq), Cs₂CO₃ (0.306 g, 0.936 mmol, 2.5 eq), CuI (0.214 g, 1.122 mmol, 3.0 eq), Pd₂(4-OH, 4'-OHexyl dba)₃ (0.0132 g, 5 mol%) and the aryl iodide (0.748 mmol, 2.0 eq). The reaction vessel was evacuated under high vacuum at 25 °C with stirring, and then flushed with N₂ (three cycles). Dry distilled and degassed DMF (2 mL) or 'extra dry' DMF (Acros) was then added. The vessel was sealed and heated in an oil bath at 110 °C and stirred continuously for 15 h. The mixture was then allowed to cool to 25 °C and 1 M HCl solution (2 mL) was added. The pH was then adjusted to 6.5 with 1M NaOH and the aqueous solution was extracted with a *i*PrOH: EtOAc (1:9, v/v, 5 × 50 mL) mixture, by decanting from the reaction mixture. The organic extracts were combined, dried (MgSO₄), filtered and concentrated *in vacuo* to yield a thick gum, which was dried under high vacuum (ca. 0.8 mmHg). The crude mixture was re-dissolved/suspended in MeOH:CH₂Cl₂ (1:1, 20 mL) and adsorbed onto silica-gel (approximately 0.5 g) and concentrated *in vacuo*. A short silica-gel column (approximately 10 g) was eluted using MeOH: CH₂Cl₂ (2:98 v/v, moving in stepwise increments to 10:90 by gradient elution). The fractions containing the product were combined and the solvents removed *in vacuo*, CH₂Cl₂ (10 ml) was added and then removed. The isolated product was then dried under high vacuum.

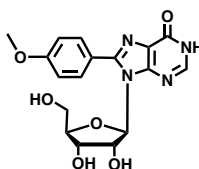
9-((2*R*,3*R*,4*S*,5*R*)-3,4-Dihydroxy-5-(hydroxymethyl)tetrahydrofuran-2-yl)-8-phenyl-1,9-dihydro-6*H*-purin-6-one, 76



TLC R_f 0.45 (30% MeOH/DCM); MP 160–162 °C (dec.); ¹H NMR (400 MHz, DMSO-*d*₆, 20 °C) δ 12.58 (br s, 1H; NH), 8.15 (s, 1H; C2-H), 7.76-7.71 (m, 2H, H-2''), 7.68-7.59 (m, 3H, H-3''), 5.74 (d, 1H, *J* = 6.3; C1'-H), 5.53-5.46 (m, 1H, C2'-OH), 5.22-5.16 (m, 1H; C3'-OH), 5.15-5.09 (m, 1H, C2'-H), 5.07-5.03 (m, 1H; C5'-OH), 4.17-4.12 (m, 1H; C3'-H), 3.98-3.92 (m, 1H; C4'-H), 3.79-3.74 (m, 1H; C5'-H₁), 3.65-3.61 (m, 1H; C5'-H₂); ¹³C NMR (100 MHz, DMSO-*d*₆, 20 °C) δ: 157.7, 149.5, 148.8, 146.6, 130.3, 129.4, 129.3, 128.9, 124.9, 89.5, 87.2, 71.1, 70.6, 61.9; ESI-MS *m/z* 213 (100),

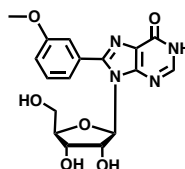
345[MH⁺](50); ESI-HRMS *m/z* 345.1198 [M+H] (calc. for C₁₆H₁₇N₄O₅ = 345.1193); IR (DMSO Solution): 3360, 3325, 2943, 1686, 1635, 1523, 1330, 980, 835 cm⁻¹.

9-((2*R*,3*R*,4*S*,5*R*)-3,4-Dihydroxy-5-(hydroxymethyl)tetrahydrofuran-2-yl)-8-(4-methoxyphenyl)-1,9-dihydro-6*H*-purin-6-one, 77



TLC Rf 0.40 (30% MeOH/DCM); MP 138–141 °C (dec.); ¹H NMR (400 MHz, DMSO-*d*₆, 20 °C) δ 8.07 (s, 1H; C2-H), 7.66 (d, *J* = 8.7 Hz, 2H, H-2''), 7.13 (d, *J* = 8.7 Hz, 2H, H-3'), 5.74 (d, 1H, *J* = 6.80; C1'-H), 5.47 (br s, 1H, C2'-OH), 5.23-5.18 (m, 1H; C3'-OH), 5.10 (dd, *J* = 6.0, 6.0 Hz, 1H, C2'-H), 5.05-5.01 (m, 1H; C5'-OH), 4.19-4.12 (m, 1H; C3'-H), 3.97-3.89 (m, 1H; C4'-H), 3.85 (s, 3H, OCH₃), 3.72-3.67 (m, 1H; C5'-H₁), 3.58-3.51 (m, 1H; C5'-H₂); ¹³C NMR (100 MHz, DMSO-*d*₆, 20 °C) δ: 162.0, 159.2, 151.3, 150.7, 148.4, 132.1, 126.8, 123.3, 115.4, 90.2, 87.9, 72.7, 72.3, 63.6, 56.8; ESI-MS *m/z* 192(100), 397[MNa⁺](20); ESI-HRMS *m/z* 397.1125 [M+Na] (calc. for C₁₇H₁₈N₄NaO₆ = 397.1119); Elemental Analysis (CHN) C: 54.47% H: 5.12% N: 14.77 (Calculated: C: 54.54% H: 4.85%; N, 14.97%); IR (DMSO Solution): 3350, 3325, 2943, 1636, 1529, 1330, 978, 836 cm⁻¹.

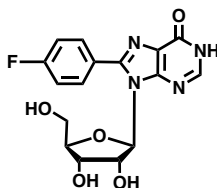
9-((2*R*,3*R*,4*S*,5*R*)-3,4-Dihydroxy-5-(hydroxymethyl)tetrahydrofuran-2-yl)-8-(3-methoxyphenyl)-1,9-dihydro-6*H*-purin-6-one, 78



TLC Rf 0.40 (30% MeOH/DCM); MP 207–209 °C (dec.); ¹H NMR (400 MHz, DMSO-*d*₆, 20 °C) δ 8.16 (s, 1H; C2-H), 7.55-7.49 (m, 1H, H-5''), 7.36-7.28 (m, 2H, H-2'', H-6''), 7.12 (d, *J* = 8.3 Hz, 1H, H-4''), 5.79 (d, 1H, *J* = 6.80; C1'-H), 5.54-5.48 (m, 1H, C2'-OH), 5.26-5.19 (m, 1H; C3'-OH), 5.14-5.08 (m, 1H, C2'-H), 5.06-5.01 (m, 1H; C5'-OH), 4.18-4.14 (m, 1H; C3'-H), 3.94-3.89 (m, 1H; C4'-H), 3.84 (s, 3H, OCH₃), 3.67-3.62 (m, 1H; C5'-H₁), 3.59-3.53 (m, 1H; C5'-H₂); ¹³C NMR (100 MHz, DMSO-*d*₆, 20 °C) δ: 160.4, 157.8, 151.8, 150.3, 147.2, 131.7, 131.4, 126.5, 123.1, 117.9, 116.4,

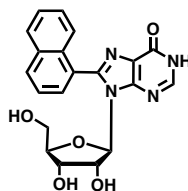
90.3, 87.5, 72.0, 71.8, 63.4, 56.7; ESI-MS m/z 192(100), 397[MNa⁺](30); ESI-HRMS m/z 397.1118 [M+Na] (calc. for C₁₇H₁₈N₄NaO₆ = 397.1119); IR (DMSO Solution): 3350, 3327, 2946, 1633, 1527, 1333, 978, 836 cm⁻¹.

9-((2*R*,3*R*,4*S*,5*R*)-3,4-Dihydroxy-5-(hydroxymethyl)tetrahydrofuran-2-yl)-8-(4-fluorophenyl)-1,9-dihydro-6*H*-purin-6-one, 79



TLC Rf 0.35 (30% MeOH/DCM); MP 196–198 °C (dec.); ¹H NMR (400 MHz, DMSO-*d*₆, 20 °C) δ 8.17 (s, 1H; C2-H), 7.72 (d, *J* = 8.7, 2H; H-2''), 7.34 (d, *J* = 8.7, 2H; H-3''), 5.73 (d, 1H, *J* = 6.3; C1'-H), 5.51-4.46 (m, 1H, C2'-OH), 5.22-5.18 (m, 1H; C3'-OH), 5.14-5.11 (m, 1H, C2'-H), 5.07-5.01 (m, 1H; C5'-OH), 4.18-4.13 (m, 1H; C3'-H), 3.97-3.92 (m, 1H; C4'-H), 3.81-3.76 (m, 1H; C5'-H₁), 3.66-3.59 (m, 1H; C5'-H₂); ¹³C NMR (100 MHz, DMSO-*d*₆, 20 °C) δ: 161.27, 152.1, 149.3, 146.9, 131.5, 130.7, 130.0, 129.7, 125.2, 89.9, 88.2, 72.6, 71.1, 62.1; ESI-MS m/z 136(100), 180(80), 385[MNa⁺](20); ESI-HRMS m/z 385.0921 [M+Na] (calc. for C₁₆H₁₅FN₄NaO₅ = 385.0919); IR (DMSO Solution): 3355, 2936, 1684, 1631, 1524, 1331, 982, 836 cm⁻¹.

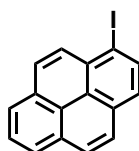
9-((2*R*,3*R*,4*S*,5*R*)-3,4-Dihydroxy-5-(hydroxymethyl)tetrahydrofuran-2-yl)-8-(naphthalen-1-yl)-1,9-dihydro-6*H*-purin-6-one, 84



TLC Rf 0.30 (25% MeOH/DCM); MP 189-191 °C (dec.); ¹H NMR (400 MHz, DMSO-*d*₆, 20 °C) δ 8.24-8.19 (m, 1H; ArH), 8.14-8.07 (m, 1H; C2-H), 7.85-7.34 (m, 6H; ArH), 5.81-5.76 (m, 1H; C1'-H), 5.48-5.41 (m, 1H, C2'-OH), 5.07-5.01 (m, 1H; C2'-H), 4.67-4.02 (m, 1H; C5'-OH), 4.23-4.16 (m, 1H; C3'-H), 4.03-3.97 (m, 1H; C4'-H), 3.78-3.72 (m, 1H; C5'-H₁), 3.67-3.59 (m, 1H; C5'-H₂); ¹³C NMR (100 MHz, DMSO-*d*₆, 20 °C) δ: 156.7, 152.4, 151.8, 148.2, 145.1, 138.1, 137.8, 128.0,

127.9, 125.9, 124.5, 123.2, 117.4, 88.8, 86.9, 74.1, 70.2, 61.0; ESI-MS m/z 183(100), 417[MNa⁺](30); ESI-HRMS m/z 417.1321 [M+Na] (calc. for C₂₀H₁₈N₄NaO₅ = 417.1324); IR (DMSO Solution): 3352, 3309, 3027, 2942, 1592, 1480, 1425, 1313, 1250, 1176, 1006, 972, 835 cm⁻¹.

1-Iodopyrene, 87²⁵¹



1-Bromopyrene (0.4 g, 1.423 mmol, 1 eqv.) was dissolved in dry THF 5 ml) and cooled to -78 °C under an argon atmosphere. *N*-Butyllithium (1.6 M in *n*-hexane; 1.1 ml; 1.71 mmol, 1.2 eqv.) was added dropwise. After 15 minutes a solution of I₂ (0.544 g; 2.14 mmol, 1.5 eqv.) in dry THF (2 ml) was added and reaction mixture was allowed to warm to room temperature overnight. For the workup the reaction mixture was concentrated *in vacuo*. H₂O (15 ml) was added to the residue and it was extracted with DCM (3×20 ml). The combined organic phases were washed with saturated sodium thiosulfate solution and H₂O. After drying over MgSO₄ and concentration under reduced pressure, the crude product was purified by column chromatography. Eluent for column chromatography: *n*-hexane/EtOAc, 50:1. Yield: 0.311 g (78 %); light yellow solid after recrystallization from MeCN to afford the pure white product.

TLC Rf 0.60 (25% EtOAc/Pet. ether, *v/v*); MP 85-87 °C; ¹H NMR (400 MHz, CDCl₃, 20 °C) δ 8.55-8.48 (m, 1H; Ar-H), 8.33-8.01 (m, 7H; Ar-H), 7.93-7.85 (m, 1H; Ar-H); ¹³C NMR (100 MHz, CDCl₃, 20 °C) δ: 137.1, 132.9, 131.8, 131.2, 131.1, 131.0, 129.8, 128.5, 127.6, 126.9, 126.4, 126.1, 125.7, 125.6, 124.9, 96.8; ESI-MS m/z 328[MH⁺](100); ESI-HRMS m/z 328.9751 [M+H] (calc. for C₁₆H₁₀I = 328.9754); IR (DMSO Solution): 3027, 1584, 1481, 1450, 1425, 1311, 1240, 1202, 1176, 1078, 1007, 963, 836, 812 cm⁻¹.

CHAPTER 6

CONCLUSIONS AND FUTURE WORK

6 Conclusions and Future Work

6.1 General Discussion

The main aim concerning the synthesis of a library of fluorescent C8-modified nucleosides, using newly developed Pd catalysts via a Sonogashira cross-coupling protocol, has been achieved. The activity of the Pd catalysts against both Sonogashira of 8-bromoguanosine/adenosine with terminal alkynes, under optimised conditions, was evaluated. Photophysical characterisation of the C8-modified nucleosides indicated that they were suitable for use as potential fluorescent probes in a biological context. The Heck cross-coupling reactions of suitably halogenated pyrimidine nucleosides have been successfully carried out, showing the versatility of the new Pd catalysts developed as part of this project.

6.2 Synthesis of Pd catalysts for 8-modified fluorescent nucleosides

Dbz ligands containing hydroxylated and alkyloxy moieties have been synthesised *via* Claisen-Schmidt condensation (under basic or acidic conditions) in good to high yields. Under basic conditions, it was found that addition of solid dry ice to adjust the pH of the hydroxylated dbz compounds enabled product yields to be increased. Under normal basic conditions yields were poor, indeed interesting colour differences were seen for the deprotonated phenolic dbz derivatives due to extended π -conjugation.

Novel Pd complexes were synthesised with the appropriate dbz ligand in the presence of PdCl₂ and NaOAc, in alcoholic solvents, in relatively good to high yields. ¹H COSY spectra revealed that most of the 'Pd-dbz' complexes possess 12 olefinic protons (thus two different Pd environments), which were proton correlated in most cases. ESI-MS, UV and CHN analysis confirmed the structures of the 'Pd-dbz' complexes. A question related to how much of the total Pd belonged to the 'Pd-dbz' complex and how much might be tied-up in the PdNPs. The active Pd/dbz ratio was thus investigated by ³¹P NMR using PPh₃, generating Pd⁰(dbz)(PPh₃)₂ *in situ*, using triethyl phosphate as a non-interfering reference compound to enable quantification. For several 'Pd-dbz' complexes the purity of the active Pd for reaction with PPh₃ was found to be lower than expected. Also, comparison between low temperature and room temperature NMR spectra of the 'Pd-dbz' complexes showed that the PPh₃ ligands were exchanging in Pd⁰(dbz-Z)(PPh₃)₂. TEM analysis showed the presence of PdNPs for the majority of the 'Pd-dbz' complexes synthesised, which are qualitatively consistent with the elemental analysis and ³¹P NMR study.

6.3 Synthesis of highly conjugated linear ethynyl nucleosides

The use of deionised and a pH between 6.5-7 water is important for the synthesis of deoxyadenosine. The Sonogashira alkylation of unprotected 8-bromoguanosine/adenosine was undertaken using various Pd catalysts, at different loadings, using Et₃N in DMF. It is important to use freshly distilled triethylamine and shorter reaction times to synthesise C8-alkynylated deoxyadenosines. Screening the activity of the novel Pd catalysts against Sonogashira and Heck cross-couplings of 8-bromoguanosine/adenosine revealed that the best catalyst was Pd₂(dba-4-OH,4'-O-hexyl)₃. Other solvent systems were also been examined, including propylene carbonate (PC). In the PC solvent, the yield for each coupling reaction was found to diminish, possibly due to lower reagent solubility. Libraries of novel C8-modified nucleosides, which contain “PhCCPhCC-” motifs, have been prepared in high yields (80-96%). The reaction conditions involved heating the reaction mixture at 110 °C for 18 or 22 h in DMF, catalysed by the optimised catalyst Pd₂(dba-4-OH,4'-O-hexyl)₃. NMR spectroscopic analysis enabled the structural information of the nucleosides to be determined. Based on the equilibrium of the *anti-syn* relationship, the dynamic behaviour of the nucleosides has been assessed, in comparison with simple natural nucleosides.

Experiments designed to assess whether the 8-alkynylguanosine could form G-quartets were carried out. However, no evidence for G-quartet formation could be gained by NMR, which may be due to the bulky structure of the modified guanosine or unfavourable formation about the purine ring system, relative to the ribose ring system.

6.4 Photophysical characterization of modified nucleosides

Photophysical characterisation of the C8-modified nucleosides has been recorded. All exhibited promising UV-vis and fluorescence properties. The modified nucleosides possess absorbance maxima shifted away from the intrinsic absorbance associated with proteins and nucleic acids. The band was slightly solvatochromic and bathochromically shifted in polar solvents (DMSO and DMF), indicating a decreasing HOMO-LUMO energy gap. The spectra for the C8-modified nucleosides analogues showed a linear decrease in absorption with decreasing concentration. This showed that aggregation of the nucleosides was not occurring at low concentrations (< 10⁻⁶ mol dm⁻³). Fluorescence spectra indicated these modified compounds were fluorescent. In DMSO, PhCCPhCC-(deoxy)adenosine had a high quantum yield (up to 0.51) and large Stokes' shift (6926 cm⁻¹), which was the best among all of the analogues tested. PhCCPhCC-(deoxy)guanosine had a lower quantum yield (up to 0.12).

Solvatochromic studies showed a relatively poor correlation between the solvent polarity and Stokes' shift for the compounds. Furthermore, the studies showed no correlation between solvents polarity and quantum yields for the parent compound. Significant fluorescence quenching was observed for the modified nucleosides compounds in water. Taking the PhCCPhCC-deoxyadenosine as example, the quantum yield decreased from 0.51 (DMSO) to 0.03 (water). The latter value is still useable in a biological context.

6.5 C-H direct arylation of nucleosides

The direct arylation reaction employs catalytic Pd and stoichiometric Cu, in the presence of carbonate base using DMF as a solvent to achieve the C-H coupling of phenyl group at C8 of inosine at 110 °C. Screening the activity of the Pd catalysts against the C-H bond direct arylation of inosine resulted in the best catalyst for this reaction being Pd₂(4-OH,4'-O-hexyl-dba)₃. Unfortunately this protocol was not effective for mediating the coupling of various other electron-donating substituents or using PC as the reaction solvent.

6.6 Future Work

Since the problem for the solid-phase synthesis was not resolved in this study, the first and most important need is to alter and improve the synthetic methodology. Due to the bulky motif linkage on the C8 position of nucleosides, attempts to introduce a more polar motif (acid group or phenyl group) at the C8 position, will most likely favour the synthesis.

Once the modified nucleotide has been synthesised, different oligonucleotides can be prepared. Various experiments can be envisaged, including the incorporation of the C8-modified nucleotides into a DNA mismatching-angled duplex (Figure 6.1). One chain has several more nucleotides than the other chain, which causes a kink in the DNA. Any reduction in duplex stability upon incorporation of the analogues can then be determined by melting temperature (T_m) measurements.

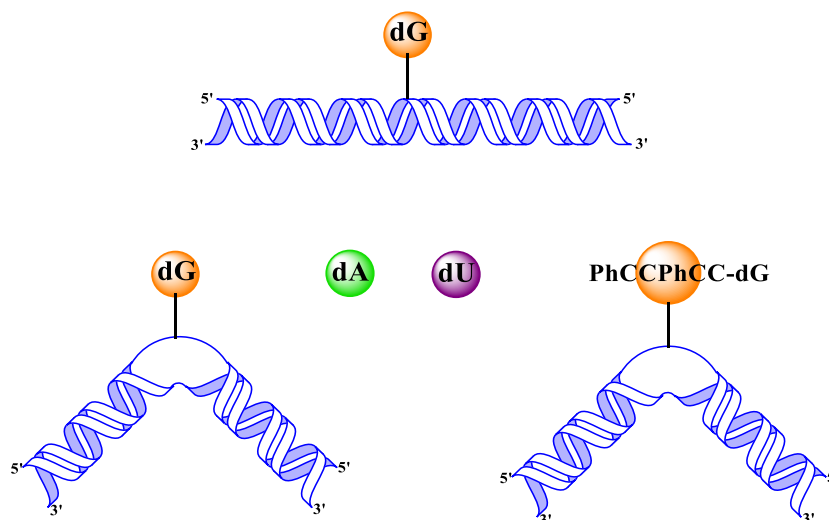


Figure 6.1 Angled DNA mismatching duplex.

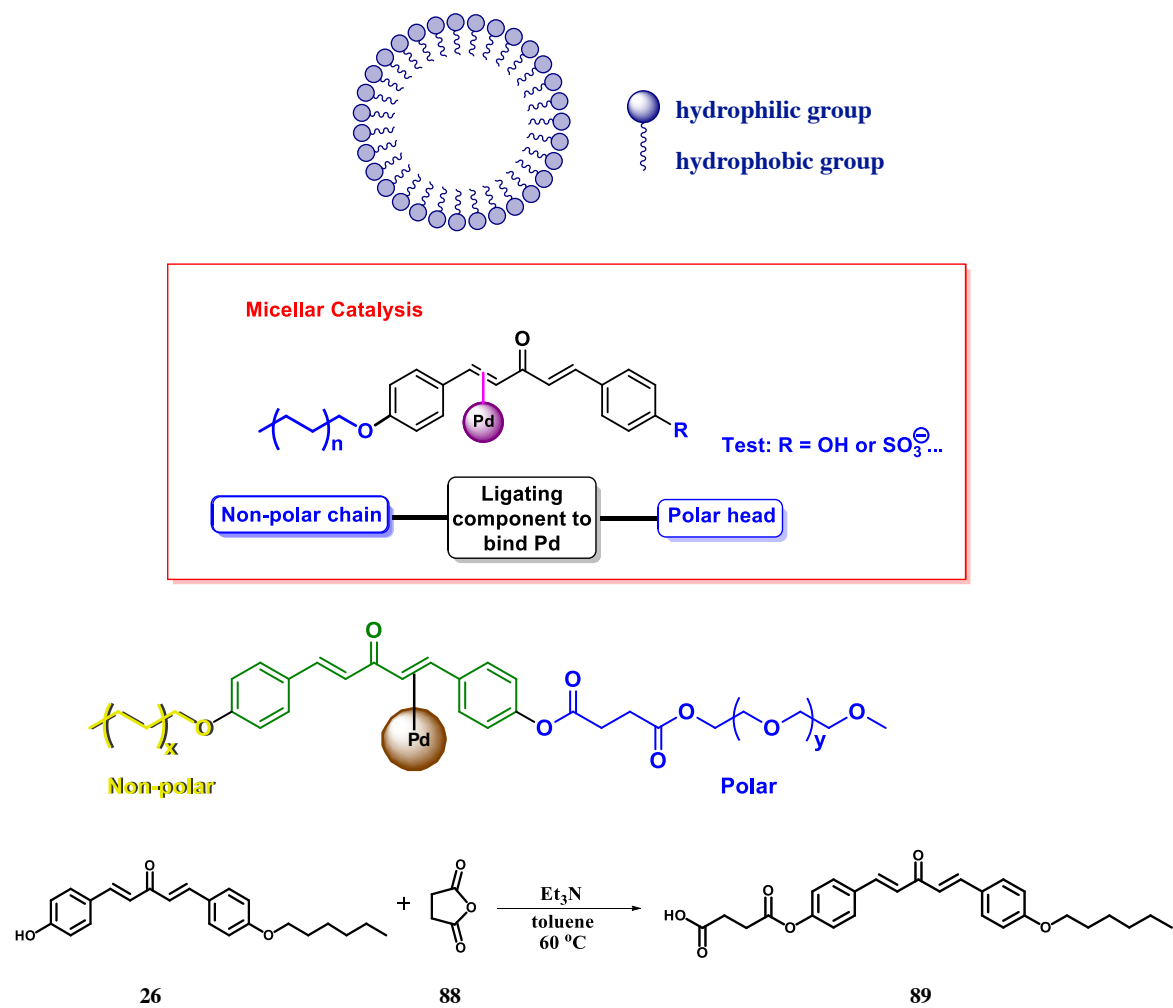


Figure 6.2 Micellar catalysis study.

For the Pd catalysis study, micellar catalysis can also be considered (Figure 6.2). A range of ligands of the type micellar, were first prepared by treatment of 4-OH,4'-alkyloxy dba ligand with succinic anhydride at 60 °C, using the method of Krasovskiy *et al.*²⁵²

Micellar catalysis is a well-known area in organic synthesis. Typically, an amphiphilic species (also called surfactant molecule or detergent) of the anionic, cationic, or non-ionic variety spontaneously aggregates in water at low concentrations forming “normal” (as opposed to “inverted”) micellar arrays, uniting a polar or ionic head and a non-polar tail within the same molecule. Such particles can be organised into spheres, rods or worms, vesicles, or combinations thereof, with their polar head groups outwardly interacting with the surrounding water, while their nonpolar subsection make up the interior. These lipophilic cores function as hosts for organic compounds; in essence, as solvent. The structure of micelle ensure the progression arranged in intermediate stage with concomitant formation of combinations of amphiphilic portions, wherein the non-polar parts stick together and are shielded from water, whereas the head groups are located in the outer regions of the aggregate.²⁵³ Given the huge influence of solvent effects in organic chemistry, variation in the nature of the amphiphile structure could well determine the level of success realised in synthetic transformations.²⁵⁴ The initial plan in this project (not fully executed) was to synthesise a surfactant compound having an amphiphilic structure: with hydrophobic chain at the inside of micellar and hydrophilic group at the outside of micellar.²⁵⁵ When the molecule with amphiphilic structure is dissolved in aqueous medium, the hydrophobic group distorts the structure of the water. As a result of this distortion, some of the surfactant molecule is expelled to the surfaces of the system with the hydrophobic groups oriented to minimise contact with the water molecules.^{256–258}

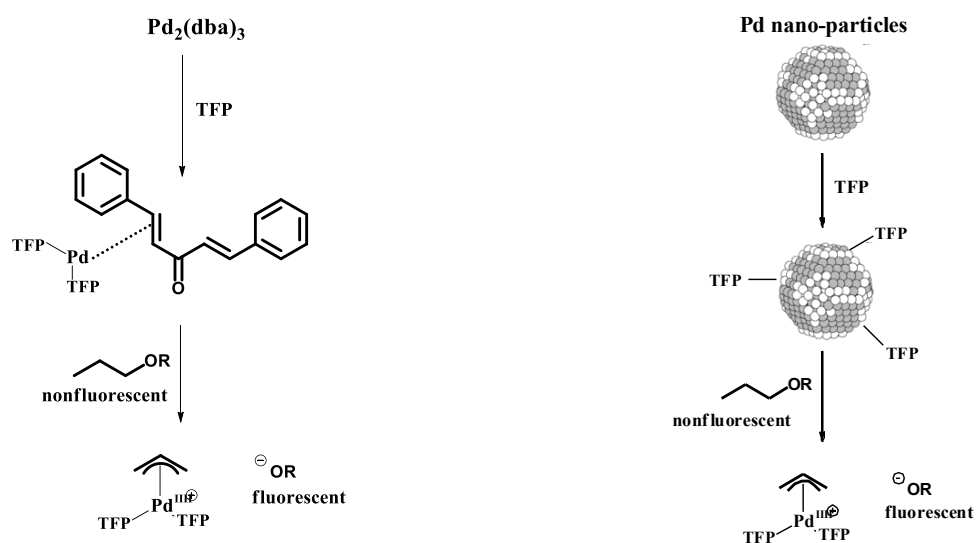
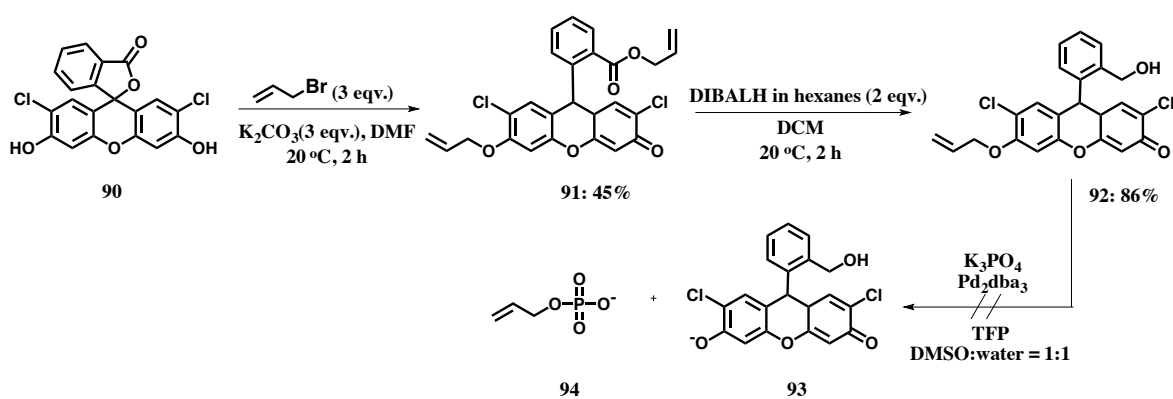


Figure 6.3 Understanding the difference between $\text{Pd}_2(\text{dba})_3$ and PdNPs.

An alternative method for determining the active Pd from the Pd catalysts can be done using a fluorescence experiment to test whether PdNPs are active (Figure 6.3). This idea is inspired by Koide and co-workers research (Scheme 6.1).²⁵⁹ Compound **92** is non-fluorescent, whereas **93** is fluorescent. The idea is to compare the reactivity of Pd₂(dba)₃ to PdNP. Simple Pd₂(dba)₃ reacts with tri(2-furyl)phosphine (TFP) to give Pd⁰(dba)(TFP)₂, which can then react with non-fluorescent **92** to generate fluorescent compound **93**. Quantification by fluorescence measurement could allow determination of total active Pd from the starting 'Pd-dba' complexes. Further, this reaction has the potential to test whether PdNPs are active catalysts in their own right, with appropriate controls in place using stabilised and well-defined PdNPs.



Scheme 6.1 Koide and co-workers fluorescent tools for sensing Pd⁰.

Abbreviations

[M]	metal
A	adenosine
A.U.	absorbance units
Abs	absorption
Ac	acetyl
AMP	adenosine monophosphate
ANS	1-aminonaphthalene-5-sulfonate
aq.	aqueous
Ar	aryl or heteroaryl
ATP	adenosine triphosphate
ave.	average
Bn	benzyl
B.P.	boiling point
Bu	butyl
C	cytosine
calc.	calculated
cat.	catalytic
CHN	analysis of carbon, hydrogen & nitrogen (elemental analysis)
cm	centimetre
cod	1,5-cyclooctadiene
conc.	concentration
COSY	correlation spectroscopy

Cp	cyclopentadienyl
CPS	counts per second
dA	2'-deoxyadenosine
dba	<i>E,E</i> -dibenzylideneacetone (1,5- <i>bis</i> -phenyl-penta-1 <i>E</i> ,4 <i>E</i> -dien-3-one)
DCM	dichloromethane
DDQ	2,3-dichloro-5,6-dicyano-1,4-benzoquinone
dec.	decomposition
DFT	density functional theory
dG	2'-deoxyguanosine
DI	deionized water
DIBALH	dissobutylaluminium hydride
DIPEA	<i>N,N</i> -diisopropylethylamine
DMAP	4- <i>N,N</i> -dimethylaminopyridine
DMF	<i>N,N</i> -dimethylformamide
DMSO	dimethyl sulfoxide
DMT	4,4'-dimethoxytrityl
DMTr	4,4'-dimethoxytrityl
DNA	deoxyribonucleic acid
EC	ethylene carbonate
eqv.	mole equivalent
ESI	electron spray ionisation
Et	ethyl
Et ₃ N	triethylamine
EtOAc	ethyl acetate

EtOH	ethanol
Fc	ferrocene
g	gram
G	guanosine
GIC ₅₀	50% growth inhibition concentration
Grad	gradient
h	hour
HOMO	highest occupied molecular orbital
HRMS	high resolution mass spectrometry
Hz	Hertz
IC	internal conversion
ICT	intramolecular charge transfer
IPA	isopropanol
ⁱ Pr	<i>iso</i> -propyl
IR	infrared
ISC	inter-system crossing
<i>J</i>	coupling constant
L	ligand
LIFDI	liquid introduced field desorption ionisation
lit.	literature
LUMO	lowest occupied molecular orbital
M	moles per decimetre cubed
<i>m/z</i>	mass-to-charge ratio
Me	methyl

MeCN	acetonitrile
MeOH	methanol
mg	milligram
min	minute
mmol	millimole
mol	mole
mol%	molar percentage
MP	melting point
MS	mass spectrometry
MW	microwave
n.d.	not detected
N.R.	no reaction
N^6	exocyclic amine on the 6 position of the purine ring
NAD	nicotinamide adenine dinucleotide
NBS	<i>N</i> -bromosuccinimide
nm	nanometres
NMR	nuclear magnetic resonance
OD	optical density
PC	propylene carbonate
PdNPs	palladium nanoparticles
Pet.	petroleum ether (40-60 °C)
Ph	phenyl
pH	potential of hydrogen
ppm	parts per million

<i>p</i> -TsOH	<i>p</i> -toluenesulfonic acid
Py	pyridine
R.T.	room temperature
R_f	retention factor
RNA	ribonucleic acid
TBAB	triethylamine bicarbonate buffer
TBAF	tetra- <i>n</i> -butylammonium fluoride
TBS	<i>tert</i> -butyldimethylsilyl
<i>t</i> Bu	<i>tert</i> -butyl
TEM	transmission electron microscopy
Temp.	temperature
TFP	tri(2-furyl)phosphine
THF	tetrahydrofuran
TLC	thin layer chromatography
T_m	melting temperature
TMS	trimethylsilyl
TMSA	trimethylsilylacetylene
TPPTS	triphenylphosphine- <i>tris</i> -sulphonate trisodium salt
TXPTS	tris(4,6-dimethyl-3-sulfanatophenyl)phosphine trisodium salt
UV	ultraviolet
vis	visible
Δf	orientation polarizability
δ	chemical shift (given in ppm)
ϵ	molar absorption coefficient

λ	wavelength (given in nm)
λ_{abs}	Absorption wavelength
λ_{em}	Emission wavelength
λ_{ex}	Excitation wavelength
Φ	fluorescence quantum yield
\AA	ångström

References

- (1) Bloomfield, V. A. *J. Polym. Sci. Macromol. Rev.* **1968**, 3, 255.
- (2) Maddox, B. *Rosalind Franklin: The Dark Lady of DNA*; New Ed edi.; HarperCollins Publishers Ltd: London, United Kingdom, 2003.
- (3) Maddox, B. *Nature* **2003**, 421, 407.
- (4) Watson J. D. and F. H. Crick. *Nature* **1957**, 737.
- (5) Stryer, L. *Biochemistry*; ed, 3rd, Ed.; W. H. Freeman and company: New York, 1988.
- (6) Alberts B., Johnson A., Lewis J., Raff. M, Roberts K., Walter P. *Molecular Biology of the Cell* ; ed, 5th, Ed.; Garland Science: New York, 2007.
- (7) Altona, C.; Sundaralingam, M. *J. Am. Chem. Soc.* **1972**, 94, 8205.
- (8) Hocquet, A.; Leulliot, N.; Ghomi, M. *J. Phys. Chem. B* **2000**, 104, 4560.
- (9) Neidle, S. *Nucleic acid structure and recognition*; Oxford University Press: Oxford, UK, 2002.
- (10) Feig, M.; Pettitt, B. M. *Biophys. J.* **1999**, 77, 1769.
- (11) Gast, K.; Zirwer, D.; Müller-Frohne, M.; Damaschun, G. *Protein Sci.* **1999**, 8, 625.

- (12) Uversky, V. N.; Narizhneva, N. V; Kirschstein, S. O.; Winter, S.; Löber, G. *Fold. Des.* **1997**, *2*, 163.
- (13) Nikolova, E. N.; Gottardo, F. L.; Al-Hashimi, H. M. *J. Am. Chem. Soc.* **2012**, *134*, 3667.
- (14) Mateos-Timoneda, M. A.; Crego-Calama, M.; Reinhoudt, D. N. *Chem. Soc. Rev.* **2004**, *33*, 363.
- (15) Gellert M., Davies D. R., Lipsett M. N.; *Proc. Natl. Acad. Sci. USA* **1962**, *48*, 2013.
- (16) Neidle, S.; Balasubramanian, S. *Quadruplex Nucleic Acids*; Neidle, S.; Balasubramanian, S., Eds.; Royal Society of Chemistry: Cambridge, 2006.
- (17) Qin, Y.; Hurley, L. H. *Biochimie* **2008**, *90*, 1149.
- (18) Eddy, J.; Maizels, N. *Nucleic Acids Res.* **2006**, *34*, 3887.
- (19) Huppert, J. L.; Balasubramanian, S. *Nucleic Acids Res.* **2007**, *35*, 406.
- (20) Cahoon, L. A.; Seifert, H. S. *Science* **2009**, *325*, 764.
- (21) Hurley, L. H. *Nat Rev Cancer* **2002**, *2*, 188.
- (22) Neidle, S.; Parkinson, G. *Nat Rev Drug Discov* **2002**, *1*, 383.
- (23) Pennarun, G.; Granotier, C.; Gauthier, L. R.; Gomez, D.; Hoffschir, F.; Mandine, E.; Riou, J.-F.; Mergny, J.-L.; Mailliet, P.; Boussin, F. D. **2005**, *24*, 2917.

- (24) Balasubramanian, S.; Hurley, L. H.; Neidle, S. *Nat. Rev. Drug Discov.* **2011**, *10*, 261.
- (25) Ruttkay-Nedecky, B.; Kudr, J.; Nejdil, L.; Maskova, D.; Kizek, R.; Adam, V. *Molecules* **2013**, *18*, 14760.
- (26) Cohen, Y.; Avram, L.; Frish, L. *Angew. Chemie Int. Ed.* **2005**, *44*, 520.
- (27) Kaucher, M. S.; Davis, J. T. *Tetrahedron Lett.* **2006**, *47*, 6381.
- (28) Sproviero, M.; Fadock, K. L.; Witham, A. A.; Manderville, R. A.; Sharma, P.; Wetmore, S. *D. Chem. Sci.* **2014**, *5*, 788.
- (29) Dumas, A.; Luedtke, N. W. *Nucleic Acids Res.* **2011**, *39*, 6825.
- (30) Aboul-ela, F.; Murchie, A. I. H.; Lilley, D. M. J. *Nature* **1992**, *360*, 280.
- (31) Sessler, J. L.; Sathiosatham, M.; Doerr, K.; Lynch, V.; Abboud, K. A. *Angew. Chemie Int. Ed.* **2000**, *39*, 1300.
- (32) S. L. Forman S. Pieraccini, G. Gottarelli, J. T. Davis, J. C. F. *J. Am. Chem. Soc.* **2000**, *122*, 4060.
- (33) C. H. Kang R. Ratliff, R. Moyzis, A. Rich, X. Z. *Nature* **1992**, *356*, 126.
- (34) G. Laughlan D. G. Norman, M. H. Moore, P. C. E. Moody, D. M. J. Lilley, B. Luisi, A. I. H. M. *Science.* **1994**, *265*, 520.

- (35) T. Sunami T. Kobuna, I. Hirao, K. Watanabe, K. I. Miura, A. Takenaka, J. K. *Nucleic Acids Res.* **2002**, *30*, 5253.
- (36) Guschlbauer W., Thiele, D.J., Chantot J. F.; *J. Biomol. Struct. Dyn.* **1990**, *8*, 491.
- (37) Davis, J. T. *Angew. Chem.* **2004**, *116*, 684.
- (38) Greco Y., N. . T. *Nat. Protoc.* **2007**, *2*, 305.
- (39) Reese, C. B. *Org. Biomol. Chem.* **2005**, *3*, 3851.
- (40) Zhang, H.; Luo, X.; Wongkhan, K.; Duan, H.; Li, Q.; Zhu, L.; Wang, J.; Batsanov, A. S.; Howard, J. A. K.; Marder, T. B.; Lei, A. *Chem. - A Eur. J.* **2009**, *15*, 3823.
- (41) Mujumdar, R. B.; Ernst, L. A.; Mujumdar, S. R.; Lewis, C. J.; Waggoner, A. S. *Bioconjug. Chem.* **1993**, *4*, 105.
- (42) Phelps, K.; Morris, A.; Beal, P. A. *ACS Chem. Biol.* **2012**, *7*, 100.
- (43) Behm-Ansmant, I.; Helm, M.; Motorin, Y. *J. Nucleic Acids* **2011**, *2011*, 1.
- (44) Sun, Y.; Li, S.; Zhou, L.; Zhong, Q.; Fang, S.; Chen, T.; Bi, L.; Mat, W.-K.; Zhao, C.; Xue, H.; Zhou, L.; Zhong, Q.; Fang, S.; Chen, T.; Bi, L.; Mat, W.-K.; Zhao, C.; Xue, H. *Appl. Microbiol. Biotechnol.* **2014**, *98*, 4095.
- (45) Lin, W. C.; Iversen, L.; Tu, H. L.; Rhodes, C.; Christensen, S. M.; Iwig, J. S.; Hansen, S. D.; Huang, W. Y. C.; Groves, J. T. *Proc. Natl. Acad. Sci.* **2014**, *111*, 2996.
- (46) Kore, A.; Charles, I. *Curr. Org. Chem.* **2012**, *16*, 1996.

- (47) Cremona, C. R. *Biophotonics* **2003**, *360*, 129.
- (48) Singh, Y.; Murat, P.; Defrancq, E. *Chem. Soc. Rev.* **2010**, *39*, 2054.
- (49) Bagshaw, C. R. *J. Cell Sci.* **2001**, *114*, 459.
- (50) Mulder, B. a.; Anaya, S.; Yu, P.; Lee, K. W.; Nguyen, A.; Murphy, J.; Willson, R.; Briggs, J. M.; Gao, X.; Hardin, S. H. *Nucleic Acids Res.* **2005**, *33*, 4865.
- (51) Kore, A. R.; Yang, B.; Srinivasan, B. *Tetrahedron Lett.* **2014**, *55*, 4822.
- (52) Draganescu, A.; Hodawadekar, S. C.; Gee, K. R.; Brenner, C. *J. Biol. Chem.* **2000**, *275*, 4555.
- (53) Yarbrough M. B.; Schlageck, J. G.; Baughman, M.; Yarbrough, L. R. *J. Biol. Chem.* **1979**, *254*, 12074.
- (54) Dhar, G.; Bhaduri, A. *J. Biol. Chem.* **1999**, *274*, 14568.
- (55) Hiratsuka, T. *Biochim. Biophys. Acta - Gen. Subj.* **1982**, *719*, 509.
- (56) Hiratsuka, T. *J. Biol. Chem.* **1985**, *260*, 4784.
- (57) Hazlett, T. L.; Moore, K. J. M.; Lowe, P. N.; Jameson, D. M.; Eccleston, J. F. *Biochemistry* **1993**, *32*, 13575.
- (58) Cremona, C. R.; Neuron, J. M.; Yount, R. G. *Biochemistry* **1990**, *29*, 3309.

- (59) Kurreck, J.; Wyszko, E.; Gillen, C.; Erdmann, V. A. *Nucleic Acids Res.* **2002**, *30*, 1911.
- (60) Mohamed, M. R.; Piacente, S. C.; Dickerman, B.; Niles, E. G. *Virology* **2006**, *349*, 359.
- (61) Montesano, L.; Glitz, D. G. *J. Biol. Chem.* **1988**, *263*, 4939.
- (62) Sontheimer, E. J. *Mol. Biol. Rep.* **1994**, *20*, 35.
- (63) Schneller, J. M.; Martin, R.; Stahl, A.; Dirheimer, G. *Biochem. Biophys. Res. Commun.* **1975**, *64*, 1046.
- (64) Nakatsuka, S.; Ohgi, T.; Goto, T. *Tetrahedron Lett.* **1978**, *19*, 2579.
- (65) Bogaerts, L. Fotochemie van het N6-acetylcytidine, 1969.
- (66) Pope, A. J.; Haupts, U. M.; Moore, K. J. *Drug Discov. Today* **1999**, *4*, 350.
- (67) Hurley, D. J.; Tor, Y. *J. Am. Chem. Soc.* **1998**, *120*, 2194.
- (68) Li, J. P.; Wang, H. X.; Wang, H. X.; Xie, M. S.; Qu, G. R.; Niu, H. Y.; Guo, H. M. *European J. Org. Chem.* **2014**, *2014*, 2225.
- (69) Hurley, D. J.; Tor, Y. *J. Am. Chem. Soc.* **2002**, *124*, 3749.
- (70) Okamoto, A.; Kanatani, K.; Saito, I. *J. Am. Chem. Soc.* **2004**, *126*, 4820.
- (71) Saito, Y.; Suzuki, A.; Imai, K.; Nemoto, N.; Saito, I. *Tetrahedron Lett.* **2010**, *51*, 2606.

- (72) Segal, M.; Fischer, B. *Org. Biomol. Chem.* **2012**, *10*, 1571.
- (73) Dziuba, D.; Pohl, R.; Hocek, M. *Chem. Commun.* **2015**, *51*, 4880.
- (74) Okamoto, A.; Tainaka, K.; Unzai, T.; Saito, I. *Tetrahedron* **2007**, *63*, 3465.
- (75) Amann, N.; Pandurski, E.; Fiebig, T.; Wagenknecht, H.-A. *Chemistry* **2002**, *8*, 4877.
- (76) Blas, J. R.; Huertas, O.; Tabares, C.; Sumpter, B. G.; Fuentes-Cabrera, M.; Orozco, M.; Ordejón, P.; Luque, F. J. *J. Phys. Chem. A* **2011**, *115*, 11344.
- (77) Gogichaishvili, S.; Johnson, J.; Gvarjaladze, D.; Lomidze, L.; Kankia, B. *Biopolymers* **2014**, *101*, 583.
- (78) Jałoszyński, P.; Jaruga, P.; Oliński, R.; Biczysko, W.; Szyfter, W.; Nagy, E.; Möller, L.; Szyfter, K. *Free Radic. Res.* **2003**, *37*, 231.
- (79) Shin, D.; Lönn, P.; Dowdy, S. F.; Tor, Y. *Chem. Commun.* **2015**, *51*, 1662.
- (80) Kawai, M.; Lee, M.; Evans, K.; Nordlund, T. *J. Fluoresc.* **2001**, *11*, 23.
- (81) Wanninger-Weiß, C.; Wagenknecht, H.-A. *European J. Org. Chem.* **2008**, *2008*, 64.
- (82) Mizuta, M.; Seio, K.; Miyata, K.; Sekine, M. *J. Org. Chem.* **2007**, *72*, 5046.
- (83) Liu, H.; Gao, J.; Kool, E. T. *J. Org. Chem.* **2005**, *70*, 639.

- (84) Lee, A. H. F.; Kool, E. T. *J. Am. Chem. Soc.* **2006**, *128*, 9219.
- (85) Wu, P.; Nordlund, T. M.; Gildea, B.; McLaughlin, L. W. *Biochemistry* **1990**, *29*, 6508.
- (86) Keller M. M., G. H. a. M. *DNA Probes*; Stockton: New York, 1989.
- (87) Bruns, R. F. C. *J. Physiol. Pharmacol.* **1980**, *58*, 673.
- (88) Jacobson, K. A. *In Comprehensive medicinal chemistry of the rational design, mechanistic study and therapeutic application of chemical compounds*; Pergamon Press: Oxford, New York, 1990.
- (89) Gudmundsson, K. S.; Daluge, S. M.; Condreay, L. D.; Johnson, L. C. *Nucleosides. Nucleotides Nucleic Acids* **2002**, *21*, 891.
- (90) Western K. H. J., E. C. . S. *Org. Chem.* **2005**, *70*, 6378.
- (91) Vigny M., P. . D. *Photochem. Photobiol.* **1974**, *20*, 15.
- (92) Madariaga, S. Teresa, Contreras, J. G. *J. Chil. Chem. Soc.* **2010**, *55*, 50.
- (93) Saito, Y.; Hanawa, K.; Motegi, K.; Omoto, K.; Okamoto, A.; Saito, I. *Tetrahedron Lett.* **2005**, *46*, 7605.
- (94) Zilbershtein-Shklanovsky, L.; Weitman, M.; Major, D. T.; Fischer, B. *J. Org. Chem.* **2013**, *78*, 11999.
- (95) Schlitt, K. M.; Millen, A. L.; Wetmore, S. D.; Manderville, R. A. *Org. Biomol. Chem.* **2011**, *9*, 1565.

- (96) Saito, Y.; Matsumoto, K.; Bag, S. S.; Misawa, A.; Saito, I. *Nucleic Acids Symp. Ser.* **2008**, *52*, 357.
- (97) A. G. Firth, K. Darley and C. G. Baumann, I. J. S. Fairlamb. *Tetrahedron Lett.* **2006**, *47*, 3529.
- (98) Sessler, J. L.; Wang, R. *Angew. Chemie Int. Ed.* **1998**, *37*, 1726.
- (99) Chianese, A. R.; Lee, S. J.; Gagné, M. R. Electrophilic activation of alkenes by platinum(II): So much more than a slow version of palladium(II). *Angewandte Chemie - International Edition*, 2007, *46*, 4042–4059.
- (100) Elsevier, C. J.; Reedijk, J.; Walton, P. H.; Ward, M. D. *Dalt. Trans.* **2003**, 1869.
- (101) Lamblin, M.; Nassar-Hardy, L.; Hierso, J. C.; Fouquet, E.; Felpin, F.-X. *Adv. Synth. Catal.* **2010**, *352*, 33.
- (102) Zhang, S.-S.; Wang, Z.-Q.; Xu, M.-H.; Lin, G.-Q. *Org. Lett.* **2010**, *12*, 5546.
- (103) Chay, R. S.; Luzyanin, K. V.; Kukushkin, V. Y.; Guedes da Silva, M. F. C.; Pombeiro, A. J. L. *Organometallics* **2012**, *31*, 2379.
- (104) Kostas, I. D.; Heropoulos, G. A.; Kovala-Demertzi, D.; Yadav, P. N.; Jasinski, J. P.; Demertzis, M. A.; Andreadaki, F. J.; Vo-Thanh, G.; Petit, A.; Loupy, A. *Tetrahedron Lett.* **2006**, *47*, 4403.
- (105) Bai, L.; Wang, J. X. *Adv. Synth. Catal.* **2008**, *350*, 315.

- (106) Tannai, H.; Koizumi, T.; Tanaka, K. *Inorg. Chim. Acta* **2007**, *360*, 3075.
- (107) Vlaar, T.; Ruijter, E.; Orru, R. V. A. *Adv. Synth. Catal.* **2011**, *353*, 809.
- (108) Lu, W.; Li, Y.; Wang, C.; Xue, D.; Chen, J.-G.; Xiao, J. *Org. Biomol. Chem.* **2014**, *12*, 5243.
- (109) Heijnen, D.; Hornillos, V.; Corbet, B. P.; Giannerini, M.; Feringa, B. L. *Org. Lett.* **2015**, *17*, 2262.
- (110) De Ornellas, S.; Williams, T. J.; Baumann, C. G.; Fairlamb, I. J. S. Royal Society of Chemistry: Cambridge, UK, 2013; pp. 409–447.
- (111) Hervé, G.; Sartori, G.; Enderlin, G.; Mackenzie, G.; Len, C. *RSC Adv.* **2014**, *4*, 18558.
- (112) Sonogashira, K.; Tohda, Y.; Hagihara, N. *Tetrahedron Lett.* **1975**, *16*, 4467.
- (113) Chinchilla, R.; Nájera, C. The Sonogashira reaction: A booming methodology in synthetic organic chemistry. *Chemical Reviews*, 2007, *107*, 874–922.
- (114) Xue, L.; Lin, Z. *Chem. Soc. Rev.* **2010**, *39*, 1692.
- (115) Barluenga, J.; Valdés, C. *Angew. Chemie Int. Ed.* **2011**, *50*, 7486.
- (116) Cho, J. H.; Shaughnessy, K. H. In *Current Protocols in Nucleic Acid Chemistry*; John Wiley & Sons, Inc.: Hoboken, NJ, USA, 2012.
- (117) Matsuda, A.; Satoh, K.; Tanaka, H.; Miyasaka, T. *Nucleic Acids Symp. Ser.* **1983**, *5*.

- (118) Cho, J. H.; Prickett, C. D.; Shaughnessy, K. H. *European J. Org. Chem.* **2010**, 2010, 3678.
- (119) Vrábel, M.; Pohl, R.; Votruba, I.; Sajadi, M.; Kovalenko, S. A.; Ernsting, N. P.; Hocek, M. *Org. Biomol. Chem.* **2008**, 6, 2852.
- (120) Firth, A. G.; Fairlamb, I. J. S.; Darley, K.; Baumann, C. G. *Tetrahedron Lett.* **2006**, 47, 3529.
- (121) Hervé, G.; Len, C. *RSC Adv.* **2014**, 4, 46926.
- (122) Western, E. C.; Shaughnessy, K. H. *J. Org. Chem.* **2005**, 70, 6378.
- (123) Capek, P.; Pohl, R.; Hocek, M. *Org. Biomol. Chem.* **2006**, 4, 2278.
- (124) Bourderioux, A.; Nauš, P.; Perlíková, P.; Pohl, R.; Pichová, I.; Votruba, I.; Džubák, P.; Konečný, P.; Hajdúch, M.; Stray, K. M.; Wang, T.; Ray, A. S.; Feng, J. Y.; Birkus, G.; Cihlar, T.; Hocek, M. *J. Med. Chem.* **2011**, 54, 5498.
- (125) Pesnot, T.; Kempster, J.; Schemies, J.; Pergolizzi, G.; Uciechowska, U.; Rumpf, T.; Sippl, W.; Jung, M.; Wagner, G. K. *J. Med. Chem.* **2011**, 54, 3492.
- (126) Cerna, I.; Pohl, R.; Hocek, M. *Chem. Commun. (Camb)*. **2007**, 4729.
- (127) Storr, T. E.; Firth, A. G.; Wilson, K.; Darley, K.; Baumann, C. G.; Fairlamb, I. J. S. *Tetrahedron* **2008**, 64, 6125.
- (128) Storr, T. E.; Baumann, C. G.; Thatcher, R. J.; De Ornellas, S.; Whitwood, A. C.; Fairlamb, I. J. S. *J. Org. Chem.* **2009**, 74, 5810.

- (129) Liang, Y.; Gloudeman, J.; Wnuk, S. F. *J. Org. Chem.* **2014**, *79*, 4094.
- (130) Fairlamb, I. J. S.; Lee, A. F. *Organometallics* **2007**, *26*, 4087.
- (131) Fairlamb, I. J. S.; Kapdi, A. R.; Lee, A. F.; McGlacken, G. P.; Weissburger, F.; de Vries, A. H. M.; Schmieder-van de Vondervoort, L. *Chem. - A Eur. J.* **2006**, *12*, 8750.
- (132) Eddy, J. W.; Davey, E. A.; Malsom, R. D.; Ehle, A. R.; Kassel, S.; Goodson, F. E. *Macromolecules* **2009**, *42*, 8611.
- (133) C. Amatore, F. Khalil, M. A. M'Barki, and L. Mottier; *Organometallics* **1993**, *12*, 3168.
- (134) Carole, W. A.; Bradley, J.; Sarwar, M.; Colacot, T. J. *Org. Lett.* **2015**, *17*, 5472.
- (135) Ananikov, S. S. Z. and V. P. *Organometallics* **2012**, *31*, 2302.
- (136) Fairlamb, I. J. S. *Org. Biomol. Chem.* **2008**, *6*, 3645.
- (137) Takahashi, Y.; Ito, T.; Sakai, S.; Ishii, Y. *J. Chem. Soc. D Chem. Commun.* **1970**, 1065.
- (138) Weber, W. M.; Hunsaker, L. A.; Abcouwer, S. F.; Deck, L. M.; Vander Jagt, D. L. *Bioorg. Med. Chem.* **2005**, *13*, 3811.
- (139) Adams, B. K.; Ferstl, E. M.; Davis, M. C.; Herold, M.; Kurtkaya, S.; Camalier, R. F.; Hollingshead, M. G.; Kaur, G.; Sausville, E. A.; Rickles, F. R.; Snyder, J. P.; Liotta, D. C.; Shoji, M. *Bioorganic Med. Chem.* **2004**, *12*, 3871.

- (140) Tenkovtsev, A. V.; Yakimansky, A. V.; Dudkina, M. M.; Lukoshkin, V. V.; Komber, H.; Häussler, L.; Böhme, F. *Macromolecules* **2001**, *34*, 7100.
- (141) Sardjiman, S. S.; Reksohadiprodo, M. S.; Hakim, L.; van der Goot, H.; Timmerman, H. *Eur. J. Med. Chem.* **1997**, *32*, 625.
- (142) Kapdi, A. R.; Whitwood, A. C.; Williamson, D. C.; Lynam, J. M.; Burns, M. J.; Williams, T. J.; Reay, A. J.; Holmes, J.; Fairlamb, I. J. S. *J. Am. Chem. Soc.* **2013**, *135*, 8388.
- (143) Franzen, S. *J. Chem. Educ.* **2011**, *88*, 619.
- (144) Goel, M.; Jayakannan, M. *J. Phys. Chem. B* **2010**, *114*, 12508.
- (145) Cao, B.; Wang, Y.; Ding, K.; Neamati, N.; Long, Y.-Q. *Org. Biomol. Chem.* **2012**, *10*, 1239.
- (146) Tatsuzaki, J.; Bastow, K. F.; Nakagawa-Goto, K.; Nakamura, S.; Itokawa, H.; Lee, K. H. *J. Nat. Prod.* **2006**, *69*, 1445.
- (147) Oguri, H.; Hishiyama, S.; Oishi, T.; Hirama, M. *Synlett* **1995**, *1995*, 1252.
- (148) McDougal, P. G.; Rico, J. G.; Oh, Y. I.; Condon, B. D. *J. Org. Chem.* **1986**, *51*, 3388.
- (149) Blackwell, J. M.; Foster, K. L.; Beck, V. H.; Piers, W. E. *J. Org. Chem.* **1999**, *64*, 4887.
- (150) Baldwin, J. E.; Adlington, R. M.; Sham, V. W.; Marquez, R.; Bulger, P. G. *Tetrahedron* **2005**, *61*, 2353.
- (151) Wee, A. G. H.; Yu, Q. *J. Org. Chem.* **2001**, *66*, 8935.

- (152) Eggers, K.; Fyles, T. M.; Montoya-Pelaez, P. J. *J. Org. Chem.* **2001**, *66*, 2966.
- (153) Wang, G. H.; Hilgert, J.; Richter, F. H.; Wang, F.; Bongard, H. J.; Spliethoff, B.; Weidenthaler, C.; Schüth, F. *Nat. Mater.* **2014**, *13*, 293.
- (154) Gniewek, A.; Trzeciak, A.; Ziolkowski, J.; Kepinski, L.; Wrzyszczyk, J.; Tylus, W. *J. Catal.* **2005**, *229*, 332.
- (155) Lin, Y.-R.; Hong, Y. L. V.; Hongs, J.-L. *Mol. Cryst. Liq. Cryst. Sci. Technol. Sect. A. Mol. Cryst. Liq. Cryst.* **1994**, *241*, 69.
- (156) H. Hashimoto, M. G. Nelson, and C. Switzer; *J. Am. Chem. Soc.* **1993**, *115*, 7128.
- (157) H. Rosemeyer E.-M. Becker, E. Feiling and F. Seela, N. R. *Bioconjugate Chem* **2002**, *13*, 1274.
- (158) J. A. Brazier J. Townsley, B. F. Taylor, E. Frary, N. H. Williams and D. M. Williams, T. S. *Nucleic Acids Res.* **2005**, *33*, 1362.
- (159) De Clercq, E. B. *Pharmacol* **1984**, *33*, 2159.
- (160) Minakawa, N.; Kojima, N.; Sasaki, T.; Matsuda, A. *Nucleosides, Nucleotides and Nucleic Acids* **1996**, *15*, 251.
- (161) Nguyen, P.; Lesley, G.; Marder, T. B.; Ledoux, I.; Zyss, J. *Chem. Mater.* **1997**, *9*, 406.
- (162) Nguyen, P.; Yuan, Z.; Agocs, L.; Lesley, G.; Marder, T. B. *Inorg. Chim. Acta* **1994**, *220*, 289.

- (163) Nguyen, P.; Todd, S.; Van den Biggelaar, D.; Taylor, N. J.; Marder, T. B.; Wittmann, F.; Friend, R. H. *Synlett* **1994**, 1994, 299.
- (164) Collings, J. C.; Parsons, A. C.; Porrès, L.; Beeby, A.; Batsanov, A. S.; Howard, J. A. K.; Lydon, D. P.; Low, P. J.; Fairlamb, I. J. S.; Marder, T. B. *Chem. Commun. (Camb)*. **2005**, 21, 2666.
- (165) Collier A., Wagner G. K.; *Synth. Commun.* **2006**, 36, 3713.
- (166) Čapek P., Hocek M.; *Synlett* **2005**, 46, 3005.
- (167) Western, E. C.; Daft, J. R.; Johnson, E. M.; Gannett, P. M.; Shaughnessy, K. H. *J. Org. Chem.* **2003**, 68, 6767.
- (168) Lakshman, M. K. C. *Org. Synth.* **2005**, 2, 83.
- (169) Hocek, M. *Eur. J. Org. Chem.* **2003**, 245.
- (170) A. G. Firth., C. G. Baumann, and I. J. S. Fairlamb;. *Nucleosides, Nucleotides and Nucleic Acids* **2011**, 30, 168.
- (171) Pneumatikakis, G. *Inorg. Chem. Acta.* **1984**, 93, 5.
- (172) Dehand J., Jordanov J.; *J. Chem. Soc. Chem. Commun.* **1976**, 598.
- (173) Crisp G. T., Gore J.; *Tetrahedron Lett.* **1997**, 53, 1523.
- (174) Flasche, W.; Cismas, C.; Herrmann, A.; Liebscher, J. *Synthesis (Stuttg)*. **2004**, 2004, 2335.

- (175) Gannett T.P, P. M. . S. *Synth. Commun.* **1993**, *23*, 1611.
- (176) M. Ikehara, M. K. *Tetrahedron Lett.* **1970**, *26*, 4251.
- (177) *Alternative Solvents for Green Chemistry*; RSC Green Chemistry; Royal Society of Chemistry: Cambridge, 2013.
- (178) Fairlamb, I. J. S., Kapdi, A. R., Lee, A. F., Sanchez, G., Lopez, G., Serrano, J. L., Perez, E. *Dalt. Trans.* **2004**, 3970.
- (179) Firmansjah, L.; Fu, G. C. *J. Am. Chem. Soc.* **2007**, *129*, 11340.
- (180) Marsh, A. J.; Williams, D. M.; Grasby, J. A. *Org. Biomol. Chem.* **2004**, *2*, 2103.
- (181) Lyttle, M. H.; Walton, T. A.; Dick, D. J.; Carter, T. G.; Beckman, J. H.; Cook, R. M. *Bioconjug. Chem.* **2002**, *13*, 1146.
- (182) Kapdi, A.; Ardhapure, A.; Sanghvi, Y. *Synthesis (Stuttg).* **2015**, *47*, 1163.
- (183) Jagtap, S. P.; Mukhopadhyay, S.; Coropceanu, V.; Brizius, G. L.; Brédas, J. L.; Collard, D. *M. J. Am. Chem. Soc.* **2012**, *134*, 7176.
- (184) Dirk, S. M.; Tour, J. M. *Tetrahedron* **2003**, *59*, 287.
- (185) Holmes, R. E.; Robins, R. K. *J. Am. Chem. Soc.* **1964**, *86*, 1242.
- (186) Roger, J.; Verrier, C.; Le Goff, R.; Hoarau, C.; Doucet, H. *ChemSusChem* **2009**, *2*, 951.

- (187) Van Roey, P.; Salerno, J. M.; Chu, C. K.; Schinazi, R. F. *Proc. Natl. Acad. Sci. U. S. A.* **1989**, *86*, 3929.
- (188) Mathé, C.; Périgaud, C. *European J. Org. Chem.* **2008**, *2008*, 1489.
- (189) Markley, J. L.; Bax, A.; Arata, Y.; Hilbers, C. .; Kaptein, R.; Sykes, B. D.; Wright, P. E.; Wüthrich, K. *J. Mol. Biol.* **1998**, *280*, 933.
- (190) Stolarski, R.; Dudycz, L.; Shugar, D. *Eur. J. Biochem.* **1980**, *108*, 111.
- (191) Plevnik, M.; Črnugelj, M.; Štimac, A.; Kobe, J.; Plavec, J. *J. Chem. Soc. Perkin Trans. 2* **2001**, 1433.
- (192) Chang, C. J.; Gomes, J. D.; Byrn, S. R. *J. Org. Chem.* **1983**, *48*, 5151.
- (193) Minakawa, N.; Kojima, N.; Matsuda, A. *J. Org. Chem.* **1999**, *64*, 7158.
- (194) Altona, C.; Sundaralingam, M. *J. Am. Chem. Soc.* **1972**, *94*, 8205.
- (195) Esho, N.; Desaulniers, J.-P.; Davies, B.; Chui, H. M.-P.; Rao, M. S.; Chow, C. S.; Szafert, S.; Dembinski, R. *Bioorg. Med. Chem.* **2005**, *13*, 1231.
- (196) Hawkins, M. E. 2008; pp. 201–231.
- (197) Wilhelmsson, L. M. *Q. Rev. Biophys.* **2010**, *43*, 159.
- (198) Srivatsan, S. G.; Weizman, H.; Tor, Y. *Org. Biomol. Chem.* **2008**, *6*, 1334.

- (199) Rist, M.; Marino, J. *Curr. Org. Chem.* **2002**, *6*, 775.
- (200) Butler, R. S.; Cohn, P.; Tenzel, P.; Abboud, K. A.; Castellano, R. K. *J. Am. Chem. Soc.* **2009**, *131*, 623.
- (201) Ogasawara, S.; Saito, I.; Maeda, M. *Tetrahedron Lett.* **2008**, *49*, 2479.
- (202) Kimura, T.; Kawai, K.; Fujitsuka, M.; Majima, T. *Tetrahedron* **2007**, *63*, 3585.
- (203) Gray, R. D.; Petraccone, L.; Trent, J. O.; Chaires, J. B. *Biochemistry* **2010**, *49*, 179.
- (204) Gray, R. D.; Petraccone, L.; Buscaglia, R.; Chaires, J. B. *Methods Mol. Biol.* **2010**, *608*, 121.
- (205) Niles, J. C.; Wishnok, J. S.; Tannenbaum, S. R. *Chem. Res. Toxicol.* **2000**, *13*, 390.
- (206) Gottarelli, G.; Masiero, S.; Mezzina, E.; Spada, G. P.; Mariani, P.; Recanatini, M. *Helv. Chim. Acta* **1998**, *81*, 2078.
- (207) Sen, D.; Gilbert, W. A sodium-potassium switch in the formation of four-stranded G4-DNA. *Nature*, 1990, *344*, 410–414.
- (208) Salgado, G. F.; Cazenave, C.; Kerkour, A.; Mergny, J. L. *Chem. Sci.* **2015**, *6*, 3314.
- (209) Zhdanov, R. I.; Zhenodarova, S. M. *Synthesis (Stuttg.)*. **1975**, *1975*, 222.
- (210) Reese, C. B. *Tetrahedron* **1978**, *34*, 3143.

- (211) Ohtsuka, E.; Ikehara, M.; Söll, D. *Nucleic Acids Res.* **1982**, *10*, 6553.
- (212) Reese, C. B. *Tetrahedron* **2002**, *58*, 8893.
- (213) Guzaev, A. P. In *Current Protocols in Nucleic Acid Chemistry*; John Wiley & Sons, Inc.: Hoboken, NJ, USA, 2013.
- (214) Sproviero, M.; Rankin, K. M.; Witham, A. A.; Manderville, R. A. *J. Org. Chem.* **2014**, *79*, 692.
- (215) King, A. O.; Negishi, E.; Villani, F. J.; Silveira, A. *J. Org. Chem.* **1978**, *43*, 358.
- (216) Rule, N. G.; Detty, M. R.; Kaeding, J. E.; Sinicropi, J. A. *J. Org. Chem.* **1995**, *60*, 1665.
- (217) Reilly, D. T.; Kim, S. H.; Katzenellenbogen, J. A.; Schroeder, C. M. *Anal. Chem.* **2015**, *87*, 11048.
- (218) Sridharan, R.; Zuber, J.; Connelly, S. M.; Mathew, E.; Dumont, M. E. *Biochim. Biophys. Acta - Biomembr.* **2014**, *1838*, 15.
- (219) Hess, S. T.; Girirajan, T. P. K.; Mason, M. D. *Biophys. J.* **2006**, *91*, 4258.
- (220) Castro, C.; Smidansky, E. D.; Arnold, J. J.; Maksimchuk, K. R.; Moustafa, I.; Uchida, A.; Götte, M.; Konigsberg, W.; Cameron, C. E. *Nat. Struct. & Mol. Biol.* **2009**, *16*, 212.
- (221) Eoff, R. L.; Choi, J. Y.; Guengerich, F. P. *J. Nucleic Acids* **2010**, *2010*, 1.

- (222) Albani, J. R. *Principles and Applications of Fluorescence Spectroscopy*; 1, Ed.; Blackwell Science: Oxford, 2007.
- (223) Jablonski, A. *Zeitschrift fur Phys.* **1935**, *94*, 38.
- (224) Crespo-Hernández, C. E.; Cohen, B.; Hare, P. M.; Kohler, B. *Chem. Rev.* **2004**, *104*, 1977.
- (225) Kwok, W.-M.; Ma, C.; Phillips, D. L. *J. Am. Chem. Soc.* **2006**, *128*, 11894.
- (226) Jameson J. F., D. M. . E. *Fluoresc. Spectrosc.* **1997**, *278*, 363.
- (227) Williams, A. T. R.; Winfield, S. A.; Miller, J. N. *Analyst* **1983**, *108*, 1067.
- (228) Dhami, S.; Mello, A. J. De; Rumbles, G.; Bishop, S. M.; Phillips, D.; Beeby, A. *Photochem. Photobiol.* **1995**, *61*, 341.
- (229) Martel, P. *J. Phys. Chem.* **1985**, *89*, 230.
- (230) Burdick & Jackson. UV Cutoff [http://macro.lsu.edu/HowTo/solvents/UV Cutoff.htm](http://macro.lsu.edu/HowTo/solvents/UV%20Cutoff.htm).
- (231) Asakura Ji, J.; Robins, M. J.; Asaka, Y.; Kim, T. H. *J. Org. Chem.* **1996**, *61*, 9026.
- (232) Bhattacharjee, S.; Khan, M. .; Chandra, H.; Symons, M. C. . *Spectrochim. Acta Part A Mol. Biomol. Spectrosc.* **1998**, *54*, 759.
- (233) Reich, N. O.; Sweetnam, K. R. *Nucleic Acids Res.* **1994**, *22*, 2089.
- (234) Nielsen, H. R.; SjoIn, K. **1974**, *34*, 3428.

- (235) Manickam, M. C. D.; Annalakshmi, S.; Pitchumani, K.; Srinivasan, C. *Org. Biomol. Chem.* **2005**, *3*, 1008.
- (236) Stiegman, A. E.; Graham, E.; Perry, K. J.; Khundkar, L. R.; Cheng, L. T.; Perry, J. W. *J. Am. Chem. Soc.* **1991**, *113*, 7658.
- (237) Stiegman, A. E.; Miskowski, V. M.; Perry, J. W.; Coulter, D. R. *J. Am. Chem. Soc.* **1987**, *109*, 5884.
- (238) Lutz, H.-P.; Luisi, P. L. *Helv. Chim. Acta* **1983**, *66*, 1929.
- (239) Kubista, M.; Sjaback, R.; Eriksson, S.; Albinsson, B. *Analyst* **1994**, *119*, 417.
- (240) Ababneh, A. M.; Large, C. C.; Georghiou, S. *Biophys. J.* **2003**, *85*, 1111.
- (241) Homocianu M., Airinei A., and Dorohoi D. O.; *Journal of Advanced Research in Physics.* **2011**, *2*, 1
- (242) Yvon, J. A Guide to Recording Fluorescence Quantum Yields
<http://www.horiba.com/fileadmin/uploads/Scientific/Documents/Fluorescence/quantumyieldstrad.pdf>.
- (243) Firth, A. G. PhD Thesis, University of York, 2008.
- (244) Das, D. K.; Makhal, K.; Bandyopadhyay, S. N.; Goswami, D. *Sci. Rep.* **2014**, *4*.
- (245) Sun, X.; Ladanyi, B. M.; Stratt, R. M. *J. Phys. Chem. B* **2015**, *119*, 9129.

- (246) Suppan, P. *J. Chem. Soc. Faraday Trans. 1 Phys. Chem. Condens. Phases* **1987**, 83, 495.
- (247) Labinger, J. A.; Bercaw, J. E. *Nature* **2002**, 417, 507.
- (248) Godula, K.; Sames, D. *Science* **2006**, 312, 67.
- (249) Bellina, F.; Cauteruccio, S.; Di Fiore, A.; Rossi, R. *European J. Org. Chem.* **2008**, 2008, 5436.
- (250) Gigante, A.; Priego, E.-M.; Sánchez-Carrasco, P.; Ruiz-Pérez, L. M.; Vande Voorde, J.; Camarasa, M.-J.; Balzarini, J.; González-Pacanowska, D.; Pérez-Pérez, M.-J. *Eur. J. Med. Chem.* **2014**, 82, 459.
- (251) Stark, T.; Suhartono, M.; Göbel, M.; Lautens, M. *Synlett* **2013**, 24, 2730.
- (252) Lipshutz, B. H.; Ghorai, S.; Abela, A. R.; Moser, R.; Nishikata, T.; Duplais, C.; Krasovskiy, A.; Gaston, R. D.; Gadwood, R. C. *J. Org. Chem.* **2011**, 76, 4379.
- (253) Vashishtha, M.; Mishra, M.; Undre, S.; Singh, M.; Shah, D. O. *J. Mol. Catal. A Chem.* **2015**, 396, 143.
- (254) Rathman, J. F. *Curr. Opin. Colloid Interface Sci.* **1996**, 1, 514.
- (255) Zuev, Y. F.; Idiyatullin, B. Z.; Fedotov, V. D.; Mirgorodskaya, A. B.; Zakharova, L. Y.; Kudryavtseva, L. A. In *Magnetic Resonance in Colloid and Interface Science*; Springer Netherlands: Dordrecht, 2002; pp. 649–654.
- (256) R.J. Hunter. *Foundations of Colloid Science*; 2nd ed.; Oxford University Press: Oxford, UK, 2001.

(257) Broxton, T. J.; Christie, J. R.; Chung, R. P. T. *J. Org. Chem.* **1988**, *53*, 3081.

(258) La Sorella, G.; Strukul, G.; Scarso, A. *Green Chem.* **2015**, *17*, 644.

(259) Song, F.; Carder, E. J.; Kohler, C. C.; Koide, K. *Chemistry* **2010**, *16*, 13500.